Komitet Krystalografii PAN
Instytut Niskich Temperatur i Badań Strukturalnych PAN
Uniwersytet Kardynała Stefana Wyszyńskiego
Polskie Towarzystwo Krystalograficzne

63 Konwersatorium Krystalograficzne

Polish Crystallographic Meeting

Warsztaty Naukowe i Walne Zgromadzenie PTKryst

Edycja on-line, 29 VI - 1 VII 2022

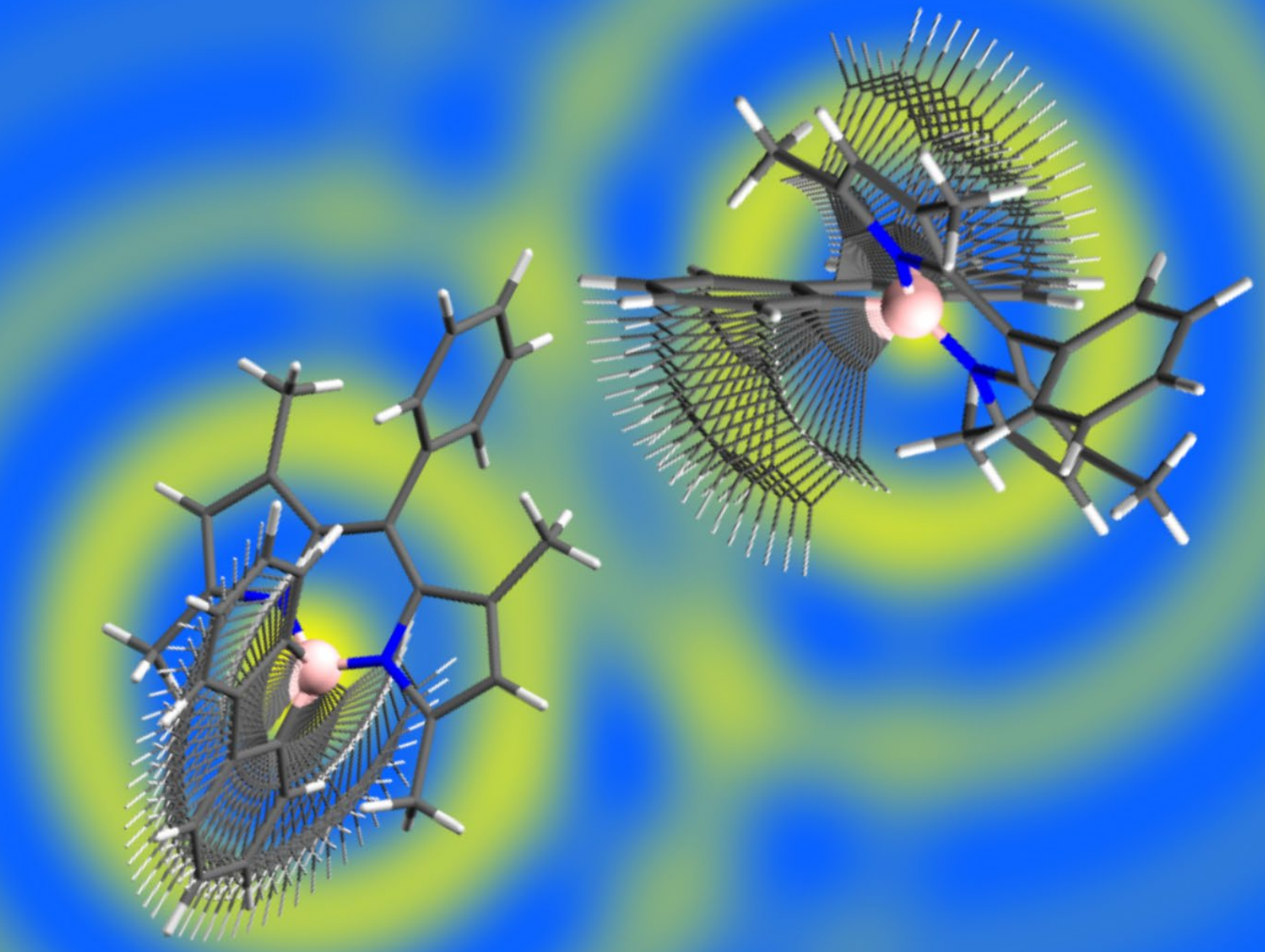

63 Konwersatorium Krystalograficzne

Edycja on-line, 29 VI – 1 VII 2022 r.

Program
Streszczenia komunikatów
Lista uczestników i autorów prac

Organizatorzy:
Komitet Krystalografii PAN
Instytut Niskich Temperatur i Badań Strukturalnych PAN we Wrocławiu
Uniwersytet Kardynała Stefana Wyszyńskiego w Warszawie
Polskie Towarzystwo Krystalograficzne

Sponsorzy:

Komitet Organizacyjny:
Marek Wołcyrz – przewodniczący, Kinga Suwińska, Marek Daszkiewicz - zastępca przewodniczącego, Anna Gągor, Daniel Lis, Vasyl Kinzhybalo, Dorota Kowalska, Tamara Bednarchuk, Piotr Rejnhardt, Dawid Drozdowski

Redakcja:
Marek Wołcyrz, Dorota Kowalska

Wydawca:
Instytut Niskich Temperatur i Badań Strukturalnych PAN, Wrocław
oraz Komitet Krystalografii PAN

ISBN 978-83-939559-8-5

Tematyka Konwersatorium obejmuje badania podstawowe i stosowane dotyczące idealnej i realnej struktury kryształów prowadzone za pomocą promieniowania rentgenowskiego uzyskiwanego zarówno tradycyjnymi metodami jak i w synchrotronach, badania przy użyciu neutronów i elektronów, zagadnienia symetrii, przemian fazowych i wzrostu kryształów, nowe metody badawcze i obliczeniowe oraz wszelkie inne aspekty krystalografii. Konwersatorium stanowi forum wymiany poglądów wszystkich polskich krystalografów.

Ilustracja na okładce: Wizualizacja rodzajów ruchów pomiędzy boracyklem oraz ligandem – z komunikatu **P-40** autorstwa Karoliny Urbanowicz, Pauliny Haliny Marek-Urban, Krzysztofa Woźniaka i Krzysztofa Durki.

PROGRAM KONWERSATORIUM I WARSZTATÓW PTKryst
PROGRAMME OF THE MEETING AND PCA WORKSHOP

Środa, 29 czerwca 2022 r. / Wednesday, June 29, 2022

9:00 – 13:30 **WARSZTATY NAUKOWE PTKryst / PCA WORKSHOP** **W**
Dyfraktometria proszkowa / Powder diffractometry
W. Łasocha, M. Kozieł, M. Oszajca, K. Nowakowska, M. Duda
Wydział Chemii Uniwersytetu Jagiellońskiego, Kraków

14:00 **WALNE ZEBRANIE SPRAWOZDAWCZO-WYBORCZE POLSKIEGO TOWARZYSTWA KRYSTALOGRAFICZNEGO / PCA GENERAL ASSEMBLY MEETING**

Czwartek, 30 czerwca 2022 r. / Thursday, June 30, 2022

9:00 – 9:05 **OTWARCIE KONWERSATORIUM / OPENING CEREMONY**

SESJA PLENARNA / PLENARY SESSION

9:05 – 9:30 Michał L. Chodkiewicz, Roman Gajda, **Krzysztof Woźniak** **O-1**
Department of Chemistry, University of Warsaw
Accurate crystal structure of ice VI from X-ray diffraction with HAR

9:30 – 9:50 **Kinga Jóźwiak**, Aneta Jezierska, Jarosław J. Panek, Andrzej Kochel, Aleksander Filarowski **O-2**
Faculty of Chemistry, University of Wrocław
Short strong hydrogen bond (SSHB) in nitrophthalic acid complexes

9:50 – 10:10 **Emilia Ganczar**, Agata Białońska **O-3**
Faculty of Chemistry, University of Wrocław
Copper(I) coordination compounds with Schiff bases as precursors to host-guest materials

10:10 – 10:30 Tamara J. Bednarchuk, **Katarzyna Helios**, Anna Kędziora, Anna Łukowiak, Michał Małaszczuk, Rafał Wysokiński, Agnieszka Wojciechowska **O-4**
Faculty of Chemistry, Wrocław University of Science and Technology; Institute of Low Temperature and Structure Research, Polish Academy of Sciences, Wrocław; Department of Microbiology, Faculty of Biological Sciences, University of Wrocław
Comprehensive studies on new isomorphous Co(II) and Zn(II) complexes with the 5-nitroorotate ligand

10:30 – 10:50	**Marzena Nowacka,** Elżbieta Nowak, Marcin Nowotny Laboratory of Protein Structure, International Institute of Molecular and Cell Biology, Warsaw **Structures of substrate complexes of foamy viral protease-reverse transcriptase**	**O-5**
10:50 – 11:00	**Piotr Rejnhardt** Institute of Low Temperature and Structure Research, PAS, Wrocław **The Polish Young Crystallographers (PYC) project**	**O-6**
11:00 – 11:30	**PRZERWA / BREAK**	
11:30 – 11:45	**Helena Butkiewicz,** Sandra Kosiorek, Volodymyr Sashuk, Oksana Danylyuk Institute of Physical Chemistry Polish Academy of Sciences, Warsaw **Crystal studies of the host-guest complexes of carboxylated pillar[n]arenes**	**O-7**
11:45 – 12:05	**Maura Malińska** Department of Chemistry, University of Warsaw **Shape and volume – molecular recognition rules of big calixarene ring**	**O-8**
12:05 – 12:25	**Anna A. Hoser,** Toms Rekis, Anders Ø. Madsen Biological and Chemical Research Centre, Faculty of Chemistry, University of Warsaw; Department of Pharmacy, University of Copenhagen **Dynamics and disorder: on the stability of pyrazinamide polymorphs**	**O-9**
12:25 – 12:40	**Maja Morawiak** Institute of Organic Chemistry, Polish Academy of Sciences, Warsaw **Thioflavin at alkaline pH – new compound and its interesting photophysical properties**	**O-10**
12:40 – 12:55	**Armand Budzianowski**, Jan K. Maurin, Katarzyna Betlejewska-Kielak National Centre for Nuclear Research, Otwock Falsified Medicines and Medical Devices Department, National Medicines Institute, Warsaw: Department of Synthetic Drugs, National Medicines Institute, Warsaw **Behind the scenes of analyses by X-ray techniques while conducting comprehensive characterization of the ketoprofen-β-cyclodextrin inclusion complex**	**O-11**
12:55 – 13:10	**Karol Wydra**, Vasyl Kinzhybalo, Jerzy Lisowski Faculty of Chemistry, University of Wrocław; Institute of Low Temperature and Structure Research, PAS, Wrocław **Tetranuclear lanthanide(III) coordination compounds of chiral 3+3 amine macrocycle**	**O-12**

13:10 – 13:30 **Konrad Dyk,** Vasyl Kinzhybalo, Marek Drozd, Grzegorz Czernel, Wojciech Grudziński, Serhii Butenko, Roman Lytvyn, Yuriy Horak and Daniel M. Kamiński **O-13**

Department of General, Coordination Chemistry and Crystallography, Institute of Chemical Sciences, Maria Curie-Skłodowska University, Lublin; Department of Structure Research, Institute of Low Temperature and Structure Research, Polish Academy of Sciences, Wrocław; Department of Biophysics, University of Life Sciences in Lublin, Lublin; Department of Biophysics, Institute of Physics, Maria Curie-Sklodowska University, Lublin; Department of Organic Chemistry, Ivan Franko National University of Lviv

Role of the molecular conformation in the polymorphism during crystal growth

13:30 – 15:00 **PRZERWA / BREAK**

15:00 – 15:30 **Felix Hennersdorf** **O-14**

Rigaku Europe SE, Neu-Isenburg

Rigaku advances in X-ray and electron crystallography

15:30 – 16:00 **Vernon Smith** **O-15**

Bruker AXS GmbH

Noble X-rays: choosing the correct X-ray wavelength for the best single-crystal structures

16:00 – 16:30 **Kristin Gratz** **O-16**

Malvern Panalytical GmbH, Kassel

New possibilities in XRD analytics with the Empyrean and Aeris system

16:30 – 18:00 **SESJA PLAKATOWA / POSTER SESSION**

Piątek, 1 lipca 2022 r. / Friday, July 1, 2022

9:00 – 10:00 **SESJA PLAKATOWA / POSTER SESSION**

SESJA PLENARNA / PLENARY SESSION

10:00 – 10:25 **Paulina M. Dominiak**, Barbara Gruza, Petr Brázda, Lukáš Palatinus, Maura Malińska, Kunal Kumar Jha, Tomasz Góral, Krzysztof Woźniak **O-17**

Department of Chemistry, University of Warsaw; Institute of Physics of the Czech Academy of Sciences, Prague; CeNT, University of Warsaw

Organic crystal structure refinement from 3D electron diffraction data

10:25 – 10:45 **Irena Jankowska-Sumara**, Marek Paściak, Jae-Hyeon Ko, Andrzej Majchrowski **O-18**

Institute of Physics, Pedagogical University of Cracow; Institute of Physics of the Czech Academy of Sciences, Prague; School of Nano Convergence Technology, Hallym University Chuncheon; Institute of Applied Physics, Military University of Technology, Warsaw

Complexity in the structural phase transition in $Pb(Hf_{0.92}Sn_{0.08})O_3$ single crystals

10:45 – 11:05 **Radosław Strzałka**, Ireneusz Bugański, Janusz Wolny **O-19**

Faculty of Physics and Applied Computer Science, AGH University of Science and Technology, Kraków

Phase transformation in a decagonal AlCuRh quasicrystal related to phason disorder

11:05 – 11:20 **Dawid Drozdowski,** Katarzyna Fedoruk, Mirosław Mączka, Jan K. Zaręba, Dagmara Stefańska, Adam Sieradzki i Anna Gągor **O-20**

Institute of Low Temperature and Structure Research, PAS, Wrocław; Faculty of Chemistry, Wrocław University of Science and Technology

Chlorek ołowiu z kationem metylohydrazoniowym – synteza i właściwości strukturalne warstwowego perowskitu hybrydowego

11:20 – 11:35 **Piotr Salwa,** Tomasz Goryczka, Maciej Zubko **O-21**

Institute of Materials Engineering, University of Silesia in Katowice, Chorzów

Structure evolution of $Ti_{50}Ni_{25}Cu_{25}$ shape memory alloy produced by high-energy ball milling

11:35 – 11:55 **Rafał Łysowski,** Ewelina Ksepko **O-22**

Faculty of Chemistry, Wrocław University of Science and Technology

Analysis of structural changes in Fe-Cu spinel-based oxygen carriers for application in chemical looping combustion process after multiple cycles of oxidation-reduction

11:55 **PRZYZNANIE DYPLOMÓW ZA NAJLEPSZE PREZENTACJE PLAKATOWE - ZAKOŃCZENIE KONWERSATORIUM**

GRANTING DIPLOMAS FOR THE BEST POSTER PRESENTATIONS - CLOSING CEREMONY

REFERATY PLENARNE
ORAL SESSIONS

O-1

ACCURATE CRYSTAL STRUCTURE OF ICE VI FROM X-RAY DIFFRACTION WITH HAR

Michał L. Chodkiewicz, Roman Gajda, Krzysztof Woźniak*

Department of Chemistry, University of Warsaw, Pasteura 1, 02-089 Warszawa, Poland

**e-mail: kwozniak@chem.uw.edu.pl*

Water is an essential chemical compound for living organisms, and twenty of its different crystal solid forms (ices) are known. Still, there are many fundamental problems with these structures such as establishing the correct positions and thermal motions of hydrogen atoms. The list of ice structures is not yet complete as DFT calculations have suggested existence for additional as of yet unknown phases. In many ice structures, neither neutron diffraction nor DFT calculations nor X-ray diffraction methods can easily solve the problem of hydrogen atom disorder or accurately determine their atomic displacement parameters. Here we present accurate crystal structures of H_2O, D_2O and mixed (50%H_2O/50%D_2O) ice VI obtained by Hirshfeld Atom Refinement (HAR)[1] against high pressure single crystal synchrotron and laboratory X-ray diffraction data. It was possible to obtain O-H bond lengths and anisotropic atomic displacement parameters for disordered hydrogen atoms which are in excellent agreement with the corresponding results of single crystal neutron diffraction data. Our results show that Hirshfeld atom refinement against X-ray diffraction data is a tool which can compete with neutron diffraction in detailed studies of polymorphic forms of ice and crystals of other hydrogen rich compounds. As neutron diffraction is relatively expensive, requires larger crystals which might be difficult to obtain, and access to neutron facilities is restricted, cheaper and more accessible X-ray measurements combined with HAR can facilitate the verification of the existing ice polymorphs and the quest for the new ones.

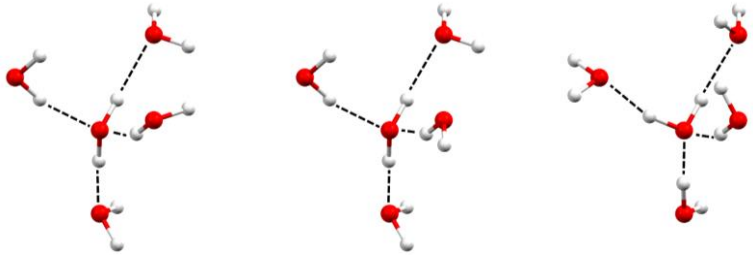

Fig. 1. Examples of water clusters considered.

Acknowledgements: Financial support of this work by the National Science Centre, Poland, through OPUS 21 grant number DEC-2021/41/B/ST4/03010 is gratefully acknowledged. The work was accomplished at the TEAM TECH Core Facility for crystallographic and biophysical research to support the development of medicinal products sponsored by the Foundation for Polish Science (FNP). The synchrotron radiation experiments were performed at the APS (Proposal No. GUP-71134) and DESY (Proposal I-20200083 EC).

References

[1] M. L. Chodkiewicz, R. Gajda, B. Lavina, S. Tkachev, V. B. Prakapenka, P. Dera, K. Woźniak, Accurate crystal structure of ice VI from X-ray diffraction with Hirshfeld Atom Refinement, *IUCRJ*, 2022, Submitted

O-2

SHORT STRONG HYDROGEN BOND (SSHB) IN NITROPHTHALIC ACID COMPLEXES

Kinga Jóźwiak, Aneta Jezierska, Jarosław J. Panek, Andrzej Kochel, Aleksander Filarowski

Faculty of Chemistry, University of Wrocław 14 F. Joliot-Curie str., 50-383 Wrocław, Poland

Nitrophthalic acid epimers are widely used as intermediates for the production of derivatives of these compounds, for instance in manufacturing dyes, plasticizers and pigments. Acid isomers are characterized by compelling catalytic properties, which is confirmed by the use of 4-nitrobenzene-1,2-dicarboxylic acid in the Diels-Alder reaction as a catalyst. As a result, a process was developed compliant with the "Principles of Green Chemistry", replacing the previously used catalysts with less toxic ones. 3-nitrobenzene-1,2-dicarboxylic acid has been applied as a substrate in the synthesis of 3-aminophthalohydrazide (luminol).

Knowledge and research on the influence of non-covalent interactions in the studied systems is extremely important in many fields of science. The intermolecular and intramolecular interactions in 3- and 4-nitrophthalic acid complexes with pyridine were analyzed by quantum-mechanical methods: (Density Functional Theory (DFT), CMPD (Car-Parrinello Molecular Dynamics)) and experimental (IR, Raman spectroscopy and X-ray diffraction) methods. The aim of the research was to present the differences between the structures of the complexes with pyridine resulting from the possibility of creating a different amount, type and strength of hydrogen bonds, the formation of planar or non-planar structures, which are greatly influenced by steric effect. The assignments of vibrational bands of the experimental spectra were made using the Potential Energy Distribution (PED) method. The spectra of the studied compounds were also measured for the deuterated derivatives (OH $\rightarrow$ OD) in order to accurately assign the experimental bands to the bridged hydrogen vibrational modes. Structural modelling of the inter- *vs.* intra- molecular hydrogen bonds equilibrium enabled one to obtain Short Strong Hydrogen Bond in our research.

Complex	HB type		D-H	H···A	D···A	D-H···A
4-nitrophthalic acid+pyridine	N(2) - H(2N) ··· O(2)	intermolecular	0.85(5)	1.85(5)	2.699(5)	176(3)
	O(1) - H(1N) ··· O(3)	intramolecular	1.33(5)	1.12(5)	2.425(4)	164(5)
3-nitrophthalic acid+pyridine	N(2) - H(2N) ··· O(4)	intermolecular	0.93(2)	1.74(2)	2.6592(14)	173(2)
	O(1) - H(1O) ··· O(4)	intramolecular	0.96(2)	1.57(2)	2.5260(13)	176(2)

Table 1. Structural parameters (in Å) for the donor-acceptor (OO) and donor-proton (OH) distances in complexes 3NAP ···Py and 4NAP ···Py (3-nitrophthalic acid with pyridine and 4-nitrophthalic acid with pyridine).

Literature

[1] K. Jóźwiak, A. Jezierska, J. J. Panek, E. A. Goremychkin, P. M. Tolstoy, I. G. Shenderovich, and A. Filarowski, Inter- vs. Intramolecular Hydrogen Bond Patterns and Proton Dynamics in Nitrophthalic Acid Associates, *Molecules* **25**, no. 20 (2020) 4720.

[2] A. Jezierska, K. Jóźwiak, J. J. Panek, A. Kochel, P. M. Tolstoy and A. Filarowski, Inter vs. intramolecular hydrogen bond in complexes of nitrophthalic acids with pyridine – in progress.

O-3

COPPER(I) COORDINATION COMPOUNDS WITH SCHIFF BASES AS PRECURSORS TO HOST-GUEST MATERIALS

Emilia Ganczar, Agata Białońska

Department of Chemistry, University of Wrocław,
14. F. Joliot-Curie, 50-383 Wrocław, Poland

Compounds with the characteristic supramolecular structure of the host−guest type are found in the area of continuous interest of the scientific world. Such compounds are attractive in the context of their physicochemical and structural properties that can be properly designed and modified [1]. Due to the architectures of the host, the host-guest crystal can be divided into two main categories: molecular complexes where convex guests adjust to a concave host, and compounds in which the packing of the host leads to the formations of the empty spaces (channel or sheets) in which guests molecules may be deposited [2]. The presence of channels in the crystal structure is attractive in the context of the exchange of guest molecules, which is used in heterogeneous catalysis, selective molecular separation, gas storage or chemical sensors. Guest particles usually plays an important role in the stabilization of the system[3]. In some cases, desolvation of the system cause huge changes in the crystal structure according to the principle of densest packing [4]. Materials that selectively and reversibly alter the host structure under the influence of guest molecules are called breathing crystals.

An interesting group of compounds are copper(I) coordination compounds with Schiff bases based on 4-amino-1,2,4-triazole. Reported previously copper(I) coordination compound with *N*-[(*E*)-(4-chlorobenzylidene)]-4*H*-1,2,4-triazol-4-amine (4ClPhtrz) has the ability to breathe. This structure is built up of cationic X-shaped units self-assembled in a way allowing formation of characteristic 1D channels occupied by solvent molecules. Desolvation of the system leads to huge reversible reorganization of its structure [5].

During the presentation our studies on breathing host-guest crystals of copper(I) coordination compound will be presented. The studies include the influence of a halogen substituent in a phenyl ring of the ligand on the mechanism of the desorption process. The ability of the system to absorb compounds of various size and shape and containing various functional groups as well as structural changes accompanying sorption – desorption processes and factors which impact the changes. We also show how the competitiveness of various halogen bonds affects the structural and sorption properties.

References

[1] J. L. Steed, J. W. Atwood, Crystal Engineering. In Supramolecular Chemistry, Wiley (2022) 537.
[2] D. J. Cram, J. M. Cram, Container Molecules and Their Guests, *R. Soc. Chem.,* **4** (1997) 1.
[3] C.-P. Li, M. Du, *Chem. Commun.,* **47** (2011) 5958.
[4] S. Kitagawa, R. Kitaura, R. S.-I. Noro, *Angew. Chemie - Int. Ed.*, **43(18)** (2004) 2334.
[5] A. Białońska, K. Drabent, B. Filipowicz, M. Siczek, *CrystEngComm,* **15** (2013) 9859.

O-4

COMPREHENSIVE STUDIES ON NEW ISOMORPHOUS Co(II) AND Zn(II) COMPLEXES WITH THE 5–NITROOROTATE LIGAND

Tamara J. Bednarchuk[a], Katarzyna Helios[b,*], Anna Kędziora[c], Anna Łukowiak[a], Michał Małaszczuk[c], Rafał Wysokiński[b] and Agnieszka Wojciechowska[b]

[a] *Institute of Low Temperature and Structure Research, Polish Academy of Sciences, Okólna 2, 50-422 Wrocław, Poland*
[b] *Faculty of Chemistry, Wrocław University of Science and Technology, Smoluchowskiego 23, 50-370 Wrocław, Poland*
[c] *Department of Microbiology, Faculty of Biological Sciences, University of Wrocław, Przybyszewskiego 63, 51-148 Wrocław, Poland*

**e-mail:katarzyna.helios@pwr.edu.pl*

5-Nitroorotic acid (5-NO_2H_3Or) is a synthetic derivative of naturally occurring orotic acid (6-carboxyuracil, vitamin B_{13}). In coordination chemistry, orotic acid is an interesting multidentate ligand, since coordination to metal ions may occur through the two deprotonated pyrimidine nitrogen atoms, the two carbonyl oxygen atoms, and also the two carboxylate oxygen atoms. As an extension of our earlier studies on metal complexes with orotic acid we have focused our attention on the coordination properties of the 5-nitroorotate ligand [1,2]. Here, I will present the results of our recently published work [1], by Helios *et al.* https://doi.org/10.1016/j.poly.2022.115830.

We have prepared and investigated two novel Co(II) and Zn(II) complexes with this ligand: tetraaqua(5-nitroorotato)cobalt(II), [Co(5-NO_2HOr)(H_2O)$_4$] (**1**) and tetraaqua(5-nitroorotato)zinc(II), [Zn(5-NO_2HOr)(H_2O)$_4$] (**2**), Fig.1.

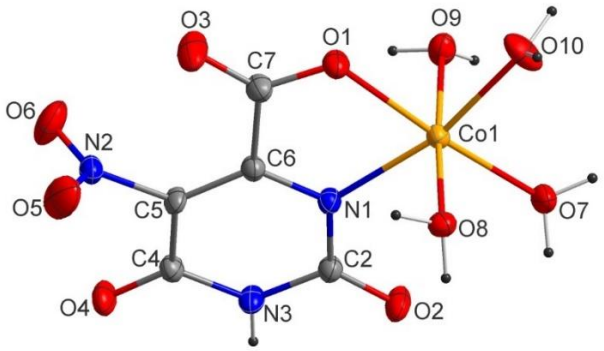

Fig. 1. The molecular structure of compounds (**1**) and (**2**) with the atom-numbering scheme (complex (**1**) is shown as an example).

Single crystal X-ray diffraction analysis has revealed that the crystals of (**1**) and (**2**) are isomorphous, both crystallize in the orthorhombic space group *Pca*2_1, Z=4; a=19.024(5), b=5.426(3), c=10.393(4) Å for (**1**) and a=18.990(5), b=5.425(3), c=10.418(4) Å for (**2**). Each metal ion is chelated by the carboxylate oxygen (O1) and the deprotonated nitrogen (N1) atoms of the 5-nitroorotate ligand. Four water molecules complete the distorted octahedral coordination sphere around the metal center with an

elongated axial M–O bonds. It is interesting that the pattern of hydrogen bonding in the crystals of (**1**) and (**2**) is somewhat different than that reported for similar metal-orotate complexes. This can be caused by the fact that no water molecules exist in the lattice of (**1**) and (**2**). Furthermore, the presence of nitro substituent in the 5-nitroorotate ligand may also contribute to a rearrangement of the hydrogen bond system (as the nitro group exhibits both the negative inductive and resonance effects). The O–H···O and N–H···O hydrogen bonds are the dominating intermolecular interactions in the crystals of (**1**) and (**2**). In addition, weak C–O···π and N–O···π intermolecular interactions promote the crystal cohesion. Close intermolecular interactions in the title compounds have been visualized using Hirshfeld surface analysis (Fig. 2).

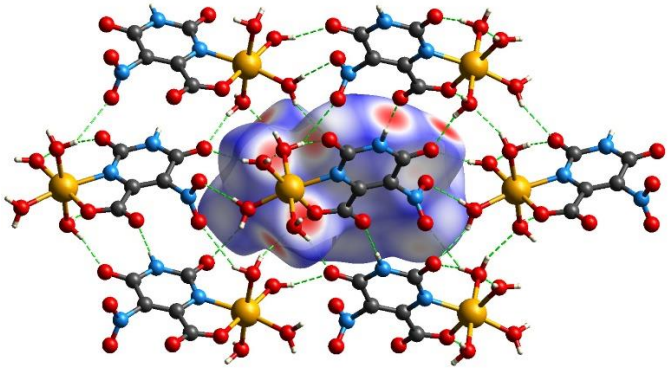

Fig. 2. Crystal-packing diagram for (**1**) with the Hirshfeld surface for the central molecule mapped with d_{norm}. The O–H···O and N–H···O hydrogen bonds are indicated by green dashed lines.

The title complexes have been characterized by FT-IR and Raman spectroscopy. Detailed interpretation of the vibrational spectra has been made on the basis of the B3LYP-calculated potential energy distribution (PED). The presented band assignment will be very helpful for the interpretation of the vibrational spectra of other metal complexes with the 5-nitroorotate ligand.

The electronic spectra (UV-Vis-NIR) and photoluminescent properties of (**1**), (**2**) and K(5-NO_2H_2Or) (**3**) have been investigated. The electronic spectrum of (**1**), in the Vis and NIR range, is characteristic of the high-spin six-coordinate Co(II) ion. The title complexes exhibit the solid-state photoluminescence at around 452 nm (**1**) and 480 nm (**2**) (λ_{ex}=335 nm). These broad emission bands can be assigned to the π*→π and/or π*→n ligand transitions.

In addition, (**1**), (**2**) and (**3**) have been studied *in vitro* for their activity against selected bacteria: one Gram-positive (*S. aureus*) and two Gram-negative (*E. coli*, *P. aeruginosa*), and one yeast (*C. albicans*). The Co(II) complex (**1**) is more effective than the other two compounds.

Literature

[1] K. Helios, T. J. Bednarchuk, R. Wysokiński, M. Duczmal, A. Wojciechowska, A. Łukowiak, A. Kędziora, M. Małaszczuk, D. Michalska, *Polyhedron* (2022) 115830.
[2] K. Helios, M. Duczmal, A. Pietraszko, D. Michalska, *Polyhedron*, **49** (2013) 259.

O-5

STRUCTURES OF SUBSTRATE COMPLEXES OF FOAMY VIRAL PROTEASE-REVERSE TRANSCRIPTASE

Marzena Nowacka, Elżbieta Nowak, Marcin Nowotny

Laboratory of Protein Structure, International Institute of Molecular and Cell Biology, Warsaw, Poland

Reverse transcriptases (RTs) are intriguing enzymes converting ssRNA to dsDNA [1]. Their activity is essential for the replication of retroviruses, which are divided into two subfamilies: Orthoretrovirinae (OV) and Spumaretrovirinae. The latter family is much more ancient and comprises five genera. Foamy viruses (FVs) have many characteristics that set them apart from OVs, including differences in the proliferation cycle [2]. Another unique feature of FVs is that their RTs contain N-terminal protease (PR) domains, which are not present in orthoretroviral enzymes [3].

For FVs, nuclear magnetic resonance (NMR) structures for the isolated prototype FV (PFV) RH domain and simian FV from macaque (SFVmcy, formerly SFVmac) PR domain have been solved [4, 5]. However, no structural information for full-length foamy viral PR-RT interacting with nucleic substrates have been reported so far.

In our study, we present crystal and cryo-electron microscopy structures of marmoset foamy virus (MFV) PR-RT. These structures represent the mode of binding of RNA/DNA and dsDNA substrates. Moreover, unexpectedly, the structures and biochemical data revealed that foamy viral PR-RTs have ability to change their oligomeric state depending on the type of nucleic acid bound. FV RTs adopt monomeric configuration in the presence of RNA/DNA hybrid and an asymmetric dimer arrangement which we observed in the presence of dsDNA.

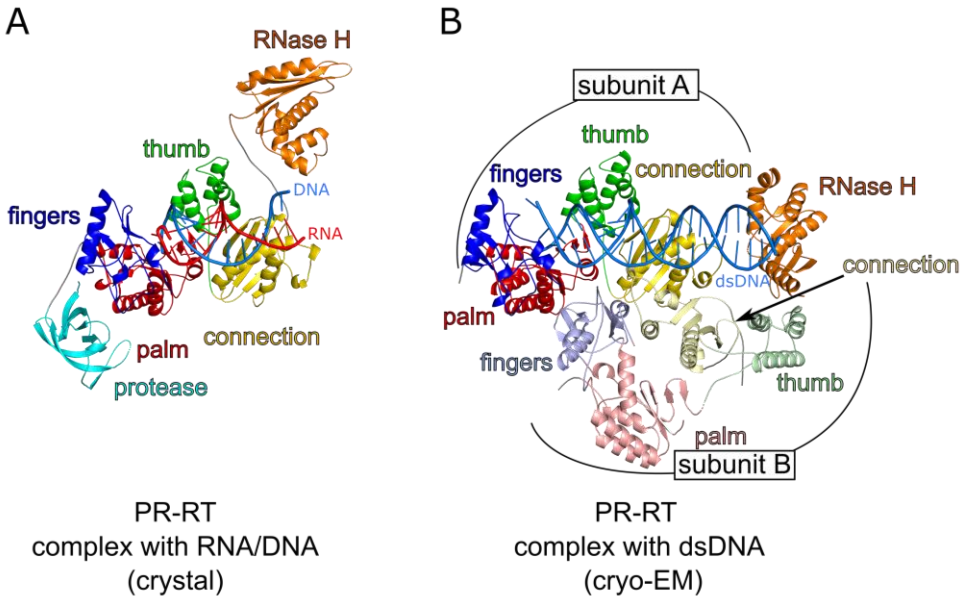

Fig. 1. Monomeric and dimeric structure of foamy viral PR-RT.

O-5

We further corroborated the monomer-dimer switch using biophysical methods. Finally, through advanced biochemical experiments we determined the mode of interaction between the mobile RNase H domain of foamy viral PR-RT with its RNA/DNA substrate. In summary, our data show a novel mode of action of an RT.

References

[1] S. F. J. L. Grice, M. Nowotny, Reverse Transcriptases, *Nucleic Acid Polymerases*. *Nucleic Acids and Molecular Biology*, **30** (2014) 189–214.

[2] A. Rethwilm, J. Bodem, Evolution of foamy viruses: the most ancient of all retroviruses. *Viruses*, **5** (2013) 2349–74.

[3] A. Schneider, D. Peter, J. Schmitt, B. Leo, F. Richter, P. Rosch, B. M. Wohrl, M. J. Hartl, Structural requirements for enzymatic activities of foamy virus protease-reverse transcriptase. *Proteins-Structure Function and Bioinformatics*, **82** (2014) 375–385.

[4] M. J. Hartl, B. M. Wohrl, P. Rosch, K. Schweimer, The solution structure of the simian foamy virus protease reveals a monomeric protein. *Journal of Molecular Biology*, **381** (2008) 141–149.

[5] B. Leo, K. Schweimer, P. Rosch, M. J. Hartl, B. M. Wohrl, The solution structure of the prototype foamy virus RNase H domain indicates an important role of the basic loop in substrate binding. *Retrovirology*, **9** (2012) 73.

O-6

THE POLISH YOUNG CRYSTALLOGRAPHERS (PYC) PROJECT

Piotr Rejnhardt

Institute of Low Temperature and Structure Research, Polish Academy of Sciences, ul. Okólna 2, 50-422 Wrocław, Poland

e-mail: p.rejnhardt@intibs.pl

The main aim of this project is to establish a section of Polish Young Crystallographers as an adhering body of Polish Crystallographic Association. The similar groups work in some of the European countries, such as Great Britain, Germany or Italy *etc*. The purpose of the PYC is to create a supportive network for young crystallographers starting out in crystallography. The PYC will offer the opportunity to exchange ideas, solve problems or promote knowledge in all areas related to crystallography. PYC will encourage interactions not only between younger scientists in the field but also with more established crystallographers and structural scientists.

The set aims for Polish Young Crystallographers are:

- Organizing first annual Polish Crystallography School for young scientists and students interested in the areas related to crystallography. It will be 3-4 days of intense crystallography learning from our domestic (and maybe in the future foreign) experts.
- Organizing one day conference as a satellite workshop to the Polish Crystallographic Meeting. It will be the opportunity for young scientists to show-case their work in the form of talks and posters in more “light” atmosphere independent from more established crystallographic community.
- Providing contact with other domestic and international young scientists organisations.
- Promoting crystallography at the Universities and in the social media (Facebook, Twitter, YouTube, *etc*).
- Cooperation with members of Polish Crystallographic Association and Crystallography Committee of the Polish Academy of Sciences.

Membership of the PYC is open to undergraduate students, graduate students and scientists who graduate within the previous five years. First of all, we need people who want to participate in the creation of our new section of Polish Young Crystallographers. The first tasks to be performed are the creation of the constitution, committee positions, financial status (annual payments from Polish Crystallographic Association, donations, grants or sponsorships), web and social pages, and logo. If you would like to join us please send me a message p.rejnhardt@intibs.pl or call me 71 3954 297.

O-7

CRYSTAL STUDIES OF THE HOST-GUEST COMPLEXES OF CARBOXYLATED PILLAR[N]ARENES

Helena Butkiewicz, Sandra Kosiorek, Volodymyr Sashuk, Oksana Danylyuk

Institute of Physical Chemistry Polish Academy of Sciences, Warsaw, Poland

Carboxylated pillar[n]arenes (n = 5, 6; CPA5, CPA6) are highly symmetrical pillar-shaped macrocycles, composed of hydroquinone units linked by methylene bridges at the para-positions, modified by ten carboxylic acid groups. Their hydrophobic, electron-rich cavities combined with water solubility make them great candidates as host molecules for various electron deficient guest or other neutral molecules. Moreover, carboxyl groups, that can take part in proton transfer, are located at the terminal positions of flexible aliphatic chains, so they can adjust to the size and shape of guests.

In 2015 Danylyuk described crystal self-assemby of CPA5 in its complex with ethanol molecules [1]. The chains of pillar[5]arenes are connected via cyclic carboxylic-carboxylic hydrogen bonds as main supramolecular motif. Introduction of tertacaine guest reorganized the formation of hydrogen bonds. Inspired by this result, we decided to investigate how guest molecules, decorated with different functional groups or metal cation, affect on the self-assembly of the host.

Here we want to present our results on the X-ray structures of CPA5 and CPA6 in the form of its host-guest complexes with viologens, guanidine and amidine compounds and metal cations. Our study on the CPA5-viologens complexes shows that the main chain motif is dictated by strong carboxylic-carboxylate hydrogen bonds [2]. Altering the guest into the amidine or guanidine molecules changes main synthon into amidinium-carboxyl/ate and guanidinium-carboxyl/ate hydrogen bonds [3]. The addition of the metal cations results in formation of coordination polymers [4]. In a broader perspective our results may have potential applications in drug delivery and molecular recognition systems.

References

[1] O. Danylyuk, V. Sashuk, *CrystEngComm*, **17** (2015) 719.
[2] H. Butkiewicz, S. Kosiorek, V. Sashuk, O. Danylyuk, *CrystEngComm*, **23** (2021) 1075.
[3] H. Butkiewicz, S. Kosiorek, V. Sashuk, M. Zimnicka, O. Danylyuk, *Cryst. Growth Des*. **22** (2022) 2854.
[4] H. Buktiewicz, V. Sashuk, O. Danylyuk, *CrystEngComm*, **23** (2021) 3265.

O-8

SHAPE AND VOLUME – MOLECULAR RECOGNITION RULES OF BIG CALIXARENE RING

Maura Malińska

Wydział Chemii, Uniwersytet Warszawski, ul. Pasteura 1, 02-093 Warszawa

Calixarenes are vase-shaped host molecules that can form complexes with one or more guest molecules. To establish molecular recognition rules, the hosts p-tert-butylcalix[6]arene [1] (TBC6) and p-tert-butylcalix[8]arene [2] (TBC8) were crystallized with different guest molecules (cyclohexane, anisole, heptane, toluene, benzene, methyl acetate, ethyl acetate, dichloromethane, chloroform, tetrahydrofuran, acetonitrile, dimethyl sulfoxide, dimethylformamide, and pyridine) and the obtained structures were characterized by X-ray diffraction. With most solvents, 1:1 and/or 1:3 TBC6-guest complexes were formed, although other stoichiometries were also observed with small guest molecules, and crystallization from ethyl acetate produced the unsolvated form. A common structural feature of most TBC(4/6/8)-guest structures is off-set bilayer packing, which is built by the strongest dimers between TBC6 which have energies lower than −110 kJ mol^{-1}. This structural feature was also present in pure TBC6 crystal structure. The incorporation of solvent molecules with volumes <100 $Å^3$ leads to the separation of the off-set bilayers, whereas larger solvent molecules prevent the formation of this layer in the crystal structures. Even though the formation of a structural motif with the tert-butyl group in the TBC6 cavity is energetically favoured, its slow rate of formation possibly limits the formation of pure TBC6 crystals. Therefore, the crystal structure of a high macrocycle-to-solvent ratio system can transform into a more thermodynamically stable crystal structure with a lower ratio through solvent evaporation and recrystallization [3]. The calculated fill percentage of the TBC6 cavity was ∼55% for apolar guests and significantly lower for polar solvents, indicating that polar molecules can bind to apolar cavities with significantly lower packing coefficients. All guest molecules that occupy the TBC6 cavity interact with the host with an energy close to −50 kJ mol^{-1}; therefore, this property does not determine molecular recognition. The ratio between the apolar surface area and the volume was used to predict the formation of inclusion versus exclusion complexes, with inclusion complexes observed at ratios <40. These findings allow the binding of potential guest molecules to be predicted and a suitable crystal packing for the designed properties to be obtained.

Literature

[1] M. Malinska, *IUCrJ*, **9** (2022) 55.
[2] A. Kieliszek and M. Malinska, *Cryst. Growth Des.*, **21** (2021) 6862.
[3] M. Malinska, *Cryst. Growth Des.*, **21** (2021) 1103.

O-9

DYNAMICS AND DISORDER: ON THE STABILITY OF PYRAZINAMIDE POLYMORPHS

Anna A. Hoser[a], **Toms Rekis**[b], **Anders Ø. Madsen**[b]

[a] *Biological and Chemical Research Centre, Faculty of Chemistry, University of Warsaw, Żwirki i Wigury 101, 02-089 Warszawa, Poland*
[b] *Department of Pharmacy, University of Copenhagen, Universitetsparken 2, Copenhagen 2100, Denmark*

In this contribution, we focus on structures and the relative stability of four pyrazinamide polymorphs. We present new single crystal X-ray diffraction data collected for all forms at 10 K and 122 K. By combining periodic *ab-initio* DFT calculations with normal mode refinement against X-ray diffraction data, we calculate both enthalpic and entropic contributions to the free energy of all polymorphs. Based on the estimated free energies, we anticipate the stability order of the polymorphs at a given temperature and predict the phase transition temperatures. We conclude that α and γ forms have higher vibrational entropy than that of β and δ and therefore they are significantly more stabilized at higher temperatures. Due to the entropy, which arises from the disorder in γ form, it overcomes form α and is the most stable form at temperatures above c.a. 500 K. Our findings are in qualitative agreement with the experimental calorimetry results.

O-10

THIOFLAVIN T AT ALKALINE pH – NEW COMPOUND AND HIS INTERESTING PHOTOPHYSICAL PROPERTIES.

Maja Morawiak

Institute of Organic Chemistry, Polish Academy of Sciences, ul. Kasprzaka 44/52, 01-224 Warsaw, Poland

We know two types of thioflavins: Thiofavin T and Thioflavin S. These dyes have been used since 1989 above all to investigate amyloid formation [1]. Thioflavin T (Basic Yellow 1, Methylene yellow, CI 49005, or ThT) is a benzothiazole salt obtained by the methylation of dehydrothiotoluidine with methanol in the presence of hydrochloric acid [2].

Thioflavin T, used as a fluorescent marker for amyloid fibers, most often works in a natural [3] or in slightly acidic environment [4]. The question is, will it work just as well at alkaline pH? It turns out that this dye undergoes hydrolysis in an alkaline environment to form disulfide – scheme 1.

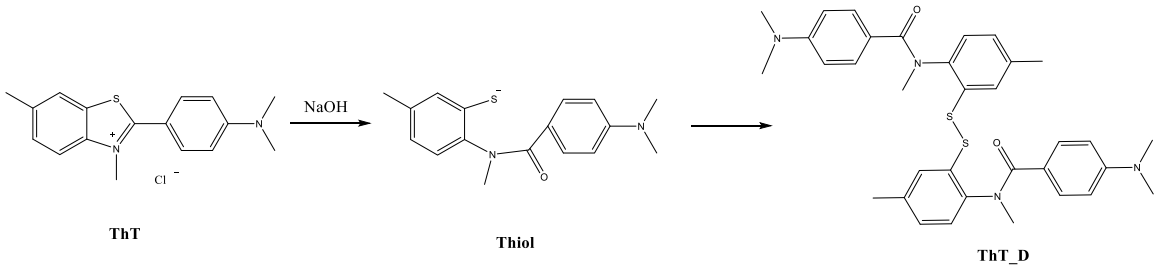

Scheme 1**.** Synthesis of bis-[2(4-dimethylamino-N-methyl-benzamido)-5-methyl-phenyl]-disulfide.

The X-ray analysis of obtained disulfide confirmed his assumed molecular structure as well as the synthesis pathway. The structure and conformation of the molecule of ThT_D in the crystal is shown in Figure 1.

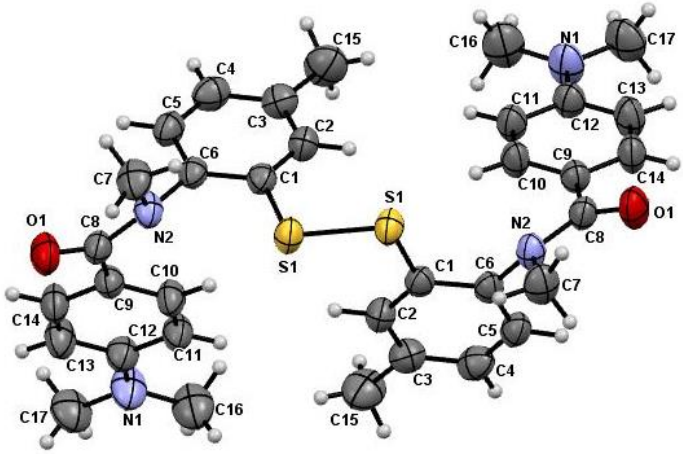

Fig. 1. A view of the molecule in conformation observed in crystal with the atom labelling scheme. Displacement ellipsoids are drawn at the 50% probability level.

The asymmetric unit contains only half of the disulfide molecule, the two halves of the molecule are related by the twofold axis [S1–S1a (a = 1–x , y, ½–z) disulfide single bond amounts 2.0315(12) Å]. The bond lengths and angles are within the normal

ranges and are comparable to those found in CCDC base [5, 6]. The disulfide creates intra- and inter-molecular hydrogen bonds that stabilize the entire system. Details of the hydrogen bonds are given in Table 1.

Table 1. Hydrogen bond distances (Å) and angles (°)

D-H ···A	D-H	H···A	D···A	Angle	Symmetry codes
C7–H7B···S1	0.96	2.90	3.377(3)	112.0	
C2–H2···S1	0.93	2.71	3.223(3)	116.0	[-x + 1, -y, -z + 1/2]
C5–H5···O1	0.93	2.49	3.204(3)	134.2	[-x + 3/2, y – 1/2, -z + 1/2]
C17–H17C···O1	0.96	2.55	3.324(4)	137.9	[x , y – 1, z]

To accomplish the description of the supramolecular connectivity in the crystal structure, a Hirshfeld surface analysis was realized. Maps of the Hirshfeld surface, shape index and curvedness were generated using the *CrystalExplorer 3.1* program [7].

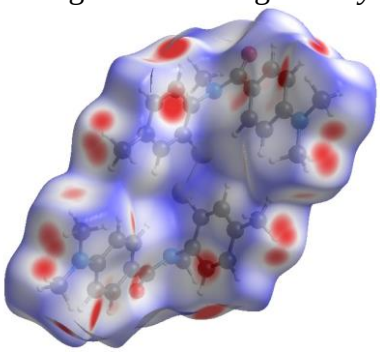

Fig. 2. Hirshfeld surface of the molecule ThT_D mapped with normalized contact distance (d_{norm}).

The obtained disulfide was subjected to absorption and fluorescence studies in order to learn about the spectroscopic properties of the new compound.

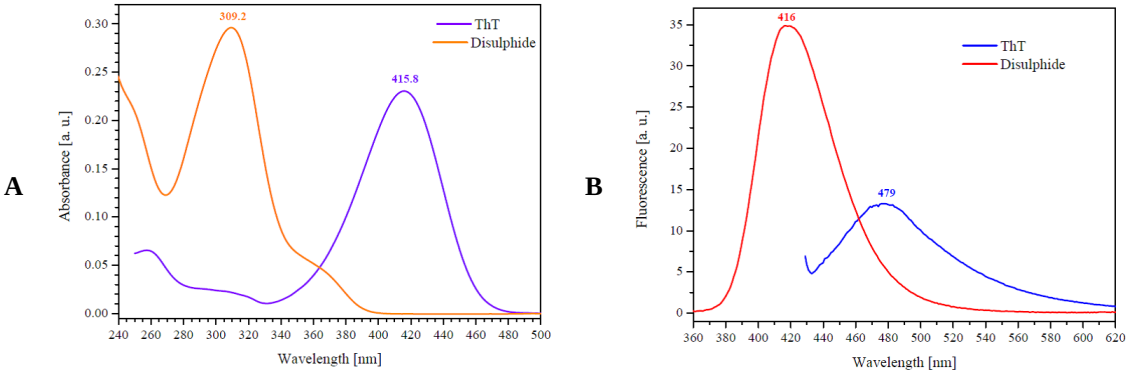

Fig. 3. Spectra of A) absorption and B) fluorescence of the obtained disulfide compared to the ThT spectra.

References

[1] K. Gade Malmos, L.M. Blancas-Mejia, B. Weber, J. Buchner, M. Ramirez-Alvarado, H. Naiki, D. Otzen, *Amyloid*, **24** (2017) 1.
[2] Y. Stremski, S. Statkova-Abeghe, A. Ivanova, P. Angelov, I. Ivanov, *Materials, Methods & Technologies*, **13** (2019) 118.
[3] S. Xu, Q. Li, J. Xiang, Q. Yang, H. Sun, A. Guan, L. Wang, Y. Liu, L. Yu, Y. Shi, H. Chen, Y. Tang, *Scientific Reports*, **6** (2016) 24793.
[4] F. Zsila, *Int. J. Biol. Mac.*, **72** (2015) 1034.
[5] L. Recané, V. Tralić-Kulenović, Z. Mihalić, G. Pavlović, G. Karminski-Zamola, *Tetrahedron*, **64** (2008) 11594.
[6] J.H. Goh, H.-K. Fun, M. Babu, B. Kalluraya, *Acta Cryst*. **E66** (2010) o292.
[7] M.J. Turner, J.J. McKinnon, S.K. Wolff, D.J. Grimwood, P.R. Spackman, D. Jayatilaka, M.A. Spackman, CrystalExplorer17.5, 2017.

O-11

BEHIND THE SCENES OF ANALYSES BY X-RAY TECHNIQUES WHILE CONDUCTING COMPREHENSIVE CHARACTERIZATION OF THE KETOPROFEN-β-CYCLODEXTRIN INCLUSION COMPLEX

Armand Budzianowski[1], Jan K. Maurin[1,2], Katarzyna Betlejewska-Kielak[3]

[1] National Centre for Nuclear Research, A. Sołtana 7, 05-400 Otwock, Poland
Armand.Budzianowski@ncbj.gov.pl
[2] Falsified Medicines and Medical Devices Department, National Medicines Institute, Chełmska 30/34, 00-725 Warsaw, Poland
j.maurin@nil.gov.pl
[3] Department of Synthetic Drugs, National Medicines Institute, Chełmska 30/34, 00-725 Warsaw, Poland
k.kielak@nil.gov.pl

The Ketoprofen-β-Cyclodextrin inclusion complex crystallized in the monoclinic system in the $P2_1$ space group [1]. The unit cell dimensions are: a=15.1158(3) Å b=32.3308(7) Å c=15.5546(2) Å, β=101.966(2) °, V=7436.4(2) Å^3. The *Vive la Différence* (VLD) cyclic phasing algorithm allowed solving of this crystal structure. For this purpose, the SIR 2014 (Semi-Invariants Representation) software was used to structure an ab-initio crystal structure determination of macromolecules [2]. The structure was refined using ShelXL software [3]. The X-Seed [4] and ShelXle [5] programs were used for structure visualization during the refinement process to rename and sort the order of atoms. The structure contains more than 200 non-hydrogen atoms and more than 200 Hydrogen atoms in an independent part of the unit cell. Although computers are faster and faster, there was a challenge connected to time-consuming to make the refinement with patience.

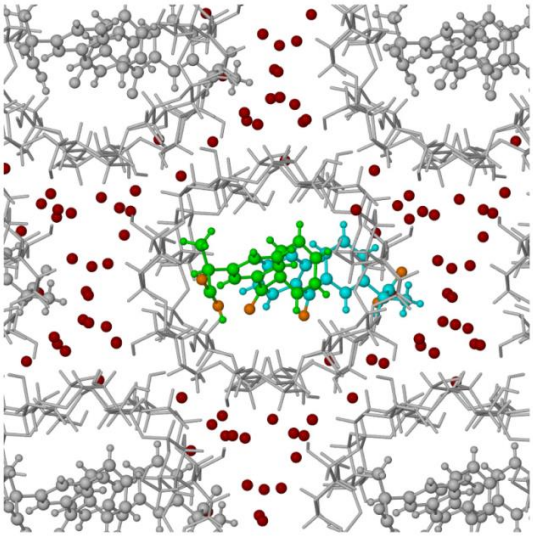

During this presentation, we will remind selected leads connected to the diffraction techniques we used in this work [1].

For the single-crystal structure that contains water molecules in the crystal structure, there are three approaches during refinement: use a larger number of isotropic oxygen atoms with partial occupation for water molecules; use a smaller number of oxygen atoms with anisotropic displacement parameters, or use a PLATON SQUEEZE procedure to omit disordered molecules of a solvent with volume up 30%. The second technique is described in Supplementary Materials [1] according to „SHELXL-93 A Program for the Refinement of Crystal Structures" and „User guide to crystal structure refinement with SHELXL", both by George Sheldrick.

O-11

Literatura
[1] K. Betlejewska-Kielak, E. Bednarek, A. Budzianowski, K. Michalska, J. K. Maurin, *Molecules*, **26(13)** (2021) 4089. DOI: 10.3390/molecules26134089.
[2] M.C. Burla, R. Caliandro, M. Camalli, B. Carrozzini, G.L. Cascarano, L. de Caro, C. Giacovazzo, G. Polidori, R. Spagna, *J. Appl. Cryst.*, **38** (2005) 381–388.
[3] G.M. Sheldrick, *Acta Cryst. C*, **71** (2015) 3–8.
[4] L.J. Barbour, *J. Supramol. Chem.*, **1** (2001) 189–191.
[5] C.B. Hübschle, G.M. Sheldrick, B. Dittrich, *J. Appl. Cryst.*, **44** (2011) 1281–1284.

O-12

TETRANUCLEAR LANTHANIDE(III) COORDINATION COMPOUNDS OF CHIRAL 3+3 AMINE MACROCYCLE

Karol Wydra[a], Vasyl Kinzhybalo[b], Jerzy Lisowski[a]

[a] *Faculty of Chemistry University of Wrocław, ul. F. Joliot-Curie 14, 50-383 Wrocław*
[b] *Institute of Low Temperature and Structural Research, ul. Okólna 2, 50-422 Wrocław*

Polynuclear coordination compounds containing carbonate-bridged lanthanide(III) ions (Ln^{III}) have drawn attention thanks to their diverse structural motifs and potentially applicable properties, including luminescence, catalysis, molecular magnetism, and medical diagnostics [1]. However, the formation of such polynuclear species is limited due to the poor complexing ability and flexible coordination sphere of Ln^{III} cations as well as various possible binding modes of carbonate ions. The polychelate or macrocyclic ligand may thus be utilized to facilitate and enhance carbonate-bridged lanthanide cluster architecture for the desired application. It is worth mentioning, that accommodation of several Ln^{III} ions close together in the cavity of suitable chiral macrocycles may result in polynuclear complexes with increased kinetic and thermodynamic stability as well as new interesting physicochemical features [2].

Here we describe the synthesis and characterization of novel series of $[Ln_4(H\mathbf{L}^{\boldsymbol{R}})_2(CO_3)_2(NO_3)_2(H_2O)_4](NO_3)_2$ coordination compounds (Ln^{III} = Sm^{III}, Eu^{III}, or Gd^{III}) with homochiral 3+3 amine macrocycle (Fig. 1) [3]. The X-ray crystal structures of these molecular species reveal the planar $Ln_4(CO_3)_2$ cluster bounded between two macrocyclic $H\mathbf{L}^{2-}$ units with highly folded conformation (Fig. 1). In the clusters each of the carbonate bridges connects three Ln^{III} ions in an interesting bis(monodentate)-bidentate (μ_3-η^1:η^1:η^2) coordination mode. The Ln^{III} ions are either eight- or nine-coordinate and are accommodated in the N_2O_2 or N_3O_3 pockets of the bis-deprotonated macrocycle $H\mathbf{L}^{2-}$, respectively. Finally, the comprehensive study was complemented by solution NMR characterization allowing for a deeper understanding of the chemical nature of the obtained coordination compounds.

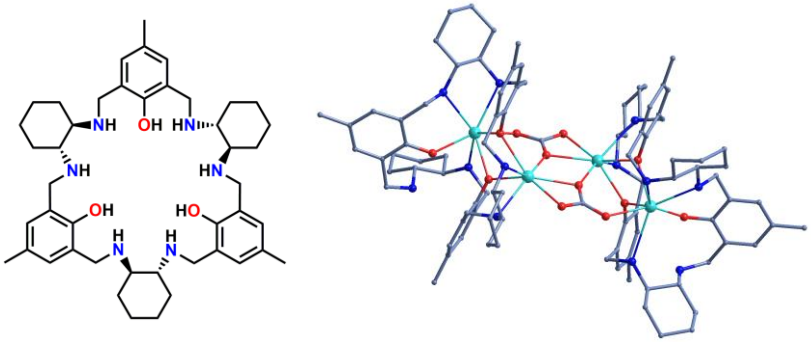

Fig. 1 (Left) The structure of macrocycle $H_3\mathbf{L}^{\mathbf{R}}$. (Right) The X-ray crystal structure of $[Eu_4(H\mathbf{L}^{\boldsymbol{R}})_2(CO_3)_2(NO_3)_2(H_2O)_4](NO_3)_2$ coordination compound (hydrogen atoms, counteranions, solvents molecules and terminal ligands are omitted for simplicity).

Literature

[1] P. Bag *et al.*, *Dalton Trans.*, **41** (2012) 3414.
[2] A. Gerus, K. Ślepokura, J. Lisowski, *Polyhedron*, **170** (2019) 115.
[3] K. Wydra, M. J. Kobyłka, T. Lis, K. Ślepokura, J. Lisowski, *Eur. J. Inorg. Chem.*, **21** (2020) 2096.

O-13

ROLE OF THE MOLECULAR CONFORMATION ON THE POLYMORPHISM DURING CRYSTAL GROWTH

Konrad Dyk[1], Vasyl Kinzhybalo[2], Marek Drozd[2], Grzegorz Czernel[3], Wojciech Grudziński[4], Serhii Butenko[5], Roman Lytvyn[5], Yuriy Horak[5], Miłosz Siczek[6] and Daniel M. Kamiński[1]

[1] Department of General, Coordination Chemistry and Crystallography, Institute of Chemical Sciences, Maria Curie-Skłodowska University, Marii Curie-Sklodowskiej 3 sq., 20-031 Lublin, Poland
[2] Department of Structure Research, Institute of Low Temperature and Structure Research, Polish Academy of Sciences, Okólna 2 str., 50-422 Wrocław, Poland
[3] Department of Biophysics, University of Life Sciences in Lublin, Akademicka 13 str., 20-950 Lublin, Poland
[4] Department of Biophysics, Institute of Physics, Maria Curie-Sklodowska University, Marii Curie-Sklodowskiej 1 sqr., 20-031 Lublin, Poland
[5] Department of Organic Chemistry, Ivan Franko National University of Lviv, 6 Kyryla I Mefidiya Str., Lviv 79005, Ukraine
[6] Department of Chemistry, University of Wrocław, 14 F. Joliot-Curie, 50-383 Wrocław, Poland

The fact that the polymorphic outcome of crystallization is the result of the interplay between relative thermodynamic stability and nucleation kinetics is well known. In this presentation, we present the synthesis of the new compound 2,5-bis(3-bromophenyl)furan (**MBPF**), for which we obtained three polymorphic structures. The studies included: structural studies of three polymorphic structures of this compound, UV-Vis spectrophotometry, circular dichroism spectroscopy studies, and theoretical approaches. The most important experimental variable in this work has been found to affect which polymorph crystallizes preferentially is the solvent. For **MBPF**, it is shown how a significantly metastable polymorph can be obtained by choosing a solvent in which nucleation of the stable form is sufficiently hindered. It is also known that the system undergoes a thermal transition of polymorphs that have been characterized by the Powder X-Ray Diffraction and differential scanning calorimetry. We have characterized the thermotropic transition of the compound under study. It was shown that the metastable polymorphs occur at temperatures close to the melting point during heating, therefore the Gibbs free energies should be similar in this temperature range. In this work, we have also unmasked the interesting influence of the surface of crystal substrate preferred crystal growth during crystallization. This work proves the importance of combining theoretical methods with experimental data to fully understand the behavior of the studied polymorphs and their correlations.

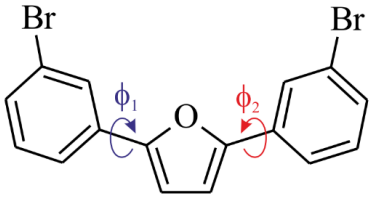

Fig. 1. Schematic of **MBPF** molecule with marked rotation angles ϕ_1 and ϕ_2 considered in this study. Scheme presents conformation where both angles are 0.

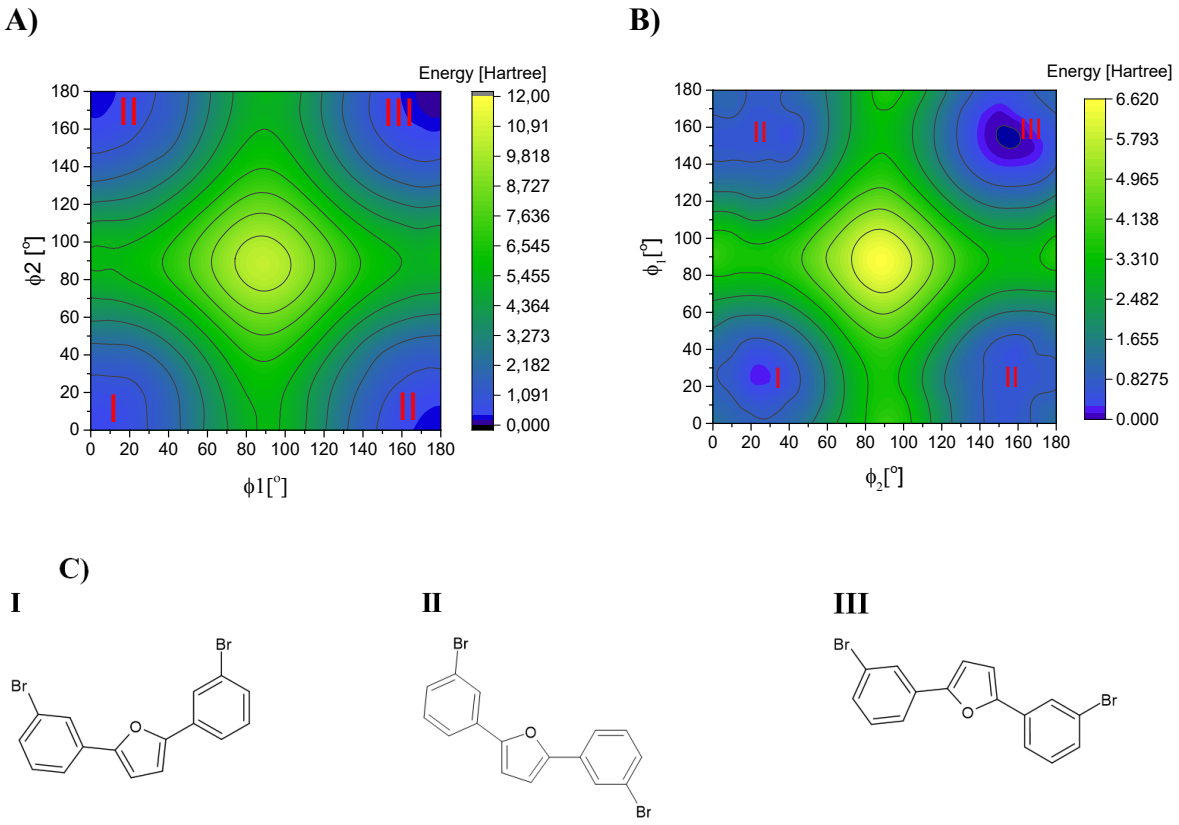

Fig. 2. Maps of the calculated energy of **MBPF** molecules as a function of the rotation angles $\phi_1$and ϕ_2. **A)** Map calculated with DFT B3LYP method; **B)** Map calculated with MP2 method; **C) MBPF** conformations corresponding to energy minima. For simplicity, the conformations are related to the position of the bromine atoms with respect to the oxygen in the furan ring. In this way, conformation **I** corresponds to both a flat as well as ~30° rotated conformation.

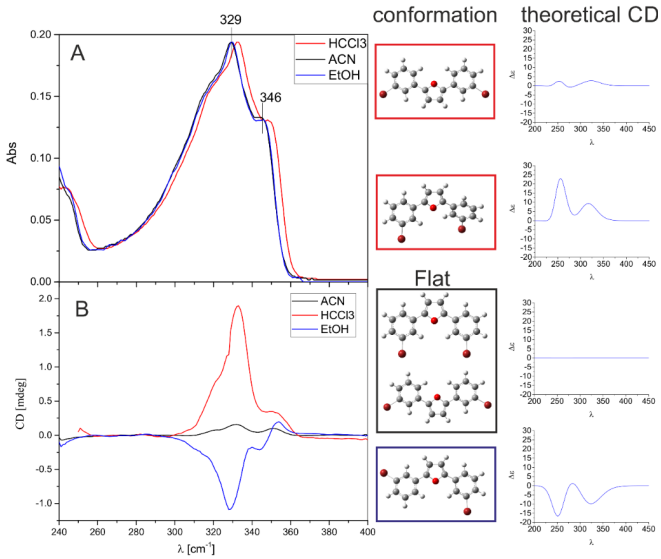

Fig. 3**. A)** UV-Vis spectra of **MBPF** in different solvents; **B)** CD spectra of **MBPF**, De expressed in units of 10^{-40}esu^{2}cm^2. On the left the calculated **MBPF** structures for different conformational minima and corresponding theoretical CD spectra. Measure spectra below 250 cm^{-1} are close to the absorption edge of solvents, thus CD spectra are strongly disturbed in this spectroscopic region.

O-14

RIGAKU ADVANCES IN X-RAY AND ELECTRON CRYSTALLOGRAPHY

Felix Hennersdorf

Rigaku Europe SE, Hugenottenallee 167, 63263 Neu-Isenburg, Germany

e-mail: felix.hennersdorf@rigaku.com

The latest range of Rigaku Oxford Diffraction instrument configurations will be summarised, and illustrated with a number of particular example applications.

The XtaLAB Synergy-ED is a new and fully integrated electron diffractometer, creating a seamless workflow from data collection to structure determination of three-dimensional molecular structures. The XtaLAB Synergy-ED is the result of an innovative collaboration to synergistically combine our core technologies: Rigaku's high-speed, high-sensitivity photon-counting detector (HyPix-ED) and state-of-the-art instrument control and single crystal analysis software platform (CrysAlisPro for ED), and JEOL's long-term expertise and market leadership in designing and producing transmission electron microscopes.

Furthermore, our X-ray diffraction instruments will be presented. The XtaLAB Synergy platform with microfocus or rotating anode sources on one side and a series of Hybrid Photon Counting (HPC) X-ray area detectors on the other side of the four-circle goniometer allows for versatile configurations perfectly adapted to the researcher's needs. These systems can be further equipped with the sample changing robot (XtaLAB Synergy Flow), an Intelligent Gonoimeter Head (IGH) for automated crystal centering, the plate scanning device XtalCheck-S or a high pressure unit.

O-15

NOBLE X-RAYS: CHOOSING THE CORRECT X-RAY WAVELENGTH FOR THE BEST SINGLE-CRYSTAL STRUCTURES

Vernon Smith

Bruker AXS GmbH, Ostliche Rheinbrueckenstrasse, Karlsruhe, Germany

Single crystal structure determination from samples containing a certain amount of heavy elements can severely suffer from absorption effects. This holds even for investigations using relatively hard radiation Mo-Kα radiation. Still harder radiation is now readily available from modern sources, such as Ag-Kα from the IμS 3.0, the IμS DIAMOND. Harder radiation not only addresses absorption issues, but also provides several further benefits like better sample transmission, higher maximum resolution, and straight forward data reduction. These properties render particularly Ag-Kα radiation ideal for advanced diffraction applications like charge density or high-pressure pressure studies or material science investigations on heavily absorbing samples in general.

However, the benefit gained from the high energy radiation can be lost if not properly reflected by the detector properties. The advanced indirect detection technology applied in PHOTON III detectors overcomes the issue. With the PHOTON III, a photon-counting detector is available, which perfectly matches the properties of hard X-ray radiation, yielding an unparalleled high quantum efficiency for Mo and Ag-radiation.

Using a number of selected examples, we will demonstrate the benefits generated combining a hard radiation source with a PHOTON III. We also will provide insights into modern indirect detector technology.

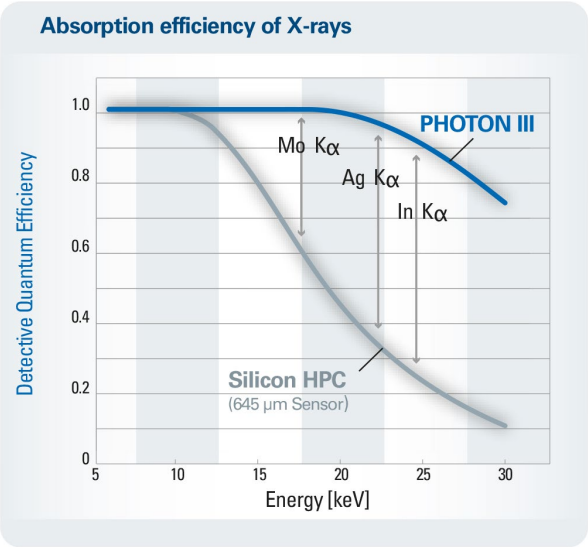

Fig. 1: PHOTON III high DQE enables quality data at higher X-ray energies.

O-16

NEW POSSIBILITIES IN XRD ANALYTICS WITH THE EMPYREAN AND AERIS SYSTEM

Kristin Gratz

Malvern Panalytical GmbH, Nuernberger Str. 113, 34123 Kassel, Germany

Listening to users of our renowned system at over a thousand universities, research centers and industries around the world, we have now redefined the concept of a multipurpose X-ray diffraction (XRD) instrument. The new Empyrean is the first fully automated multipurpose diffractometer that allows the largest variety of measurements without any manual intervention. Our newly designed MultiCore Optics featuring iCore and dCore take care of the work. The MultiCore Optics do not need any human intervention.

How can you best explore and optimize your materials? What do you need to adjust to move your research forwards? How quickly can you qualify and ship your product? X-ray diffraction is a well-established, non-destructive way of getting to the heart of crystalline materials and finding the answers to these questions. So you might not think it could be improved. But a fresh look, smart design, and advanced technology always make for a good upgrade. So, building on over 70 years of experience, we're proud to present Aeris – our super-compact, fully capable X-ray diffractometer. Aeris continually raises the bar for powder X-ray diffraction – and, with its new flexibility in measurement and automation, it's sure to provide solutions for you. Want to know more? Take a closer look... WORK SAFELY. Aeris lets you choose how to introduce new samples: manually or via automated systems. You can load your samples safely and precisely on its positioning stations and change them without disturbing ongoing measurements.

O-17

ORGANIC CRYSTAL STRUCTURE REFINEMENT FROM 3D ELECTRON DIFFRACTION DATA

Paulina M. Dominiak[1], Barbara Gruza[1], Petr Brázda[2], Lukáš Palatinus[2], Maura Malinska[1], Kunal Kumar Jha[3], Tomasz Góral[3], Krzysztof Woźniak[1,3]

[1] Department of Chemistry, University of Warsaw, Poland
[2] Institute of Physics of the Czech Academy of Sciences, Czech Republic
[3] CeNT, University of Warsaw, Poland

In recent years, one can observe spectacular developments of the 3D electron diffraction (3D ED) methods. Practitioners of this method are learning how to improve data collection, among others how to diminish radiation damage and how to deal with dynamical scattering, data processing and refinement. Currently, available structures from 3D ED reach R-factors even below 10% and resolution around d_{min} = 0.5 Å. Refinement with a dynamical approach [1] against such data allows for observation of residual density in bonding paths or lone electron pair regions. Therefore, it is possible and profitable to use more sophisticated aspherical models of atomic electrostatic potential instead of standard independent atom model (IAM).

We have already proposed transferable aspherical atom model (TAAM) refinements against 3D ED data in kinematic approximation [2]. Now TAAM is coupled with dynamical refinement and available in Jana2020 [3]. Here, we present refinements of exemplary organic crystal structures, urea and α-glycine, with application of kinematic approach. Next, we show refinement of 1-methyluracil crystal structure against d_{min} = 0.56 Å data with TAAM model in the dynamical approach. There is a visible clearing of the residual density maps, also lowering of the maximum and minimum residual values and a further lowering of R-factors. In the future, we will go beyond TAAM and refine the parameters of the multipole model.

Acknowledgments: This research was funded by National Science Centre, Poland 2020/39/I/ST4/02904 and University of Warsaw IDUB grant BOB-IDUB-622-20/2021 (“lnfrastructure for Cryomicroscopy and Electron Diffraction Core Facility”).

References

[1] L. Palatinus, V. Petricek, and C. A. Correa, *Acta Crystallogr. A*, **71** (2015), 235–244.
[2] B. Gruza, M. L. Chodkiewicz, J. Krzeszczakowska, and P. M. Dominiak, *Acta Crystallogr. A*, **76** (2020), 92–109.
[3] V. Petrícek, M. Dusek, and L. Palatinus, *Zeitschrift für Krist. - Cryst. Mater.*, **229** (2014), 345–352.

O-18

COMPLEXITY IN THE STRUCTURAL PHASE TRANSITIONS IN $Pb(Hf_{0.92}Sn_{0.08})O_3$ SINGLE CRYSTALS

Irena Jankowska-Sumara[1], Marek Paściak[2], Jae-Hyeon Ko[3], Andrzej Majchrowski[4]

[1] Institute of Physics, Pedagogical University of Cracow, Kraków, Poland
[2] Institute of Physics of the Czech Academy of Sciences, Prague, Czech Republic
[3] School of Nano Convergence Technology, Hallym University Chuncheon 24252, Korea
[4] Institute of Applied Physics, Military University of Technology, Warsaw, Poland

$Pb(Hf_{1-x}Sn_x)O_3$ single crystals with x=0.08 were characterized using single-crystal X-ray diffraction and Raman scattering in the wide temperature range. The information on the structure of two intermediate phases, situated between low-temperature antiferroelectric AFE1 and high temperature paraelectric (PE) phases has been obtained. The lower-temperature intermediate AFE2 phase is characterized by incommensurate displacive modulations in the Pb sublattice. The higher temperature intermediate IM phase is characterized by distortion of oxygen octahedra, and large disorder coming from lead ions represented by X-ray diffuse scattering. Optical phonons and phase transitions in $Pb(Hf_{1-x}Sn_x)O_3$ single crystals were investigated by temperature-dependent Raman spectra. It was found that several soft modes control the phase transition between two antiferroelectric phases pointing to its displacive character, whereas both soft and central modes were observed in the paraelectric phase.

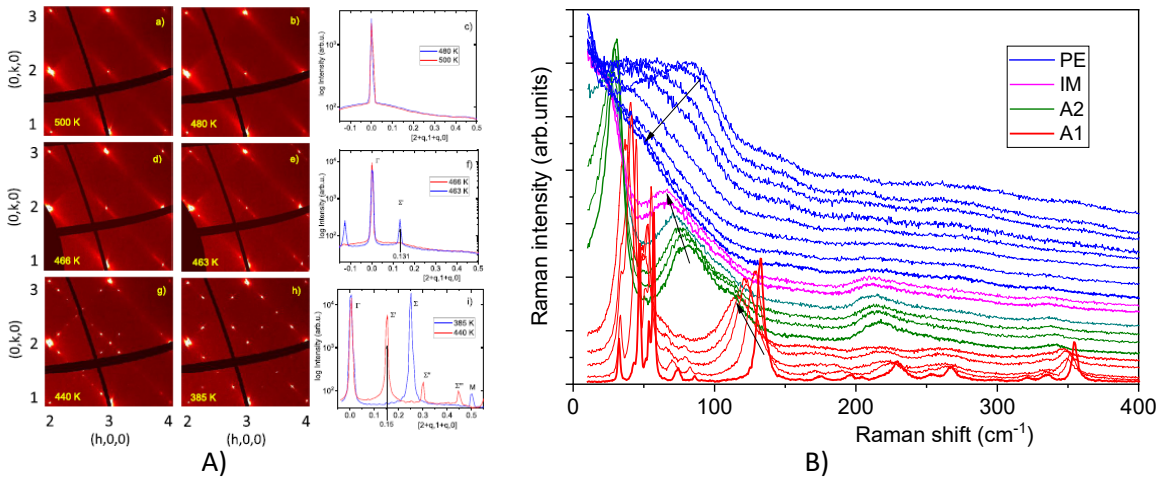

Fig. 1. A) Reciprocal space map in the (*hk0*) plane in the pseudocubic reference frame of PHS-23 in different temperatures a) 500 K, b) 480 K d) 469 K, e) 463 K, g) 440 K, h) 385 K. Intensity profiles along [-1 1 0] pseudocubic direction correspond to (c) PE and IM phase f) near IM-AFE2 phase transition, i) AFE2 and AFE1 phase. B) Raman spectra of the PHS-8 single crystal at selected temperatures between 78 and 873 K corresponding to different phases. All spectra are corrected for the temperature factor and vertically displaced for clarity.

O-19

PHASE TRANSFORMATION IN A DECAGONAL Al-Cu-Rh QUASICRYSTAL RELATED TO PHASON DISORDER

R. Strzałka*, I. Bugański, J. Wolny

Faculty of Physics and Applied Computer Science, AGH University of Science and Technology, Krakow, Poland

**e-mail: strzalka@fis.agh.edu.pl*

Since the beginning of research on the structure of quasicrystals, the challenging question about the stability of these phases has not been answered with a clear answer [1]. The use of two competing mechanisms of structure stabilization (through entropy or energy minimization) in quasicrystals finds only partial theoretical and experimental verifications. In our presentation, we will present the results of the refinement of the Al-Cu-Rh decagonal structure model based on high-temperature data [2] using a new phason approach [3,4] and a generalized Penrose tiling (GPT) as a quasilattice [5]. Diffraction data were collected at temperatures 293 K and 1013-1223 K. A correlation was observed between lattice parameters and the maximum residual electron density was observed, indicating a phase transformation at around 1083-1153 K. At the same temperatures, the minima of values of moments, which model the phasonic flips, are observed, leading to the conclusion that the transition to a more stable phase is related to phason disorder.

The occurrence of the additional 5^{th} atomic surface in GPT can be obtained by phasonic fluctuation in the ideal structure. In the consecutive refinement we observed that the atomic distribution of an 5^{th} atomic surface correlates with the stability of a structure at the temperature of approximately 1153 K, which could indicate the influence of the phason disorder on the stabilization of the structure [6].

Acknowledgements: The authors acknowledge financial support from the Polish National Science Center under grant no. 2019/33/B/ST3/02063.

Literature

[1] M. de Boissiue, *Chem. Soc. Rev.*, **20** (2012) 6778.
[2] P. Kuczera, J. Wolny, W. Steurer, *Acta Cryst. B*, **70** (2014) 306.
[3] I. Buganski, R. Strzalka, J. Wolny, *Acta Cryst. A*, **75** (2019) 352.
[4] I. Buganski, R. Strzalka, J. Wolny, *J. App. Cryst.*, **53** (2020) 904.
[5] M. Chodyn, P. Kuczera, J. Wolny, *Acta Cryst. A*, **71** (2015) 161.
[6] I. Bugański, R. Strzałka, J. Wolny, *Acta Cryst. A* (accepted).

O-20

CHLOREK OŁOWIU Z KATIONEM METYLOHYDRAZONIOWYM – SYNTEZA I WŁAŚCIWOŚCI STRUKTURALNE WARSTWOWEGO PEROWSKITU HYBRYDOWEGO

Dawid Drozdowski[a,*], Katarzyna Fedoruk[b], Mirosław Mączka[a], Jan K. Zaręba[b], Dagmara Stefańska[a], Adam Sieradzki[b] i Anna Gągor[a]

[a] Instytut Niskich Temperatur i Badań Strukturalnych PAN, ul. Okólna 2, 50-422 Wrocław
[b] Politechnika Wrocławska, ul. Wybrzeże Wyspiańskiego 27, 50-370 Wrocław

**e-mail: d.drozdowski@intibs.pl*

Perowskity hybrydowe (tj. organiczno-nieorganiczne, 3D HOIPs) o wzorze sumarycznym ABX_3, zbudowane są z sieci oktaedrów BX_6 połączonych narożami, a składnik organiczny „A" położony jest w lukach między oktaedrami [1]. Związki te są przedmiotem intensywnych badań z uwagi na ich unikalne właściwości fizykochemiczne. Najlepiej poznane 3D HOIPs, w których „A" to kation metyloamoniowy (MA^+) lub formamidyniowy (FA^+), „B" to kation ołowiowy, a „X" to anion halogenku (Br, Cl, I), stanowią główny komponent perowskitowych ogniw słonecznych [2], wykazują m.in. wysoką wydajność kwantową luminescencji (PLQY) i konwersji energii, przestrajalność barw emisji oraz ponadprzeciętną mobilność nośników ładunków [3, 4]. Ograniczeniem dla zastosowań technologicznych tych materiałów jest ich wrażliwość na wilgoć oraz degradacja chemiczna. Zwiększoną stabilność oraz poprawę niektórych właściwości (np. PLQY) obserwuje się w warstwowych perowskitach hybrydowych (2D HOIPs) o wzorze A_2BX_4, w których warstwy połączonych narożami oktaedrów oddzielone są kationami organicznymi [5].

W naszej grupie badamy 3D i 2D HOIPs z kationem metylohydrazoniowym (MHy^+). Materiały z MHy^+ cechują nowe i ciekawe właściwości – analogi 3D krystalizują w fazie polarnej i wykazują efekty nieliniowe (np. generacja drugiej harmonicznej), natomiast w strukturach 2D zaobserwowano rekordowo niskie odległości międzywarstwowe [6, 7].

Tematem prezentacji są przemiany fazowe w kryształach MHy_2PbCl_4 oraz wpływ struktury krystalicznej na właściwości optyczne i dielektryczne [8]. Pomiary dyfrakcyjne wykazały istnienie trzech faz polimorficznych w tych związkach. Faza wysokotemperaturowa (I) o symetrii *Pmmn* jest izostrukturalna względem dotychczas opublikowanych analogów MHy_2PbBr_4 i MHy_2PbI_4 [6, 7], i charakteryzuje się nieporządkiem pozycyjnym kationów MHy^+, zlokalizowanych na płaszczyźnie zwierciadlanej *m*. W temperaturze 332 K/338 K przy chłodzeniu/grzaniu zachodzi przemiana fazowa do fazy modulowanej (II) o symetrii opisanej w grupie nadprzestrzennej $Pmmn(00\gamma)s00$ z wektorem modulacji $\mathbf{q} \cong 0.25\mathbf{c^*}$. Obecność fazy modulowanej zaobserwowano również dla MHy_2PbBr_4, jednakże wąski zakres temperaturowy występowania tej fazy (ok. 15 K) oraz słaba intensywność refleksów satelitarnych uniemożliwiły wyznaczenie grupy nadprzestrzennej. W temperaturze 205 K/224 K następuje kolejne obniżenie symetrii do jednoskośnej, polarnej grupy $P2_1$ (III), charakteryzującej się uporządkowanymi aminami i znaczną dystorsją oktaedrów

$PbCl_6$. W fazie III tworzy się kompletny układ wiązań wodorowych pomiędzy cząsteczkami MHy^+ oraz pomiędzy MHy^+ a szkieletem nieorganicznym. Pomiary SHG oraz piroprądu potwierdzają polarny charakter tej fazy.

Badania zostały sfinansowane ze środków Narodowego Centrum Nauki, w ramach projektu OPUS 18 (2019/35/B/ST5/00043).

Literatura

[1] D. B. Mitzi, *Progress in Inorganic Chemistry*, Wiley (1999).
[2] H. J. Snaith, *J. Phys. Chem*., **4(21)** (2013) 3623-3630.
[3] H. Mehdi *et al., RSC Adv*., **9** (2019) 12906–12912.
[4] H. Ball *et al., Energy Environ. Sci*., **6** (2013) 1739−1743.
[5] X. Gao *et al., Adv. Sci.*, **22(6)** (2019) 1900941.
[6] M. Mączka *et al., Chem. Mater*., **32(4)** (2020) 1667−1673.
[7] M. Mączka *et al., Chem. Mater*., **33** (2021) 2331−2342.
[8] K. Fedoruk *et al.*, praca nieopublikowana, 2022.

O-21

STRUCTURE EVOLUTION OF $Ti_{50}Ni_{25}Cu_{25}$ SHAPE MEMORY ALLOY PRODUCED BY HIGH-ENERGY BALL MILLING

Piotr Salwa, Tomasz Goryczka, Maciej Zubko

Institute of Materials Engineering, University of Silesia in Katowice, 75 Pułku Piechoty 1A, 41-500 Chorzów

Ni-Ti based Shape Memory Alloys are known for their shape memory effect being the strongest than any of the most used SMA. While shape memory effect can occur at various temperatures ranging from -120°c to 140°C, specific transformation temperature and overall profile can be adjusted by tailoring chemical composition of the alloy. Additional control over shape memory effect characteristics can be obtained by influencing microstructure of produced alloy and modifying its grain size [1].

Addition of copper to NiTi alloy strongly affects its shape memory effect and phase transition characteristics. Under 20 at.% addition of Cu causes widening of hysteresis loop, however additional stage of the martensitic transition appears at 15at.%. Increasing Cu content to 25at.% leads to narrow hysteresis loop and one stage martensitic transformation in temperature range from room temperature to around 80°C [2-4].

Thus possibility of producing amorphous/nanocrystalline $Ti_{50}Ni_{25}Cu_{25}$ alloy, which would undergo martensitic transformation, directly from commercially available elemental powders (purity 99,7%) by high-energy ball milling method was studied.
Structure and morphology of produced alloys at various milling times and after crystallization at 600°C were examined by X-ray diffraction, electron microscopy – both SEM and TEM methods. Increased milling time led to decreasing in average crystallite size from 6,5 nm at 50 hrs to approx. 2 nm after 100hrs of milling time. Additionally extending grinding time to 140 hrs resulted in formation of areas of the B19 martensite and $Ti_2(Ni,Cu)$ phase in as milled alloys. After crystallization average crystallite size increased to 11 nm [5].

Literature

[1] T. W. Duerig, K. N. Melton, D. Stockel & C. M. Wayman, EngineeringAspects of Shape Memory Alloys. London: Butterworth-Heinemann (1990).
[2] Bricknell RH, Melton KN & Mercier, The structure of NiTiCushape memory alloys. *Metall Mater Trans A*, **10** (1979) 693–697.
[3] J. van Humbeeck, Shape memory materials: State of the art and requirements for future applications. *J Phys IV France*, **07** (1997) C5-3–C5-12.
[4] W. J. Moberly, J. L. Proft, T. W. Duerig & R. Sinclair, Twinless martensite in TiNiCu shape memory alloys. *Mater Sci Forum*, **56–58** (1990) 605–610.
[5] T. Goryczka,P. Salwa & M. Zubko, High-Energy Ball Milling Conditions in Formation of NiTiCu. *Shape Memory Alloys. Microscopy and Microanalysis*, **28(3)** (2022) 939-945. doi:10.1017/S143192762101271X

O-22

ANALYSIS OF STRUCTURAL CHANGES IN Fe–Cu SPINEL–BASED OXYGEN CARRIES FOR APPLICATION IN CHEMICAL LOOPING COMBUSTION PROCESS AFTER MULTIPLE CYCLES OF OXIDATION–REDUCTION

Rafał Łysowski*, Ewelina Ksepko

Wrocław University of Science and Technology
Department of Engineering and Technology of Chemical

**e-mail: rafal.lysowski@pwr.edu.pl*

Chemical Looping Combustion is new, emerging technology that could find application for solid fuel combustion. In this process, system of two reactors is used (fuel and air reactor). Fuel is combusted by oxygen released from material called oxygen carrier (OC), which is circulating between reactors. Since fuel has no contact with atmospheric air, production of thermal nitrogen oxides is reduced almost to zero. Oxygen carrier for practical application in CLC has to fulfil certain requirements like low cost, high reactivity toward certain fuels and most important – to maintain its physicochemical properties during many cycles of reactions. Oxygen carrier can undergo unfavourable chemical changes like partial decomposition or formation of new unreactive phases due to reaction with ash residues.

In this work, spinel structure materials based on iron and copper oxides for CLC application were synthesized using solid state method. Obtained spinels were tested for their oxygen transport capacities in wide range of temperatures (800-1000°C) to measure CLOU (Chemical Looping with Uncoupling properties).

Crystal structures of both fresh and spent OCs were examined using X-Ray diffractometry and Rietveld method for determination of their structure and stability after multiple redox cycles in different temperatures.

Acknowledgement: The work was financed from the National Science Centre Poland, Project No. 2020/37/B/ST5/01259.

PLAKATY

POSTERS

P-01

STRUCTURAL CHARACTERIZATION OF COPPER SENSING BACTERIAL HISTIDINE KINASE

Anna Cociurovscaia, Grzegorz Bujacz, Agnieszka Pietrzyk-Brzezińska

Institute of Molecular and Industrial Biotechnology, Stefanowskiego 2/22, 90-537 Lodz

The *Escherichia coli* CusS histidine kinase is a component of the bacterial two-component signal transduction system CusS-CusR, engaged in sensing copper ions excess and activating the transcription of chemiosmotic efflux pump CusCFBA [1]. The classical histidine kinase is a transmembrane multidomain protein, which propagates recognized signal from periplasmic space toward the cytoplasmic catalytic kinase core, through the coordinated conformational change of its subsequent domains. In response, the catalytic kinase core binds ATP, autophosphorylates a histidine residue, and transfers the phosphate group to the cognate response regulator, which recognizes the target operon and regulates its transcription [2]. Due to the antibacterial properties of copper, it is abundantly used in healthcare settings [3]. Therefore, new structural studies aiming at understanding the rapid phosphotransfer mechanism will reveal the crucial role of the CusS kinase core in bacterial copper resistance.

Using X-ray crystallography, the crystal structure of the CusS kinase core was determined at the resolution of 1.4 Å. The cytoplasmic catalytic domains ensemble in the homodimer. The CusS structure determination allowed studying intramolecular and intermolecular interactions crucial for the mechanism of CusS autophosphorylation. Based on obtained structural data, conserved catalytic and structural motifs were identified and described. All conserved motifs classify CusS into the Type I family of histidine kinases, the most common group of these enzymes constituting 72% of all histidine kinases.

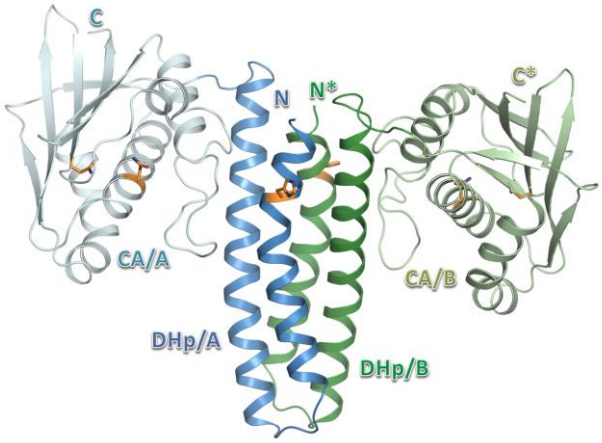

Fig. 1. The overall structure of CusS catalytic kinase core.

Literature

[1] G.P. Munson, D.L. Lam, F.W. Outten, T.V. O'Halloran, *J. Bacteriol.*, **182** (2000) 5864-5871.
[2] C.P. Zschiedrich, V. Keidel, H. Szurmant, *J Mol Biol.*, **428 (19)** (2017) 3752-3775.
[3] E. Dauvergne, C. Mullie, *Antibiotics*, **286 (10)** (2021).

P-02

PACKING ANALYSIS OF GLUCOSE/ XYLOSE ISOMERASE UNDER AREAS OF EXPECTED CHANGES INDUCED BY HIGH-PRESSURE

Agnieszka Klonecka[1,2], Joanna Sławek[1], Maciej Kozak[1,3]

[1] SOLARIS National Synchrotron Radiation Center, Jagiellonian University, ul. Czerwone Maki 98, 30-392 Kraków.
[2] Faculty of Physics, Astronomy and Applied Computer Science, Jagiellonian University, ul. Łojasiewicza 11, 30-348 Kraków.
[3] Faculty of Physics, Adam Mickiewicz University in Poznań, ul. Poznańskiego 2, 61-614 Poznań.

The stability and possible changes in the structure of biomacromolecules at high-pressure remains largely unexplored. The impact of high pressure on the protein structure and properties is particularly relevant for enzymes, which find a wide range of industrial applications such as biotechnology, food chemistry, food processing, and others.

While studying protein molecules, especially under extreme conditions it is crucial to investigate their structure since it is closely related to their function. It is known that the protein structure can be disturbed or even destroyed during chemical or thermal-denaturation processes. In contrast, pressure does not destabilize the protein's structure uniformly. The influence of pressure depends on the type of protein (at the level of the secondary, tertiary, and quaternary structures). Additionally, the content of cavities, pores, and channels is also significant. With a pressure increase, the spaces can be modulated. As a result, the number of water molecules penetrating the void may alter causing a change in the protein conformation [1].

Glucose/xylose isomerase is widely used in the food industry and biotechnology. The enzyme catalyzes the reversible isomerization of glucose to fructose and xylulose to xylose. It applies in the production of high-fructose corn syrup and bioethanol from hemicelluloses [2]. Bioethanol finds application as a fuel additive [3]. Additionally, glucose/xylose isomerase is often considered a model protein in many molecular studies [4].

As an introduction to the further high-pressure study, an extensive analysis of the glucose/xylose isomerase structures under ambient conditions was performed. The glucose/xylose isomerase most commonly crystallizes in space group I222. In this work, 93 models of glucose/xylose isomerase from *Streptomyces rubiginosus* in this symmetry were identified and analyzed.

During the packing analysis, all protein structures were divided according to unit cell parameters, ligands present in the structure, and crystallization conditions. The protein molecules were then superposed, and representatives of each group were selected. Those were later used as an input for the packing analysis of elementary cells, and the most important intra- and intermolecular contacts (in quaternary, tertiary, and secondary structures) were identified. Based on the results of this analysis, it will be possible to determine the structural elements that could be destroyed first in high-pressure testing. Since the effect of pressure on voids in a protein's structure depends on their nature, the channels and pores were divided into hydrophobic and hydrophilic. It

expects these regions to be the first to be altered by the impact of high-pressure. The high-pressure diffraction experiments using synchrotron radiation are planned soon.

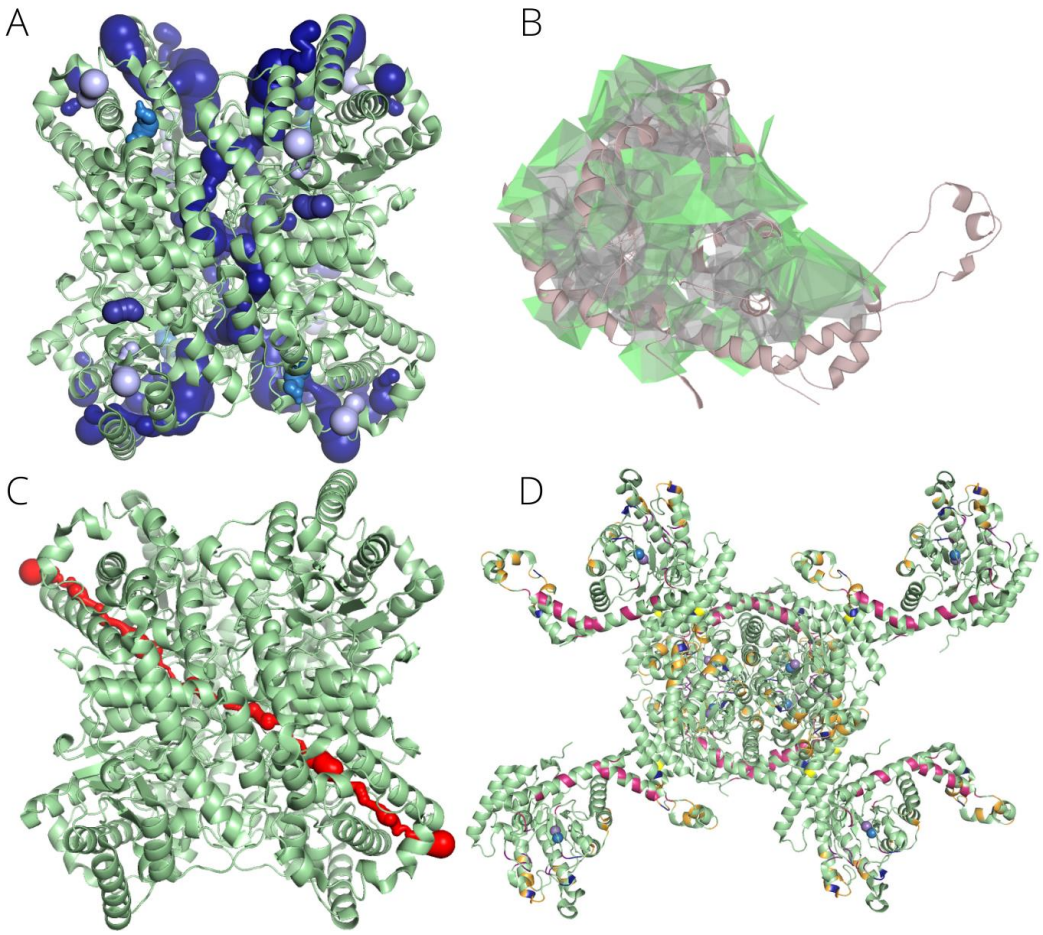

Fig. 1. (A) Channels in the protein tetramer (blue- channels, green- protein). (B) Cavities in the protein structure (green- cavities, beige- protein). (C) Pore in the protein tetramer (red- pore, green- protein). (D) The most important bonds in the quaternary structure (pink, orange, and blue-amino acids present in the tetramer bonds, (yellow- amino acids present in bonds between tetramers, green- protein).

Analysis showed that the models are similar to each other. This indicates that the structure of glucose/xylose isomerase is very stable, which makes this protein a good target for high-pressure studies.

This work was supported by research grant PRELUDIUM BIS (grant ID: 2020/39/O/ ST4/ 03465) from National Science Centre (Poland).

Literature

[1] K. Kurpiewska, K. Lewiński, *Central European Journal of Biology*, **5(5)** (2010) 531–542.
[2] S. H. Bhosale, M. B. Rao, V.V. Deshpande, *Microbiology and Molecular Biology Review*, **60(2)** (1996) 280–300.
[3] T. Komorowicz, J. Magiera, *Wydawnictwo Politechniki Krakowskiej* (2008).
[4] K. H. Nam, *Applied Sciences*, **12(1)** (2022) 428.

P-03

LESSONS FROM RANDOM MUTAGENESIS OF *E. COLI* NTN-AMIDOHYDROLASE: THE EFFECT OF MULTIPLE SUBSTITUTIONS IN THE ACTIVE SITE ON AUTOCATALYTIC MATURATION OF ECAIII

Joanna I. Loch[1], Agnieszka Klonecka[1], Kinga Kądziołka[1], Piotr Bonarek[2], Jakub Barciszewski[3], Barbara Imiolczyk[3], Krzysztof Brzezinski[3], Miroslaw Gilski[3,4], Mariusz Jaskolski[3,4]

[1]Faculty of Chemistry, Jagiellonian University, Krakow, Poland
[2]Faculty of Biochemistry, Biophysics and Biotechnology, Jagiellonian University, Krakow, Poland
[3]Institute of Bioorganic Chemistry, Polish Academy of Sciences, Poznan, Poland
[4]Faculty of Chemistry, A. Mickiewicz University, Poznan, Poland

L-Asparaginases are enzymes that hydrolyze L-Asn to L-Asp and ammonia. *E. coli* genome encodes L-asparaginases from two different structural classes: Class 1 (EcAI and EcAII) and Class 2 (EcAIII) [1]. EcAIII belongs to Ntn-amidohydrolases, which are produced as inactive precursors and develop their catalytic activity in an autoproteolytic maturation process [2]. In this work, a series of new EcAIII variants (Fig. 1) obtained by random mutagenesis within the active site area were studied using structural, biophysical, and bioinformatic methods.

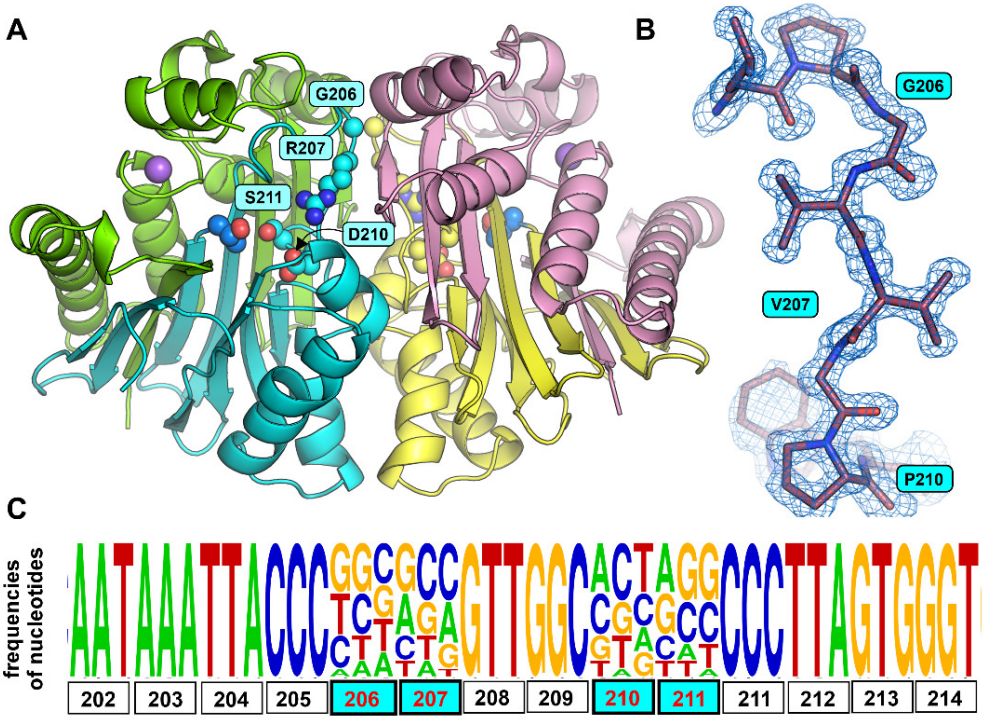

Fig. 1. (A) The EcAIII structure with mutation sites targeted in this work marked in cyan boxes. (B) The 2Fo-Fc electron density map (1.50 σ) of the mutated peptide of variant RDM1-19 (1.20 Å resolution). (C) Nucleotide frequencies at the mutation sites.

Activity tests revealed that all analyzed mutants have abolished L-asparaginase activity; however, some of them retained the ability to undergo autoproteolytic maturation. The nine determined crystal structures (1.20-2.55Å resolution) showed that the EcAIII fold is flexible enough to accommodate different types of mutations; nevertheless, these substitutions have a variable impact on protein stability. The conclusions from the analysis of structure-function relationships in this series of new EcAIII variants were grouped into six lessons focused on: (1) adaptation of the EcAIII fold to new substitutions; (2) the role of Arg207 in L-asparaginase activity; (3) networking of residues as a prerequisite of autoprocessing; (4) the complexity of the autoprocessing initiation; (5) conformational changes observed in the inactive variants; and (6) cooperativity of the EcAIII dimer subunits. Furthermore, we classified the structural requirements of autocleavage initiation.

The lessons from our work provide useful hints for enzyme engineering aimed at designing Ntn-hydrolases for antileukemic applications. The currently used Class 1 enzymes of bacterial origin induce severe side effects, and thus better, or at least different, therapeutics are highly required. Promising candidates could be sought among Ntn-amidohydrolases, such as EcAIII. However, native Ntn-amidohydrolases have too low substrate affinity, and thus enzyme engineering would be required to improve their catalytic properties for therapeutic applications.

Work supported by National Science Centre (NCN, Poland) grant 2020/38/E/NZ1/00035.

References

[1] J.I. Loch, M. Jaskolski, *IUCrJ* **8** (2021) 514–521
[2] K. Michalska, A. Hernandez-Santoyo, M. Jaskolski, *J. Biol. Chem.* **283** (2008) 13388–13397

P-04

STRUCTURAL STUDIES OF *RHIZOBIUM ETLI* INDUCIBLE ASPARAGINASE MUTANTS

K. Pokrywka[1], B. Imiołczyk[1], M. Grzechowiak[1], J. Loch[2], M. Gilski[1,3], M. Jaskólski[1,3]

[1]*Institute of Bioorganic Chemistry, Polish Academy of Sciences, Poznan, Poland*
[2]*Faculty of Chemistry, Jagiellonian University, Krakow, Poland*
[3]*Department of Crystallography, Faculty of Chemistry, A. Mickiewicz University, Poznan, Poland*

L-Asparaginases are a large family of enzymes, grouped into three structural Classes. Some Class 1 asparaginases from bacteria are used to treat acute lymphoblastic leukemia (ALL) and lymphosarcoma. Unfortunately, these therapeutic regimens are often associated with a number of serious side effects. Alternative sources of therapeutic asparaginases have thus been sought, and the inducible *Rhizobium etli* enzyme (ReAV) emerges as an interesting candidate.

ReAV differs significantly in sequence from other microbial asparaginases, indicating a different catalytic mechanism of asparagine hydrolysis. The crystal structure of ReAV [1] shows a protein folded as some β-lactamases, but forming a unique dimeric assembly. The active site of ReAV contains two Ser-Lys tandems, centered around the hydrated Ser48 residue and located in the close vicinity of a Zn^{2+} cation, which has an unusual coordination sphere created by two cysteines, a lysine and a water molecule. The presence of a Zn^{2+} cation in the active site area is unique to ReAV; however the metal ion is not necessary for catalysis. Another characteristic residue of ReAV is an oxidized Cys249, which is involved in a network of H-bonds comprising the active site area.

To decipher the catalytic mechanism of ReAV, the most conspicuous residues implicated by the crystal structure, i.e. the two Ser-Lys tandems (Ser48-Lys51 and Ser80-Lys263), the residues involved in zinc coordination (Cys135, Lys138, Cys189), and the relatively distant Cys249, were subjected to site-directed mutagenesis and substituted with Ala. All eight alanine mutants were studied using biophysical and structural methods. With the exception of the K138A mutant, all the created ReAV muteins lost the ability to hydrolyze L-asparagine, as clearly demonstrated by the Nessler method. This confirms the significance of the implicated residues in catalysis. The replacement of Ser48 and Ser80 by Ala affected the protein stability and folding, as indicated by CD spectra and low expression yields. We were able to crystallize mutants: K51A, S80A, C135A, K138A, C189A and K263A, and solve their X-ray crystal structures. The structures reveal some intriguing variations in the active site area. With alanine substitutions of Cys135, Lys138 and Cys189, the zinc coordination site fell apart and the mutants are unable to bind Zn. Moreover, the absence of the Zn^{2+} cation affected the oxidation state of Cys249, which no longer carried a chemical modification. The K51A and K263A mutations disrupted the network of H-bonds in the active site region and modified the hydration pattern of Ser48. Work supported by National Science Centre (NCN, Poland) grant 2020/37/B/NZ1/03250.

References

[1] J.I.Loch *et al.*, *Nature Commun*., **12** (2021) 6717.

P-05

STRUCTURAL CHANGES IN A NEW VARIANT OF *E. COLI* NTN-AMIDOHYDROLASE INDUCED BY THE PRESENCE OF POTASSIUM CATIONS

Anna Ściuk[1], Miłosz Ruszkowski[2], Krzysztof Lewiński[1], Mariusz Jaskolski[2,3], Joanna Loch[1]

[1] Faculty of Chemistry, Jagiellonian University, Krakow, Poland
[2] Institute of Bioorganic Chemistry, Polish Academy of Sciences, Poznan, Poland
[3] Faculty of Chemistry, A. Mickiewicz University, Poznan, Poland

L-Asparaginases catalyze the hydrolysis of L-asparagine to L-aspartate with the release of ammonia. Class 2 L-asparaginases belong to the N-terminal nucleophile (Ntn) amidohydrolase superfamily. They can be divided into K-dependent and K-independent enzymes [1]. A structural element present in all Class 2 enzymes is the Stabilization Loop that is responsible for establishing a geometrical lock on the nucleophilic threonine [1]. The conformation of the Stabilization Loop is usually supported by an Na^+ cation with an octahedral coordination sphere provided by six main-chain C=O groups. The K-Dependent enzymes from plants also have an Activation Loop, which acts as a regulator of enzymatic activity [2]. The presence of K^+ coordinated within the Activation Loop allows the substrate to anchor in the active site (ON mode). The absence of K^+ in the Activation Loop causes a structural rearrangement switching the enzyme to the OFF mode [3]. It was shown that K-sensitivity can be introduced into a K-independent enzyme, *e.g.* PvAIII from *Phaseolus vulgaris*, via site-directed mutagenesis [4].

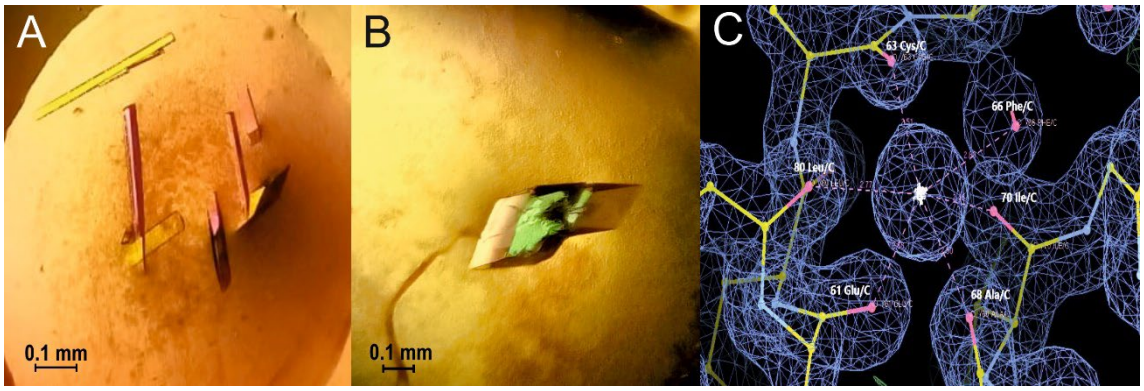

Fig. 1. Morphology of the crystals of the V120S mutant obtained in presence of (A) NaCl and (B) KCl. The 2Fo-Fc electron density map (1.0σ) of the K^+ coordination site in the Stabilization Loop of variant V120S (1.55 Å resolution).

EcAIII is a K-independent L-asparaginase encoded by the *E. coli* genome. To explore whether K-sensitivity can be activated in this bacterial enzyme, a new variant of EcAIII, with a V120S mutation in the Activation Loop area, was generated and its properties were studied by X-ray crystallography. The V120S mutant was crystallized in two different conditions, viz. in the presence of NaCl or KCl (Fig. 1). The structures of these crystals (1.55–1.70 Å resolution) were analyzed to visualize the

differences in the Stabilization Loop as well as in the region corresponding to the Activation Loop. In the Na^+ form, the structure replicates the standard conformation of the EcAIII enzyme. In the crystals obtained in the presence of KCl, a K^+ ion was coordinated not only in the Stabilization Loop (Fig. 1), but was also found close to the V120S mutation site, in the region corresponding to the Activation Loop of K-dependent enzymes. The K^+ cation bound near the V120S mutation has an interesting octahedral coordination sphere including Glu234, which in WT EcAIII stabilizes the orientation of Arg207 for accurate presentation of the L-Asn substrate to the active site apparatus.

Work supported by National Science Centre (NCN, Poland) grant 2020/38/E/NZ1/00035.

References

[1] J. Loch, M. Jaskolski, *IUCrJ.*, **8** (2021) 514-531.
[2] M. Bejger *et al*., *Acta Cryst.*, D**70** (2014) 1854–1872.
[3] K. Michalska *et al*., *J. Biol. Chem.*, **283** (2008) 13388–13397.
[4] E. Ajewole *et al.*, *FEBS J*., **285** (2018) 1528–1539.

P-06

HOW THE HALOGEN BONDS ALLOW CRYSTAL OF COPPER(I) COORDINATION COMPOUND TO BREATHE

Emilia Ganczar, Agata Białońska

Department of Chemistry, University of Wrocław,
14. F. Joliot-Curie, 50-383 Wrocław, Poland

The host-guest materials are at the heart of the scientific world due to their wide range of applications and the huge structural diversity[1]. Due to the architectures of the host, the host-guest crystal can be divided into two main categories: molecular complexes where convex guests adjust to a concave host [2], and compounds in which the packing of the host leads to the formations of the empty spaces (channel or sheets) in which guests molecules may be deposited. Taking into account how guest release can affect host framework and interactions within it, the host-guest systems can be divided into few groups – rigid, able for reorientation and able for reorganization. In the third group, guest release causes reorientation of the host framework, which is accompanied by reorganization of interactions (breaking of ones and formation of others) within it [3].

On the poster results of our studies on breathing host-guest crystals of copper(I) coordination compound will be presented. The studies include the ability of the system to absorb compounds of various size and shape and containing various functional groups as well as structural changes accompanying sorption – desorption processes and factors which impact the changes. We also show how the competitiveness of various halogen bonds affects the structural and sorption properties.

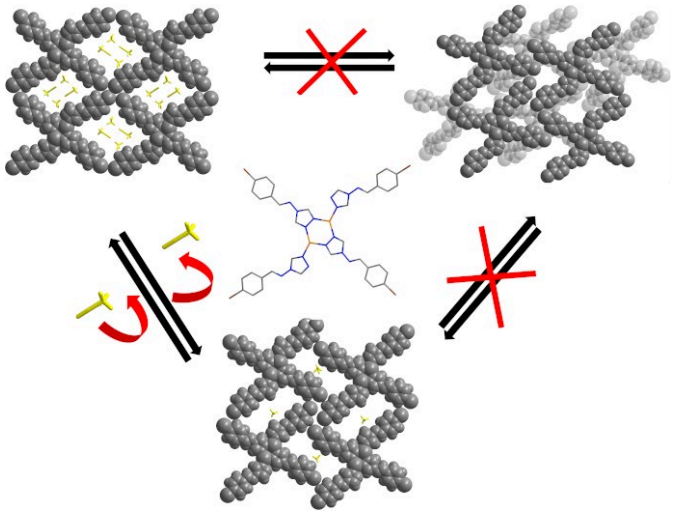

References

[1] J. L. Steed, J. W. Atwood, Crystal Engineering. In Supramolecular Chemistry, Wiley (2022) 537.
[2] D. J. Cram, J. M. Cram, Container Molecules and Their Guests, *R. Soc. Chem.,* **4** (1997) 1.
[3] S. Kitagawa, R. Kitaura, R. S. -I. Noro, *Angew. Chemie - Int. Ed.*, **43(18)** (2004) 2334.

P-07

SYNTHESIS, STRUCTURAL CHARACTERIZATION AND BIOLOGICAL ACTIVITY OF NEW 6-METHYL-2-PHENYLPYRIMIDINE SCHIFF BASE DERIVATIVES

Iwona Bryndal[1], Anna Pyra[2], Marcin Stolarczyk[1], Aleksandra Mikołajczyk[3], Agnieszka Matera-Witkiewicz[3]

[1] Department of Organic Chemistry and Pharmaceutical Technology, Faculty of Pharmacy, Wroclaw Medical University, 211A Borowska, 50-556 Wrocław,
[2] Faculty of Chemistry, University of Wroclaw, 14 Joliot-Curie, 50-383 Wrocław
[3] Screening Laboratory of Biological Activity Tests and Collection of Biological Material, Faculty of Pharmacy, Wroclaw Medical University, 211A Borowska, 50-556 Wrocław

Pyrimidine is widely found in nature as a component of nucleic acids (cytosine, thymine, and uracil) and many other natural and synthetic compounds, including drugs, and it is known over time as a potent pharmacophore. In our previous studies, we observed that 5-hydroxymethylpyrimidine with a tetrasulfide bridge at the 4-position has interesting antibacterial and antifungal properties [1], particularly, the hydroxylation of 4-[(4-chlorobenzyl)sulfanyl]-5,6-dimethyl-2-phenylpyrimidine to its 5-hydroxymethyl derivative enhances the cytotoxicity significantly towards both, i.e. the cancer (HeLa, K562 and CFPAC) and normal (HUVEC) cell lines [2]. Furthermore, pyrimidines possessing a 4-benzylsulfanyl group exhibit stronger toxicity than their 4-amino analogues [3]. The crystal structures of such 5-hydroxymethylpyrimidines display the one-dimensional hydrogen-bonded network created by O-H···O or O–H···N intermolecular interactions, involving primarily –OH moieties as donors [2-3]. In our further the studies on 4-aminopyrimidine we were mainly focused on its 5-aminomethyl derivatives and products of their cyclization with aldehyde, especially the 5-[(4-ethoxyanilino)methyl]-*N*-(4-fluorophenyl)-6-methyl-2-phenylpyrimidin-4-amine and its Schiff base [4]. Both of these compounds differ in conformation and interaction modes, molecules are linked into chains with N–H···N hydrogen bonds or C–H···O interactions and they also vary in also biological activities [4]. The presence of the –C=N– bond in the studied molecules increases their activity, indicating that 5-iminomethylpyrimidine could serve as a potent core for further drug discovery research.

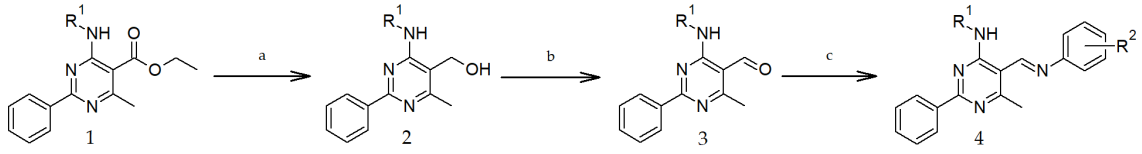

Scheme 1. The synthetic routes to studied compounds (R^1-allyl/aryl, R^2-aryl substituents). Conditions: a) $LiAlH_4$, THF; b) PCC, DCM, 3 h; c) aromatic amine, $In(OTf)_3$, 72 h.

Based on the above information and considering the need to discover and develop active agents, we synthesized ten new Schiff bases, 5-iminomethyl-6-methyl-2-

phenylpyrimidine derivatives (Scheme 1), bearing potentially biologically active functionalities and studied their cytotoxic activity *in vitro* towards the normal (RPTEC) and the cancer (AGS, HeLa, HepG2, A172, Caco-2) cell lines. The structures of the obtained compounds were established by spectroscopy techniques (ESI-MS, FTIR, ^{1}H and ^{13}C NMR). In order to extend the current knowledge about the features responsible for the biological activity of the new 5-iminomethylpyrimidine derivatives, the X-ray single-crystal analyses were carried out and their results are presented here for several newly obtained compounds.

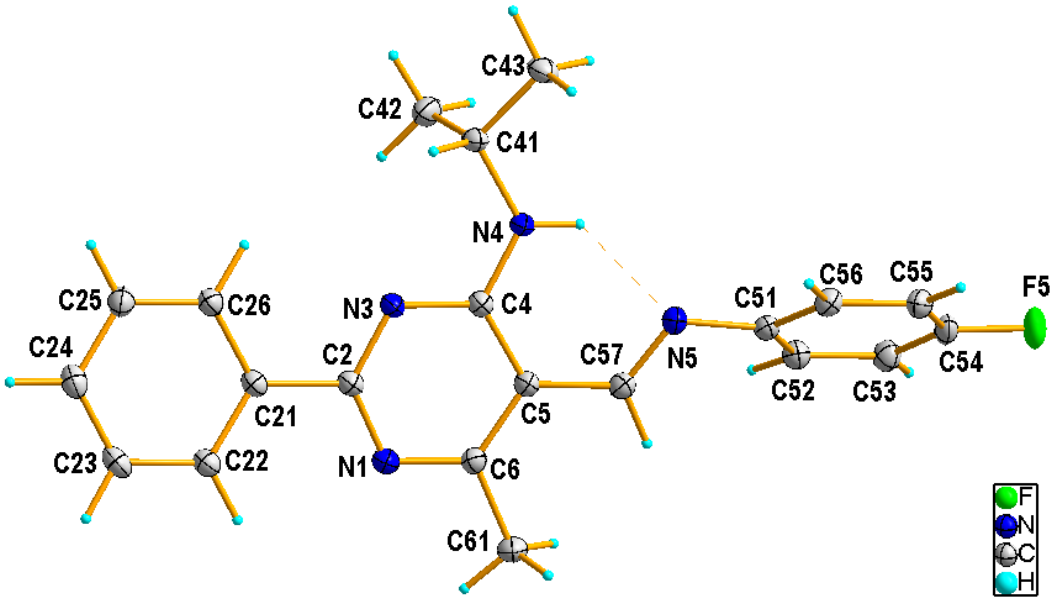

Fig. 1. The molecular structure of 5-{[(4-fluorophenyl)imino]methyl}-6-methyl-2-phenyl-N-(propan-2-yl)pyrimidin-4-amine, showing the atom-numbering scheme and displacement ellipsoids drawn at the 50% probability level. H atoms are shown as small spheres of arbitrary radii. The dashed line (in black) indicates the N–H···N hydrogen bond.

References

[1] J. Cieplik, M. Stolarczyk, J. Pluta, O. Gubrynowicz, I. Bryndal, T. Lis, M. Mikulewicz, *Acta Pol. Pharm*., **72** (2015) 53.
[2] M. Stolarczyk, I. Bryndal, A. Matera-Witkiewicz, T. Lis, K. Królewska-Golińska, M. Cieślak, J. Kaźmierczak-Barańska, J. Cieplik, *Acta Crystallogr. C*, **74** (2018) 1138.
[3] M. Stolarczyk, Agnieszka Matera-Witkiewicz, A. Wolska, M. Krupińska, A. Mikołajczyk, A. Pyra, I. Bryndal, *Materials*, **14** (2021) 6916.
[4] M. Stolarczyk, A. Wolska, A. Mikołajczyk, I. Bryndal, J. Cieplik, T. Lis, A. Matera-Witkiewicz, *Molecules*, **26** (2021) 2296.

P-08

ANIONIC SUBSTRUCTURES IN HYPODIPHOSPHATE SALTS AND CO-CRYSTALS OF HETEROCYCLIC COMPOUNDS

Daria Budzikur, Katarzyna Ślepokura

University of Wrocław, Faculty of Chemistry, 14. F. Joliot-Curie, 50-383 Wrocław

Heterocycles are organic compounds in which at least one atom in the ring is an element other than carbon. The most common heteroatoms are nitrogen, oxygen and sulphur. Many natural products and most drugs possess heterocyclic rings. Antibiotics, dyes of flowers and other plants, oxygen-transporting compounds in living organisms, as well as DNA components are heterocyclic compounds.

The first salts of hypodiphosphoric acid (PP) containing heterocyclic cations were described in 2018 [$(AdeH^+)_2(H_2P_2O_6)\cdot 2H_2O$ and $(AdeH^+)_2(H_2P_2O_6)$] as model systems for the study of hydrogen bonds in adenine-hypodiphosphate (Ade-PP) system, playing an important role in stabilizing the crystals of nucleoside hypodiphosphate esters [1]. Subsequent research on the organic hypodiphosphates focused on tetraalkylammonium [2], imidazolium [3] and aminopyridinium compositions [4]. It turned out that both the PP anions and the acid molecules tend to form inorganic substructures of diverse dimensionalities. Continuing our research, we present the results of X-ray structural studies of a series of hypodiphosphates containing non-aromatic heterocyclic cations. In pyrrolidinium hypodiphosphate $(PyrrH)_3(H_2P_2O_6)(H_3P_2O_6)\cdot(H_4P_2O_6)$ for example, a previously unexplored anion substructure architecture was observed (Fig. 1).

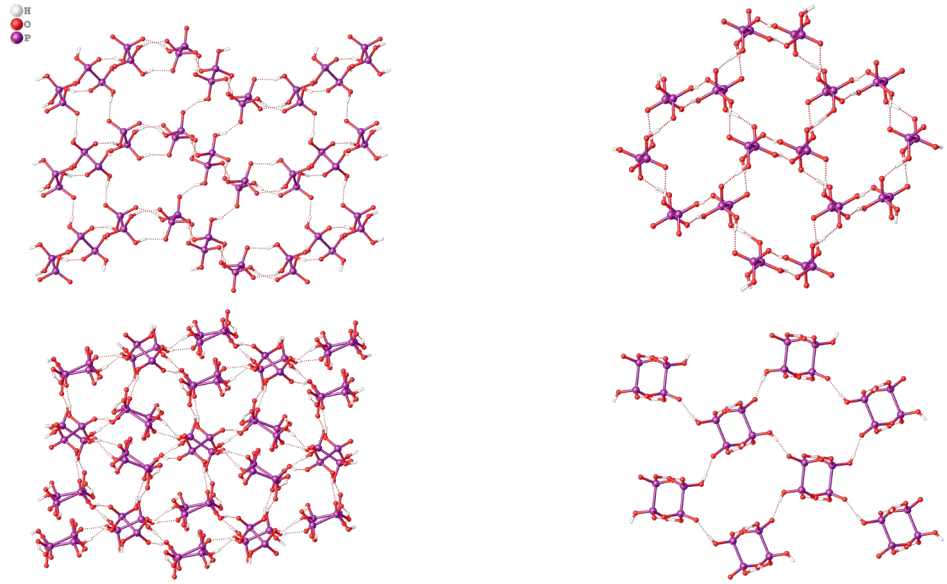

Fig. 1. Top and side views of different hypodiphosphate 3D substructures in $(PyrrH)_3(H_2P_2O_6)(H_3P_2O_6)\cdot(H_4P_2O_6)$ (left) and $(ThiazH)(H_3P_2O_6)$ (Thiaz – thiazolidine; right).

References

[1] M. Otręba, D. Budzikur, Ł. Górecki, K. Ślepokura, *Acta Cryst. C*, **74** (2018) 571.
[2] M. Emami, K. Ślepokura, M. Trzebiatowska, N. Noshiranzadeh, V. Kinzhybalo, *CrystEngComm*, **20** (2018) 5209.
[3] D. Budzikur, P. Szklarz, V. Kinzhybalo, K. Ślepokura, *Acta Cryst. B*, **76** (2020) 939.
[4] D. Budzikur, V. Kinzhybalo, K. Ślepokura, *CrystEngComm*, (2022) DOI: 10.1039/D2CE00261B.

P-09

STRUKTURY KRYSTALICZNE WIELORDZENIOWYCH SILANOTILANÓW CYNKU I KADMU Z PIPERAZYNĄ I 1,4-BIS(3-AMINOPROPYLO)PIPERAZYNĄ

Bartosz Cieśla, Agnieszka Pladzyk, Daria Kowalkowska-Zedler

Katedra Chemii Nieorganicznej, Wydział Chemiczny, Politechnika Gdańska, ul. Narutowicza 11/12, 80-233 Gdańsk

Związki kompleksowe pierwiastków o konfiguracji d^{10}, takich jak Zn(II) i Cd(II) wykazują ciekawe właściwości adsorpcyjne, luminescencyjne, czy też zdolność katalizowania reakcji chemicznych [1-5]. Z tego powodu, zainteresowanie tą grupą związków dalej utrzymuje się na wysokim poziomie i ukierunkowane jest na otrzymanie związków o pożądanych właściwościach.

W badaniach realizowanych przez naszą grupę wykorzystywane są ligandy silanotiolanowe, w tym tri-*tert*-butoksysilanotiol (tBuO)$_3$SiSH [6-8]. Związek pełni rolę tiolanowego liganda S-donorowego, a dzięki swej budowie i względnej odporności na hydrolizę pozwala na prowadzenie syntez w warunkach atmosferycznych i otrzymywanie związków kompleksowych o zróżnicowanych geometriach i budowie. W ramach badań, których wyniki zostaną zaprezentowane podczas konferencji otrzymano dwa nowe związki: wielordzeniowy [Cd{SSi(OtBu)$_3$}$_2$(μ-ppz)]$_n$ **(1)** (Rys. 1) i dwurdzeniowy [Zn$_2$\{SSi(OtBu)$_3$\}$_4$(μ-bapp)] **(2)** (Rys. 2). Związek **(1)** został otrzymany w reakcji [Cd{SSi(OtBu)$_3$}$_2$]$_2$ z piperazyną (ppz), natomiast związek **(2)** w reakcji Zn(acac)$_2$ z (tBuO)$_3$SiSH i 1,4-*bis*(3-aminopropylo)piperazyną (bapp).

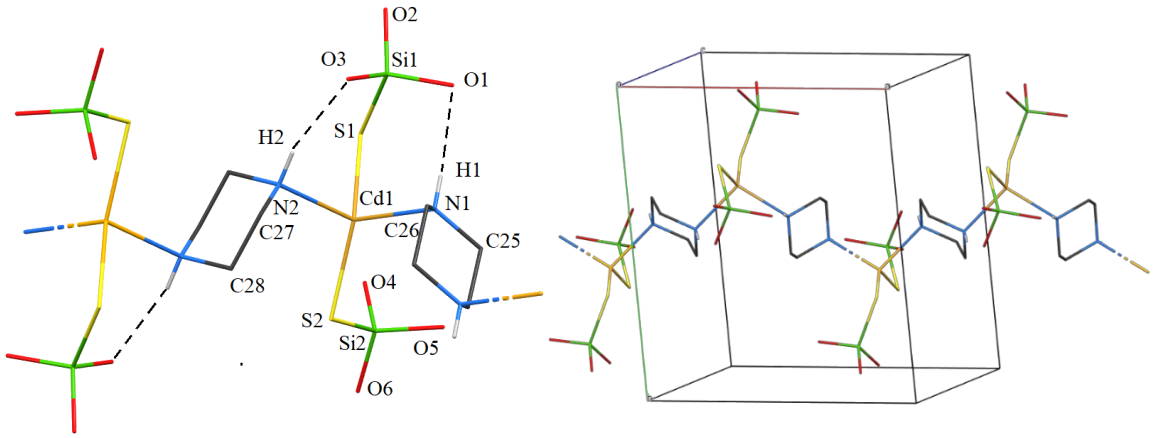

Rys. 1. Struktura molekularna związku **(1)** (po lewej) oraz jego upakowanie w komórce elementarnej, widok wzdłuż osi *c* (po prawej). Dla czytelności rysunku pominięto grupy *tert*-butylowe. Numeracja atomów dla części symetrycznie niezależnej.

Oba prezentowane związki kompleksowe **(1)** i **(2)** krystalizują w układzie trójskośnym w grupie przestrzennej *P*-1. Parametry komórki elementarnej wynoszą a=10,522(12), b=13,85(2), c=14,994(16) Å, α=66,58(12), β=85,85(9), γ=88,65(11)˚ oraz a=8,9281(3), b=14,4533(5), c=16,5969(5) Å, α=75,962(3), β=82,217(3), γ=79,017(3)˚, odpowiednio dla związku **(1)** oraz **(2)**. W obu przypadkach na centrach

metalicznych tworzą się rdzenie koordynacyjne o geometrii tetraedrycznej i wzorze MN_2S_2 (M=Cd dla **(1)**, M=Zn dla **(2)**).

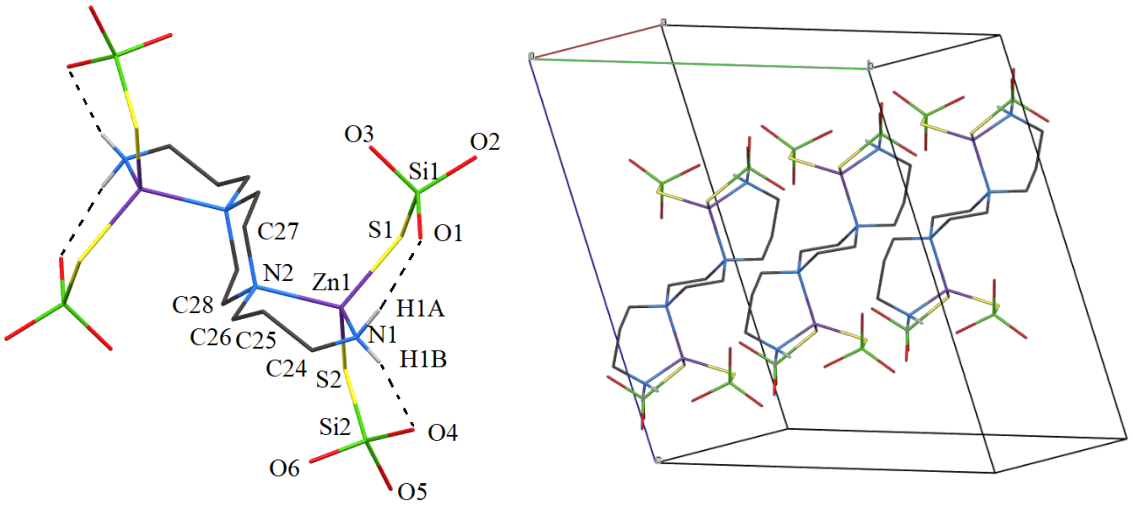

Rys. 2. Struktura molekularna związku **(2)** (po lewej) oraz jego upakowanie w komórce elementarnej, widok wzdłuż osi *a* (po prawej). Dla czytelności rysunku pominięto grupy *tert*-butylowe. Numeracja atomów dla części niezależnej.

W obydwu kompleksach centrum metaliczne jest koordynowane przez dwie reszty silanotiolanowe, pełniące rolę ligandów S-terminalnych. Zastosowanie różnych ligandów N-donorowych pozwoliło na powstanie różnych struktur kompleksów. W kompleksie **(1)** piperazyna pełni rolę liganda mostkowego łączącego kolejne jony Cd(II) tworząc 1D polimer koordynacyjny. Natomiast w związku **(2)** ligand bapp pełni rolę liganda mostkowego między jonami Zn(II) w strukturze dwurdzeniowego kompleksu, pełnią równocześnie rolę liganda N,N-chelatującego poszczególne centra metaliczne.

Struktura obydwu związków jest stabilizowana poprzez wewnątrzcząsteczkowe wiązania wodorowe typu N_{ppz}—H···O_{TBST} (D···A = 2.972(6) Å oraz 3.067(6) Å) **(1)** oraz N_{bapp}—H···O_{TBST} (D···A = 2.983(5) Å oraz 2.960(5) Å) **(2)**.

Dla otrzymanych związków planowane jest określenie ich właściwości spektralnych i termicznych.

Literatura

[1] A. Pladzyk *et al.*, *Coordination Chemistry Reviews*, **437** (2021) 213761.
[2] P. Maślewski *et al.*, *Inorg. Chim. Acta*, **459** (2017) 22–28.
[3] D. Kowalkowska-Zedler *et al.*, *CRYSTENGCOMM*, **19(25)** (2017) 3506–3518.
[4] A. Pladzyk *et al.*, *Chemistry – An Asian J.*, **10** (2015) 2388–2396.
[5] A. Pladzyk *et al.*, *OPTICAL MATERIALS*, **36(2)** (2013) 554–561.
[6] A. Herman *et al.*, *Z. anorg. allg. Chem.*, **450** (1979) 178–182.
[7] W. Wojnowski *et al.*, *Z annorg. allg. Chem.*, **403** (1974) 186–192.
[8] R. Piękoś *et al.*, *Z. anorg. allg. Chem.*, **318** (1962) 212–216.

P-10

STRUKTURA KRYSTALICZNA I ODDZIAŁYWANIA MIĘDZYCZĄSTECZKOWE W NOWYCH KOMPLEKSACH DIALKILOARYLOKSYGALOWYCH Z N-HETEROCYKLICZNYMI KARBENAMI

Anna M. Dąbrowska*, Izabela D. Madura, Paweł Horeglad

Wydział Chemiczny Politechniki Warszawskiej, ul. Noakowskiego 3, 00-664 Warszawa

**e-mail: anna.dabrowska.dokt@pw.edu.pl*

Kompleksy dialkiloaryloksygalowe z N-heterocyklicznymi karbenami (NHC) są nową i wciąż niepoznaną klasą kompleksów $R_2Ga(OR)NHC$. Kompleksy tego typu z ligandem *o*-metoksyfenylowym wykazują interesującą zmienność sposobu upakowania cząsteczek w kryształach – obecność grupy aryloksylowej pozwoliła np. zaobserwować nietypową wśród kompleksów dialkiloalkoksy- i dialkiloaryloksygalowych z NHC strukturę wykazującą porowatość.

Wszystko wskazuje na to, że dla kompleksów $Me_2Ga(OC_6H_4OMe)NHC$, budowa NHC jest głównym czynnikiem wpływającym na strukturę tych kompleksów w ciele stałym. Jak dotąd nie podjęto jednak próby analizy tej zależności. Zrozumienie jej jest istotne z punktu widzenia potencjalnego projektowania materiałów porowatych opartych na kompleksach galowych.

Na moim posterze zaprezentuję wyniki analizy zmian oddziaływań międzycząsteczkowych i ich hierarchizacji w kompleksach $Me_2Ga(OC_6H_4OMe)NHC$ w zależności od budowy N-heterocyklicznego karbenu, z wykorzystaniem karbenów symetrycznych i asymetrycznych (Rysunek 1).

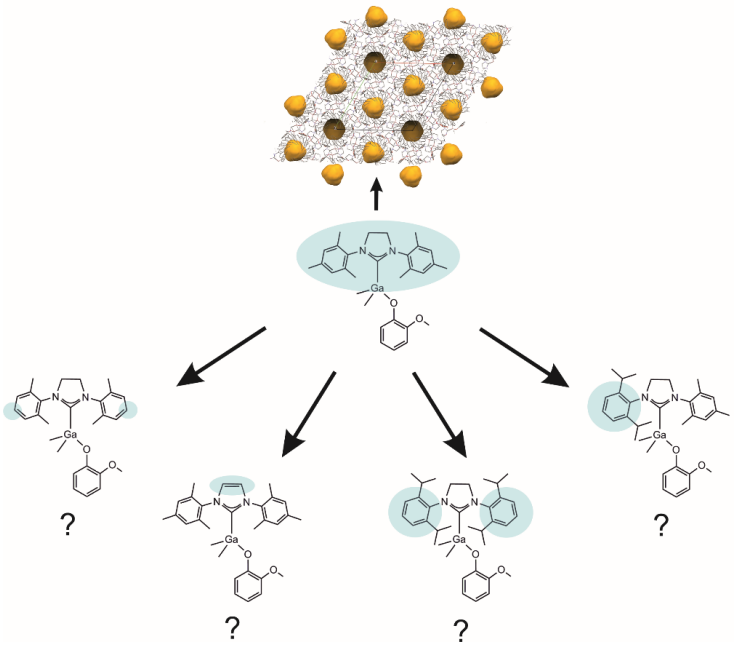

Rys. 1. Zastosowane modyfikacje NHC w kompleksach $Me_2Ga(OC_6H_4OMe)NHC$.

Badania finansowane były z grantu Preludium 2016/23/N/ST5/03338.

P-11

CRYSTAL STRUCTURE OF THE $ErNi_{4.09}Si_{0.91}$

Bohdana Belan[1], Mariya Dzevenko[2], Dorota A. Kowalska[3], Roman Gladyshevskii[1]

[1]Department of Inorganic Chemistry, Ivan Franko National University of Lviv, Kyryla i Mefodia Str. 6, 79005 L'viv, Ukraine
[2]Heroes of Kruty Lviv State Lyceum with enhanced military and physical training, Pasichna Str. 68, 79038 L'viv, Ukraine
[3]Institute of Low Temperature and Structure Research, Polish Academy of Sciences, ul. Okólna 2, 50-422 Wrocław, Poland

Interactions of the components in the Er-Ni-Si ternary system has been studied twice at two different temperatures. According to the authors [1], the 11 intermetallic compounds have been found at 870 K. Xiang Chen and co-authors have found 17 ternary compounds in this system at 770 K [2]. Among these compounds was ternary silicide $ErNi_4Si$, the crystal structure of which has been determined by X-ray powder method. This compound is isotypical to YNi_4Si structure type: space group *Cmmm* (#65) $a = 4.7918(6)$, $b = 8.1253(9)$, $c = 3.9131(2)$ Å [3].

We have succeded in the attempt to synthesize the $ErNi_4Si$ compound at 870 K. Our sample was prepared by melting the components under argon in an arc furnace and was annealed at 870 K under vacuum for 720 h. Single crystals were selected from the sample by mechanical fragmentation. The composition of the investigated single crystal was analyzed by EDS employing a scanning electron microscope (FEINovaNonoSEM 230) equipped with an EDAX Genesis XM4 spectrometer. The experimentally determined composition of the grain (17±2 at.% Er : 60±2 at.% Ni : 23±2 at.% Si) is rather close to the composition calculated from the structure refinement. The crystal structure of the $ErNi_4Si$ compound was investigated by X-ray single-crystal diffraction. X-ray diffraction was performed at room temperature on an Oxford Diffraction X'calibur four-circle diffractometer (Mo$K\alpha$ radiation). The structure was solved by direct methods and refined by the SHELX-2018/3 program package [4] with anisotropic atomic displacement parameters. The compound crystallizes in the YNi_4Si-type: space group *Cmmm*, Pearson code *oS*12, $Z = 2$; $a = 4.8516(10)$, $b = 8.4764(13)$, $c = 3.9629(5)$ Å, $V = 162.97(5)$ Å^3; $R1 = 0.0356$, $wR2 = 0.0895$, for 139 independent reflections with $I > 2\sigma(I)$ and 16 variables. The final atomic positional and displacement parameters of the compound are listed in the Table 1. The crystallographic positions 2*c* and 4*j* are fully occupied by Er and Ni, respectively. However, the positions 4*e* and 2*a* are occupied by the mixture of the Ni and Si atoms. Therefore, the refined composition of the compound can be described as $ErNi_{4.09}Si_{0.91}$.

The interatomic distances (δ), the values of interatomic distances reductions from the sum of atomic radii and coordination numbers of atoms for $ErNi_{4.09}Si_{0.91}$ are listed in Table 2 (values of the atomic radii are taken from [5]: r(Er) = 1.757 Å, r(Ni) = 1.240 Å, r(Si) = 1.170 Å). The majority of interatomic distances are in good agreement with the sum of atomic sizes. The projection of the crystal structure of $ErNi_{4.09}Si_{0.91}$ on the *ab*-plane and the coordination polyhedra of the atoms are shown in Fig. 1. The coordination polyhedra for the Er atoms have 20 vertices. The nickel atoms centre the icosahedra. Twelve neighbors surround the mixture of *M*1 and *M*2 atoms and their polyhedra can be described as slightly distorted icosahedra.

P-11

Table 1. Atomic coordinates and thermal displacement parameters for $ErNi_{4.09}Si_{0.91}$.

Atom	Wyckoff Site	*G*	*x*	*y*	*z*	U_{eq}, Å^2
Er	2*c*	1	1/2	0	1/2	0.0233(5)
Ni	4*j*	1	0	0.1677(2)	0	0.0193(6)
*M*1	4*e*	0.73Ni + 0.27Si	1/4	1/4	0	0.0219(8)
*M*2	2*a*	0.68Ni + 0.32Si	0	0	0	0.0210(7)

Atom	U_{11}	U_{22}	U_{33}	$U_{23} = U_{13}$	U_{12}
Er	0.0323(8)	0.0273(7)	0.0102(6)	0	0
Ni1	0.0265(13)	0.0259(12)	0.0055(10)	0	0
*M*1	0.040(2)	0.026(3)	0.012(2)	0	0
*M*2	0.0268(14)	0.0301(13)	0.0062(10)	0	0.0047(10)

Table 2. Interatomic distances (δ), Δ values ($\Delta = 100(\delta - \sum r)/\sum r$, where $\sum r$ is the sum of the respective atomic radii) and coordination numbers (CN) of $ErNi_{4.09}Si_{0.91}$ compound ($r(M1) = 0.73r_{Ni} + 0.27r_{Si}$, $r(M2) = 0.68r_{Ni} + 0.32r_{Si}$).

Atoms		δ, Å	Δ, %	CN	Atoms		δ, Å	Δ, %	CN
Er	4 Ni	2.8120	-6.2	20	Ni	4 *M*1	2.4260	-1.4	12
	2 Ni	2.8170	-6.0			2 *M*2	2.4390	-0.8	
	4 *M*2	3.1320	5.3			2 Ni	2.7980	12.8	
	8 *M*1	3.1440	5.6			2 Er	2.8120	-6.2	
	2 Er	3.9630	12.8			1 Er	2.8170	-6.0	
*M*1	4 Ni	2.4260	-1.4	12		1 Ni	2.8430	14.6	
	2 *M*1	2.4260	-0.7		*M*2	4 Ni	2.4390	-0.8	12
	2 *M*2	2.4420	0.1			4 *M*1	2.4420	0.1	
	4 Er	3.1440	5.6			4 Er	3.1320	5.3	

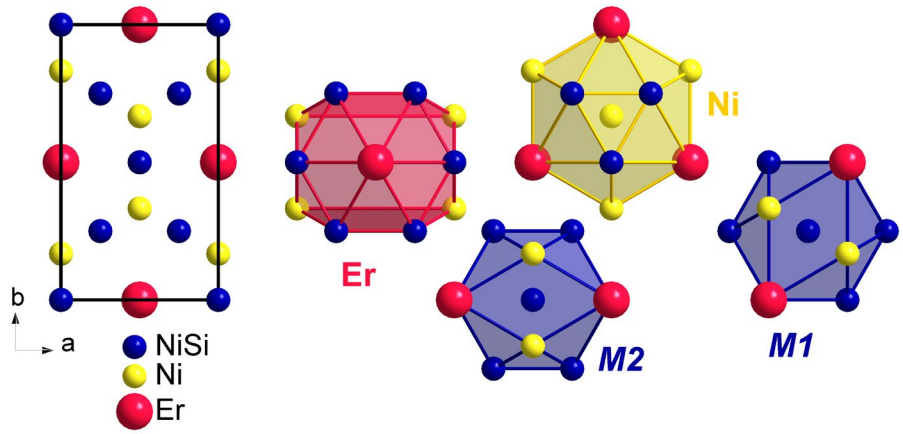

Fig. 1. A projection of the $ErNi_{4.09}Si_{0.91}$ unit cell on *ab*-plane (left) and view of the coordination polyhedra of the atoms (right).

Literature

[1] Matvijishyn R. *Thesis*, Lviv National University, 2010 (in Ukraine).
[2] Xiang Chen, Chao Ni, Dang-Chao Wang, J. Phase Equilib. Diffus., **41** (2020) 138–147.
[3] Villars P., Cenzual K., Eds. *Pearson's Crystal Data: Crystal Structure Database for Inorganic Compounds* (release 2018/19); ASM International®: Materials Park, Ohio (USA), 2018.
[4] G.M. Sheldrick, *Acta Crystallogr. A* **64** (2015) 3-8.
[5] J. Emsley, *The Elements*, 3-th edition. Oxford University Press, Oxford, 1998.

P-12

NEW STRUCTURE TYPE OF THE $Pr_3Ni_4Si_2$

Bohdana Belan[1], Mariya Dzevenko[2], Marek Daszkiewicz[3], Roman Gladyshevskii[1]

[1]Department of Inorganic Chemistry, Ivan Franko National University of Lviv, Kyryla i Mefodia Str. 6, 79005 L'viv, Ukraine
[2]Heroes of Kruty Lviv State Lyceum with enhanced military and physical training, Pasichna Str. 68, 79038 L'viv, Ukraine
[3]Institute of Low Temperature and Structure Research, Polish Academy of Sciences, ul. Okólna 2, 50-422 Wrocław, Poland

The exploration of Pr-Ni-Si system has been represented only by testing the existence of compounds with definite composition or structure [1]. During our investigation of this system, we have found the new compound $Pr_3Ni_4Si_2$. Herein we present the results of the crystal structure determination of $Pr_3Ni_4Si_2$, which is the first representative of a new structure type.

The sample with composition $Pr_{33.3}Ni_{44.4}Si_{22.2}$ was melted under argon in an arc furnace, and annealed at 870 K under vacuum for 350 h. Single crystals were selected from the sample by mechanical fragmentation. They exhibit metallic lustre whereas the ground powders are dark grey. The reflections intensities were measured with graphite-monochromatized Mo *K*α radiation on an Xcalibur Atlas CCD diffractometer. The structure was refined by the full-matrix least-squares method on F^2 using SHELXL-2018/3 [2]. The composition of the investigated single crystal was analyzed in a scanning electron microscope (FEINovaNonoSEM 230) with an EDAX Genesis XM4 spectrometer. The experimentally determined composition of the grain (39±2 at.% Pr : 48±2 at.% Ni : 13±2 at.% Si) is rather close to the composition calculated from the structure refinement.

The present investigation led to the following data for the crystal structure and the refined composition $Pr_3Ni_4Si_2$: own structure type, Pearson symbol *mS*36, space group *C*2/*c*, a = 15.710(2), b = 5.8354(9), c = 7.4442(11) Å, β = 102.004(15), R = 0.0664, R_w = 0.1531. The refined atomic coordinates and displacement parameters are the following: Pr1: 4*e*, 0, 0.3779(4), ¼, U_{eq} = 0.0188(6) Å^2; Pr2: 8*f*, 0.84606(10), 0.1099(3), 0.55036(19), U_{eq} = 0.0201(6) Å^2; Ni1: 8*f*, 0.0355(2), 0.1489(6), 0.6113(4), U_{eq} = 0.0212(9) Å^2; Ni2: 8*f*, 0.2870(2), 0.1545(6), 0.6629(5), U_{eq} = 0.0221(9) Å^2; Si: 8*f*, 0.3395(5), 0.1089(13), 0.3921(10), U_{eq} = 0.0181(17).

The interatomic distances (δ), the values of interatomic distances reductions from the sum of atomic radii and coordination numbers of atoms for $Pr_3Ni_4Si_2$ listed in Table 1 (values of the atomic radii are taken from [3]: r(Pr) = 1.877 Å, r(Ni) = 1.240 Å, r(Si) = 1.170 Å). The majority of interatomic distances are in good agreement with the sum of atomic sizes. Some Ni-Pr interatomic distances are rather short and one Pr2-Si is longer in comparison with the sum of the respective atomic radii.

The projection of the crystal structure of $Pr_3Ni_4Si_2$ on the *ac*-plane and the coordination polyhedra of the atoms are shown in Fig. 1. The coordination polyhedra for the Pr atoms have from 19- to 20- vertices and consist of the atoms of all sorts. The coordination polyhedrons of the Ni1 atoms (CN = 9) can be described as distorted icosahedra. Ten neighbors surround both the Ni2 and Si atoms.

P-12

Table 1. Interatomic distances (δ), Δ values ($\Delta = 100(\delta - \sum r)/\sum r$, where $\sum r$ is the sum of the respective atomic radii) and coordination numbers (CN) of $Pr_3Ni_4Si_2$ compound.

Atoms		δ, Å	Δ, %	CN	Atoms		δ, Å	Δ, %	CN
Pr1	2 Ni1	2.951(7)	-3.8	20	Ni1	1 Si	2.424(0)	0.6	9
	2 Ni1	3.040(3)	-0.9			1 Ni1	2.498(10)	0.7	
	2 Si	3.226(12)	7.6			1 Ni1	2.544(13)	2.6	
	2 Si	3.266(29)	8.9			1 Pr2	2.812(24)	-8.3	
	2 Ni2	3.279(9)	6.9			1 Pr2	2.850(11)	-7.1	
	2 Ni1	3.327(2)	8.4			1 Pr2	2.925(7)	-4.7	
	2 Pr2	3.830(13)	4.8			1 Pr1	2.951(7)	-3.8	
	2 Pr2	3.936(13)	7.7			1 Pr1	3.040(3)	-0.9	
	2 Pr2	3.942(19)	7.8			1 Pr1	3.327(2)	8.4	
	2 Pr1	3.986(0)	9.0		Ni2	1 Si	2.317(9)	-3.9	10
Pr2	1 Ni2	2.809(17)	-8.4	19		1 Si	2.346(10)	-2.7	
	1 Ni1	2.812(24)	-8.3			1 Si	2.384(5)	-1.1	
	1 Ni1	2.850(11)	-7.1			1 Ni2	2.702(15)	9.0	
	1 Ni1	2.925(7)	-4.7			1 Pr2	2.809(17)	-8.4	
	1 Ni2	2.992(4)	-2.5			1 Pr2	2.992(4)	-2.5	
	1 Si	3.047(1)	1.6			1 Pr2	3.156(12)	2.9	
	1 Si	3.134(1)	4.5			1 Pr1	3.279(9)	6.9	
	1 Si	3.146(1)	4.9			1 Pr2	3.294(19)	7.4	
	1 Ni2	3.156(12)	2.9			1 Pr2	3.462(3)	12.8	
	1 Si	3.291(5)	9.8		Si	1 Ni2	2.317(9)	-3.9	10
	1 Ni2	3.294(19)	7. 4			1 Ni2	2.346(10)	-2.7	
	1 Pr2	3.377(10)	-7.6			1 Ni2	2.384(5)	-1.1	
	1 Ni2	3.462(3)	12.8			1 Ni1	2.424(0)	0.6	
	1 Pr1	3.830(13)	4.8			1 Pr2	3.047(1)	1.6	
	1 Si	3.918(35)	30.7			1 Pr2	3.134(1)	4.5	
	1 Pr1	3.936(13)	7.7			1 Pr2	3.146(1)	4.9	
	2 Pr2	3.937(1)	7.7			1 Pr1	3.226(12)	7.6	
	1 Pr1	3.942(19)	7.8			1 Pr1	3.266(29)	8.9	
						1 Pr2	3.291(5)	9.8	

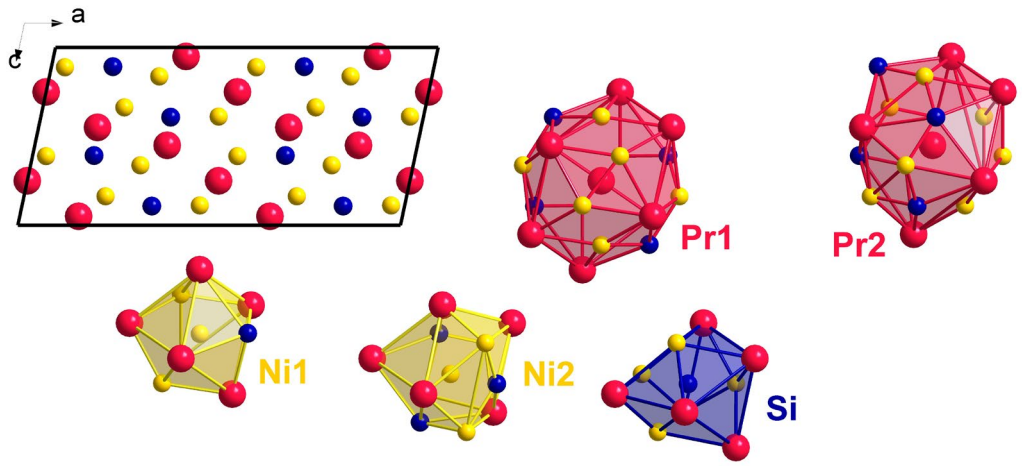

Fig. 1. A projection of the $Pr_3Ni_4Si_2$ unit cell on *ac*-plane and a view of the coordination polyhedra of the atoms.

Literature

[1] Villars P., Cenzual K., Eds. *Pearson's Crystal Data: Crystal Structure Database for Inorganic Compounds* (release 2018/19); ASM International®: Materials Park, Ohio (USA), 2018.

[2] G.M. Sheldrick, *Acta Crystallogr. A* **64** (2015) 3-8.

[3] J. Emsley, *The Elements*, 3-th edition. Oxford University Press, Oxford, 1998.

P-13

THE RESULTS OF SYNTHESIS AND STRUCTURAL ANALYSIS OF GOLD(III) COMPLEXES WITH 3-CYANOPYRIDINE AND 2-CYANOPYRIDINE

Maciej Ejnik, Anna Ciborska, Anna Dołęga

Department of Inorganic Chemistry, Faculty of Chemistry,
Gdansk University of Technology, Narutowicza 11/12, 80-233 Gdańsk

Cyanopyridines are pyridine derivatives with nitrile group attached to the aromatic ring. Three isomers are possible, which differ in the position of the nitrile group and these are 2-, 3- and 4-cyanopyridine. The compounds may act as monodentate ligands in metal complexes, due to the lone electron pair, located on the basic, pyridyl nitrogen. They may also function as bridging ligands, however the nitrile nitrogen is weaker base than pyridinic one, therefore it less often acts as an electron donor.[1] So far only one structure of gold complex with cyanopyridine has been reported , the one with 4-cyanopiridine.[2]

Here we present the results of structural analysis of two molecular gold complexes with 2-cyanopyridine (compound **1**) and 3-cyanopyridine (compound **2**). The formulas of the complexes are shown in Scheme I and the molecular structures in Figure 1. The compounds were obtained by direct reactions of the chloroauric acid and the respective cyanopyridine isomer. Both reactions were carried out in acetonitrile, however compound **2** crystallized directly from the reaction mixture, whilst crystals of compound **1** were obtained by recrystallization carried out in methanol.

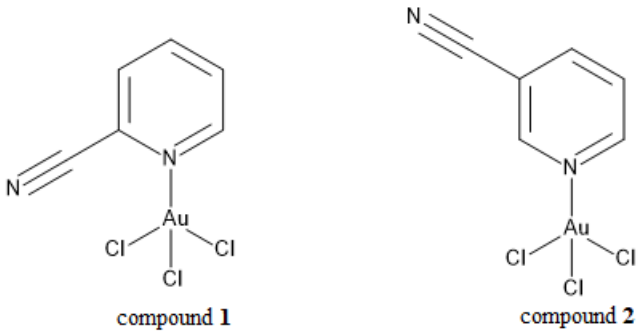

Scheme 1. Formulas of compound **1** and compound **2**.

The inability of compound **1**, to crystallize directly from reaction mixture, was associated with different molecular interactions, ensuing from differences in ligand structure. These issues will be further discussed in a poster.

Compound **1** crystallizes in a $P2_1/c$ symmetry group of a monoclinic system with a = 10.2825(4) Å, b = 6.9557(4) Å, c = 13.8459(5) Å, β= 100.834(3)°. The gold atom is characterized by a coordination number C.N. equal to 4. The geometry of the compound can be therefore characterized by the geometric index τ_4 which, for discussed compound, is equal to 0.034. It indicates, that discussed geometry is almost purely square planar.[3]

P-13

The central Au1 atom in **1** is connected to three chlorine atoms by bonds, two of which slightly differ by length: Au1–Cl2 2.276(1) Å, and Au1–Cl3 2.280(1) Å, whereas third bond is significantly shorter: Au1–Cl1 2.257(1) Å. Central gold atom Au1 is also bonded to pyridinic nitrogen atom N1 by the shortest of discussed bonds Au1–N1 2.046(3) Å.

Compound **2** crystallizes in a $P2_1/n$ symmetry group of a monoclinic system with a = 10.6363(19) Å, b = 6.7871(13) Å, c = 13.955(2) Å, β = 103.476(14)°. The gold atom is also characterized by coordination number C.N. = 4, with yet lower geometric index parameter τ_4, which for the discussed compound is equal to 0.022.

The central Au1 atom is bonded to three chlorine atoms by bonds, which lengths are more differentiable than in compound **1**, however there is still a possibility to indicate a pair of bonds with more consistent lengths: respectively Au1–Cl2 2.261(1) Å and
Au1–Cl 3 2.269(2) Å and a third bond, noticeably longer than two others: Au1–Cl1 2.286(2) Å. Central gold atom Au1 is also bonded to pyridinic nitrogen atom N1 by the shortest of discussed bonds Au1–N1 2.047(5) Å.

The details of the crystal structures of both complexes, explanations of the differences in crystal packing as well as comparison of all three complexes will be further discussed in a poster.

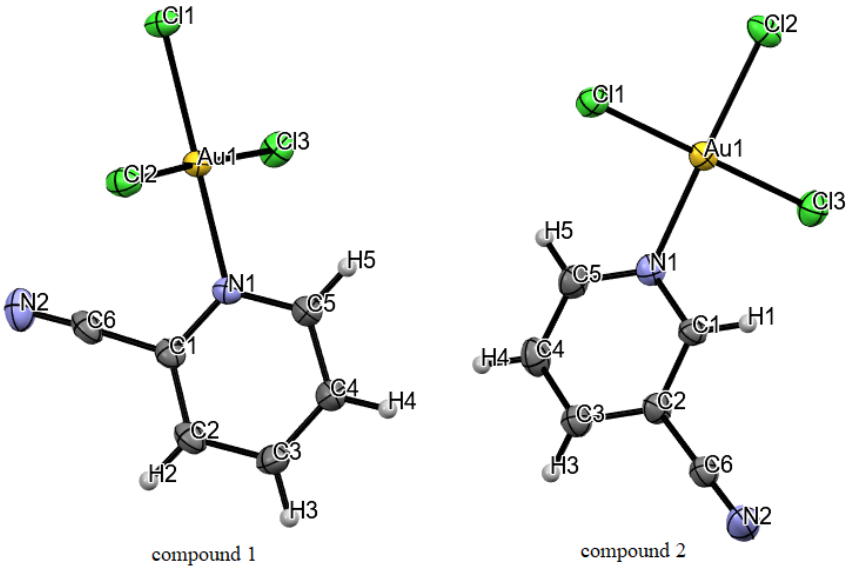

Fig 1. Molecular structures of compound **1** and compound **2**.

References

[1] K. Gutmańska, A. Ciborska, Z. Hnatejko, A. Dołęga, *Polyhedron*, **220** (2022) 115831
[2] R. Mohammad-Nataj, A. Abedi, V. Amani, *Synth. React. Inorg. Met. Org. Chem.*, **43** (2013) 1375.
[3] L Yang, D.R Powell, R.P. Houser, *Dalton Trans.*, **9** (2007) 955.

P-14

SYNTEZA I CHARAKTERYSTYKA N,C–METALOCYKLICZNYCH ZWIĄZKÓW PALLADU (II) OTRZYMANYCH NA DRODZE FUNKCJONALIZACJI WIĄZANIA C–H

Jarosław Fornalski, Nurbey Gulia

Wydział Chemii, Uniwersytet Wrocławski, ul. F. Joliot-Curie 14, 50-383 Wrocław

Związki metalocykliczne stanowiące produkt pośredni w reakcji funkcjonalizacji wiązania C–H, cieszą się niemalejącym zainteresowaniem świata nauki [1]. Powodem jest szeroka gamma reakcji organicznych wykorzystujących zjawisko prekoordynacji w celu selektywnej funkcjonalizacji słabo reaktywnych wiązań C–H. Pallad jest metalem wysoce reaktywnym w tym ujęciu, dlatego jego związki są często wykorzystywane jako katalizatory aktywacji C–H. Wybrane do badań układy są produktami pośrednimi w reakcjach funkcjonalizacji wiązań C(sp^2)–H. [3][4]

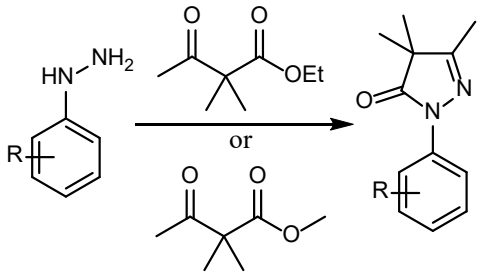

W ramach przeprowadzonych badań otrzymano N,C-metalocykliczne związki palladu (II) na drodze bezpośredniej funkcjonalizacji wiązania C–H. Badane układy reprezentują cyklometalację na węglu o hybrydyzacji sp^2. Przebieg reakcji prowadzono w różnych warunkach i przy zmiennej stechiometrii ligandu/metalu. Otrzymane związki kompleksowe zbadano metodami spektroskopowymi oraz rentgenografia strukturalną. Rysunki poniżej prezentują struktury zbadanych związków palladu (II).

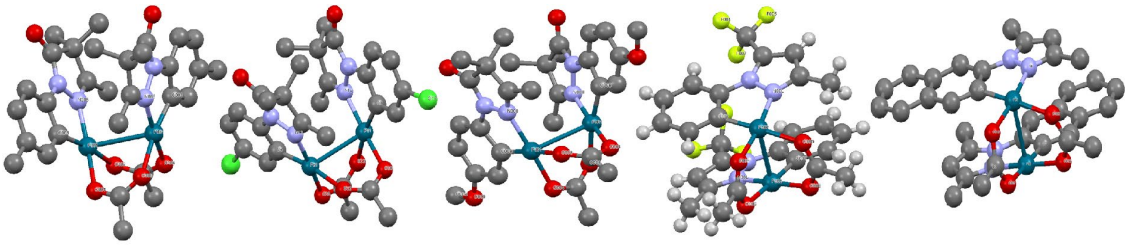

Literatura

[1] N. Gulia, O.Daugulis, *Angew. Chem. Int. Ed.,* **2017**, 56, 3630.
[2] S. H. Kwak, N. Gulia, O. Daugulis, *J. Org. Chem*., **2018**, 83, 5844.
[3] A. K. Cook, M. S. Sanford, *J. Am. Chem. Soc.,* **2015**, 3109-3118.
[4] Z. Ren, G. Dong, *Organometallic*, **2016**, 1057-1059.

P-15

SQUARIC ACID COMPLEXES WITH PYRIDINE CARBOXYLIC ACID ISOMERS – X-RAY, THERMAL AND THEORETICAL STUDIES

Mateusz Gołdyn[a,*], Julia Skowronek[a], Elżbieta Bartoszak-Adamska[a], Anna Komasa[a], Aneta Lewandowska[b], Zofia Dega-Szafran[a]

[a] *Crystallography Department, Faculty of Chemistry, Adam Mickiewicz University, Uniwersytetu Poznańskiego 8, 61-614 Poznań*
[b] *Department of Polymers, Faculty of Chemical Technology, Institute of Chemical Technology and Engineering, University of Technology, Berdychowo 4, 60-965 Poznań*

**e-mail: mateusz.goldyn@amu.edu.pl*

Looking for new medicinal substances with specific pharmacological properties as well as satisfactory physicochemical parameters, like good solubility and permeability, low toxicity, thermal or chemical stability, is one of the goals of pharmaceutical industry. Often these substances need to be modified to improve their properties. One of the way is the synthesis of drug-containing molecular or ionic complexes (cocrystals or salts) by numerous techniques[1]. It is critical to design cocrystallizations by selecting an appropriate coformer based on the knowledge of crystal engineering tools[2].

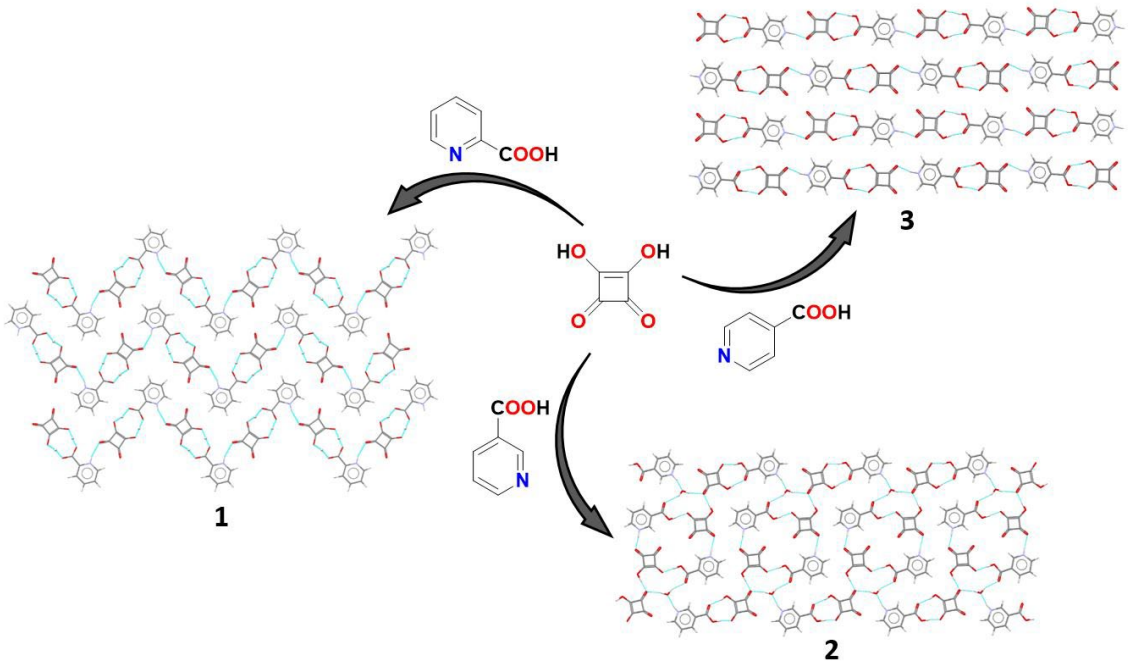

Fig. 1. Pyridine carboxylic acid cocrystallization with squaric acid as a coformer leading to **1**, **2** and **3** complexes (**1**– picolinic acid squaric acid adduct, **2** – nicotinium hydrogen squarate hemihydrate, **3** – isonicotinium hydrogen squarate).

Pyridine carboxylic acids, biologically active compounds have been cocrystallized with squaric acid (3,4-dihydroxycyclobut-3-ene-1,2-dione), increasingly

used as an organic reagent. Squaric acid and its derivatives show promising pharmacological properties[3]. The crystal structure of adducts **1**, **2** and **3** obtained by solution cocrystallization was determined using single-crystal X-ray diffraction. Structural studies showed the ionic nature of **2** and **3**, while **1** was classified as a salt-cocrystal continuum. Molecules in the crystal lattice of **1**, **2** and **3** are connected by strong O–H···O and N–H···O hydrogen bonds. In the structures optimized at the APF-D/6-311++G(d,p) level of theory, no proton migration from the squaric acid to the zwitterionic form of the pyridine carboxylic acid was observed. The complexes show high density, determined by X-ray measurements (1.638 – 1.677 gcm^{-3}). Thermal analysis reveals high thermal stability of obtained adducts. The values of their melting point are in the range of 260-280 ^{o}C.

Acknowledgement
MG thanks the National Science Centre (grant PRELUDIUM no. 2021/41/N/ST5/00503) for financial support and Adam Mickiewicz University for funds from the Initiative of Excellence – Research University (IDUB) program obtained in the PhD Minigrants competition no. 017 (research grant no. 017/02/SNŚ/0005). The computations supported in part by PL-Grid Infrastructure were performed at the Poznań Supercomputing and Networking Center. MG and EBA thank prof. Maria Gdaniec for the fruitful discussions on twinning.

References

[1] A. Karagianni, M. Malamatari and K. Kachrimanis, *Pharmaceutics*, 2018, 10, 18.
[2] G. R. Desiraju, *Crystal Engineering: The Design of Organic Solids*, Elsevier, 1989.
[3] J. Chasák, V. Šlachtová, M. Urban and L. Brulíková, *Eur J Med Chem*, 2021, 209, 112872.

P-16

STRUCTURE - ACTIVITY RELATIONSHIP OF AMIDRAZONE DERIVATIVES

Klaudia Górska[1], Małgorzata Szczesio[1], Katarzyna Gobis[2], Izabela Korona-Głowniak[3]

[1] Institute of General and Ecological Chemistry, Faculty of Chemistry, Lodz University of Technology, 116 Żeromskiego Street, 90-924 Lodz, Poland
[2] Department of Organic Chemistry, Medical University of Gdansk, M. Skłodowskiej-Curie 3a Street, 80-210 Gdansk, Poland
[3] Department of Pharmaceutical Microbiology, Medical University of Lublin, Chodźki 1, 20-093 Lublin, Poland

Tuberculosis (TB) is a well-known disease that is caused by the *Mycobacterium tuberculosis* bacteria. Due to occurrence of resistant strains, it is still highly dangerous. Until the coronavirus pandemic, TB was the leading cause of death from a single infectious agent [1].

Amidrazones derivatives show significant antituberculosis activity [2]. Therefore, three new ones were synthesized. Their structures confirmed by the single crystal X-ray diffraction. Their antibacterial and antifungal activities were evaluated and ADMET analysis was also performed.

The packing of compounds in the element cell and the interactions were analysed. All of them have showed intermolecular hydrogen bonds and additionally compound **3** pi - stacking interactions. Moreover, **2** was crystallized in zwitterionic form.

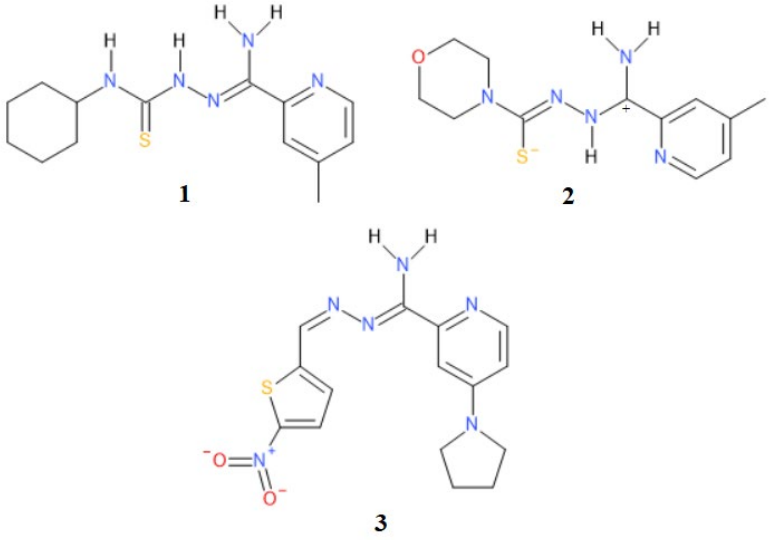

Rys. 1. Chemical structures of compounds **1**, **2** and **3**.

References

[1] Global Tuberculosis Report 2021 [accessed: 11.06.2022 https://www.who.int/ health-topics/ tuberculosis#tab=tab_1].

[2] L. Mazur, J. Saczewski, K. N. Jarzembska, K. Szwarc-Karabyka, R. Paprocka, and B. Modzelewska-Banachiewicz, *CrystEngComm.*, **20** (2018) 29.

P-17

ZWIĄZKI INTERKALACYJNE TLENKU ARSENU(III) Z CHLORKAMI LITOWCÓW

Piotr A. Guńka

Wydział Chemiczny, Politechnika Warszawska, ul. Noakowskiego 3, 00-664 Warszawa

Tlenek arsenu(III) tworzy stechiometryczne związki z halogenkami potasu i amonu. Zostały one odkryte już w XIX wieku, ale do połowy XX wieku nie została określona struktura krystaliczna tych związków.[1-4] Połączenia te okazały się związkami interkalacyjnymi, w których elektrycznie naładowane warstwy, zbudowane z równoimiennych jonów, są ułożone naprzemiennie i rozdzielone przez elektrycznie obojętne warstwy As_2O_3 (patrz Rysunek 1). Interkalaty, zawierające kationy potasu i amonu ,zbudowane są z heksagonalnych, niepofałdowanych warstwy As_2O_3, zaś te, zawierające mniejsze kationy sodu, zbudowane są z pofałdowanych warstw tlenkowych o niższej symetrii.[3,4]

W tym wystąpieniu przedstawiona zostanie struktura pierwszych uwodnionych związków interkalacyjnych tlenku arsenu(III) chlorkami potasu, rubidu i cezu o wzorze ogólnym $MCl{\cdot}As_2O_3{\cdot}½H_2O$ (gdzie M = K, Rb, Cs) oraz $KCl{\cdot}As_2O_3{\cdot}3H_2O$. Struktura tych połączeń opisana została zarówno z wykorzystaniem metod dyfrakcyjnych jak również spektroskopowych takich jak spektroskopia rezonansu jądrowego w ciele stałym oraz spektroskopia w podczerwieni ATR-FTIR.

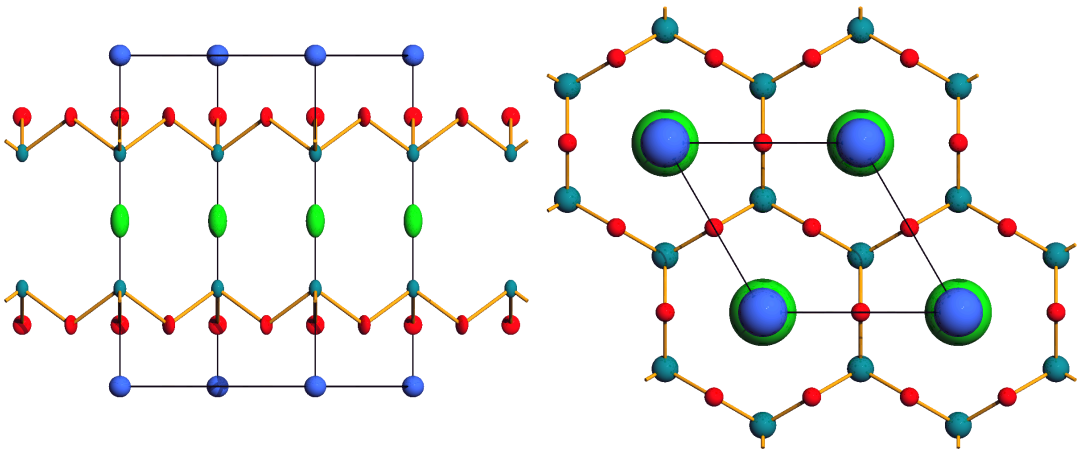

Rys. 1. Struktura krystaliczna interkalatu $KCl{\cdot}2As_2O_3$. Widok wzdłuż kierunku [120] (po lewej) i [001] (po prawej). Anizotropowe czynniki temperaturowe zaznaczono z prawdopodobieństwem 50% po lewej stronie, zaś po prawej stronie zastosowano model prętowo-kulowy. Atomy As, K, Cl i O zostały zaznaczono kolorami odpowiednio ciemnozielonym, niebieskim, jasnozielonym i czerwonym.

Literatura

[1] F. Rüdorff ,*Ber. Dtsch. Chem. Ges.* **19** (1886) 2668.
[2] M. Edstrand, G. Blomqvist, *Arkiv för kemi.* **8** (1955) 245.
[3] F. Pertlik, *J. Solid State Chem.* **70** (1987) 225.
[4] F. Pertlik, *Monatsh. Chem.* **119** (1988) 451.

P-18

ANTIMONY(III) PHTHALOCYANINE COMPLEXES OBTAINED IN OXIDATION CONDITIONS

Jan Janczak

Institute of Low Temperature and Structure Research, Polish Academy of Sciences, Okólna 2, 50-422 Wrocław, Poland

Phthalocyanine and its metal complexes are still very intensively studied due to their various technological applications. However, the metallophthalocyanines with group 15 elements were ignored for a long time until the first derivatives of bismuth and antimony were identified [1,2], and their structural characterizations are still less explored [3]. The variable valency of these metals depending on the reaction conditions (III or V) can lead to the formation of various MPc derivatives. SbPc derivatives can be promising candidates for new drugs because they are stable, powerful electron donors/acceptors, and some derivatives undergo facile Sb^{III}/Sb^{V} conversion under mild conditions

In the present work, the synthesis, X-ray structural characterization of novel antimony(III) phthalocyanine complexes obtained by direct reaction of antimony powder with phthalonitrile under iodine vapor atmosphere, $(Sb^{III}Pc)(I_3)\cdot\frac{1}{2}(I_2)$ – (**1**) or iodine monobromide atmosphere, $[(SbPc)_2(Sb_2I_8)(SbBr_3)]_2$ – (**2**) are reported. Both complexes crystallize in the centrosymmetric space group of the triclinic system with two molecules per unit cell. The molecular structures of the asymmetric unit of $(Sb^{III}Pc)(I_3)\cdot\frac{1}{2}(I_2)$ – (**1**) and $[(SbPc)_2(Sb_2I_8)(SbBr_3)]_2$ – (**2**) are illustrated in Figure 1.

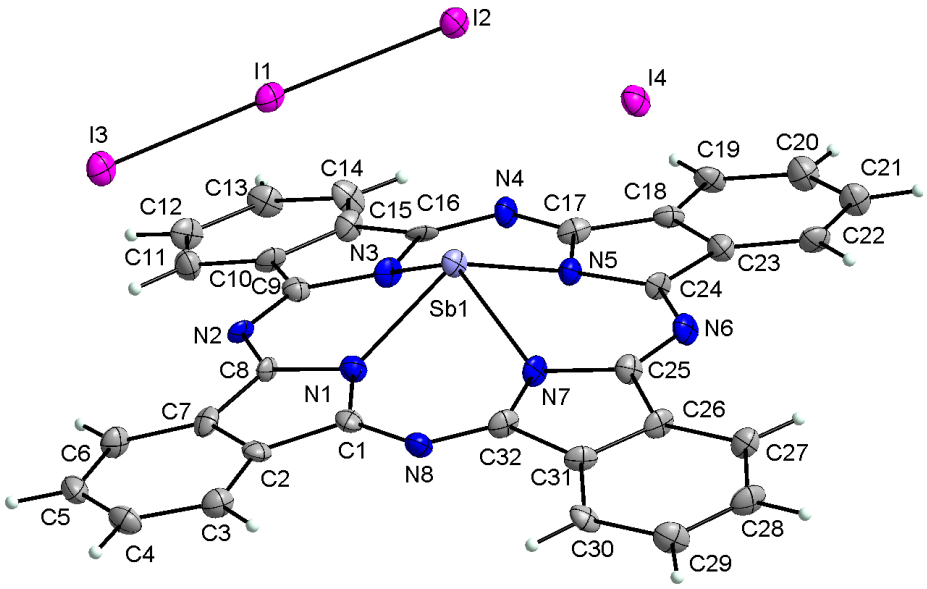

(a)

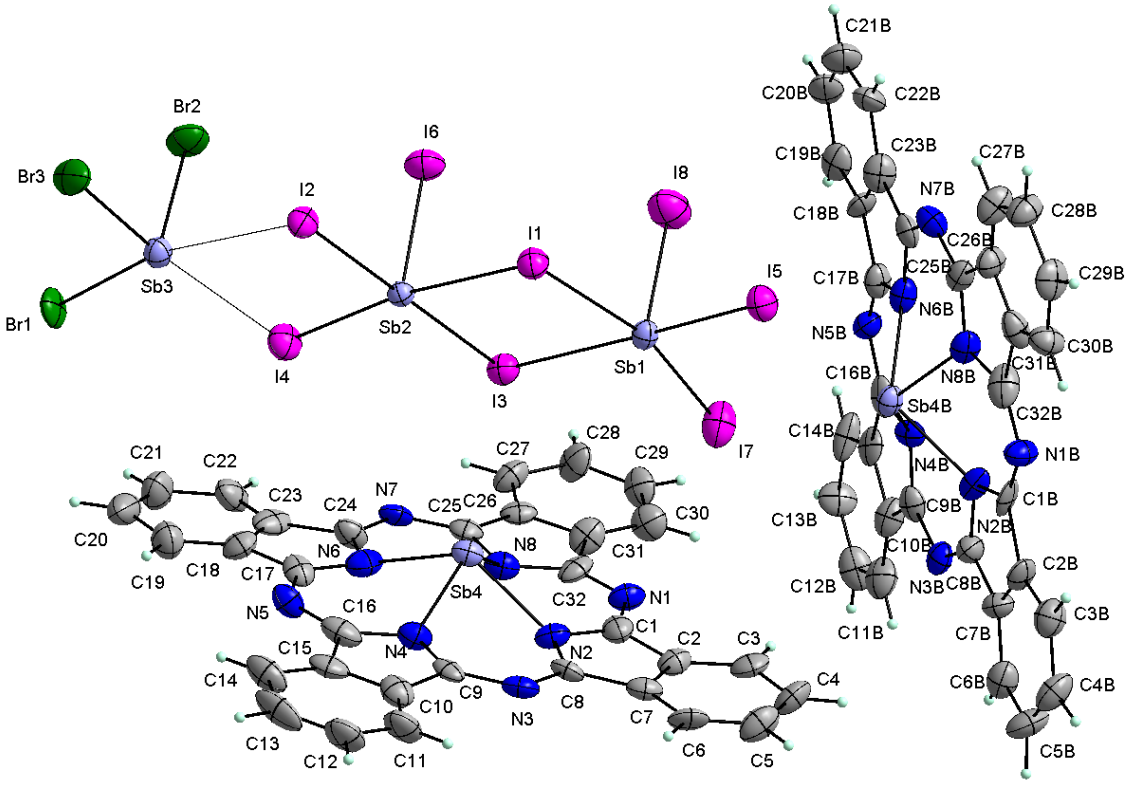

(b)

Fig. 1. View of the asymmetric unit of **1** (a) and **2** (b).

Details of the structures of both antimony(III) phthalocyanine complexes as well as their optical properties will be presented on poster. Moreover, the oxidation process of both antimony(III) phthalocyanine complexes to antimony(V) phthalocyanine complexes monitored by UV-Vis will be presented. Both investigated antimony(III) phthalocyanine complexes are intriguing from the point of view of potential use as an infrared cut-off filter for plasma displays, silicon photodiodes or charge-generating material.

References

[1] (a) H.Isago, Y. Kagaya, *Bull. Chem. Soc. Jpn*. **67** (1994) 383–389; (b) H. Isago, Y. Kagaya, *Bull. Chem. Soc.Jpn.* **69** (1996) 1281–1288.

[2] (c) H. Isago, Y. Kagaya, S.-L. Nakajima, *Chem Lett.* **32** (2003) 112–113; (d) H. Isago, K. Miura, M. Kanesato, *J. Photochem. Photobiol. A: Chem*. **197** (2008) 313–320.

[3] (a) R. Kubiak, M. Razik, *Acta Cryst*. C**54** (1998) 583–485; (b) R. Kubiak, J. Janczak, M. Razik, *Inorg. Chim. Acta* **293** ((1999) 155–159; (c) J. Janczak, R. Kubiak, A. Jezierski, *Inorg. Chem*. **38** (1999) 2043–2049; (d) J. Janczak, R. Kubiak, J. Richter, H. Fuess, *Polyhedron* **18** (1999) 2775–2780; (e) J. Janczak, R. Kubiak, *Acta Cryst*. C**57** (2001) 55–57; (f) J. Janczak, Y.M. Idemori; *Acta Cryst*. C**58** (2002) m23–m25; (g) J. Janczak, R. Kubiak, *Acta Cryst*. C**59** (2003) m70–m72; (h) G.J. Perpetuo, J. Janczak, *Acta Cryst*. E**61** (2005) m2003–m2005; (i) G.J. Perpetuo, J. Janczak, *Acta Cryst*. C**62** (2006) m323–m326; (j) J. Janczak, *J. Mol. Struct*. **965** (2010) 125–130.

P-19

SYNTEZA HEKSABORANU BARU Z WĘGLANU BARU I AMORFICZNEGO BORU

Róża Jastrzębska i Maciej Dranka

Wydział Chemiczny Politechniki Warszawskiej, ul. Noakowskiego 3, 00-664 Warszawa

Heksaborany należą do grupy związków o wysokiej twardości, wysokiej temperaturze topnienia i niskiej pracy wyjścia [1,2]. Mimo że pierwsze ich syntezy zostały przeprowadzone w XX wieku, to nadal poszukiwane są wygodniejsze i lepsze metody ich otrzymywania. Dużo uwagi poświęca się także na optymalizację syntez i poznanie mechanizmów reakcji dla już poznanych procedur. Jedną z możliwych dróg otrzymania heksaboranów metali ziem alkalicznych jest reakcja w fazie stałej węglanów metali z amorficznym borem. Jej zaletą jest stosunkowo niska temperatura prowadzenia syntezy. Za wyjątkiem jednej publikacji z początku lat osiemdziesiątych brak jest jednak innych doniesień o jej wykorzystaniu [2].

W ramach przeprowadzonych badań wykazałam, że stosując powyższa metodę możliwe jest otrzymanie heksaboranu baru już w temperaturze poniżej 1000°C. Badania obejmowały określenie wpływu temperatury prowadzenia procesu, stosunku molowego użytych wyjściowych reagentów i czasu ogrzewania na otrzymywane w wyniku reakcji produkty.

Skład mieszanin poreakcyjnych określano na podstawie analizy fazowej opartej o rentgenowskie pomiary dyfrakcyjne na materiałach proszkowych. Dodatkowo, w celu uzupełnienia informacji o przebiegu reakcji, przeprowadzono pomiary termograwimetryczne z detekcją gazów.

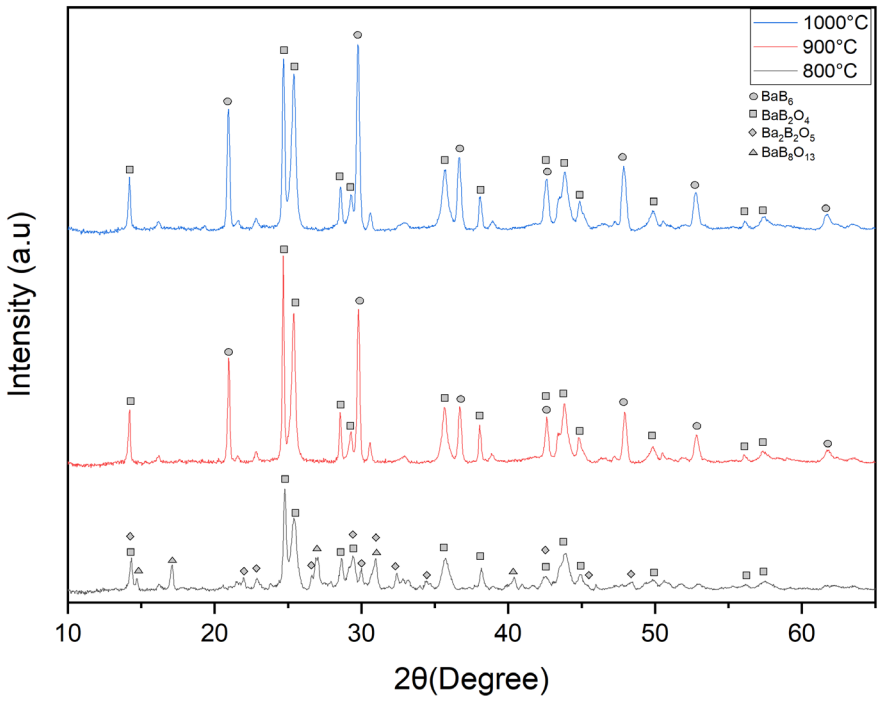

Rys. 1. Dyfraktogramy mieszanin poreakcyjnych dla stosunku molowego $BaCO_3$:B = 1:8 i czasu wygrzewania równego 8 h.

Praca powstała w wyniku realizacji projektu „Szkoła Orłów” współfinansowanego ze środków Unii Europejskiej w ramach Europejskiego Funduszu Społecznego, Programu Operacyjnego Wiedza Edukacja Rozwój, Oś priorytetowa III – Szkolnictwo Wyższe dla gospodarki i rozwoju, Działanie 3.1. Kompetencje w szkolnictwie wyższym.

Literatura

[1] G. Min, S. Zeng, Z. Zou, H. Yu, J. Han, *Meter. Lett.*, **57** (2003) 1330–1333.
[2] T. Aida, Y. Honda, S. Yamamotto, et. al., *J. Appl. Phys.*, **52** (1981) 1022.

P-20

CRYSTAL AND MOLECULAR STRUCTURE OF NEW BIOLOGICALLY ACTIVE CHIRAL SULFONAMIDES WITH PYRAZOLO[4,3-*e*][1,2,4]TRIAZINE CORE

Zbigniew Karczmarzyk[1], Mariusz Mojzych[1] and Mateusz Kciuk[2,3]

[1] Faculty of Science, Siedlce University of Natural Sciences and Humanities, 3 Maja 54, 08-110 Siedlce
[2] Department of Molecular Biotechnology and Genetics, University of Lodz, Banacha Street 12/16, 90-237 Lodz
[3] Doctoral School of Exact and Natural Sciences, University of Lodz, Banacha Street 12/16, 90-237 Lodz

The search for new lead structures and chemical entities for the development of new effective anticancer agents is an increasingly important task in medicinal chemistry. This trend of global research includes work on the use of 1,2,4-triazine scaffold as a source for the design of biologically relevant molecules with well-known broad biological applications [1]. Thus, the 1,2,4-triazine ring is an eminent structural motif found in plentiful natural and synthetic biologically active compounds [2].Some interesting and little studied in the group of 1,2,4-triazines condensed with a five-membered heterocycle is the pyrazolo[4,3-e][1,2,4]triazine ring system. The combination of this heterocyclic core with the sulfonamide group resulted in a new series of derivatives with antitumor activity. Few groups of pyrazolo[4,3-e][1,2,4]triazine sulfonamides were prepared as inhibitors of carbonic anhydrase hCA IX and XII with antitumor activity [3,4]. Here we report the synthesis and crystal and molecular structure of two new sulfonamides with pyrazolo[4,3-e][1,2,4]trazine ring system **1** and **2**.

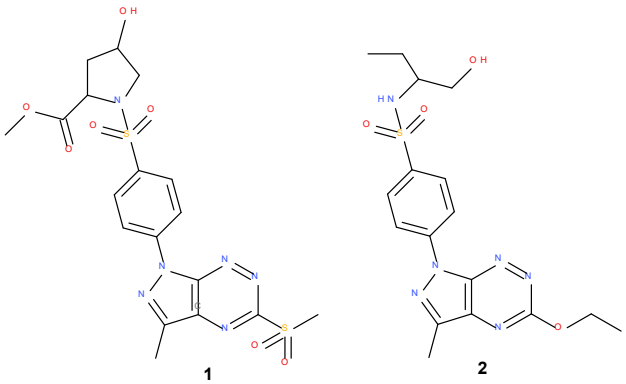

1 **2**

References

[1] S. Cascioferro, B. Parrino, V. Spanò, A. Carbone, A. Montalbano, P. Barraja, P. Diana, G. Cirrincione, *Eur. J. Med. Chem.*, **142** (2017) 328.
[2] L. Yurttas, G. A. Ciftci, H. E. Temel, B. N. Saglik, B. Demir, S. Levent, *Anticancer Agents Med. Chem.*, **17** (2017) 1846
[3] M. Mojzych, A Bielawska, K Bielawski, M. Ceruso, C. T. Supuran, *Bioorg. Med. Chem.,* **22** (2014) 2643.
[4] M. Mojzych, M. Ceruso, A. Bielawska, K. Bielawski, E. Fornal, C. T. Supuran, *Bioorg. Med. Chem.,* **23** (2015) 3674.

P-21

ENERGIE ODDZIAŁYWAŃ PAR CZĄSTECZKOWYCH W STRUKTURACH KRYSTALICZNYCH MIKONAZOLU

Hanna Kaspiaruk i Lilianna Chęcińska

Wydział Chemii, Uniwersytet Łódzki, ul. Pomorska 165, 90-236 Łódź

Mikonazol, (*RS*)-1-[2-(2,4-dichlorobenzyloksy)-2-(2,4-dichlorofenylo)etylo]-1*H*-imidazol, jest lekiem przeciwgrzybiczym, należącym do grupy pochodnych imidazolu, wykazuje szerokie spektrum działania przeciwko różnym grzybom, drożdżom i wybranym bakteriom Gram-dodatnim [1]. W ramach naszych badań zostały otrzymane nowe formy mikonazolu: czysta forma mikonazolu (MIC), monosolwat z etanolem (MIC-EtOH) oraz monohydrat (MIC-H_2O). Struktura krystaliczna mikonazolu w formie hemihydratu (MIC-0.5H_2O) jako jedyna została opublikowana ponad 40 lat temu [2]. W celu podkreślenia różnic pomiędzy czystą formą mikonazolu a postaciami solwatowanymi zostały obliczone modelowe energie par cząsteczkowych [3] a na ich podstawie zostały wygenerowane ramy energetyczne [4] dla wszystkich badanych kryształów. Energie par molekularnych dominujących kontaktów międzycząsteczkowych zostały oszacowane w zakresie 20 - 70 kJ/mol. Zdecydowanie, największy wkład elektrostatyczny obserwuje się dla oddziaływań typu O-H···N pomiędzy rozpuszczalnikiem a cząsteczką mikonazolu, natomiast składowa dyspersyjna determinuje oddziaływania typu π···π. Z porównania postaci czystej mikonazolu z solwatomorfami wynika, że cząsteczka rozpuszczalnika (etanolu lub wody) wpływa zarówno na strukturę molekularną mikonazolu, jak i strukturę krystaliczną odmian solwatomorficznych.

Literatura

[1] P. R. Sawyer, R. N. Brogden, R. M. Pinder, T. M. Speight, G. A. Avery, *Drugs*, **9** (1975) 406–423.
[2] O. M. Peeters, N. M. Blaton, C. J. De Ranter, *Bull. Soc. Chim. Belg*, **88** (1979) 265–272.
[3] M. J. Turner, S. Grabowsky, D. Jayatilaka, M. A. Spackman, *J. Phys. Chem. Lett*, **5** (2014) 4249–4255.
[4] M. J. Turner, S. P. Thomas, M. W. Shi, D. Jayatilaka, M. A. Spackman, *Chem. Commun*, 51 (2015) 3735–3738.

P-22

ADENOSINE 5′-DIPHOSPHATE (ADP) POTASSIUM SALTS – CRYSTAL STRUCTURES, DEHYDRATION AND PHASE TRANSITION

Oskar Kaszubowski, Katarzyna Ślepokura

Faculty of Chemistry, University of Wrocław,
14 F. Joliot-Curie, 50-383 Wrocław, Poland

Adenosine 5′-diphosphate (ADP) belongs to group of adenyl nucleotides, which are commonly found in living cells of almost all organisms. They serve many key functions, including taking part in the biosynthesis of nucleic acids [1]. Adenine ribonucleotides, in particular diphosphate and triphosphate, have been recognized as playing an important role in a variety of biological effects. They are responsible for the regulation of many enzymes [2], controlling processes of muscle contraction [3], activation of platelets [4] and all stages of cellular respiration: glycolysis, citric acid cycle and oxidative phosphorylation [5,6].

Four different potassium salts of ADP: K(ADP)·4H_2O, K(ADP)·2H_2O, K(H_5O_2)(ADP)$_2$·4.25H_2O and K(ADP), formed by dehydration of K(ADP)·2H_2O (Fig. 1), were structurally characterised with the use of single-crystal X-ray crystallography. A phase transition takes place in K(H_5O_2)(ADP)$_2$·4.25H_2O crystals (Fig. 2), which results, among others, in changing the space group from $P2_12_12$ to $P2_12_12_1$ (on cooling) and doubling one of the unit cell parameters. The transition temperature was determined by DSC and is about 280 K.

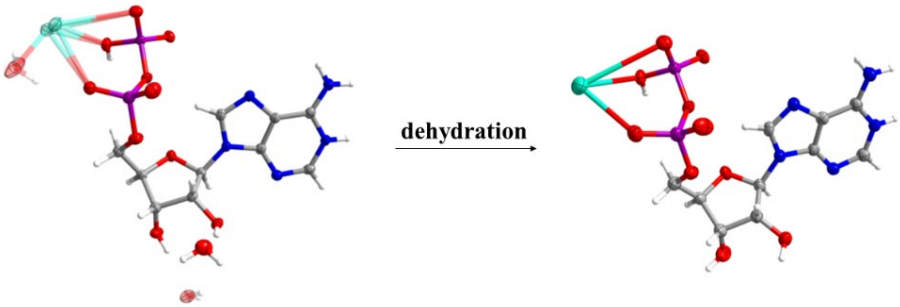

Fig. 1. Asymmetric units of K(ADP)·2H_2O (left) and K(ADP) (right).

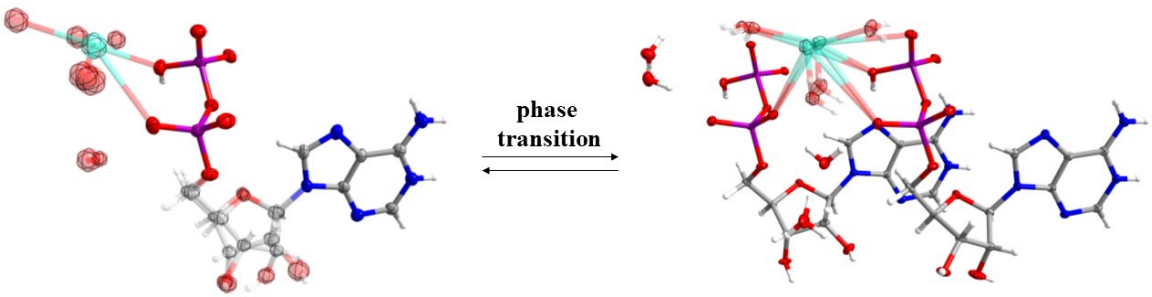

Fig. 2. Asymmetric units of K(H_5O_2)(ADP)$_2$·4.25H_2O in high-temperature phase (left) and low-temperature phase (right).

In all crystal structures, chains and layers motifs are observed (Fig. 3 and Fig. 4), which are stabilized by a network of hydrogen bonds formed, among others, by water molecules, the oxygen atoms of the diphosphate and the hydroxyl groups of ribose, as well as the nitrogen atoms of the Hoogsteen and Watson-Crick edges of nucleobase.

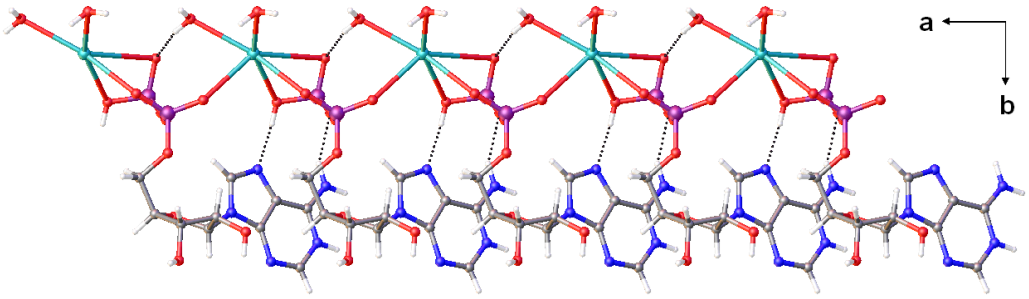

Fig. 3. Chain formed by ADP^{-} anions and K^{+} cations in the crystal of $K(ADP)\cdot 4H_2O$. Some water molecules are omitted for clarity. Selected hydrogen bonds are marked with black dotted lines.

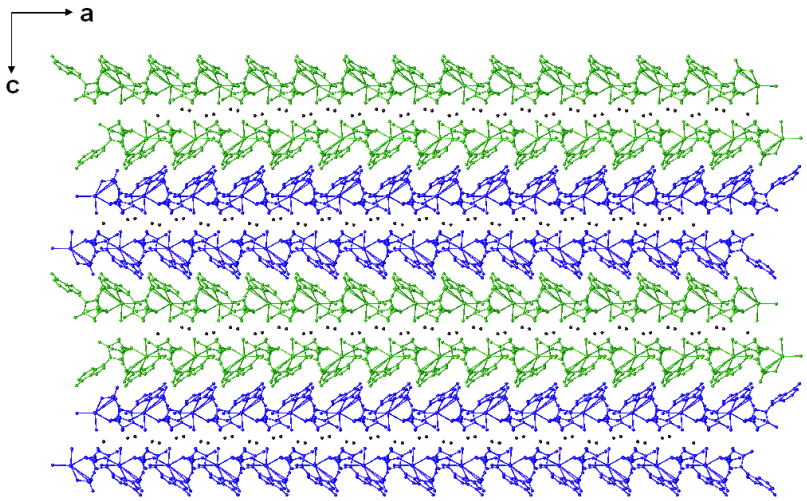

Fig. 4. Separated by water molecules (marked in black) bilayers in the crystal of $K(ADP)\cdot 4H_2O$ formed by two antiparallel layers (marked in green and blue).

References

[1] H. G. Khorana, *Pure Appl. Chem*. **17** (1968) 349–382.
[2] D. E. Atkinson, G. M. Walton, *J. Biol. Chem.* **242** (1967) 3239–3241.
[3] R. Cooke, E. Pate, *Biophys. J.* **48** (1985) 789–798.
[4] S. Murugappa, S. P. Kunapuli, *Front. Biosci*. **11** (2006) 1977–1986.
[5] E. N. Maldonado, J. J. Lemasters, *Mitochondrion*. **19** (2014) 78–84.
[6] A. M. Bertholet, E. T. Chouchani, L. Kazak, A. Angelin, A. Fedorenko, J. Z. Long, S. Vidoni, R. Garrity, J. Cho, N. Terada, D. C. Wallace, B. M. Spiegelman, Y. Kirichok, *Nature* **571** (2019) 515–520.

P-23

CRYSTAL STRUCTURES OF NOVEL MONO– AND BIS(TETRAZOL–2–YL)COUMARIN-BASED DERIVATIVES

Marcin Kaźmierczak, Miłosz Siczek, Robert Bronisz

Wydział Chemii, Uniwersytet Wrocławski, ul. F. Joliot-Curie 14, 50-383 Wrocław

N-substituted tetrazoles are exploited in coordination chemistry as monodontate donor groups. 1-substituted derivatives usually coordinates through *exo* positioned nitrogen atom N4 [1]. They can form with 3d metal ions octahedral complexes in which six rings form first coordination sphere. The important group constitute Fe(II) complexes because they can exhibit thermally induced spin crossover. 2-substituted regioisomers form besides homoleptic complexes of compositions of first coordination spheres [Fe(tetrazol-2-yl)$_6$] also heteroleptic systems [Fe(tetrazol-2-yl)$_4$(L)$_2$] in which axial positions are occupied by small alcohol or nitrile molecules (L) [2]. Both groups of coordination compounds based on second tetrazole regioisomer can undergo thermally induced spin crossover, too.

Spin crossover can be induced by temperature, light irradiation or application of pressure. Change of spin state can involve serious structural changes, thus, influencing other incorporated functionalities. On the other hand spin state can be affected by structural changes associated for example with structural phase transitions or triggered by host-guest interactions. Therefore we decided to combine tetrazole donor delivering spin crossover property with multifunctional moieties potentially revealing sensitivity towards change of spin state and concomitantly being an origin of chemical transformations affecting structure, thus, an ability to change of spin state. In this communication we present two novel ligands containing 2-substituted tetrazole as donor groups. Their characteristic is presence of methylene spacer linking flat coumarin moiety with tetrazole ring.

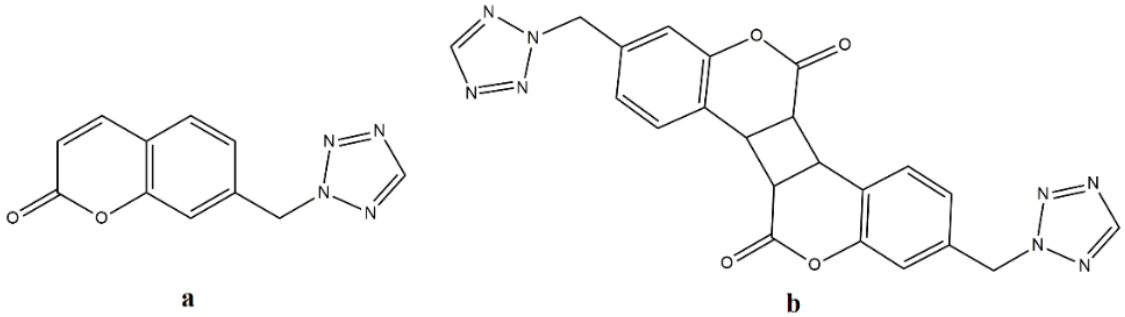

a **b**

Fig 1. Molecular structures of **L1** (a), **L2** (b).

Crystals of ligand **L1** (Fig. 1a) were obtained by slow evaporation of ethanol. **L1** crystallizes in *P-1* space group (a= 4.283, b= 9.818, c= 12.061, α= 84.15, β= 81.63, γ= 79.91). The *syn* head-to-head isomer of **L2** (Fig. 1b) crystallizes in *P-1* space group (a= 6.594, b= 12.455, c= 12.673, α= 101.05, β= 99.32, γ= 97.19). Formation of **L2** is connected with appearance of cyclobutane ring and the same vanishing of double bond of coumarin fragment. Moreover vanishing of double bond. There will be details presented on the poster concerning crystal structures of **L1** and **L2**.

References

[1] a) J. Kusz, P. Gütlich, H. Spiering; *Top Curr. Chem.*, **234** (2004) 129-153; b) R. Bronisz; *Inorg. Chem*.,**46** (2007) 6733–6739.

[2] a) M. Książek, M. Weselski, M. Kaźmierczak, A. Tołoczko, M. Siczek, P. Durlak, J. A. Wolny, V. Schünemann, J. Kusz, R. Bronisz, *Chem. Eur. J.*, **26** (2020) 14419–14434; b) R. Bronisz *Inorg. Chim. Acta*, 357 (2004) 396–404.

P-24

SODIUM HYPODIPHOSPHATES AND THEIR DEHYDRATION STUDIES

Marta Otręba[a], Rafał Lipiński[a], Aleksandra M. Sokołowska[a], Katarzyna Ślepokura[a] and Vasyl Kinzhybalo[b]

[a] *Faculty of Chemistry, University of Wrocław, 14 F. Joliot-Curie, 50-383 Wrocław*
[b] *Institute of Low Temperature and Structure Research, 2 Okólna, 50-422 Wrocław*

Alkali metal hypodiphosphates are the best studied group of hypodiphosphoric acid compounds [1]. Nevertheless, crystal structures of sodium hypodiphosphates reported so far include only four hydrated salts: $Na(H_3P_2O_6)\cdot H_2O$, $Na_2(H_2P_2O_6)\cdot 6H_2O$, $Na_3(HP_2O_6)\cdot 9H_2O$ and $Na_4(P_2O_6)\cdot 10H_2O$ [2-5]. Therefore in the course of systematic studies on hypodiphosphates we have undertaken the synthesis, crystal structure determination and dehydration studies of the missing members of the group (Fig. 1). The following compounds were obtained and analysed: $Na(H_3P_2O_6)$ (triclinic), $Na(H_3P_2O_6)$ (monoclinic), $Na_2(H_2P_2O_6)$, $Na_2(H_2P_2O_6)\cdot 2H_2O$, $Na_2(H_2P_2O_6)\cdot 6H_2O$ (new modification), $Na_5(H_2P_2O_6)(HP_2O_6)\cdot 21H_2O$, $Na_3(HP_2O_6)$ and $Na_4(P_2O_6)$. The details on structural features of the obtained compounds will be presented.

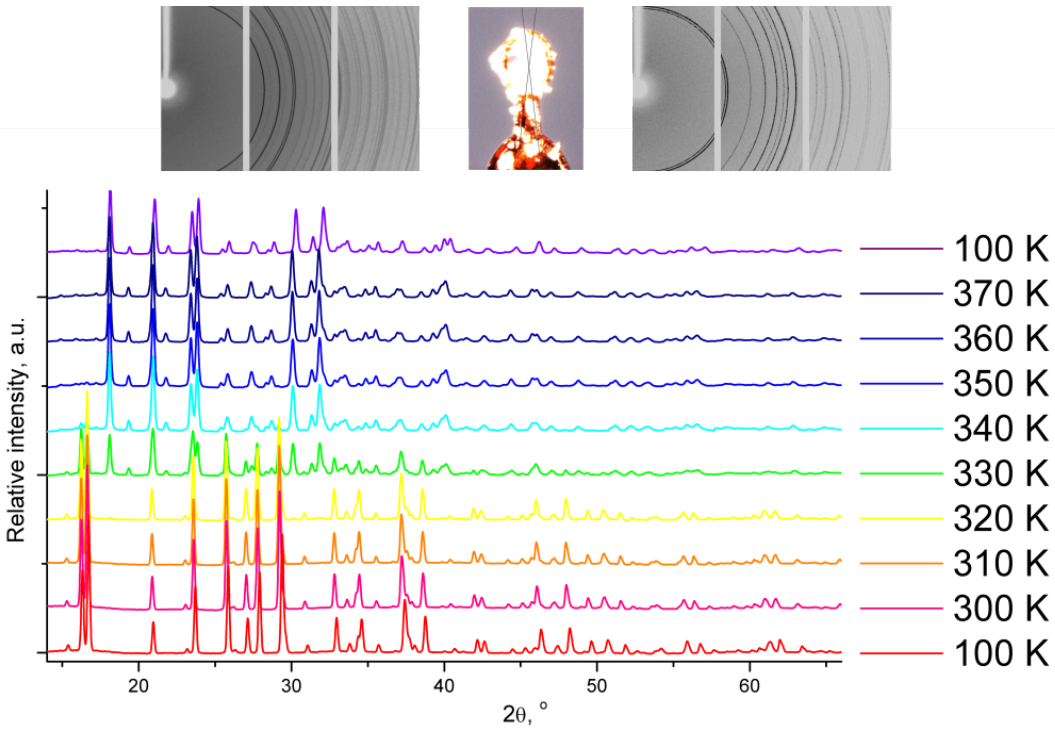

Fig. 1. Dehydration of $Na(H_3P_2O_6)\cdot H_2O$ evidenced by micro powder X-ray diffraction.

References

[1] V. Kinzhybalo, M. Otręba, K. Ślepokura, T. Lis, *Wiad. Chem.*, **75** (2021) 423.
[2] V. Kinzhybalo, K. Ślepokura, B. Szafranowska, E. Karaś, *54 Konwersatorium Krystalograficzne, V Sesja Naukowa i Warsztaty PTK*, Wrocław, 5–7 VII 2012, 231.
[3] R. L. Collin, M. Willis *Acta Crystallogr. B*, **27** (1971) 291.
[4] D. S. Emmerson, D. E. C. Corbridge, *Phosphorus*, **4** (1974) 207.
[5] M. Gjikaj, P. Wu, W. Bruckner, *Z. Anorg. Allg. Chem.*, **638** (2012) 2144.

P-25

HYDROGEN BOND PROPERTIES IN SELECTED NAPHTHO- AND ANTHRAQUINONE DERIVATIVES ON THE BASIS OF CAR-PARRINELLO MOLECULAR DYNAMICS

Beata Kizior[1], Jarosław J. Panek[2], Bartłomiej M. Szyja[1] and Aneta Jezierska[2]

[1] Wrocław University of Science and Technology, Institute of Advanced Materials, ul. Gdańska 7/9, 50-344 Wrocław, Poland
[2] University of Wrocław, Faculty of Chemistry, ul. F. Joliot-Curie 14, 50-383 Wrocław, Poland

Naphtho- and anthraquinone are attractive group of compounds for study using computational chemistry methods. They have complex molecular structures and show a variety of properties interesting from material science point of view [1]. For example, they are employed as electrode-active materials for flow batteries [2] and long-life lithium-organic batteries [3]. In our work, we focused on intra- and intermolecular interactions present in the crystal structures of naphtho- and anthraquinone derivatives (see Figure 1) [4]. The detailed analysis of such interactions sheds more light onto molecular level processes involving the molecules, e.g. aggregation processes, proton transfer phenomenon etc., which are important to design new molecules with desired physico-chemical properties. In turn, the Car-Parrinello molecular dynamics (CPMD) was applied to reproduce molecular properties of hydrogen bridges.

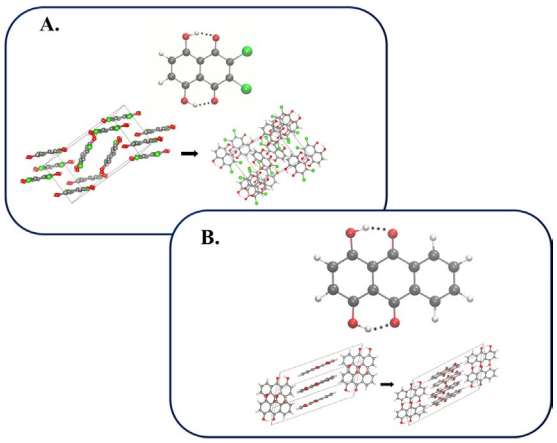

Figure 1. Structures of A. 2,3-dichloro-5,8-dihydroxy-1,4-naphthoquinone and B. 1,4-dihydroxy anthraquinone.

Ab initio molecular dynamics simulations were performed using Car-Parrinello molecular dynamics [5] in vacuo and in the crystalline phase. The PBE functional [6,7] and Troullier-Martins pseudopotentials [8] were used in the study for both phases. A kinetic energy cutoff of 80 Ry was employed. The CPMD simulations were carried out at 295 K temperature, controlled by a Nosé-Hoover thermostat [9,10]. The time-step was set to 3 au. The fictitious electron mass parameter was equal to 400 au. The initial part of the simulations was taken as an equilibration (ca. 1,8 ps) and it was excluded during the data analyses. The CPMD trajectories were collected for 20 ps for both compounds in both phases.

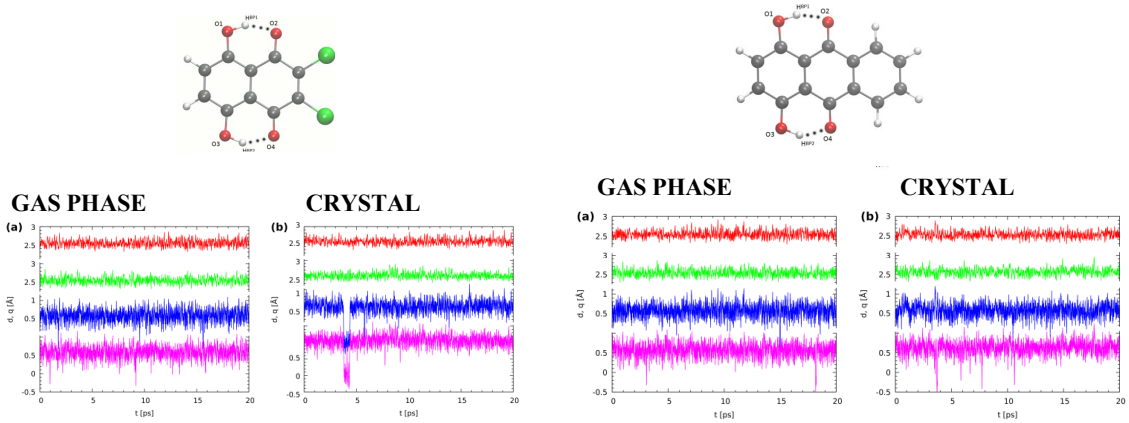

Fig. 2. Time evolution of the metric parameters of the O-H..O hydrogen bridges in the investigated systems, (a): HBQ in the gas phase, (b): HBQ in the crystal. Two upper lines: donor-acceptor distances d, two lower lines: the corresponding proton position parameters q (defined as $dH^{BP}...O - dOHBP$). Color coding is as follows: red - d(O1...O2), green - d(O3...O4), blue - q(O1-H^{BP}1-O2), pink - q(O3-^{HBP2}-O4).

The CPMD results indicate that the protons are very labile in the hydrogen bridges of the studied compounds (see Figure 2). Short proton transfer (PT) and proton-sharing events were observed and correlation between was noticed, especially for the first investigated system.

Acknowledgments

The Authors thank the Wrocław Center for Networking and Supercomputing (WCSS) and Academic Computer Centre Cyfronet AGH (PL-Grid infrastructure Prometheus) for CPU time and technical support.

Literature

[1] J. R. Widhalm, D. Rhodes, *Hortic. Res.*, **3** (2016).
[2] L. Tong, M. A. Goulet, D. P. Tabor, E. F. Kerr, D. D. Porcellinis, E. M. Fell, A. Aspuru-Guzik, R. G. Gordon, M. J. Aziz, *Energy Lett.*, **4** (2019) 1880-1887.
[3] L. Joungphil, K. Hoon, J. Moon, *Chem. Mater.*, **28** (2016) 2408–2416.
[4] B. Kizior, J. J. Panek, B. M. Szyja, A. Jezierska, *Symmetry*, **13** (2021) 564.
[5] R. Car, M. Parrinello, *Phys. Rev. Lett.*, **55** (1985) 2471–2474.
[6] J. Perdew, M. Ernzerhof, K. Burke, *J. Chem. Phys.*, **105** (1996) 9982–9985.
[7] J. Perdew, K. Burke, M. Ernzerhof, *Phys. Rev. Lett.*, **78** (1997) 1396–1396.
[8] N. Troullier, J. L. Martins, *Phys. Rev. B*, **43** (1991) 1993–2006.
[9] S. Nosé, *J. Chem. Phys.*, **81** (1984) 511–519.
[10] W. Hoover, *Phys. Rev. A*, **31** (1985) 1695–1697.

P-26

CRYSTAL STRUCTURE OF A MONONUCLEAR COBALT(II) COMPLEX WITH SCHIFF BASE

Hubert Kleinschmidt, Anna Dołęga and Magdalena Siedzielnik

Department of Inorganic Chemistry, Faculty of Chemistry,
Gdansk University of Technology, G. Narutowicz 11/12, 80-233 Gdańsk

Metal complexes of Schiff bases owe the long-lasting attention to their potential applications in many areas: medicine as antibacterial, antifungal, anticancer agents, corrosion inhibition and other applications that utilize their thermal, magnetic, optical and electrical properties. Moreover many Schiff base complexes of metal ions show high catalytic activity and are efficient catalysts in homogeneous and heterogeneous reactions.[1-4]

Within this study new mononuclear complex **C1** with the formula of [Co(**L1**)$_2$] (**HL1**: 2-(5-methylpyridin-2-ylimino)methyl)-6-methoxyphenol) has been synthesised and characterized by X-ray diffraction analysis.

The compound was obtained by reacting the formerly synthesised Schiff base (**L1**) with cobalt(II) acetate in ethanol followed by the addition of Et_3N. Crystals suitable for X-ray analysis were obtained at +4°C. In the independent part of the unit cell two conformers of **C1** are found; the two molecules differ from each other exclusively in the orientation of one of their methoxy groups (compare the position of C atoms labelled C8/C50).

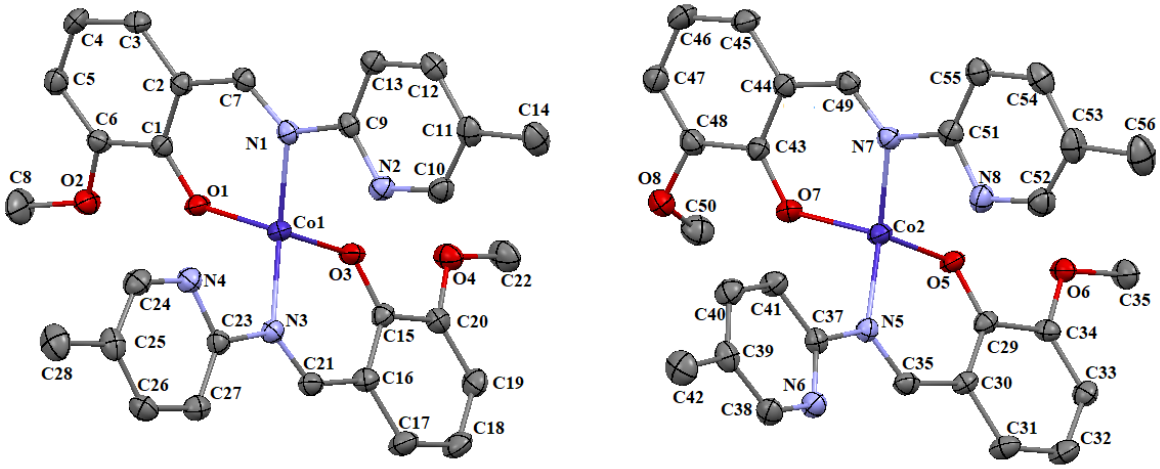

Fig. 1. Molecular structure of **C1**. Thermal ellipsoids at 50%. Hydrogen atoms have been omitted for clarity. Bond lengths [Å]: Co1—O1 1.9385(19), Co1—O3 1.946(2), Co1—N3 1.986(3), Co1—N1 1.997(3), Co2—O5 1.908(2), Co2—O7 1.933(2), Co2—N7 1.985(3), Co2—N5 2.001(3). Angles [°]: O1—Co1—O3 102.70(9), O1—Co1—N3 111.42(9), O3—Co1—N3 93.31(9), O1—Co1—N1 92.51(9), O3—Co1—N1 113.91(9), N3—Co1—N1 139.07(10), O5—Co2—O7 113.76(9), O5—Co2—N7 117.36(10), O7—Co2—N7 93.02(9), O5—Co2—N5 97.19(9), O7—Co2—N5 106.28(9), N7—Co2—N5 129.30(10).

The crystallographic data for the title compound were collected on an STOE IPDS II diffractometer at 120.0 K using Mo Kα radiation of a microfocus X-ray source.

P-26

C1 crystallizes in a monoclinic system in $P2_1/c$ space group. The unit cell parameters are as follows: a = 13.6519(4) Å, b = 13.7225(5) Å, c = 26.1260(8) Å, β = 90.899(3)°, V = 4893.8(3) $Å^3$ and Z= 4. Quality parameters of the solution are $R_1[I > 2\sigma(I)]$= 0.0475, wR_2 (all data)= 0.0779, R_{int}= 0.040, GOOF= 1.062. Asymmetric unit contains two molecules.

It is an example of a mononuclear cobalt complex, where two imine molecules are coordinated to the cobalt atom. Cobalt atom forms four bonds to its neighbor atoms in tetrahedral geometry. The lengths of nitrogen-cobalt and oxygen-cobalt bonds are in accordance with those founded in the literature.

Literature

[1] M. N. Uddin, S. S. Ahmed, S. M. Alam Rahatul, *J. Coord. Chem.*, **73** (2020), 3109–3149.

[2] M. Ikram, S. U. Rehman, S. Rehman, R. J. Baker, C. Schulzke, *Inorg. Chim. Acta.*, **390** (2012) 210–216.

[3] V. Kuchtanin, L. Kleščíková, M. Šoral, R. Fischer, Z. Růžičková, E. Rakovský, J. Moncoľ, P. Segľa, *Polyhedron*, **117** (2016) 90–96.

[4] A. Sakthivel, K. Jeyasubramanian, B. Thangagiri, J. Dhaveethu Raja, *J. Mol. Struct.*, **1222 (**2020) 1–14.

P-27

SOLE KWASU FENAMOWEGO I TOLFENAMOWEGO Z AMANTADYNĄ

Marta S. Krawczyk

Wydział Farmaceutyczny, Uniwersytet Medyczny im. Piastów Śląskich we Wrocławiu, ul. Borowska 211, 50-556 Wrocław

Kontynuując badania nad kokryształami i solami substancji leczniczych z grupy niesteroidowych leków przeciwzapalnych (NLPZ) z amantadyną, przedstawiono struktury soli kwasów fenamowego i tolfenamowego z amantadyną. Kokrystalizacja i synteza soli substancji leczniczych są obiecującymi metodami stosowanymi celem uzyskania poprawy właściwości fizykochemicznych i farmakologicznych farmaceutyków [1]. Kwasy: mefenamowy, tolfenamowy, flufenamowy i meklofenamowy znane są jako leki należące do grupy NLPZ. Wyjątkiem jest kwas fenamowy, który ze względu na niepożądane efekty uboczne nie ma zastosowania w medycynie, stanowi natomiast strukturę modelową. Amantadyna (1-aminoadamantan) jest lekiem przeciwwirusowym oraz stosowana jest w leczeniu choroby Parkinsona. Jako lek przeciwwirusowy amantadyna hamuje uwalnianie wirusowego genomu w zakażonej komórce. W stężeniach terapeutycznych hamuje ona replikację wirusa grypy A [2].

Kryształy badanych soli kwasów tolfenamowego i fenamowego z amantadyną otrzymano w wyniku krystalizacji z alkoholu etylowego. W kryształach kationy uprotonowanej amantadyny oddziałują z anionami kwasów fenamowych poprzez wiązania wodorowe N–H···O tworzone pomiędzy grupą NH_3^+ a grupą karboksylanową. W kryształach nie występują cząsteczki rozpuszczalnika, co czyni je obiecującymi układami do dalszych badań aktywności biologicznej.

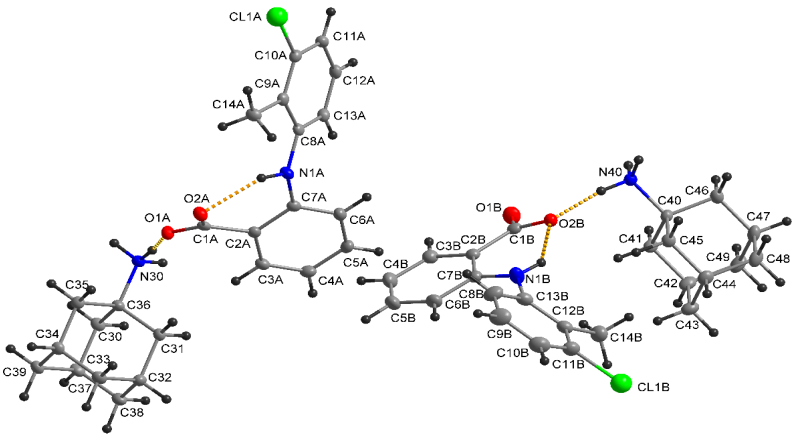

Rys. 1. Struktura soli kwasu tolfenamowego z amantadyną.

Źródło finansowania: Uniwersytet Medyczny we Wrocławiu, grant SUBZ.D050.22.025.

Literatura

[1] M. Guo, X. Sun, J. Chen, T. Cai, *Acta Pharm Sin B*., **11(8)** (2021), 2537.
[2] G. Hubsher, M. Haider, M. S. Okun, *Neurology*, **78(14)** (2012), 1096.

P-28

NOWY POLIMER KOORDYNACYJNY 3D – SYNTEZA SOLWOTERMALNA W REAKTORZE BERGHOF

Kamil Twaróg, Andrzej Kochel

Wydział Chemii, Uniwersytet Wrocławski, F. Joliot-Curie 14, Wrocław

Polimery koordynacyjne są jednym z wiodących wątków badań w światowych ośrodkach badawczych. Dynamiczny rozwój i rosnące zainteresowanie tego typu połączeniami wiąże się przed wszystkim z możliwością otrzymywania nowych materiałów o funkcjonalnych właściwościach fizykochemicznych. Otrzymano solwotermalnie polimer koordynacyjny 3D $\{[Cu_3(C_{14}H_8N_3O_2)_2(H_2O)_2][BF_4]_2\}_n$, który krystalizuje w układzie rombowym i wykazuje unikalną trójwymiarową strukturę.

Dla polimeru wykonano badania magnetyczne w zakresie temperatur 2-300 K. Analizując przebieg $\chi_m T$ można zaobserwować, że nie zmienia się on aż do temperatury około 35K, a następnie zaczyna rosnąć stąd możemy wnioskować, że w zakresie niskich temperatur obserwowany wzrost $\chi_m T$ może mieć charakter oddziaływań ferromagnetycznych pomiędzy jonami Cu(II), które są przekazywane poprzez sieć wiązań wodorowych.

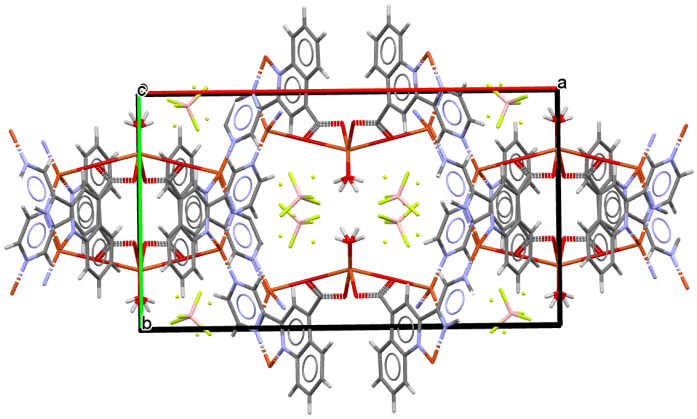

Rys. 1. $\{[Cu_3(C_{14}H_8N_3O_2)_2(H_2O)_2][BF_4]_2\}_n$.

P-29

AMMONIUM HYPODIPHOSPHATES: SYNTHESIS, CRYSTAL STRUCTURES, PHASE TRANSITION AND DEHYDRATION

Paulina Kurowska[1], **Daria Budzikur**[1], **Vasyl Kinzhybalo**[2], **Katarzyna Ślepokura**[1]

[1] *University of Wroclaw, Faculty of Chemistry, 14 F. Joliot-Curie, 50-383 Wroclaw*
[2] *Institute of Low Temperature and Structure Research, Polish Academy of Sciences, 2 Okólna, 50-422 Wroclaw*

The crystal structure of diammonium hypodiphosphate $(NH_4)_2(H_2P_2O_6)$ was reported in 1964, based on which the structural formula of hypodiphosphoric acid $(H_4P_2O_6)$ was confirmed [1]. In the 21st century, a reversible solid-state phase transition and the related ferroelectricity of the diammonium salt was revealed [2]. No other crystal structures of ammonium hypodiphosphates have been reported so far [3]. The following new ammonium compounds will be presented: two polymorphic (triclinic and monoclinic) forms of $(NH_4)(H_3P_2O_6)$, $(NH_4)_5(H_2P_2O_6)(HP_2O_6)\cdot H_2O$, $(NH_4)_3(HP_2O_6)$, $(NH_4)_4(P_2O_6)$ and $(NH_4)_4(P_2O_6)\cdot H_2O$. An order-disorder phase transition in the triclinic $(NH_4)(H_3P_2O_6)$ was structurally characterised. Dehydration of crystal hydrates was analysed by hot-stage microscopy and PXRD. Two types of dimensionalities of the hypodiphosphate substructures are present in the crystals: 3D in monoammonium salts and 0D (dimers or isolated anions) in the remaining (Fig. 1), while $H_2P_2O_6^{2-}$ anions in $(NH_4)_2(H_2P_2O_6)$ formed 1D ribbons.

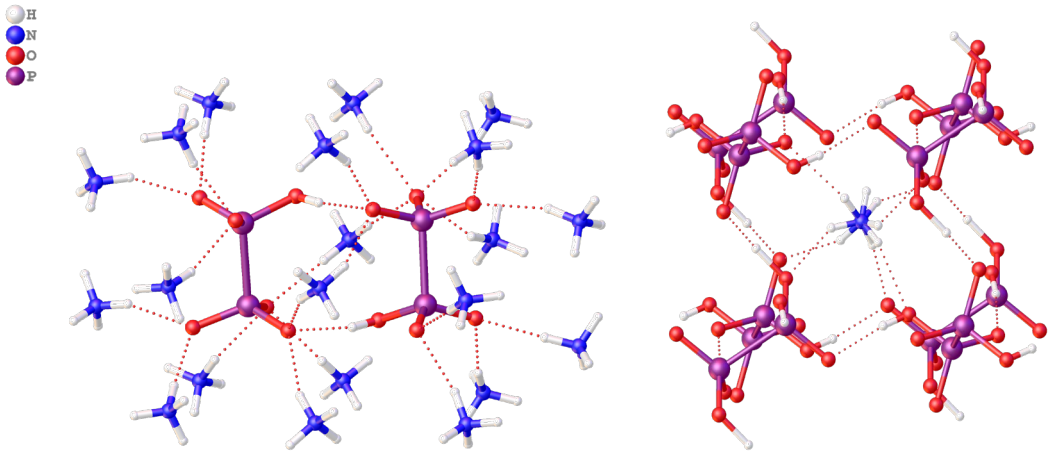

Fig. 1. Hypodiphosphate dimer and 3D cage in $(NH_4)_3(HP_2O_6)$ (left) and high temperature phase of the triclinic $(NH_4)(H_3P_2O_6)$ (right), and their interactions with NH_4^+ cations. Disorder of NH_4^+ and one of the hypodiphosphate hydrogen atoms in $(NH_4)(H_3P_2O_6)$ is shown. Hydrogen bonds are shown with dashed lines.

Literature

[1] A. Wilson, H. McD. McGeachin, *Acta Crystallogr.*, **17** (1964) 1352.
[2] P. Szklarz, M. Chański, K. Ślepokura, T. Lis, *Chem. Mater.*, **23** (2011) 1082.
[3] V. Kinzhybalo, M. Otręba, K. Ślepokura, T. Lis, *Wiad. Chem.*, **75** (2021) 423.

P-30

POLYMORPHISM AND STRUCTURAL DIVERSITY IN ORGANOBORON LUMINESCENT COMPLEXES

Paulina H. Marek-Urban[1,2], **Krzysztof Woźniak**[2], **Krzysztof Durka**[1]

[1] *Faculty of Chemistry, Warsaw University of Technology, Noakowwskiego 3, 00-664 Warsaw*
[2] *Faculty of Chemistry, Warsaw University, Pasteura 1, 02-093 Warsaw*

Reactive oxygen species (ROS) are intensively used in many areas of chemistry, for example in synthesis [1], water purification [2], and finally in medicine in photodynamic therapy [3] and photoinactivation of microorganisms [4]. Therefore, vast research is devoted for development of efficient photosensitizers, capable of ROS generation upon irradiation, especially focusing on heavy-atom free catalysts.

Our recent studies show that organoboron complexes exhibiting *spiro* geometry can be used as effective photosensitizers [5]. In the complexes boron atom plays a role of a node separating perpendicularly oriented donor (cyclic organoboron moiety) and acceptor (N,O ligand) molecular sites. However, in such compounds mechanism of generation of excited triplet states and thus reactive oxygen species is unknown. Our findings suggest that perpendicular geometry as well as conformation lability might play a crucial role in triplet states generation.

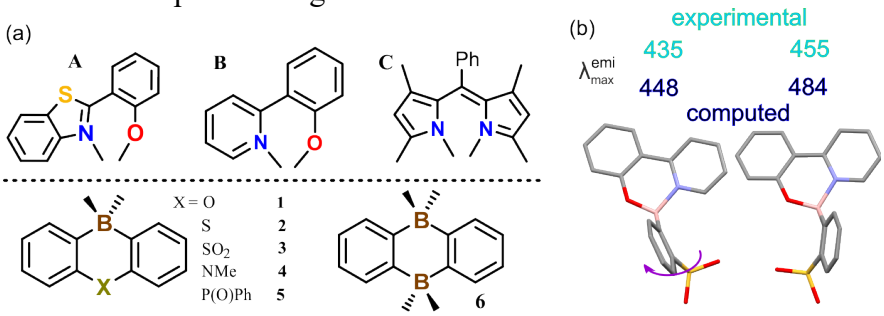

Fig.1. (a) Scheme of analysed complexes. (b) structural differences in polymorphic forms of **SO2-pp** with experimental and theoretical values of emission maxima.

We have synthetized a series of 30 complexes with (N,O)-ligands. Structural analysis of the complexes proved structural lability of the compounds, as compounds are prone to formation of polymorphic forms and solvates, where different relative localization of organoboron part and ligand can be observed. Herein we present structural and theoretical investigation of conformational lability of the organoboron complexes and its structure-luminescence properties relationship.

References

[1] A. Ghogare *et al.*, *Chem. Rev.*, **17** (2016) 9994.
[2] R. Bonnett *et al.*, *Water Res.*, **40** (2006) 1269.
[3] A. Kamkaew *et al.*, *Chem. Soc. Rev.*, **42** (2013) 77.
[4] F. Vatansever *et al.*, *FEMS Microbiol. Rev.*, **27** (2013) 955.
[5] P. H. Marek-Urban *et al.*, *J. Org. Chem.*, **86** (2021) 12714.

P-31

STRUCTURAL ANALYSIS OF RESONANCE ASSISTED HYDROGEN BONDS INVOLVING THE PHOSPHORYL GROUP (RAHB-P)

Przemysław Nowak[a,*], Anna Pietrzak[a], Marta K. Dudek[c], Jacek Koszuk[b], Tomasz Janecki[b], Wojciech M. Wolf[a]

[a] *Institute of General and Ecological Chemistry, Łódź University of Technology*
[b] *Institute of Organic Chemistry, Łódź University of Technology*
[c] *Centre of Molecular and Macromolecular Studies, Polish Academy of Sciences, Łódź, Poland*

**e-mail: nowakprzemek0@gmail.com*

A hydrogen bond is one of the interactions which may be found in all types of matter. In the human body, hydrogen bonds determine the double helix structure of DNA or participate in enzymatic reactions. One of the few hydrogen bond types is the resonance assisted hydrogen bond. This bond is characterized by alternating single and double bonds between an acceptor and a donor. This interaction occurs in many chemical compounds, where the acceptor and donor are atoms of carbon, sulfur, oxygen, or nitrogen. However, these bonds involving the phosphoryl group (RAHB-P) are scarce. Here we reported RAHB-P stabilizing the conformation of organophosphorus compounds (i.e., derivatives of 3-(diethoxyphosphoryl)-1,2-dihrydroquinolin-4-ols). The effect was characterized by SC-XRD and the ^{1}H NMR analyses.

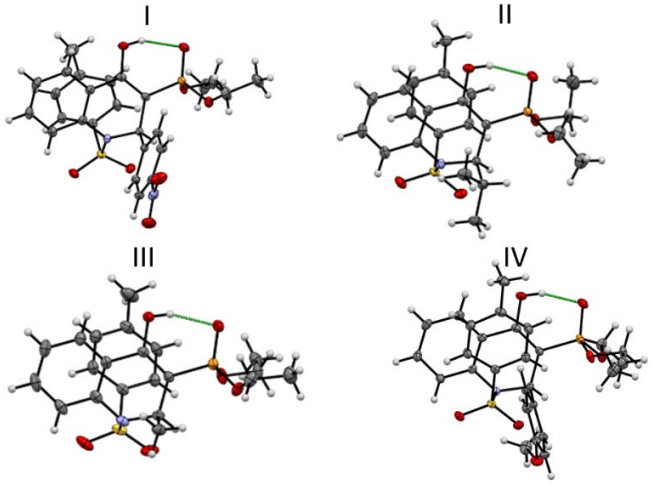

Fig. 1. Structures of derivatives of 3-(diethoxyphosphoryl)-1,2-dihrydroquinolin-4-ols . Intramolecular hydrogen bonds are marked with broken green lines. Displacement ellipsoids are drawn at the 50% probability level.

Structural Data:

(I) a=8.7017(4), b=10.1160(7), c=16.0888(5) [Å], α=93.901(3) β=95.514(6), γ=114.150(6) [°], *P*-1, Z=2, R= 0.029, S=1.031, T=100(2) K; **(II)** a=9.2048(2), b=19.4487(2), c=13.3777(3) [Å], **a**=90 **b**=90.034(2) **g**=90 [°], $P2_1/n$, Z=4, R=0.028, S= 1.033, T=100(2) K**; (III)** a=10.5517(2), b=14.4734(3), c=16.4385(2) [Å], a=64.579(3) b=83.184(2) c=71.998(2) [°], *P*-1, Z=4, R=0.032, S= 1.035, T=100(2) K; **(IV)** a=10.7031(9), b=20.6165(2), c=12.0046(6) [Å], a=90 b=99.437(2) g=90 [°], $P2_1/n$, Z=4, R=0.029, S= 1.025, T=100(2) K.

P-32

SYNTHESIS AND STRUCTURAL ANALYSIS OF NEW SALTS OF ACYCLOVIR WITH 2,6–DIHYDROXYBENZOIC ACID

Weronika Nowak*, Mateusz Gołdyn, Elżbieta Bartoszak-Adamska

Faculty of Chemistry, Adam Mickiewicz University, Uniwersytetu Poznańskiego 8, Poznań 61-614, Poland

**e-mail: wernow@amu.edu.pl*

Acyclovir (ACV, 2-amino-1,9-dihydro-9-[(2-hydroxyetoxy)methyl]-3*H*-purin-6-one) is an analog of guanosine where the ribose ring is replaced by a side chain. ACV is an antiviral agent commonly used to treat infections such as herpes simplex, HSV-1 and HSV-2, herpes zoster and chickenpox [1]. Acyclovir is widely used in medicine, although its solubility in water is low - 1.62 mg mL^{-1}. As a result, the permeability and bioavailability of this active pharmaceutical ingredient (API) are only 15-30% [2]. According to the Biopharmaceutical Classification System (BCS), acyclovir is classified into Class III (400 mg tablet strength), while in some countries it can be classified into group IV due to the higher drug strength (800 mg) [3].

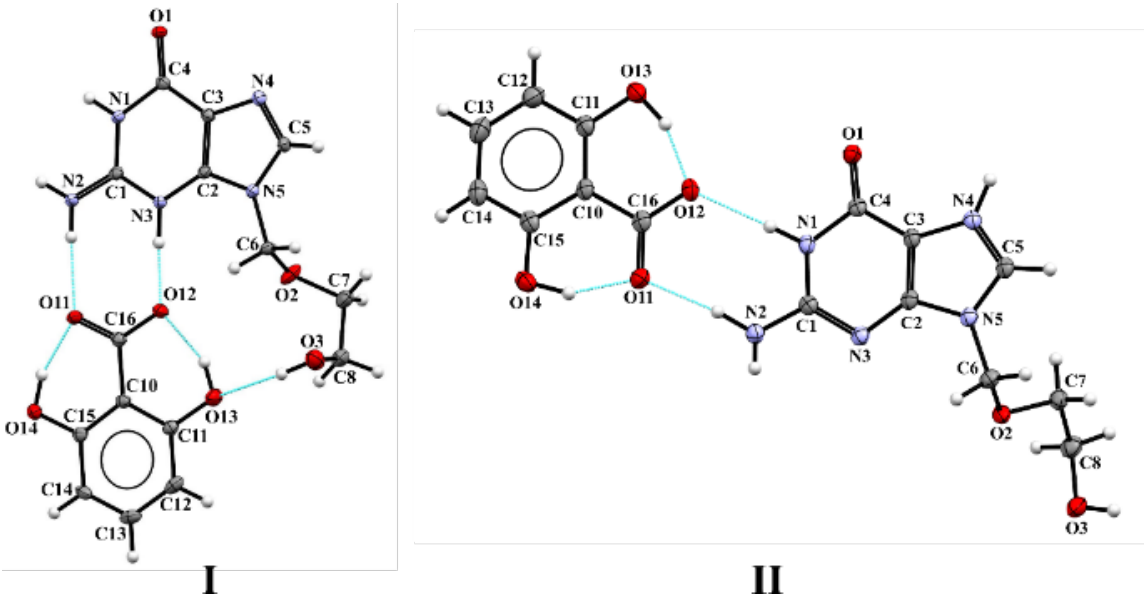

Fig. 1. ORTEP representation of the asymmetric unit of acyclovirium 2,6-dihydroxybenzoate salts (I and II forms).

To improve the solubility of the tested API, acyclovir was cocrystallized with 2,6-dihydroxybenzoic acid as a coformer using various techniques, i.e. solvent evaporation, neat grinding and solvent-drop grinding, and microwave-assisted slurry cocrystallization. Powder diffraction and a single crystal X-ray analysis allowed us to identify and characterize two forms (I and II) of ACV·26DHBA salt (Fig. 1).

Acknowledgement
The authors thank the PRELUDIUM grant No. 2021/41/N/ST5/00503 of the National Science Center in Poland for financial support, as well as by Adam Mickiewicz University from the funds of the Initiative of Excellence – Research University (IDUB) program in PhD Minigrants competition no. 017 (research grant 017/02/SNŚ/0005).

References

[1] D. Richards, A. Carmine, R. Brogden, R. Heel, T. Speight & G. Avery, *Drugs*, **26** (1983) 378.
[2] Y. Yan, J. M. Chen & T. B. Lu, *CrystEngComm*, **15** (2013) 6457.
[3] M. Karpe, N. Mali, V. Kadam, *Journal of Applied Pharmaceutical Science*, **02(03)** (2012) 101–105.

P-33

COPPER(I) π,σ-COORDINATION COMPOUNDS WITH 1-ALLYL-3-NORBORNAN-THIOUREA AND N-ALLYLCYTISINE: SYNTHESIS AND STRUCTURAL CHARACTERIZATION

Yurii Slyvka[1],*, Evgeny Goreshnik[2], Nazariy Pokhodylo[1], Marian Mys'kiv[1]

[1] *Ivan Franko National University of Lviv, 79005 Lviv, Ukraine*
[2] *Jožef Stefan Institute, Jamova 39, SI-1000 Ljubljana, Slovenia*

**e-mail: yurii.slyvka@lnu.edu.ua*

The aim of this work is to develop a novel Cu(I) π,σ-coordination compounds with the two allyl-containing ligands, i.e. 1-allyl-3-norbornan-thiourea (*Anor*) and allylcytisine (*Actis*). Crystals of the corresponding coordination compounds **1** and **2** (Table 1) were obtained under the conditions of the alternating-current electrochemical technique [1-3] starting from the acetonitrile solution of *Anor* and copper(II) nitrate or the ethanol solution of *Actis* and copper(II) chloride on copper electrodes. Diffraction data for compexes **1** and **2**, as well as for organic ligands (*Anor* and *Actis*), were collected on an Agilent Gemini A four-circle diffractometer with Atlas CCD detector using Cu K_a radiation (λ = 1.54184 Å).

Table 1. Selected crystal data for studied compounds.

Compound	Space group	V, Å^3	Z	Density, g/cm^3
Anor	$P2_1/c$	1157.17(8)	4	1.207
[Cu(*Anor*)(CH_3CN)](NO_3) (**1**)	$P2_12_12_1$	1624.69(5)	4	1.541
Actis	$P2_12_12_1$	1211.53(10)	4	1.263
{*Actis*(H^+)}[Cu_8{*Actis*(H^+)}Cl_{10}] (**2**)	$P1$	1011.24(8)	1	2.176

Anor crystallizes as a mixture of *Anor*((*2S*)-*exo*) and *Anor*((*2R*)-*exo*) enantiomers which statistically occupy the same position with an occupancy ratio of 0.637(7) : 0.363(7) (Fig. 1). In the crystal structure of coordination compound **1** two *Anor exo*-isomers also statistically occupy the same position (with an occupancy ratio of 0.564(9) : 0.436(9)) [4].

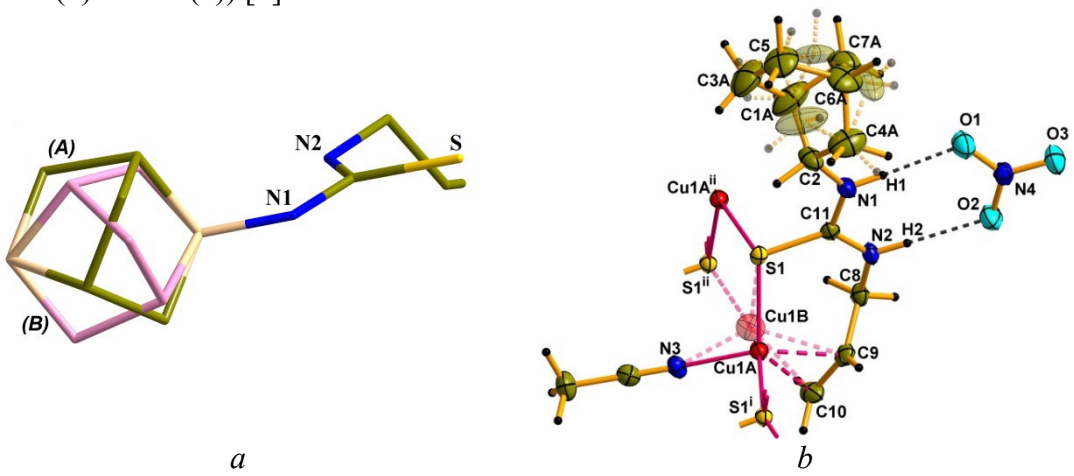

a *b*

Fig. 1. (*a*) Superposition of *(2S)-exo* (Part *A*) & *(2R)-exo* (Part *B*) enantiomers in *Anor* structure. H-atoms are omitted for clarity. (*b*) Fragment of **1** crystal structure. Symmetry codes: (*i*) x+1/2, −y+1/2, −z+1; (*ii*) x−1/2, −y+1/2, −z+1. One of the disordered positions of Cu(I) with lower S.O.F. and the position of *Anor*(*(2R)-exo*) are shown in semi-transparent mode.

P-33

Anor molecules in **1** are π,σ-coordinated with the Cu(I) ion through an allylic C=C bond and a thiourea S atom in a bridging mode. Cu1 is disordered over two sites (Cu1A and Cu1B) with an occupancy ratio of 0.972(3) : 0.028(3) due to the concurrent participation of the sulfur atoms of the adjacent thiourea ligands. Both Cu1A and Cu1B have a nearly trigonal-pyramidal coordination environment containing the η^2-allyl group and an S atom of the same *Anor* molecule, as well as an acetonitrile N atom in the basal plane. The apical position of the Cu(I) polyhedron is occupied by the bridging S atom of the nearest organic molecule. As a result, Cu(I) ions bind *Anor* molecules into infinite cationic coordination polymer $\{[Cu(Anor)(CH_3CN)]^+\}_n$.

Coordination compound **2** crystallizes in the acentric space group *P*1, with two *Actis*(H^+) cations, eight Cu(I) and ten Cl ions per unit cell. The organic cations are two conformers, which arise from the rotation of the N-allyl substituent relative to the N2—C12 bond by 102.6(8)°. One of the organic cations is π-coordinated to Cu(1) through allylic C=C bond, while the second *Actis*(H^+) cation is involved into hydrogen bonding only. Both these organic particles form extensive cationic pairs {*Actis*(H^+)….*Actis*(H^+)} through N—H···O bonding and π…π-stacking and contribute to the organisation of an unusual anionic chain. Within the chain there are seven crystallographically independent copper(I) ions, which form the specific $\{Cu_7\{Actis(H^+)\}Cl_{10}\}$ subunits, linked by linearly-arranged Cu^+ cations and bridging μ_3-Cl anions into 1*D*-polymer. The main feature of the subunit is the presence of cuprophilic interactions (2.81-2.85 Å) defined by geometrically distinct coordination environments of σ-bonded Cu(I) ions that possess trigonal, closed to trigonal pyramidal, distorted tetrahedral and T-shaped arrangements.

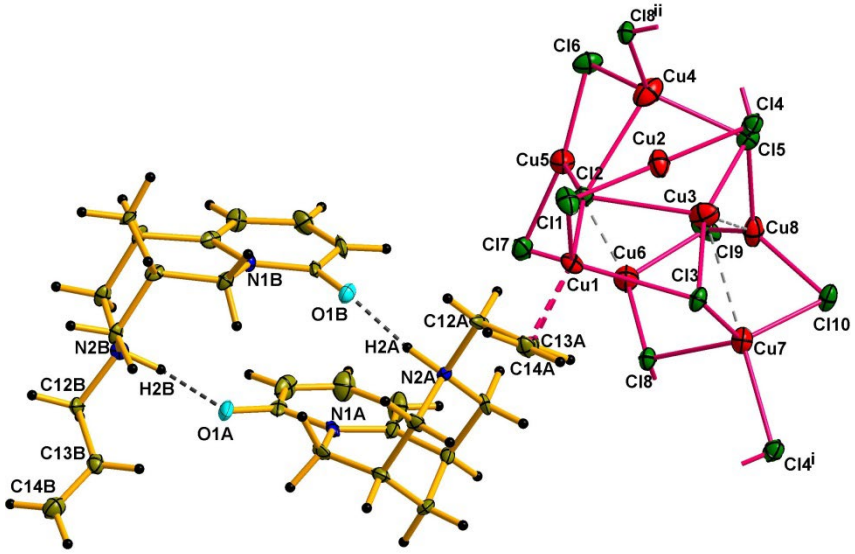

Fig. 2. The independent part in crystal structure of **2**. Symmetry codes: (*i*) *x*+1, *y*, *z*; (*ii*) *x*−1, *y*, *z*.

Literature

[1] Yu.I. Slyvka, O.V. Pavlyuk, M.Yu. Luk'yanov, M.G. Mys'kiv, *Ukraine Patent UA 118819*, Bull. № 16 (2017).

[2] Yu. Slyvka, E. Goreshnik, G.Veryasov, D. Morozov, A.A. Fedorchuk, N.Pokhodylo, I.Kityk, M. Mys'kiv, *J. Coord. Chem.*, **72** (2019) 1049–1063.

[3] D.A. Kowalska, V. Kinzhybalo, Yu.I. Slyvka, M. Wołcyrz, *Acta Crystallogr. B*., **77** (2021) 241–248.

[4] Yu. Slyvka, A.A. Fedorchuk, E. Goreshnik, N. Pokhodylo, J. Jedryka, K. Ozga, M. Mys'kiv, *Polyhedron*, **211** (2022) 115545.

P-34

ANALYSIS OF FLUORESCENT PROPERTIES OF CHINOLINE SALTS

Paulina Sobczak, **Agata Trzęsowska-Kruszyńska**

Institute of General and Ecological Chemistry, Faculty of Chemistry, Łódź University of Technology, Żeromskiego 116, 90-924 Łódź

Recently, research on the possibility of obtaining compounds exhibiting fluorescent properties in a solid has become very important due to their wide range of applications, e.g. in materials [1] and medicine [2]. The fluorescence of organic compounds in the solid-state depends not only on the structure of the fluorophore, but also on the packing of molecules in the crystal net and the intermolecular interactions. The fine-tuning of the emission wavelength as well as the fluorescence intensity can be achieved by the chemical modification of the compounds. An example of this strategy is the introduction of different substituents to the molecular structure of the compounds. This approach allows to consciously modify the fluorescent properties as well as control the fluorescence phenomenon, and thus allows to obtain a structure with the desired properties of light emission.

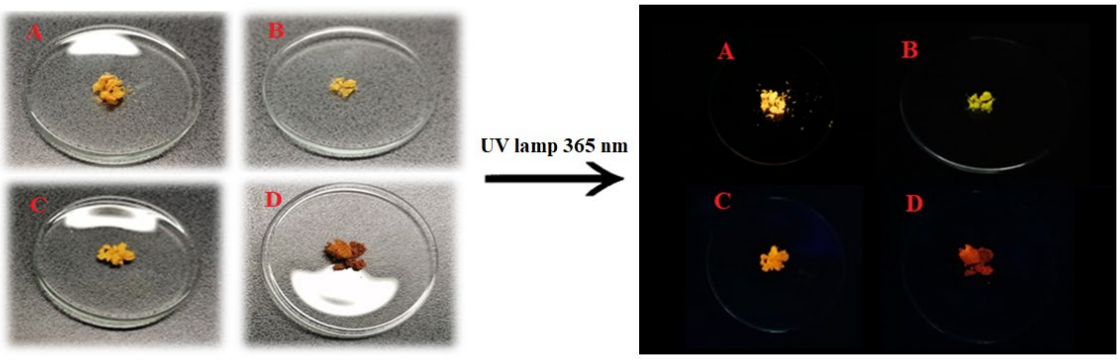

Fig. 1. The influence of introducing different substituents into the molecular structure on the fluorescent properties of quinoline salts.

The main aim of the research was to analyze the influence of introducing different substituents into the molecular structure of the compound on their fluorescent properties.

The research included the synthesis of quinoline salts and the characterization of the properties of the obtained compounds using the method of X-ray diffraction, infrared (IR) spectroscopy, X-ray powder diffraction and fluorescence spectroscopy methods (including excitation—emission matrix–EEM).

References

[1] Y. Shi, F. Zhang, R. J. Linhardt, *Dyes Pigm.*, **188** (2021) 109136.
[2] K. Li, T-B. Ren, S. Huan, L. Yuan, X-B. Zhang, *J. Am. Chem. Soc.*, **143** (2021) 21143–21160.

P-35

AMMONIUM AND POTASSIUM SALTS OF CYCLIC DIHYDROXYACETONE PHOSPHATE

Aleksandra R. Sokołowska, Katarzyna Ślepokura

University of Wrocław, Faculty of Chemistry, 14. F. Joliot-Curie, 50-383 Wrocław

Dihydroxyacetone phosphate (DHAP) is an example of a phosphate that has a great biological importance. Its cyclic form, cyclic dihydroxyacetone phosphate (cDHAP), gained interest across the years. Successful synthesis of cDHAP promised a possibility of obtaining a variety of biologically important molecules and its analogues [1]. DHAP and cDHAP are said and proven to exist in 2 forms – as a ketone and as a hydrate (*gem*-diol) [2] (Figure 1).

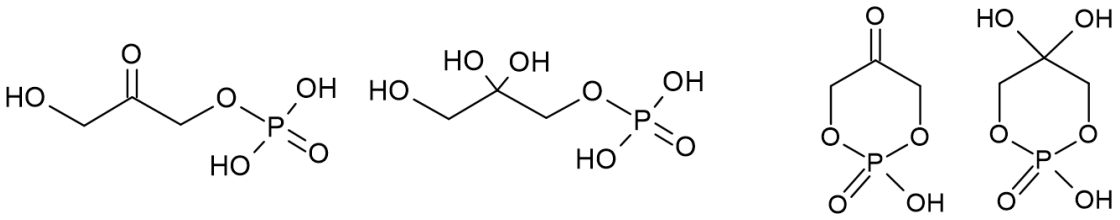

Fig. 1. Structures of DHAP and cDHAP in two forms.

In solid state, the most common conformation of six-membered O/P/O/C/C/C is chair [3]. What is interesting is the difference between ring conformations of acidic cDHAP forms – hydrate (cDHAP-H) takes chair conformation while ketone (cDHAP-K) – a skew one, which is a rare occurrence. Although cDHAP-H seems to take up the most common conformation, it is not a perfect chair – it is distorted towards envelope form [2]. So far, no crystal structures of the cDHAP salts have been reported.

As a continuation of our research on cDHAP [2,4], the crystal structures of two new salts will be presented – ammonium and potassium, NH_4(cDHAP-H) and K(cDHAP-H) (Figure 2). In both crystals, the 1,3,2-dioxaphosphorinane ring is found to adopt a chair conformation.

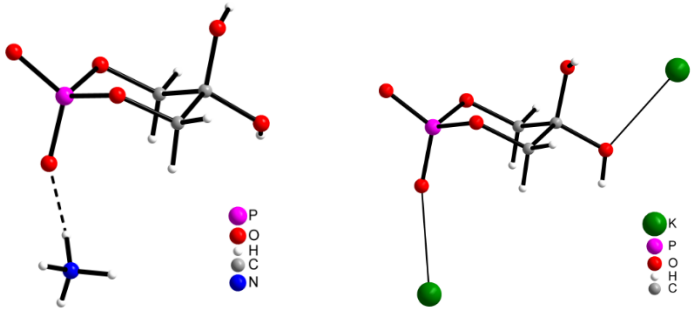

Fig. 2. Asymmetric units of NH_4(cDHAP-H) and K(cDHAP-H) (site-occupation factors of K^+ = 0.5).

Literature

[1] S. Goswami, A. K. Adak, *Tetrahedron Lett.*, **43** (2002) 504.
[2] K. Ślepokura, *Carbohydr. Res.*, **368** (2013) 97.
[3] K. Ślepokura, *Carbohydr. Res.*, **343** (2008) 114.
[4] M. Klimecka, *Cykliczne fosforany organiczne*, praca licencjacka, Uniwersytet Wrocławski, 2016.

P-36

PROJEKTOWANIE FUNKCJONALNYCH HYDROKSYBENZOKSAZYN

Magdalena Stępień, Edyta Kierasińska, Małgorzata Gazińska, Jolanta Ejfler

Wydział Chemii, Uniwersytet Wrocławski, 50-383 Wrocław,
Katedra Inżynierii i Technologii Polimerów, Wydział Chemii, Politechnika Wrocławska, 50-370 Wrocław

Polibenzoksazyny to klasa polimerów alternatywna do klasycznych żywic fenolowych, charakteryzująca się unikalnymi właściwościami, które stanowią o ich szerokim spektrum aplikacyjnym. Materiały polimerowe na bazie polibenzoksazyn są stosowane, m.in.: w przemyśle lotniczym, kosmicznym, ochronie środowiska, robotyce, medycynie. [1] Otrzymywane są w termicznej polimeryzacji 1,3-benzoksazyn, przebiegającej w zielonym procesie, bez katalizatorów i produktów ubocznych. [2]

Sterowana funkcjonalizacja benzoksazyn umożliwia zaprojektowanie właściwości takich materiałów polimerowych na etapie syntezy monomerów. Natomiast, elastyczność motywu strukturalnego monomerów otwiera możliwości szeregu modyfikacji, w tym indukowania wiązań wodorowych, które mogą wprowadzić nowe funkcje jak pamięć kształtu, czy właściwości autoregeneracyjne. [3] Odpowiednio zaprojektowane hydroksybenzoksazyny są platformą do syntezy nowych monomerów, obniżają skutecznie temperaturę polimeryzacji oraz modyfikują architekturę łańcucha polimerowego.

Otrzymano zbiór nowych orto-hydroksybenoksazyn $_{OHtBu}Bx^{R}$, które polimeryzują w niższych temperaturach niż ich analogii bez grup hydroksylowych w rdzeniu aromatycznym $_{OHtBu}Bx^{R}$ < $_{tBu}Bx^{R}$. Otwarcie pierścienia heterocyklicznego w polimeryzacji takich monomerów jest aktywowane przez zewnątrz-cząsteczkowe wiązania wodorowe i jest kluczowe w tworzeniu nietypowej, nowej struktury łańcucha polibenzoksazyn.

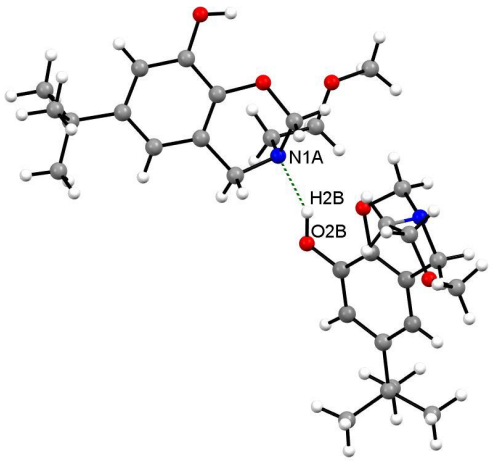

Literatura

[1] W. Ma, Z. Ma, Y. Cai, R. Du, Z. Xu, K. Jia, *ASC Material Letters*, 2020, 1575-1582.
[2] D. Trybuła, A. Marszałek-Harych, M. Gazińska, D. Jędrzkiewicz, S. Berski, J. Ejfler, *Macromolecules* , **53** (2020), 8202-8215.
[3] B. Kiskan, *Reactive and Functional Polymers*, **129**, (2018), 76-88.

P-37

STRUCTURES OF NEW PIPERAZINE DERIVATIVES

Jaroslaw Sukiennik[a], Katarzyna Gobis[b], Andrzej Fruzinski[a], Malgorzata Szczesio[a]

[a] Institute of General and Ecological Chemistry, Faculty of Chemistry, Lodz University of Technology, Zeromskiego 116, 90-924 Lodz, Poland
[b] Department of Organic Chemistry, Medical University of Gdansk, M. Sklodowskiej-Curie 3a, 80-210 Gdansk, Poland

Piperazine is one of important building block used in variety of compounds. Piperazine and triazolo-pyrazine have promising antimicrobial activity against gram-positive and gram-negative bacteria and yeast[1,2]. Their benzimidazole derivatives demonstrate biological activity against tuberculosis[3,4]. As a building block, piperazine also have much to offer.

Presented compound have very similar structure (Table, Scheme), and promising ADME analysis results.

No	a, b, c [Å]	α, β, γ [°]	Space group	R [%]
1	8.12850(10) 8.90820(10) 26.0412(3)	91.0710(10)	P $2_1/n$	3.38
2	8.02926(10) 9.32434(12) 26.0349(4)	90.1831(13)	P $2_1/n$	3.61
3	9.30960(10) 10.01480(10) 12.9361(2)	106.2890(10) 103.0470(10) 98.7360(10)	P $\bar{1}$	3.1

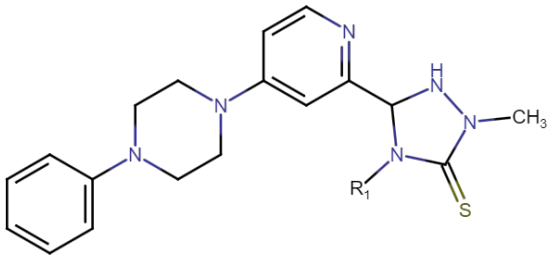

R^1 = Et, Pr, Bn

[1] M. Patil, A. Noonikara-Poyil, S.D. Joshi, S.A. Patil, S.A. Patil, A.M. Lewis, A. Bugarin, *Molecular Diversity*, **26** (2022) 827–841.
[2] A. Mermer, O. Faiz, A. Demirbas, N. Demirbas, M. Alagumuthu, S. Arumugam, *Bioorganic Chemistry*, **85** (2019) 308–318.
[3] M. Krause, H. Foks, E. Augustynowicz-Kopeć, A. Napiórkowska, M. Szczesio, K. Gobis, *Molecules*, **23** (2018) 985.
[4] A. Wang, S. Xu, Y. Chai, G. Xia, B. Wang, K. Lv, C. Ma, D. Wang, A. Wang, X. Qin, M. Liu, Y. Lu, *European Journal of Medicinal Chemistry*, **218** (2021) 113398.

P-38

CRYSTAL STRUCTURES AND ANTIBACTERIAL ACTIVITY OF [4-OXO-5-(PYRIDYLMETHYLIDENE)-2-SULFANYLIDENE-1,3-THIAZOLIDYN-3-YL]ALKANOIC ACIDS

Waldemar Tejchman[a], **Izabela Korona-Głowniak**[b], **Agnieszka-Skórska-Stania**[c], **Agnieszka Kania**[a] **and Ewa Żesławska**[a]

[a] *Institute of Biology, Pedagogical University, Podchorążych 2, 30-084 Kraków*
[b] *Department of Pharmaceutical Microbiology, Medical University of Lublin, Chodźki 1, 20-093 Lublin*
[c] *Faculty of Chemistry, Jagiellonian University, Gronostajowa 2, 30-387 Kraków*

Rhodanine derivatives show interesting biological properties *e.g.* antimicrobial, antiviral, anticancer, antiinflammatory [1] and are also used in the dye sensitized solar cells [2]. In our previous research [3], we obtained 5-arylidene-3-carboxyalkylrhodanine derivatives containing tertiary amine group bounded to aromatic ring with promising antibacterial activity. At present, our interest is focused on chemical modifications among different location of nitrogen atom. Thus, we decided to check whether the presence of a heterocyclic nitrogen atom in the aromatic ring would significantly improve antibacterial activity. Furthermore, we examined the influence of the linker length between the carboxyl group and rhodanine ring on the antibacterial activity.

In order to investigate structural properties of selected synthesized compounds, we determined the crystal structures of 4-[4-oxo-5-(pyridin-3-ylmethylidene)-2-sulfanylidene-1,3-thiazolidin-3-yl]butanoic acid (**1**), 4-[4-oxo-5-(pyridin-4-ylmethylidene)-2-sulfanylidene-1,3-thiazolidin-3-yl]butanoic acid (**2**) and 6-[4-oxo-5-(pyridin-2-ylmethylidene)-2-sulfanylidene-1,3-thiazolidin-3-yl]hexanoic acid (**3**).

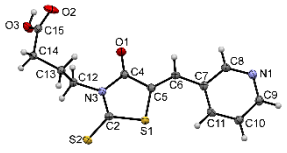

1

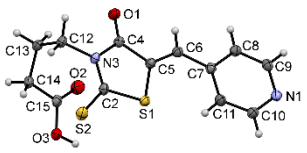

2

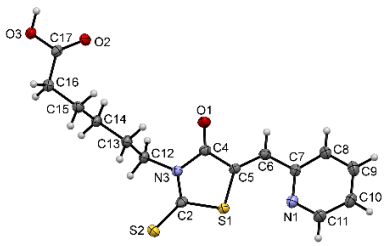

3

We analyzed the impact of nitrogen atom positions on the crystal and molecular structures, as well as the length of the linker between the rhodanine ring and carboxyl group on the intermolecular interactions. The packing of the molecules is determined by O-H···N, O-H···O, C-H···O and C-H···S intermolecular interactions. The presented compounds were also evaluated towards their *in vitro* antimicrobial activity. For compound **3**, showing higher antibacterial activity in comparison to other two, it is observed 1.5 N···S interaction between the sulfur atom of rhodanine ring and the nitrogen atom in the pyridine ring.

References

[1] D. Kaminskyy, A. Kryshchyshyn, R. Lesyk, *Eur. J. Med. Chem*., **140** (2017) 542.
[2] J. Sivanadanam *et al*., *Int. J. Hydrog. Energy*, **43** (2018) 4691.
[3] W. Tejchman, I. Korona-Głowniak, A. Malm *et al*., *Med. Chem. Res*., **26** (2017) 1316.

P-39

CRYSTAL STRUCTURE OF 1,3−DI(1,2,3−TRIAZOL−1−YL)PROPAN−2−YL STEARATE

Aleksandra Tołoczko, Miłosz Siczek, Robert Bronisz

Wydział Chemii, Uniwersytet Wrocławski, ul. F. Joliot-Curie 14, 50-383 Wrocław

1,ω-di(azolyl)alkanes (azolyl = 1,2,3-triazol-1-yl, tetrazol-1-yl, tetrazol-2-yl) are well known bridging molecules which form with 3d metal ions coordination polymers. Similarly to mono alkylazoles, they are prone to form with Fe(II) compounds exhibiting thermally induced change of spin state. Generally it was established that cooperativity of spin crossover is reduced with an increase of carbon atoms in alkyl chain of bridging molecule. Nevertheless other structural properties related, in particular, to occurrence of structural phase transitions can affect spin crossover. 1,4-di(5-ethyl-1,2,3-triazol-1-yl)butane (ebbtr) forms with Fe(II) 2D network $[Fe(\mathbf{ebbtr})_2(CH_3CN)_2](ClO_4)_2 \cdot 4CH_3CN$ [1]. In this compound takes place sequence of LS→HS→LS→HS transitions, associated with reorientation of coordinated/noncoordinated solvent molecules as well as with the deformation and the mutual shift of the polymeric units. It was found that an exchange of perchlorate on triflate anion resulted in formation of 2D net in which occurrence of normal and reverse hysteresis is driven by structural phase transitions related to: *trans-trans→gauche-trans* conformational changes of ebbtr molecules [2]. Importance of conformational changes was also notices for 2D network $[Fe(\mathbf{bbtre})_3](ClO_4)_2 \cdot 2CH_3CN$ (bbtre = 1,4-di(1-ethyl-1,2,3-triazol-5-yl)butane) in which two ways spin crossover is associated with conformational changes of alkyl spacer in bbtre molecule [3]. Thus, it is clearly visible that presence of conformationally labile fragments can be a source of structural phase transitions decisive about course of spin crossover.

Continuing our studies we have prepared novel family of potentially structurally labile ligands in which additional side chain was introduced into central carbon atom of propylene linker (Fig. 1). 1,3-di(1,2,3-triazol-1-ylo)propan-2-yl stearate has been obtained in a reaction of 1,3-di(1,2,3-triazol-1-ylo)propan-2-ol with stearoyl chloride in a mixture of dichloromethane and pyridine (5:1 v/v).

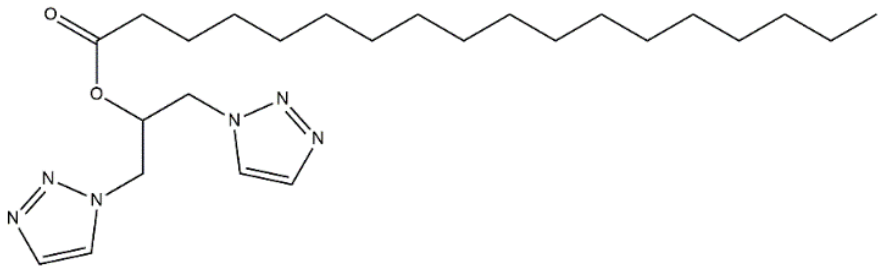

Fig 1. Molecular structure of 1,3-di(1,2,3-triazol-1-yl)propan-2-yl stearate.

Crystals of 1,3-di(1,2,3-triazol-1-yl)propan-2-yl stearate were obtained by slow evaporation of acetonitrile. Compound crystallizes in *P-1* space group (a= 5.376, b= 8.037, c= 31.169 Å, α= 85.72, β= 88.55, γ= 75.00). There will be details presented on the poster concerning crystal structures of the ligand.

P-39

References
[1] M. Weselski, M. Książek, D. Rokosz, A. Dreczko, J. Kusz, R. Bronisz, *Chem. Commun*., **54** (2018) 3895.
[2] M. Weselski, M. Książek, P. Mess, A. Dreczko, J. Kusz, R. Bronisz, *Chem. Commun*., **55** (2019) 7033.
[3] M. Książek, M. Weselski, A. Dreczko, V. Maliuzhenko, M. Kaźmierczak, A. Tołoczko, J. Kusz, R. Bronisz, *Dalton Trans*., **49** (2020) 9811.

P-40

BADANIA STRUKTURALNE I TEORETYCZNE KOMPLEKSÓW BODIPY OPARTYCH NA RÓŻNYCH RDZENIACH BORACYKLICZNYCH

Karolina Urbanowicz[a], **Paulina Halina Marek-Urban**[a,b], **Krzysztof Woźniak**[b], **Krzysztof Durka**[a]

[a] *Wydział Chemiczny Politechniki Warszawskiej, ul. Noakowskiego 3, 00-664 Warszawa*
[b] *Wydział Chemii Uniwersytetu Warszawskiego, Pasteura 1, 02-093 Warszawa*

Kompleksy BODIPY stanowią szeroką grupę luminescencyjnych pochodnych 4,4-difluoro-4-boro-3*a*,4*a*-diaza-*s*-indiacenu. Mogą zostać użyte jako chemosensory [1], barwniki używane do znakowania biomolekuł [2] czy jako fotouczulacze do zastosowań w terapii fotodynamicznej [3] i fotoinaktywacji mikroorganizmów [4]. Dotychczas modyfikacje strukturalne umożliwiające cząsteczkom kompleksów wydajne generowanie stanów trypletowych, a w konsekwencji produkcji reaktywnych form tlenu, odbywały się na ligandzie, co ograniczało dalsze zmiany w obrębie struktury cząsteczki w celu zwiększenia np. hydrofilowości związku lub poprzez wprowadzenie atomów ciężkich (np. jodu), co mogłoby zwiększyć ciemną cytotoksyczność związków.

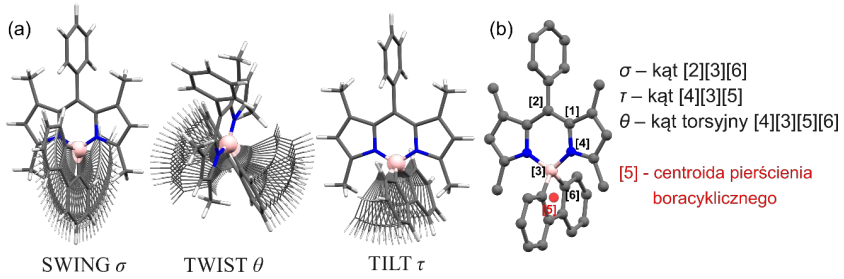

Rys. 1. (a) Wizualizacja rodzajów ruchów pomiędzy boracyklem oraz ligandem oraz (b) ich definicja.

Niedawno zostały opisane kompleksy BODIPY oparte na rdzeniach boracyklicznych, w które okazały się obiecującymi katalizatorami homofazowymi [5]. W niniejszej pracy przedstawiam wyniki badań strukturalnych dotyczących szeregu kompleksów BODIPY różniących się podstawnikiem boracyklicznym, z których część została zmodyfikowana hydrofilowymi grupami w celu poprawy ich rozpuszczalności w środowisku polarnym. Porównanie struktur molekularnych związków wskazuje na istnienie pewnej ograniczonej labilności konformacyjnej pomiędzy częścią boracykliczną a ligandem, odpowiednio donorem i akceptorem. Zdefiniowane zostały trzy rodzaje ruchów do opisu tego efektu – swing (ruch wahadłowy), tilt (pochylenie) oraz twist (skręcenie). Zakresy labilności omawianych kompleksów zostały wyznaczone w sposób ilościowy dzięki obliczeniom kwantowo-chemicznym. Omawiana labilność zdaje się grać istotną rolę przy rozważaniu mechanizmu generowania stanów trypletowych w tych układach.

Literatura

[1] X. Qi *et al.*, *J. Org. Chem.*, **71** (2006) 2881.
[2] M. Landrum *et al.*, *The Plant Journal*, **62** (2010) 529.
[3] A. Kamkaew *et al.*, *Chem. Soc. Rev.*, **42** (2013) 77.
[4] Q. Shi *et al.*, *Photodiagnosis and Photodynamic Therapy*, (2022) 102901.
[5] P. Marek-Urban *et al.*, *J. Org. Chem.*, **86** (2021) 12714.

P-41

LABILNOŚĆ KONFORMACYJNA I POLIMORFIZM W POCHODNYCH KOMPLEKSÓW BODIPY MODYFIKOWANYCH PODSTAWNIKIEM STYRENOWYM

Karolina Wrochna[a], Paulina H. Marek-Urban[a,b], Karolina Urbanowicz[a], Krzysztof Woźniak[b], Krzysztof Durka[a]

[a] *Wydział Chemiczny, Politechnika Warszawska, ul. Noakowskiego 3, 00-664 Warszawa*
[b] *Wydział Chemii, Uniwersytet Warszawski, ul. Pasteura 1, 02-093 Warszawa*

Choroby nowotworowe są niewątpliwie jednym z największych problemów współczesnej medycyny. Intensywnie poszukiwane są nowe metody walki z nowotworami, które byłyby mniej obciążające od obecnie stosowanych. Terapia fotodynamiczna (PDT) polegająca na wprowadzeniu fotouczulacza do komórek nowotworowych, a jego wzbudzeniu, co prowadzi do generowania reaktywnych form tlenu, które unieszkodliwiają komórki nowotworowe. [1] Odpowiednie projektowanie fotouczulaczy jest kluczowe, do uzyskania pożądanych cech, takich jak absorpcja promieniowania w zakresie światła czerwonego [2], czy możliwość przechodzenia przez błony komórkowe. [3]

W niniejszej pracy prezentuję nową klasę fotouczulaczy do zastosowań w PDT opartą na znanej strukturze barwników BODIPY zawierających rdzeń borafluorenu. W celu przesunięcia maksimum absorbcji w zakres światła czerwonego przeprowadzono modyfikacje polegające na wydłużeniu układu wiązań π-sprzężonych, z kolei polepszenie rozpuszczalności związku w wodzie uzyskano poprzez wprowadzono do struktury ugrupowań polieterowych.

Przeprowadzono analizę strukturalną uzyskanych pochodnych. Wykonane badania wskazują na znaczącą labilność konformacyjną w obszarze wprowadzonego podstawnika styrenowego. W przypadku trzech pochodnych zaobserwowano tworzenie się form polimorficznych. Dodatkowo, w celu przeanalizowania zakresu labilności konformacyjnej przeprowadzono skan hiperpowierzchni energii wewnętrznej cząsteczki na drodze obliczeń kwantowochemicznych. Postuluje się, że omawiana labilność może odpowiadać za zdolność generowania stanów trypletowych w tej klasie związków, a więc i pośrednio odpowiadać za zdolność do generowania reaktywnych form tlenu.

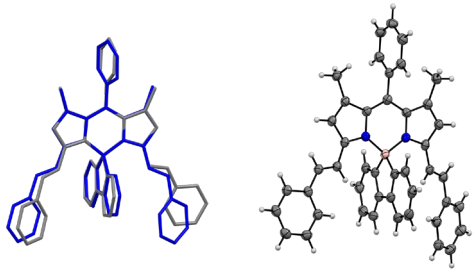

Rys 1. (a) Nałożenie struktur polimorficznych jednej z omawianych struktur (**Bf-A-St2**) oraz (b) rysunek ORTEP kompleksu **Bf-A-St2** (elipsoidy drgań termicznych na poziomie 50 % prawdopodobieństwa).

Literatura

[1] Samuel G. Awuah, Youngjae You, *RSC Adv.*, **2** (2012) 11169–11183.
[2] Michele M. Kim, Arash Darafsheh, *Photochemistry and Photobiology*, **96** (2020) 280–294.
[3] Z. Wang, M. Ivanov, Y. Gao, L. Bussotti, P. Foggi, H. Zhang, N. Russo, B. Dick, J. Zhao, M. Di Donato, G. Mazzone, L. Luo, M. Fedin, *Chem. - Eur. J.*, **26(5)** (2020) 1091−1102.

P-42

BADANIA STRUKTURALNE ZWIĄZKÓW KOORDYNACYJNYCH TYPU [RU(H)(CO)(N^N)(TPP)$_2$](PF$_6$) WYKAZUJĄCYCH WŁAŚCIWOŚCI LUMINESCENCYJNE

Waldemar Wysocki, Anna Kamecka, Zbigniew Karczmarzyk

Instytut Nauk Chemicznych,Uniwersytet Przyrodniczo-Humanistyczny w Siedlcach, ul. 3 Maja 54, 08-110 Siedlce

Badania zależności pomiędzy strukturą a właściwościami emisyjnymi kompleksów metali przejściowych cieszą się niesłabnącym zainteresowaniem zarówno z teoretycznego punktu widzenia, jak i ze względu na ich potencjalne zastosowania praktyczne. Związki rutenu (II) testowane są w kontekście ich wykorzystania, jako domieszek w warstwach emisyjnych materiałów typu OLED czy fotouczulaczy w ogniwach słonecznych (dye-sensitized solar cells – DSCC) [1]. Należy także wspomnieć o ich licznych zastosowaniach biofizycznych m.in. jako sensory, sondy DNA czy testy immunologiczne [2].

Dogodną metodą otrzymywania związków koordynacyjnych typu $[Ru(H)(CO)(N^N)(tpp)_2]^+$ (tpp – trifenylofosfina oraz N^N – ligandy α-diiminowe) jest synteza z wykorzystaniem prekursora w postaci kompleksu $[Ru(H)_2(CO)(tpp)_3]$ [3,4]. W badanych reakcjach powstają kationowe kompleksy, które następnie są izolowane w postaci soli poprzez dodanie do mieszaniny reakcyjnej nadmiaru KPF_6. Otrzymane związki koordynacyjne zostały scharakteryzowane za pomocą metod spektroskopowych: ^{1}H NMR, ^{31}P NMR, FT-IR i UV-VIS [5].

W prezentowanym komunikacie przedstawiamy syntezę, struktury krystaliczne i właściwości luminescencyjne dwóch związków koordynacyjnych rutenu (II): heksafluorofosforanu karbonylo-(hydrydo)-(1,10-fenantrolino)-bis(trifenylofosfino)-rutenu (II) (**1**) oraz heksafluorofosforanu karbonylo-(hydrydo)-(2,2'-bichinolino)-bis(trifenylofosfino)-rutenu (II) (**2**).

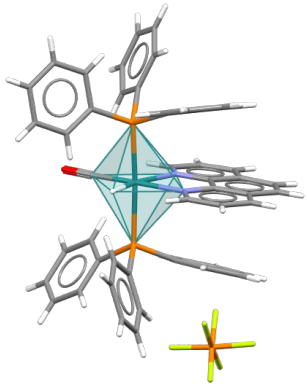

(**1**)

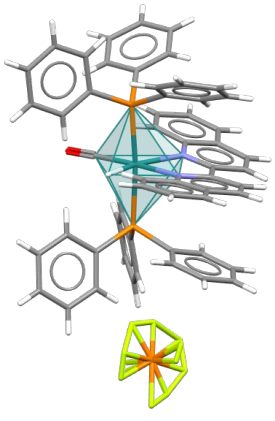

(**2**)

Związki koordynacyjne tego typu wykazują silne właściwości luminescencyjne w temperaturze 77 K, a ich czasy życia molekuły w stanie wzbudzonym są długie i wynoszą od kilkudzisięciu mikrosekund do kilku milisekund (τ_{em} ~ 62–2300 μs).

P-42

W zależności od skoordynowanego liganda N^N następuje zmiana natury stanu wzbudzonego ^{3*}[Ru(H)(CO)(N^N)(tpp)$_2$]+…PF_6– ze stanu ^{3*}MLCT do wyraźnie zaznaczonego stanu ^{3*}LC zlokalizowanego w obrębie liganda N^N [5]. Dla większości badanych kompleksów emitujących w temperaturze 298 K wyznaczone zostały wydajności kwantowe emisji (ϕ_{em} ~ 0.08–1.3 %) oraz czasy życia molekuły wzbudzonej (τ_{em} ~ 0.097–7.25 μs) [5]. W temperaturze pokojowej procesy dezaktywacji bezpromienistej w przypadku kompleksów Ru (II) są dużo szybsze, co związane jest z obecnością wzbudzonego stanu ^{3*}MC o względnie niskiej energii.

Dane krystalograficzne:

Związek (***1***): $C_{49}H_{39}N_2OP_2Ru*PF_6$, M_r = 979.80, układ jednoskośny, $P2_1/n$, a = 10.592 (2), b = 21.310 (18), c = 22.107 (3) Å, β = 97.439 (12), V = 4948 (4) Å^3, Z = 4, D_x = 1.315 gcm^{-3}, μ = 0.472 mm^{-1}, *MoKα*, λ = 0.71073 Å, T = 296 (2) K, R = 0.0594 dla 6551 refleksów.

Związek (***2***): $C_{55}H_{43}N_2OP_2Ru*PF_6$, M_r = 1055.89, układ trójskośny, P-1, a = 11.527 (2), b = 12.480 (3), c = 16.788 (3) Å, α = 89.77 (3), β = 84.56 (3), γ = 86.20 (3)°, V = 2398.8 (9) Å^3, Z = 2, D_x = 1.462 gcm^{-3}, μ = 0.493 mm^{-1}, *MoKα*, λ = 0.71073 Å, T = 296 (2) K, R = 0.0365 dla 8743 refleksów.

Literatura

[1] C. A. Bignozzi, R. Argazzi, R. Boaretto, E. Busatto, S. Carli, F. Ronconi, S. Caramori, *Coord. Chem. Rev.*, **257** (2013) 1472.

[2] D. L. Maa, V. P. Y. Maa, D. S. H. Chana, K. H. Leunga, H. Z. Hea, Ch. Leung, *Coord. Chem. Rev.*, **256** (2012) 3087.

[3] F. Yu, W-K. Chu, C. Shen, Y. Luo, J. Xiang, S-Q. Chen, C-C. Ko, T-C. Lau, *Eur. J. Inorg. Chem*, **24** (2016) 3892.

[4] H. Samouei, V. V. Grushin, *Organometallics*, **32** (2013) 4440.

[5] A. Kamecka, W. Muszyńska, A. Kapturkiewicz, *J. Lumin.*, **192** (2017) 842.

P-43

NOWY IZOMORFICZNY ZWIĄZEK KOORDYNACYJNY TERBU(III)

Patrycja Wytrych, Józef Utko, Tadeusz Lis, Łukasz John

Wydział Chemii Uniwersytetu Wrocławskiego, 14 F. Joliot-Curie, 50-383 Wrocław

Terb jest pierwiastkiem *f*-elektronowym należącym do grupy lantanowców. W naturze nie występuje w stanie wolnym, ale jego związki wchodzą w skład wielu minerałów, jak np. monacyt czy euksenit. W zależności od temperatury, terb może wykazywać interesujące właściwości magnetyczne. Ponadto, kationy Tb^{3+} dają charakterystyczny jasnożółty kolor podczas fluorescencji [1]. Terb najczęściej występuje na +3 stopniu utlenienia, ale znane są też związki, w których kation jest na +4 stopniu utlenienia, jak np. TbO_2 czy TbF_4 [2]. Ze względu na swoje charakterystyczne właściwości, związki terbu znalazły zastosowanie w materiałach półprzewodnikowych i luminescencyjnych [3].

Silanole, czyli krzemowe analogami alkoholi, to grupa związków zawierających co najmniej jedną grupę Si-OH. Związki te charakteryzują się wysoką reaktywnością i właściwościami kwasowo-zasadowymi. W porównaniu z alkoholami, silanole są mocniejszymi kwasami, ale słabszymi zasadami [4]. Czterokoordynacyjny atom krzemu w cząsteczce silanolu może być połączony z różną liczbą grup hydroksylowych, a także z podstawnikami organicznymi lub pojedynczymi atomami [5]. Związki te znalazły szereg zastosowań w wielu dziedzinach nauki, jak np. chemia materiałowa czy synteza organiczna [4]. W reakcjach ze związkami metali, silanole tworzą metalasiloksany zawierające fragment Si-O-M, które mogą zostać wykorzystane w roli katalizatorów reakcji chemicznych [5].

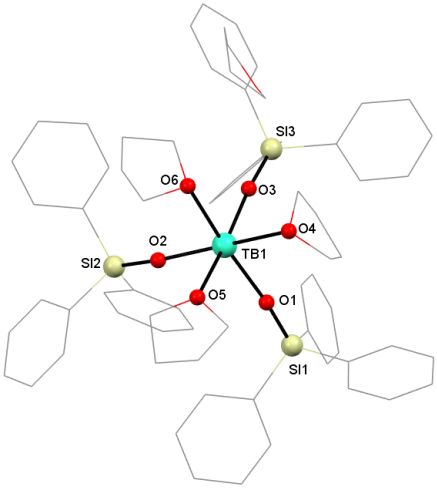

Rys. 1. Struktura krystaliczna $[Tb(OSiPh_3)_3(THF)_3]\cdot THF$.

Celem pracy była synteza związku koordynacyjnego zawierającego kation lantanowca i anion trifenylosilanolanowy (Ph_3SiO^-). W reakcji zastosowano wcześniej opisany związek litu $[Li_4(OSiPh_3)_4(THF)_2]$ [7] oraz bezwodny chlorek terbu(III). Otrzymano izomorficzny związek terbu(III), którego budowa odpowiada opisanym już

związkom ceru(III), prazeodymu(III), neodymu(III), iterbu(III), lantanu(III) i dysprozu(III) [8,9,10,11]. Kolejnym etapem prac będzie zbadanie właściwości magnetycznych i luminescencyjnych $[Tb(OSiPh_3)_3(THF)_3]\cdot THF$.

Podziękowania: Prezentowane wyniki realizowane były w ramach zadań badawczych w grancie OPUS o numerze 2020/39/B/ST4/00910.

Literatura

[1] Shimada, T.; Ohno, Y.; Okazaki, T.; et al. *Physica E: Low-dimensional Systems and Nanostructures*, **21** (2004) 1089.
[2] Gruen, D. M.; Koehler, W. C.; Katz, J. J. (April 1951). "Higher Oxides of the Lanthanide Elements: Terbium Dioxide". *Journal of the American Chemical Society*, **73** (4): 1475
[3] Hammond, C. R. (2005). "The Elements". In Lide, D. R. (ed.). *CRC Handbook of Chemistry and Physics* (86th ed.). Boca Raton (FL): CRC Press.
[4] V. Chandrasekhar, R. Boomishankar, S. Nagendran, *Chemical Reviews*, **12** (2004) 5847.
[5] M. Jeon, J. Han, J. Park, *ACS Catalysis*, **8** (2012) 1539.
[6] N. T. Tran, T. Min, A. K. Franz, *Chem. – Eur. J.*, **17** (2011) 9897.
[7] P. Wytrych, J. Utko, J. Kłak, M. Ptak, M. Stefański, T. Lis, J. Ejfler, Ł. John, *Molecules*, **27** (2022) 147.
[8] P. S, Gradeff, K. Yunlu, T. J. Deming, J. M. Olofson, R. J. Doedens, W. J. Evans, *Inorg. Chem.*, **29** (1990) 420.
[9] M. J. McGeary, P. S. Coan, K. Folting, W. E. Streib, K. G. Caulton, *Inorg. Chem.*, **30** (1991) 1723.
[10] Z. Xie, K. Chui, Q. Yang, T. C. W. Mak, J. Sun, *Organometallics*, **17** (1998) 3937.
[11] T. J. Boyle, S. D. Bunge, P. G. Clem, J. Richardson, J. T. Dawley, L.A.M. Ottley, M. A. Rodriguez, B. A. Tuttle, G. R. Avilucea, R. G. Tissot, *Inorg. Chem*., **14** (2005) 1588

P-44

HYDRAZONAMIDE DERIVATIVES OF PYRAZINE AND PYRIDINE: STRUCTURE-ACTIVITY RELATIONSHIP

Dagmara Ziembicka[a], **Katarzyna Gobis**[a], **Małgorzata Szczesio**[b]

[a] *Department of Organic Chemistry, Medical University of Gdańsk, Gen. J. Hallera 107, 80-416, Gdańsk*
[b] *Institute of General and Ecological Chemistry, Technical University of Łódź, Żeromskiego 116, 90-924, Łódź*

Intensifying the search for new drug is one of the pillars of the strategy created by World Health Organization's which aims to end the global tuberculosis epidemic by 2035 [1].

Our team's study of compounds exhibiting anti-tuberculosis activity focused on hydrazonamide derivatives of pyrazine and pyridine as structural analogues of the clinically used drugs as pyrazinamide and isoniazid. The synthesized compounds **1–3** possess a chlorine atom at the 6-position on the aromatic ring and a thiosemicarbazide chain terminated with appropriate amine at the 2-position (Fig. 1). Because derivatives showed diverse *in vitro* tuberculostatic activity (MIC 0,5−2 and 512 μg/ml), we attempted to solve the crystal structure in a search for relationships between activity and specific intramolecular interactions causing the conformation of the molecule.

Determination of the spatial structure (Tab. 1) revealed that the molecules crystallize in various forms: neutral or zwitterionic (Fig. 1). The zwitterionic structure tends to enhance planarity of a molecule, which in turn were observed probably due to the establishment of a strong intramolecular hydrogen bond. The studies reported allowed to confirm our working hypothesis that capable of adopting a planar conformation by the molecules is a prerequisite for their tuberculostatic activity [2].

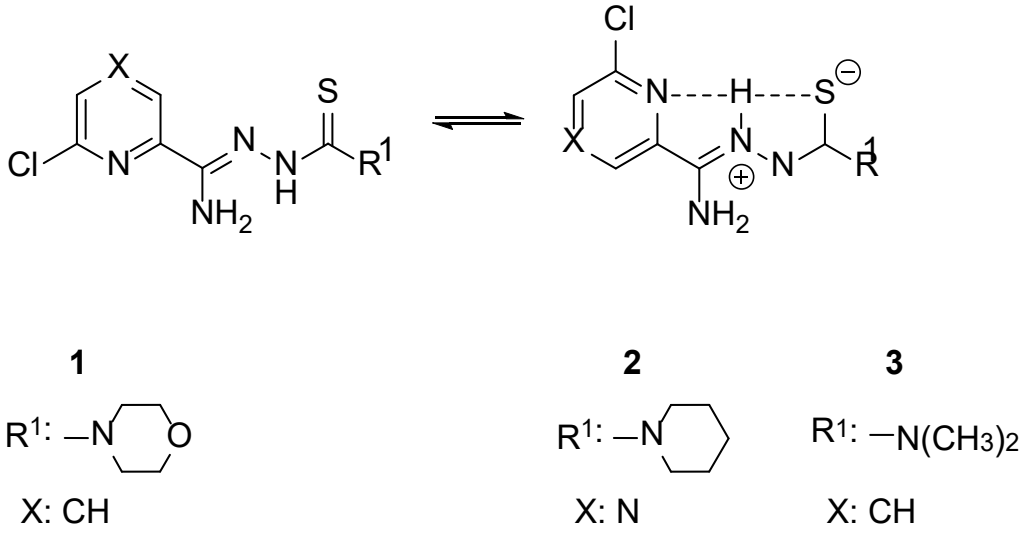

Fig. 1. The structure of compounds **1–3** and their form (neutral or zwitterionic).

Tab. 1. Crystallographic parameters of compounds **1–3**.

Compound	Space group	Unit cell parameters [Å,°]	R1 [%]
1	$P2_1/c$	7.7678, 26.4167, 6.7311 108.691	3.2
2	*Pbca*	9.6742, 14.9323, 38.6477	2.8
3	$P2_1/n$	5.5564, 11.9900, 17.3584	2.9

References

[1] Global Tuberculosis Report 2021. Geneva: World Health Organization (2021).
[2] M. L. Główka, D. Martynowski, A. Olczak, C. Orlewska, H. Foks, J. Bojarska, M. Szczesio, J. Gołka, *Journal of Chemical Crystallography*, **35** (2005) 477–480.

P-45

INTERACTION ENERGIES IN THE STRUCTURE OF 1,3-DIACETYLPYRENE INVESTIGATED UNDER HIGH PRESSURE

Aleksandra Zwolenik and Anna Makal

Faculty of Chemistry, University of Warsaw, Pasteura 1, 02-093 Warsaw

Pyrene derivatives exhibit interesting electronic and photophysical properties, which is why they are intensively investigated for a wide range of applications. Due to the presence of π-stacking interactions, they are a good example of organic semiconductors, while their fluorescent properties make them commonly used as dyes, e.g. for structural studies of proteins, DNA or lipid membranes. The occurrence of polymorphic varieties causes that the number of possible applications and the use of their properties is significantly increasing.

So far, only one polymorphic form of 1,3-diacetylpyrene has been described in the literature [1]. We discovered new polymorphic form of this compound and determined its crystal structure. In this work, we focused on studying interaction energies between molecules in its structure. To be able to do this, a series of diffraction experiments in the applied pressure range 0-1.7 GPa were performed. We investigated how the applied pressure influences the unit cell parameters and the UV-Vis spectrum of this compound. For the structures of both polymorphs at atmospheric pressure and the structure of the new polymorph at the applied pressure of 1.7 GPa, the interaction energies was calculated using CrystalExplorer17. The results were visualized using energy frameworks [2], and on their basis, conclusions were drawn as to how the intermolecular interactions affect the properties of this compound.

Bibliography

[1] S. K. Rajagopal, A. M. Philip, K. Nagarajan, M. Hariharan, *Chem. Commun*. **50(63)** (2014) 8644–8647.
[2] C. F. Mackenzie, P.R. Spackman, D. Jayatilaka, M. A. Spackman, *IUCrJ*, **4(5)** (2017) 575–587.

P-46

SUBSTITUENTS POSITION EFFECT ON THE CRYSTAL STRUCTURES OF ARYLPIPERAZINE DERIVATIVES OF 3-(2,4-DICHLOROBENZYL)-5,5-DIMETHYLHYDANTOIN

Ewa Żesławska[1], Wojciech Nitek[2] and Jadwiga Handzlik[3]

[1] Institute of Biology, Pedagogical University, Podchorążych 2, 30-084 Kraków
[2] Faculty of Chemistry, Jagiellonian University, Gronostajowa 2, 30-387 Kraków
[3] Jagiellonian University Medical College, Department of Technology and Biotechnology of Drugs, Medyczna 9, 30-688 Kraków

Civilization diseases are becoming huge problem of our society due to their increasing occurrence and the lack of effective therapy in many cases. Among them, the great place goes to central nervous system (CNS) disorders such as depression, demention or Alzheimer's and Parkinson's diseases. These irregularities are caused by dysfunction of proteins responsible for signal transmission in the body, especially within brain. To these proteins belong, *inter alia*, serotonin receptors consisting of seven classes (5-HT_1-5-HT_7) and adrenergic receptors (type α_1, α_2 i β) [1,2]. Due to the large variety of these receptors, it is necessary to search for selective ligands. A useful tool in the search for structural differences in ligands is X-ray crystal structure analysis.

The arylpiperazine derivatives of hydantoin display a variety of biological actions, especially for the treatment of CNS diseases [3]. Recently, a series of arylpiperazine derivatives of 3-(2,4-dichlorobenzyl)-5,5-dimethylhydantoin was obtained. We have performed crystal structure analysis for four derivatives, namely: 3-(2,4-dichlorobenzyl)-1-[3-(4-phenylpiperazin-1-yl)-2-hydroxypropyl]-5,5-dimethyl-imidazolidine-2,4-dione (**I**), 3-(2,4-dichlorobenzyl)-1-[3-(4-(3,4-dimethylphenyl)-piperazin-1-yl)-2-hydroxypropyl]-5,5-dimethylimidazolidine-2,4-dione (**II**), 3-(2,4-dichlorobenzyl)-1-[3-(4-(3,4-dichlorophenyl)piperazin-1-yl)-2-hydroxypropyl]-5,5-dimethylimidazolidine -2,4-dione (**IIIa**) and 3-(2,4-dichlorobenzyl)-1-[3-(4-(2,3-dichlorophenyl)piperazin-1-yl)-2-hydroxypropyl]-5,5-dimethylimidazolidine-2,4-dione (**IIIb**).

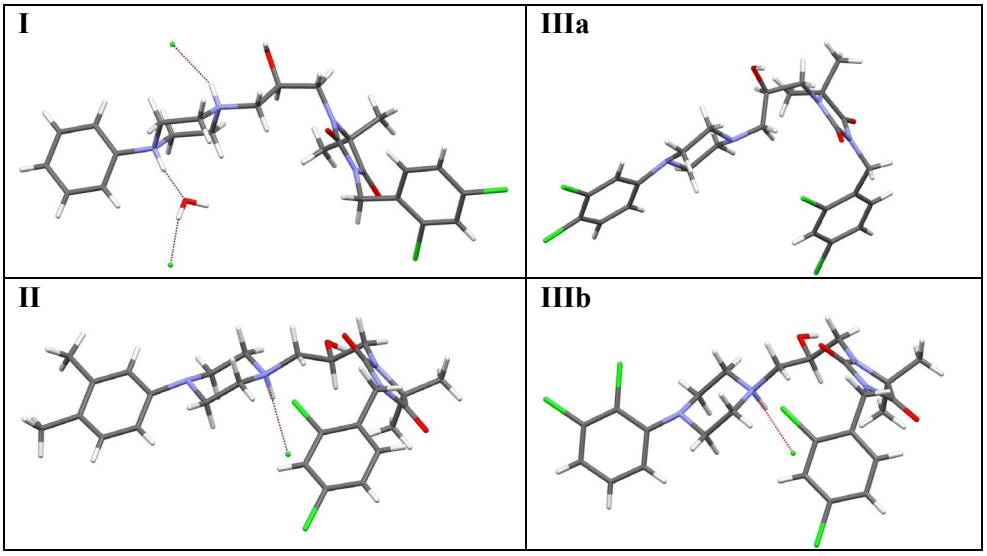

In the presented crystal structures we have analyzed the impact of methyl (**II**) and chlorine substituents (**IIIa** and **IIIb**) on the geometry of (**I**), as well as on the intermolecular interactions.

References

[1] M. Pytliak, V. Vargova *et al*., *Physiol. Res.*, **60** (2011) 15.
[2] A. D. Strosberg, *Protein Sci*., **2** (1993) 1198.
[3] J. Handzlik, A. J. Bojarski, G. Satała *et al*., *Eur J Med Chem.*, **78** (2014) 324.

P-47

STRUCTURAL AND SPECTROSCOPIC PROPERTIES GOVERNED BY METALLOPHILIC INTERACTIONS IN THE SERIES OF NOVEL RHODIUM COMPLEXES

Patryk Borowski[1], Radosław Kamiński[1], Damian Paliwoda[2], Carla Pretorius[3], Alice Brink[3], Andreas Roodt[3], Federico Cova[4], Katarzyna N. Jarzembska[1]

[1] Department of Chemistry, University of Warsaw, Żwirki i Wigury 101, 02-089, Warsaw (Poland)
[2] Université de Montpellier, ICGM, CNRS, 34293 Montpellier (France)
[3] University of the Free State, Nelson Mandela Drive, 9300 Bloemfontein (South Africa)
[4] European Synchrotron Radiation Facility, 71 Avenue des Martyrs, Grenoble (France)

pz.borowski2@student.uw.edu.pl

High pressure X-ray crystallography constitutes an important tool to study phase transitions, behavior of various materials at extreme conditions, as well as to monitor structure-property relationships in crystals. In the current study a series of high pressure single crystal XRD experiments were conducted for a series of rhodium(I) complexes. The primary aim of the study was to thoroughly investigate high-pressure impact on metallophilic Rh---Rh interactions propagating along the [001] direction and the effect of the observed structural changes on the spectroscopic properties of the examined rhodium(I) organometallic compounds. Therefore, molecular structures under various pressure, charge distribution, metal---metal interactions, and spectroscopic features were analysed both experimentally and computationally.

For a model **Rh-dbm** complex presented in Figure1 below two types of Rh···Rh contacts can be distinguished. The shorter distance is equal to 3.5517(5) Å, whereas the longer one - 3.6279(5) Å. In general, both distances shorten along with the pressure increase converging to about 2.9 Å at 10 GPa.

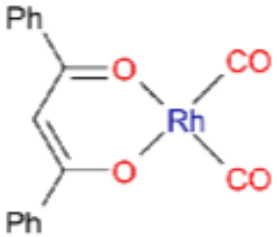

Fig. 1. Selected square-planar Rh complex (Ph= phenyl).

The authors thank the SONATA BIS grant (No. 2020/38/E/ST4/00400) of the National Science Centre in Poland, University of Warsaw, for financial support. The Wrocław Centre for Networking and Supercomputing (grant No. 285) is gratefully acknowledged for providing computational facilities. The in-house X-ray diffraction experiments were carried out at the Department of Physics, University of Warsaw, on Rigaku Oxford Diffraction SuperNova diffractometer, which was co-financed by the European Union within the European Regional Development Fund (POIG.02.01.00-14.122/09).

P-48

STRUKTURY MAGNETYCZNE ZWIĄZKÓW $R_2Ni_{1.78}In$ (R = Tb, Ho, Er, Tm) BADANE METODĄ DYFRAKCJI NEUTRONÓW

Stanisław Baran[1], Aleksandra Deptuch[2], Andreas Hoser[3], Bogusław Penc[1], Yuriy Tyvanchuk[4], Andrzej Szytuła[1]

[1] Instytut Fizyki im. M. Smoluchowskiego, Uniwersytet Jagielloński, ul. Łojasiewicza 11, 30-348 Kraków, Polska
[2] Instytut Fizyki Jądrowej im. H. Niewodniczańskiego, Polska Akademia Nauk, ul. Radzikowskiego 152, 31-342 Kraków, Polska
[3] Helmholtz-Zentrum Berlin für Materialien und Energie GmbH, Hahn-Meitner Platz 1, 14109 Berlin, Niemcy
[4] Zakład Chemii Analitycznej, Lwowski Uniwersytet Narodowy im. I. Franki, Kyryla i Mefodiya 6, 79005 Lwów, Ukraina

Struktury magnetyczne związków międzymetalicznych $R_2Ni_{1.78}In$ (R = Ho, Er, Tm), krystalizujących w grupie przestrzennej *P4/mbm* (nr. 127), zostały określone z wykorzystaniem dyfrakcji neutronów [1]. Pomiary wykonano na dyfraktometrze E6 w Helmholtz-Zentrum Berlin für Materialien und Energie GmbH w Berlinie w 1.6 K oraz powyżej temperatury Néela dla każdego ze związków. Dozwolone przez symetrię struktury magnetyczne zostały określone z użyciem programu Basireps [2], natomiast ostateczne modele otrzymano poprzez dopasowanie Rietvelda w programie FullProf [2]. Dla R = Tb wykorzystano analizę symetrii by potwierdzić strukturę magnetyczną zaprezentowaną w [3].

Wszystkie badane związki są antyferromagnetykami o strukturze magnetycznej opisanej wektorem propagacji w postaci $\mathbf{k} = [k_x, k_x, ½]$ (Rys. 1). Dla R = Tb, Er, Tm struktura magnetyczna jest współmierna, o k_x = ¼, natomiast dla R = Ho jest niewspółmierna, o k_x = 0.3074(4). Momenty magnetyczne, zlokalizowane wyłącznie na atomach pierwiastków ziem rzadkich R, są zorientowane prostopadle do płaszczyzny (001) dla R = Tb, Ho oraz leżą na płaszczyźnie (001) dla R = Er, Tm. W tym drugim przypadku, uzyskanie wiarygodnych wartości momentu magnetycznego na wszystkich atomach R wymaga opisu struktury magnetycznej z użyciem dwóch wektorów: $\mathbf{k}$ = [¼, ¼, ½] dla atomów w położeniach (x_R, x_R + ½, ½) i (1 − x_R, ½ − x_R, ½) oraz $\mathbf{k}'''$ = [−¼, ¼, −½] dla atomów w położeniach (x_R + ½, 1 − x_R, ½) i (½ − x_R, x_R, ½). Różne orientacje momentu magnetycznego dla różnych R można tłumaczyć w oparciu o teorię pola krystalicznego (czynnik Stevensa ma wartości ujemne dla Tb, Ho oraz dodatnie dla Er, Tm [4]). Wartości momentów magnetycznych w 1.6 K dla R = Tb, Er, Tm wynoszą odpowiednio 7.55(5) μ_B, 6.5(1) μ_B, 6.09(4) μ_B, natomiast dla R = Ho amplituda modulacji momentu magnetycznego jest równa 7.93(8) μ_B.

P-48

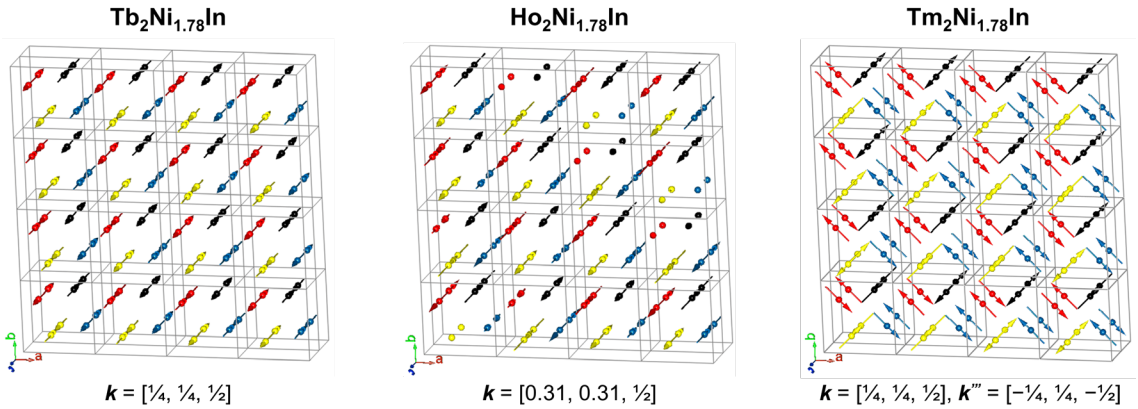

Rys. 1. Struktury magnetyczne związków $R_2Ni_{1.78}In$ (R = Tb, Ho, Tm) w 1.6 K [1]. Dla R = Er, uporządkowanie momentów jest takie samo jak dla R = Tm [1]. Struktura magnetyczna $Tb_2Ni_{1.78}In$ jest opisana także w [3,5].

Literatura

[1] S. Baran, A. Deptuch, A. Hoser, B. Penc, Yu. Tyvanchuk, A. Szytuła, *Acta Cryst. B*, **77** (2021) 824.
[2] J. Rodríguez-Carvajal, *Physica B*, **192** (1993) 55.
[3] A. Szytuła, S. Baran, A. Hoser, Ya. M. Kalychak, B. Penc, Yu. Tyvanchuk, *Acta Phys. Pol.*, **124** (2013) 994.
[4] K. W. H. Stevens, *Proc. Phys. Soc. A*, **65** (1952) 209.
[5] MAGNDATA: A Collection of magnetic structures with portable cif-type files, #1.653, http://webbdcrista1.ehu.es/magndata/index.php?this_label=1.652.

P-49

STRUCTURAL AND SPECTROSCOPIC INVESTIGATIONS OF A RUTHENIUM COMPLEX CONTAINING TWO AMBIDENTATE LIGANDS

Krystyna A. Deresz[1], D. Jacewicz[2], D. Schaniel[3], R. Kamiński[1], K. N. Jarzembska[1]

[1]Department of Chemistry, University of Warsaw, Warsaw, Poland
[2]Department of Chemistry, University of Gdansk, Gdansk, Poland
[3]Department of Chemistry, University of Lorraine, Nancy, France

Photocrystallography is a group of methods based on X-ray diffraction used for determination of structural changes in crystals under light irradiation. Besides X-Ray photocrystallography, techniques such as spectroscopy can be used to shed some light onto structural changes and dynamics of temperature- and light-induced processes, e.g. isomerization reactions. Linkage isomerization in this method can be traced thanks to the characteristic bands of ambidentate ligands. Important advantage of applying spectroscopy to photocrystallographic investigations is the experiment time, which is shorter than that needed for the diffraction experiment. It allows to select the optimal excitation wavelength, as well as to examine the relaxation of the sample. Such information constitutes a good starting point for X-ray diffraction measurements, where changes can be traced with atomic resolution (thus the metastable species can be detected more accurately) but experiments are much longer.

An important element of photocrystallographic investigations is structural analysis. It allows to determine the isomerization potential of the examined compound, mostly by analyzing intermolecular interactions in the crystal lattice and energies of different linkage isomers. Moreover, by means of theoretical calculations, bands in the spectrum can be assigned to specific vibrations in a molecule which significantly facilitates the analysis of the experiments.

For the purpose of this presentation a ruthenium complex containing two ambidentate ligands: –NO and –DMSO, was chosen. Using the solid-state IR technique optimal excitation wavelength was established along with the optimal irradiation time facilitating the maximum reaction conversion. Further, the temperature range at which the compound switches was determined, whereas the metastable linkage isomer relaxation time was examined under various conditions. In order to interpret IR spectra linkage isomers of the studied compound were modelled at the B3LYP/LANL2DZ level of theory and analyzed – both their relative molecular energies and the corresponding IR spectra. The most important intermolecular interactions and their energies of the ruthenium complex were also analyzed and calculated at the B3LYP/LANL2DZ level of theory.

The authors thank the PRELUDIUM BIS grant (No. 2019/35/O/ST4/04197) from the National Science Center, the European Regional Development Fund (POIG.02.01.00-14-122/09), and the Wrocław Center for Networking and Supercomputing (Grant No. 285) for research funding, and the University de Lorraine, France.

P-50

PHASE TRANSITIONS IN DIELECTRIC PERCHLORATE

Monika Trzebiatowska[1], Dorota A. Kowalska[1], Marek Gusowski[2], Ewelina Jach[2], Agnieszka Ciżman[2]

[1] *Institute of Low Temperature and Structure Research, Polish Academy of Sciences, Okólna 2, 50-422 Wrocław, Poland*
[2] *Faculty of Fundamental Problems of Technology, Wrocław University of Science and Technology, Wybrzeże Wyspiańskiego 27, 50-370, Wrocław, Poland*

The crystals of tetrapropylammonium perchlorate, $TePrAClO_4$, undergo two reversible phase transitions: at ~284 K (PT1) and ~445 K (PT2). The observed phase transitions, distinct dielectric and relaxation effects are due to the dynamic motions of the organic cations and anionic framework. The crystals becomes ordered at low temperatures, then disordered at room temperature and highly disordered at high temperatures. Until now, the study of this interesting compound has been limited to its ordered low temperature phase (LT, Fig. 1a) [1].

The X-ray single crystal diffraction studies shows that at room temperature (RT) the structure is orthorhombic and accommodates *Pnam* space group with cell parameters: $a = 13.644(4)$, $b = 12.257(4)$, $c = 9.758(3)$ Å; $V = 1634.4(9)$ Å^3; $Z = 4$ [2]. The asymmetric unit comprises two disordered ions: $TePrA^+$ with C and H atoms disordered over a mirror plane perpendicular to the *c*-axis direction and ClO_4^- with disordered O atoms (Fig. 1b).

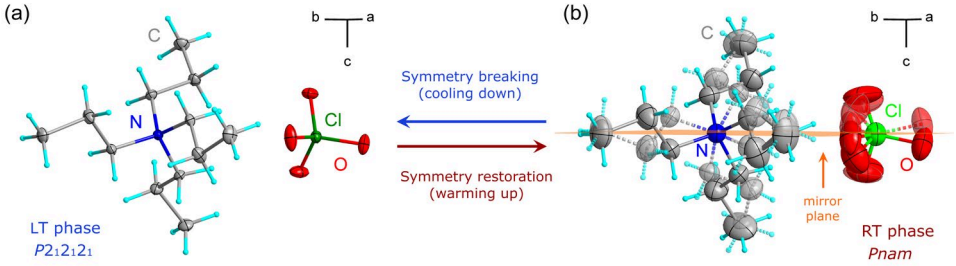

Fig. 1. The symmetry change in $TePrAClO_4$ as the temperature increases from (a) LT to (b) RT phase.

The comparable values of changes in wavenumber and FWHM shifts (IR and Raman spectroscopy) in the case of tetrapropylammonium and perchlorate ions around PT1 and slightly more significant changes for organic cations (juxtaposed with perchlorate ions) in PT2 lead to the conclusion that PT1 is equally driven by motions of the two ions, while PT2 is more influenced by the motions of organic cations. The PT2 with its large entropy change resembles the behavior found in liquid crystals. The dielectric function values can be switched and tuned in the low- and high-dielectric states, which may indicate the potential application of this material in sensors or actuators.

References

[1] T. Fujihara, M. Kato, A. Nagasawa, Tetra-n-Propylammonium Perchlorate. *Acta Crystallogr. E*, **61(5)** (2005) 1439–1440.
[2] M. Trzebiatowska, D. A. Kowalska, M. Gusowski, E. Jach, A. Ciżman, Nonobvious behavior of an obvious material – phase transitions in dielectric perchlorate. *J. Phys. Chem.* – under review.

P-51

NIETYPOWE PRZEJŚCIE FAZOWE W KRYSZTALE $(C_2H_{10}N_2)_2[ZnBr_4]Br_2$

Monika K. Krawczyk[a], Zbigniew Czapla[b] i Vasyl Kinzhybalo[c]

[a] *Instytut Fizyki Doświadczalnej, Uniwersytet Wrocławski, plac Maksa Borna 9, 50-204 Wrocław*
[b] *Katedra Fizyki, Politechnika Opolska, ul. Ozimska 75, 45-370 Opole*
[c] *Instytut Niskich Temperatur i Badań Strukturalnych, PAN, ul. Okólna 2, 50–422 Wrocław*

Otrzymano i wyizolowano w postaci krystalicznej nową sól cynku(II) o wzorze $(C_2H_{10}N_2)_2[ZnBr_4]Br_2$, zawierającą jony $ZnBr_4^{2-}$, Br^- i kationy etylenodiamoniowe $(C_2H_{10}N_2)^{2+}$ (Rys. 1). Związek krystalizuje w układzie jednoskośnym, w grupie przestrzennej $P2_1/m$. W krysztale jony $ZnBr_4^{2-}$ leżą na płaszczyźnie *m*, natomiast jony Br^- i kationy $(C_2H_{10}N_2)^{2+}$ leżą w pozycjach ogólnych. Badania metodą DSC i TGA wykazały, że kryształ ulega odwracalnemu przejściu fazowemu w temperaturze około 253 °C (podczas ogrzewania), blisko jego temperatury rozkładu (około 265 °C) i ~248 °C (podczas chłodzenia). Badany kryształ jest izomorficzny z kryształem soli $(C_2H_{10}N_2)_2[CuBr_4]Br_2$ [1]. Zanany jest również analogiczny związek $(C_2H_{10}N_2)_2[ZnCl_4]Cl_2$ [2], który krystalizuje w układzie rombowym. Podczas krystalizacji $(C_2H_{10}N_2)_2[ZnBr_4]Br_2$ pojawiają się niekiedy kryształy zbliźniaczone z pojedynczą płaszczyzną zbliźniaczenia (100) oraz kryształy, w których występuje więcej niż jedna płaszczyzna zbliźniaczenia, co potwierdzają obserwacje mikroskopowe. Biorąc pod uwagę symetrię kryształu zbliźniaczenia te można opisać jako strukturę domenową typu ferroelastycznego. Podczas ogrzewania kryształu w temperaturze przemiany fazowej pojawia się dodatkowa struktura domenowa ze ścianami domenowymi nachylonymi do płaszczyzny (100) pod kątem około 45°, która nie zanika po schłodzeniu do temperatury pokojowej.

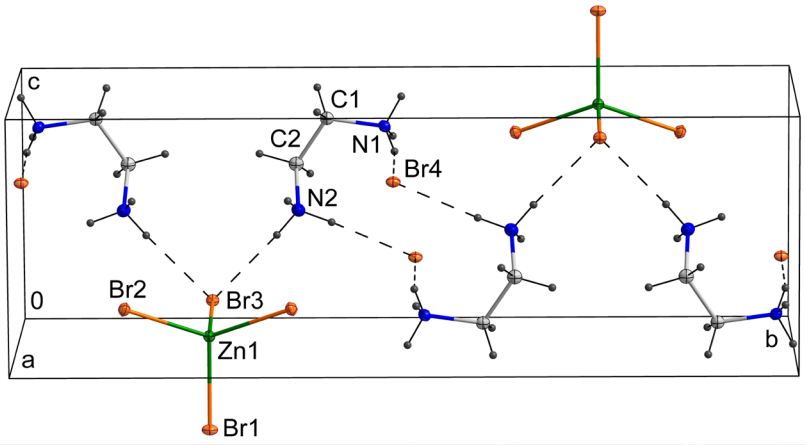

Rys. 1. Struktura kryształu $(C_2H_{10}N_2)_2[ZnBr_4]Br_2$ w temperaturze 100 K. Elipsoidy drgań atomów C, N, Br i Zn przedstawiono z 50% prawdopodobieństwem.

Literatura

[1] D. N. Anderson, R. D. Willett, *Inorg. Chim. Acta*., **5** (1971) 41.
[2] D.-H. He, Y.-Y. Di, B. Wang, W.-Y. Dan, Z.-C. Tan, *Termochimica Acta*, **506** (2010) 41.

P-52

HIGH PRESSURE STUDIES ON COUPLING BETWEEN SPIN CROSSOVER AND STRUCTURAL PHASE TRANSITIONS IN 2D COORDINATION POLYMERS

Maria Książek[1], Joachim Kusz[1], Damian Paliwoda[2], Marek Weselski[3] i Robert Bronisz[3]

[1] Institute of Physics, University of Silesia, 75 Pułku Piechoty 1, 41-500 Chorzów
[2] Laboratoire de Chemie de Coordination, CNRS & Université de Toulouse (UPS, INP) 31400 Toulouse
[3] Faculty of Chemistry, University of Wrocław, F. Joliot-Curie 14, 50-383 Wrocław

Spin crossover depends on reversible switching of electronic configuration which can be triggered by a change of temperature, by light irradiation or by an application of pressure. Studies on family of 2D coordination polymers $[Fe(bbtr)_3]X_2$ (bbtr=1,4-di(1,2,3-triazol-1-yl)butane, Fig. 1; X=ClO_4^-, BF_4^-) showed the occurrence of very abrupt and hysteretic thermally induced spin crossover in perchlorate analogue ($T_{1/2}^{\downarrow}$=101 K and $T_{1/2}^{\uparrow}$=109 K) [1, 2]. Spin crossover in this complex is associated with the structural phase transition (T_{PT}=125 K). In contrast cooling of sample of tetrafluoroborate analogue with scan rate 1K/min does not involve change of spin state of Fe(II) ions. Nevertheless, this complex exhibits very interesting properties related to light induced spin state switching because below 65 K, because it is possible to achieve permanent HS→LS(r-LIESST) or LS→HS(LIESST) switching [3]. Therefore in order to gain a knowledge about differences in spin crossover properties of bbtr based systems we have performed single crystal synchrotron radiation studies to about 2.0 GPa. These experiments revealed the possibility to trigger HS→LS transition which is preceded by the occurrence of the structural phase transition. Concomitantly high pressure studies carried out for Zn(II) analogue does not reveal~~ed~~ the occurrence of the structural phase transition.

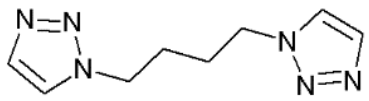

Fig. 1. Molecular structure of bbtr.

Unit cell parameters and the volume of the unit cell decrease with increasing the applied pressure and the SCO is shifted to the room temperature.

Details, concerning the results of magnetic and high pressure single crystal synchrotron radiation diffraction studies of $[Fe(bbtr)_3](BF_4)_2$, $[Fe(bbtr)_3](ClO_4)_2$, their Zn(II) analogues and for selected solid solutions $[Fe(bbtr)_3](BF_4)_{2x}(ClO_4)_{2(1-x)}$ will be presented on the poster.

References

[1] R. Bronisz, *Inorg. Chem.*, **44** (2005) 4463.
[2] J. Kusz, R. Bronisz, M. Zubko, G. Bednarek, *Chem. Eur. J.*, **17** (2011) 6807.
[3] I. Krivokapic, P. Chakraborty, R. Bronisz, C. Enachescu, A. Hauser, *Angew. Chem. Int. Ed.*, **49** (2010) 8509.

P-53

VARIABLE TEMPERATURE AND SPATIO-TEMPORAL STUDIES OF SPIN CROSSOVER IN SOLID SOLUTIONS $[Fe(bbtr)_3](BF_4)_{2x}(ClO_4)_{2(1-x)}$ $(0.1 \leq x \leq 0.9)$

Maria Książek[1], Joachim Kusz[1], Marek Weselski[2] i Robert Bronisz[2]

[1]Institute of Physics, University of Silesia, 75 Pułku Piechoty 1, 41-500 Chorzów
[2]Faculty of Chemistry, University of Wrocław, F. Joliot-Curie 14, 50-383 Wrocław

The coordination compound $[Fe(bbtr)_3](BF_4)_2$ (bbtr=1,3-di(1,2,3-triazol-1-yl)butane) is isostructural with $[Fe(bbtr)_3](ClO_4)_2$ which exhibits thermally induced spin crossover [1]. In perchlorate the spin crossover is proceeded by the structural phase transition P-3→P-1 [2].

Nevertheless the research conducted so far has not revealed the ability to thermally induced spin transition in tetrafluoroborate. Moreover, in spite of structural similarity of both complexes the structural phase transition was not revealed this compound. Recently we have found that spin crossover in another coordination polymer $[Fe(ebtz)_2(C_2H_5CN)_2](BF_4)_2$ (ebtz=1,2-di(tetrazol-2-yl)ethane) occurs during cooling at $T_{1/2}^{\downarrow}$=80 K and is kinetically very slow [3]. Thank to very slow spin crossover in this complex we were able to perform spatio-temporal studies at the lowest accessible temperature that is at 80 K. Performed measurements allowed to recognize decoupling of some structural changes from spin switching. Therefore, taking into account that the possible barrier in observation of a spin crossover in $[Fe(bbtr)_3](BF_4)_2$ could be caused by slowness of the structural process, we have again undertaken magnetic and structural studies. Repeated magnetic studies revealed that the tetrafluoroborate, however, exhibits spin crossover but the HS→LS transition is very slow and occurs during cooling in temperature below 80 K. The key to understanding why the spin crossover in tetrafluoroborate occurs far below spin crossover temperature than in perchlorate analogue requires to establish whether spin crossover is associated with structural phase transition. Thus, we have decided to synthesize series of solid solutions $[Fe(bbtr)_3](BF_4)_{2x}(ClO_4)_{2(1-x)}$ $(0.1 \leq x \leq 0.9)$ in order to reveal dependence between temperatures of spin crossover and structural phase transitions. What is important, we have supposed that the preparation of samples rich for tetrafluoroborate anion ($x < 0.4$) will allow to shift the spin crossover temperature to 80 K or slightly above the one, thus, giving an opportunity to perform spatio-temporal measurements revealing order of events, that is, spin crossover and structural phase transition.

On the poster there will be presented details concerning results of the magnetic and structural studies of $[Fe(bbtr)_3](BF_4)_2$, $[Fe(bbtr)_3](ClO_4)_2$, their Zn(II) analogues and solid solution $[Fe(bbtr)_3](BF_4)_{2x}(ClO_4)_{2(1-x)}$ (x= 0.1-0.9).

References

[1] R. Bronisz, *Inorg. Chem.*, **44** (2005) 4463.
[2] J. Kusz, R. Bronisz, M. Zubko, G. Bednarek, *Chem. Eur. J.*, **17** (2011) 6807.
[3] M. Książek, M. Weselski, M. Kaźmierczak, A. Tołoczko, M. Siczek, P. Durlak, J. A. Wolny, V. Schönemann, J. Kusz, R. Bronisz, *Chem. Eur. J.*, **17** (2020) 14419.

P-54

ROZMIAROWE PRZEMIANY FAZOWE POD CIŚNIENIEM – BAZA DANYCH
SIZE-INDUCED PHASE TRANSITIONS UNDER HIGH PRESSURE - DATABASE

Paweł E. Tomaszewski

Instytut Niskich Temperatur i Badań Strukturalnych, Polska Akademia Nauk, ul. Okólna 2, 50-422 Wrocław

Prezentowana baza danych stanowi dopełnienie wcześniej opracowanych danych o strukturalnych przemianach fazowych w kryształach, PTDB. Pierwsza baza obejmuje przemiany zachodzące przy zmianie temperatury, druga – przy zmianie ciśnienia zewnętrznego. Modne od wielu lat badania nanokryształów zaowocowały bazą przemian rozmiarowych. Teraz przyszedł czas na ostatnie zestawienie – przemian fazowych obserwowanych pod ciśnieniem a wywołanych zmianą wielości krystalitów.

O ile opis temperaturowych i ciśnieniowych przemian fazowych nie stanowi specjalnego problemu (zarówno wyznaczanie temperatury jak i ciśnienia zostało już wystarczająco dobrze opanowane), to pomiary dla nanokryształów, zwłaszcza pod ciśnieniem, napotykają na poważne problemy metodologiczne. Dlatego wszelkie zestawienia czy porównania danych literaturowych są obarczone dużymi i niewyznaczalnymi błędami. W zasadzie, co publikacja, to inne dane. I praktycznie nie ma możliwości standardowego opisu. Wiadomo, że wyznaczenie wielkości krystalitów to poważne zagadnienie metrologiczne (i nie chodzi tu tylko o podawane wartości do… dziesięciu miejsc po przecinku!). Do tego dochodzi kwestia różnych definicji czyli określenia, kiedy zachodzi przemiana fazowa (należy pamiętać, że w pomiarach ciśnieniowych kolejne punkty pomiarowe są zazwyczaj dosyć od siebie oddalone).

Na prezentowaną bazę zostały więc nałożone silne ograniczenia. Zestawienie obejmuje tylko przemiany zachodzące przy rosnącym ciśnieniu i w temperaturze pokojowej. Jeżeli autorzy wyraźnie zaznaczyli różnice w przemianach pod ciśnieniem (kwazi)hydrostatycznym i niehydrostatycznym, to takie dane zostały osobno zamieszczone w tabeli (jednak pominięte zostały przypadki, gdy pod ciśnieniem hydrostatycznym nie obserwowano przemiany fazowej). Uwzględnione zostały wyniki badań na próbkach proszkowych o (prawie) kulistych kształtach ziaren (pominięte zostały więc wszelkie krystality nitkowate, podłużne, płytkowe). Należy zresztą pamiętać, że kształt krystalitów na istotny wpływ na występowanie przemiany, jej charakter i na ciśnienie przemiany. Jeżeli dostępne są dane dla rożnych wielkości ziaren, to zostały one przedstawione według rosnącej wartości. W większości przypadków zarówno wielkość krystalitów, jak i wartość ciśnienia, zostały podane bez uwzględnienia miejsc po przecinku. W ten sposób, dane w bazie są w pewien sposób umowne. Dodatkowo podane zostało odniesienie do odpowiedniej przemiany fazowej dla kryształu objętościowego. Tu mamy do czynienia w zasadzie z dwoma przypadkami: albo przemiana rozmiarowa dla nanokryształu zachodzi przy wyższym ciśnieniu (typ „A”) lub przy niższym (typ „C”). Sporadycznie spotyka się przemiany dla takiego samego ciśnienia (typ „B”). Jeśli jednak w nanokrysztale obserwowana jest

przemiana, której nie ma dla kryształu objętościowego, to w tabeli bazy pojawia się znak „---”.

Prezentowana baza przemian rozmiarowych pod ciśnieniem obejmuje 191 rodzajów przemian obserwowanych dla 244 próbek pochodzących z 122 kryształów. Dane pochodzą z analizy 350 publikacji.

kryształ	**ziarno [nm]**	**faza nisko-ciśnieniowa**	**p_{tr} [GPa]**	**faza wysoko-ciśnieniowa**	**typ**	**p_{bulk} [GPa]**	**literatura**
Ag	5-10	*Fm*3*m*	10	trig.	---	---	08KoK

P-55

CHARGE DENSITY ANALYSIS OF TWO NEW ORGANIC SALTS CONTAINING TYRAMINE

Szymon Grabowski and Marlena Gryl

Faculty of Chemistry, Jagiellonian University, Gronostajowa 2, 30-387 Kraków

Two new organic salts were obtained using the slow evaporation crystallization technique: Lpyrtyr (from L-pyroglutamic acid and tyramine) and (R)-mantyr (from R-mandelic acid and tyramine). Both structures contain tyramine which is an extraordinary building block in crystal engineering. In particular, tyramine is found in many co-crystals and salts. Thus, it is proven to interact with a diversity of components [1]. An opposed example can be molecules like R-mandelic acid, which rarely forms multicomponent solids. Therefore, classical crystal structure analysis and charge density studies were undertaken to understand why tyramine is a good coformer for cocrystallization, even for difficult compounds like R-mandelic acid.

Comparing the conformation of tyramine cation from different organic salts (CSD), it can be seen that this component has conformational flexibility due to various spatial arrangements of the side alkyl chain (Fig. 1).

Another interesting fact is that in the Lpyrtyr structure, there are no hydrogen bonds between any tyramine cations. However, in (R)-mantyr tyramine cation forms five different interactions with (R)-mandelic anion. Based on these two facts, it can be said that this component also exhibits substantial synthon formation flexibility.

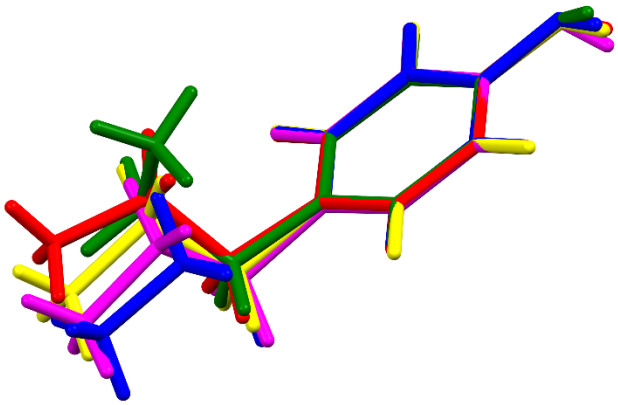

Fig. 1. Comparison of tyramine cation from different organic salts from CSD. Red – from Lpyrtyr; magenta – from (R)-mantyr; green, yellow, blue – other salts.

Using the multipolar Hansen-Coppens model [2], the accurate charge density distribution was determined in these two salts, and interaction energies [3] were compared. Bond paths and critical points of electron density distribution in the asymmetric units of both structures are presented in Fig. 2. In Lpyrtyr, the strongest interaction (about -13 kcal/mol) can be found between two different ions. Nevertheless, L-pyroglutamic anions are connected similarly as in the structure of the substrate (Ref. BOBQOA). In the second structure, the sum of hydrogen bonds energies between cation

and anion is -19.53 kcal/mol, while there is only one interaction with an energy -1.40 kcal/mol between tyramine cations. Weak C-H···π interactions between cations and anions additionally stabilize the obtained crystal structure.

The interaction analysis has proven that several aspects should be taken into account to evaluate the probability of multicomponent structure formation:

(a) conformational and synthon formation flexibility,

(b) lock and key molecular recognition mechanisms and

(c) strategies for enforcing heterosyntons formation like mimicking interactions from target structure or enabling completely new, more energetically favourable ones.

All those aspects are found in the structures containing tyramine, making this molecule a valuable coformer in crystal engineering [4].

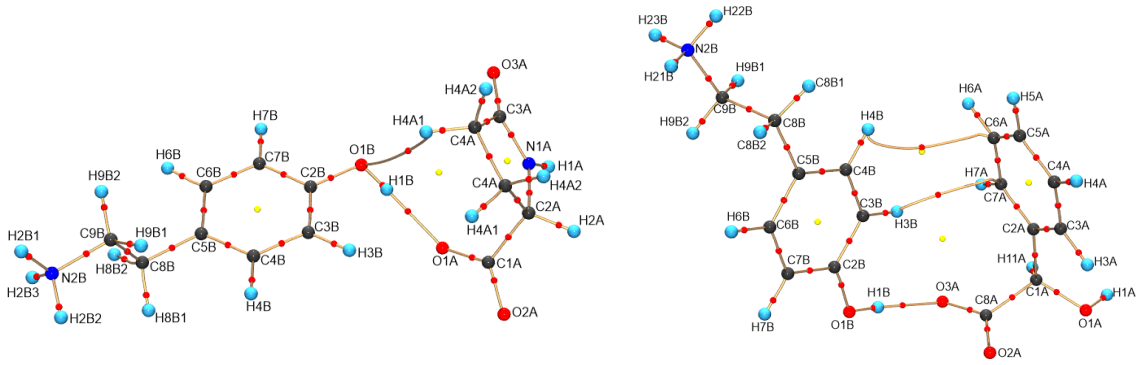

Fig. 2. Bond paths and critical points of electron density in the asymmetric units of Lpyrtyr (left) and (R)-mantyr (right). Red dots – bond critical points, yellow dots – rings critical points.

Literature

[1] N. E. B. Briggs, A. R. Kennedy & C. A. Morrison, *Acta Cryst. B*, **68** (2012) 453–464.
[2] N. K. Hansen & P. Coppens, *Acta Cryst. A*, **34** (1978) 909-921.
[3] E. Espinosa, E. Molins, C. Lecomte, *Chem. Phys. Lett.*, **285** (1998) 170−173.
[4] S. Grabowski & M. Gryl (2022) – in preparation for publication.

P-56

INFLUENCE OF TEMPERATURE AND PRESSURE ON THE STABILITY OF 3,4-DIAMINO-1,2,4-TRIAZOLE AS A POTENTIAL SUBSTRATE FOR THE PRODUCTION OF WARFARE EXPLOSIVES

Patrycja Kądziałka[a,b], Piotr Rejnhardt[b], Svitlana V. Shishkina[c], Marek Daszkiewicz[b]

[a] *Faculty of Chemistry, Wroclaw University of Science and Technology, Wybrzeże Wyspiańskiego 27, 50-370 Wroclaw, Poland*
[b] *Institute of Low Temperature and Structure Research, Polish Academy of Science, Okólna 2, 50-422 Wroclaw, Poland*
[c] *SSI "Institute for Single Crystals", National Academy of Science of Ukraine, 60 Nauky Ave., 61001 Kharkiv, Ukraine*

Heterocyclic diamines are widely used reagents in organic synthesis due to their ability to form cyclic fragments. They represent very convenient building blocks for preparation of various pharmaceutical substances and compounds possessing biological activity [1,2]. Besides, triazoles possess a large number of energetic N–N and C–N bonds and therefore belong to large number of energetic materials, which decompose to dinitrogen and release energy [3]. It is well known that introduction amino groups improve thermal stability. In this view 3,4-diamino-1,2,4-triazole (DAT) is good candidate as energetic material. Although a few salts of DAT are known in the literature [3], there is lack information about thermal stability and compressibility of DAT itself. Our X-ray diffraction studies reveal only one phase present in the range of 300-100 K and up to 1.15 GPa. Thermal expansion and compressibility coefficients are positive along all main directions. However, respective indicatrices shows large anisotropy of both thermal expansion and compressibility (Figure 1). The results of our studies indicate potential application of DAT as safe substrate in production of warfare agents, where the extreme conditions are required.

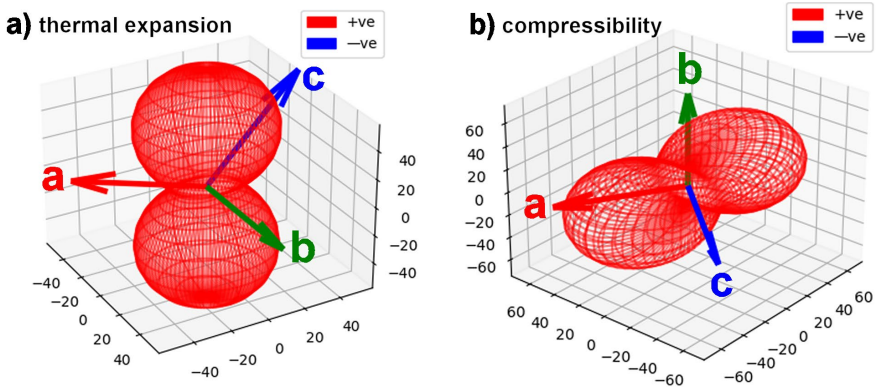

Fig. 1. (a) Thermal expansion and (b) compressibility indicatrices for DAT.

References

[1] H. D. Jakubke, H. Jeschkeit, *Aminosauren, Peptide, Proteine*, Akademie-Verlag, Berlin, (1982).
[2] M. A. E. Shaban, A. Z. Nasr and A. E. A. Morgaan, *Pharmazie*, **57** (2002) 442.
[3] J.-T. Wu, J.-G. Zhang, X. Yin, Z.-Y. Cheng, C.-X. Xu, *New J. Chem.*, **39** (2015) 5265.

P-57

LATTICE PARAMETER AND DENDRITIC STRUCTURE OF SINGLE-CRYSTALLINE TURBINE BLADES MADE OF CMSX-4 SUPERALLOY

Jacek Krawczyk* and Włodzimierz Bogdanowicz

Institute of Materials Engineering, Faculty of Science and Technology, University of Silesia in Katowice, 75 Pułku Piechoty 1a St., 41-500 Chorzów, Poland

**e-mail: jacek.krawczyk@us.edu.pl*

Components of aviation and industrial gas turbines are expected to operate in harsh working conditions, such as high temperature, high pressure, and complex dynamic loading conditions. Hence, the casts of these components are widely produced as single-crystalline using nickel- or cobalt-based superalloys. The high-temperature strength of Ni-based superalloys is caused by the alloy structure of the γ′ cuboidal precipitates surrounded by the net of thin channels of the γ matrix. Due to the similar crystal structures and lattice parameters of γ and γ′ phases, the interphase boundaries are coherent, and the alloy may be regarded as single-crystalline. Large γ/γ′ lattice misfits influence the yield strength, creep life, and rupture life, so its analysis is essential for blade durability.

The analyzed blades were made of CMSX-4® nickel-based superalloy using the Bridgman directional solidification at a 3 mm/min withdrawal rate. During solidification, groups of the γ-phase dendrites are formed with preferred [001]-type crystal orientation. The dendritic structure and the distribution of the γ′-phase lattice parameter ($a_{\gamma'}$) along selected measurement lines traced in the longitudinal section of a model single-crystalline blade were studied. It was established that there is a correlation between the value of the $a_{\gamma'}$ and the predomination of initial or ending fragments of the secondary dendrite arms. It is most noticed in the areas where the dendrite growth conditions are similar to steady. They are located in the center and near the root's selector extension (SE) area. The correlation has been related to the dendritic segregation mechanism. It was shown that in the single-crystalline blades obtained by the directional crystallization using a spiral selector, the "walls" of the primary dendrite arms that grow at a low angle to the blade axis are created. It was found that the value of the lattice parameter $a_{\gamma'}$ is decreased near such "walls". Additionally, it was found that competitive growth of the dendrites may occur at a distance of even several millimeters from the bottom surface of the root. The first-time applied X-ray diffraction measurements of $a_{\gamma'}$ made in a single-pass along the line allow the analysis of the dendritic segregation in the whole blade cast [1,2].

References

[1] J. Krawczyk, W. Bogdanowicz, *Materials*, **15** (2022) 781.
[2] J. Krawczyk, W. Bogdanowicz, J. Sieniawski, *Materials*, **14** (2021) 3842.

P-58

NEGATIVE THERMAL EXPANSION IN DIMETHYLAMMONIUM NITROPRUSSIDE

Andrzej Okuniewski[a,b], **Damian Paliwoda**[b] **and Gábor Molnár**[b]

[a] *Department of Inorganic Chemistry, Faculty of Chemistry, Gdańsk University of Technology, 11/12 G. Narutowicza Str. 80-233 Gdańsk, Poland*
[b] *Laboratoire de Chimie de Coordination, Centre National de la Recherche Scientifique & Université de Toulouse (UPS, INP), 31077 Toulouse, France*

The title compound, dimethylammonium nitroprusside (**DMANP**), was synthesized by a double-step exchange. Firstly, the commercially available salts – sodium nitroprusside dihydrate and silver nitrate – were reacted in stoichiometric ratio to obtain insoluble silver nitroprusside:

$$Na_2[Fe(CN)_5NO]_{(aq)} + 2\ AgNO_{3(aq)} \rightarrow Ag_2[Fe(CN)_5NO]_{(s)} + 2\ NaNO_{3(aq)}$$

After washing with water, a stoichiometric amount of dimethylammonium chloride was added to obtain the final product (accompanied with silver chloride deposition):

$$Ag_2[Fe(CN)_5NO]_{(s)} + 2\ Me_2NH_2Cl_{(aq)} \rightarrow (Me_2NH_2)_2[Fe(CN)_5NO]_{(aq)} + 2\ AgCl_{(s)}$$

After evaporation of excessive water, large needle-shaped crystals were formed. Recrystallization was needed to obtain the crystals of the size suitable for the X-ray experiments. Measurements were performed on the Rigaku Synergy XtaLAB diffractometer equipped with a HyPix-6000HE hybrid photon count detector at temperatures varying from 100 to 300 K. The low-temperature structure is depicted in Fig. 1.

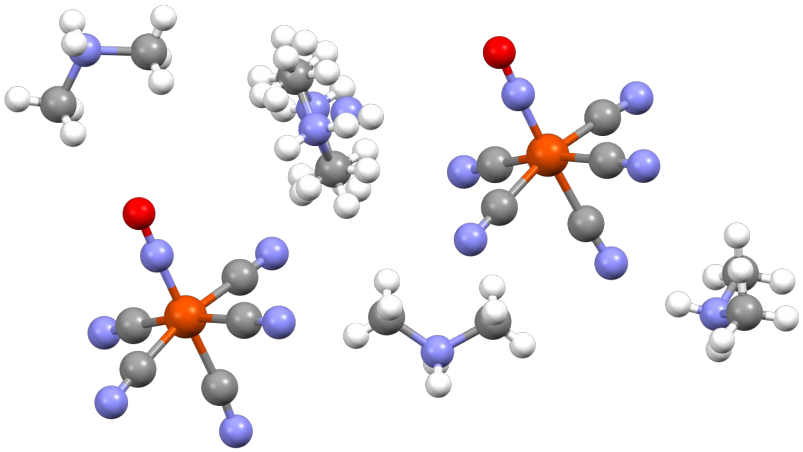

Fig. 1. A quarter of the unit cell content (grown asymmetric unit) of the **DMANP** measured at 100 K.

The asymmetric unit of the crystal is composed of four halves of $Me_2NH_2^+$ cations and two halves of $[Fe(CN)_5NO]^{2-}$ anions. All fragments lay on the mirror plane defined by the slightly non-co-linear Fe–N–O atoms. One of the dimethylammonium cations is disordered. In 100 K 33% of disordered cations lie on the mirror plane, while 67% are out-of-plane. This disorder is rationalized by the hydrogen bonding with surrounding CN groups of nitroprusside anions.

Recently similar compounds were described in the literature, where one of the dimethylammonium ions is interchanged with sodium [1] or potassium [2]. Namely $Na(Me_2NH_2)[Fe(CN)_5NO]$ and $K(Me_2NH_2)[Fe(CN)_5NO]$. Both of them exhibit molecular switching properties under temperature change or irradiation with light.

Preliminary diffraction studies on **DMANP** show that this compound exhibits negative temperature expansion in the crystallographic direction *b* (see Fig. 2).

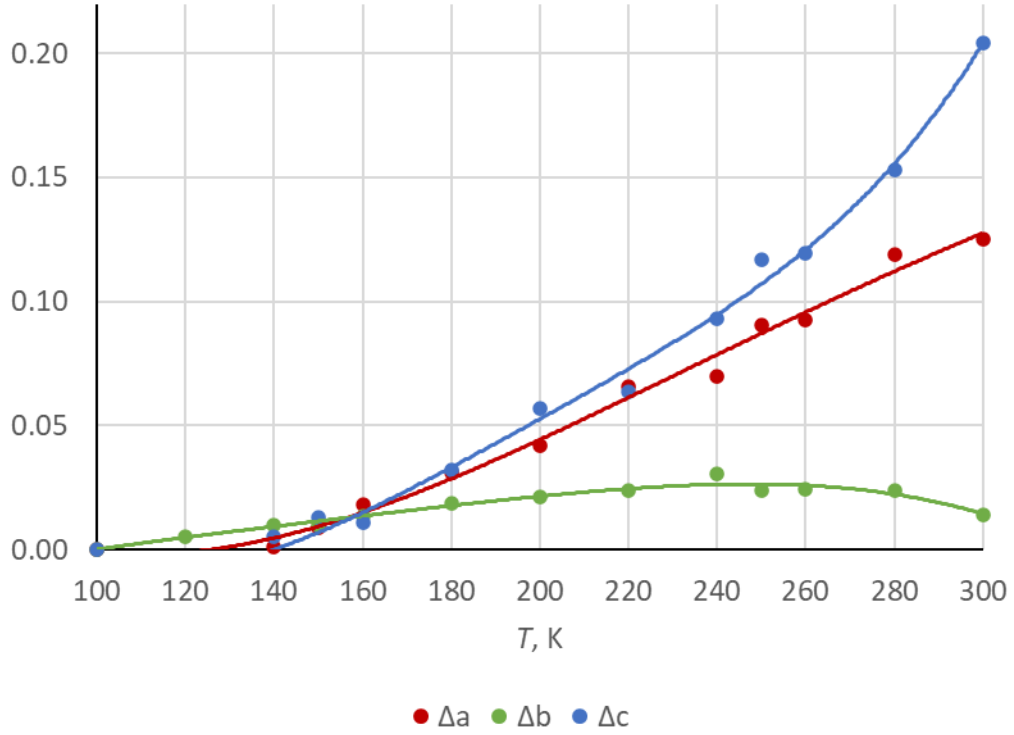

Fig. 2. The plot of unit cell parameters changes with temperature (defined as difference of the unit cell parameter value at the current temperature and its value at 100 K). Points 100, 150, 200, 250, and 300 were measured upon heating, while points 280, 260, 240, 220, 180, 160, 140, and 120 were measured upon cooling.

More structural details and molecular switching properties will be discussed within a poster.

References

[1] W.-J. Xu, K. Romanyuk, J. M. G. Martinho, Y. Zeng, X.-W. Zhang, A. Ushakov, V. Shur, W.-X. Zhang, X.-M. Chen, A. Kholkin, J. Rocha, *J. Am. Chem. Soc.*, **142** (2020) 16990–16998.

[2] R.-G. Qiu, X.-X. Chen, R.-K. Huang, D.-D. Zhou, W.-J. Xu, W.-X. Zhang, X.-M. Chen, *Chem. Commun.*, **56** (2020) 5488–5491.

P-59

DECOUPLING SPIN-CROSSOVER AND STRUCTURAL PHASE TRANSITION IN Fe(II) MOLECULAR COMPLEX

Damian Paliwoda, Laure Vendier, Gabor Molnár, Azzedine Bousseksou

Laboratoire de Chimie de Coordination, CNRS & Université de Toulouse (UPS, INP), 31077 Toulouse, France

Spin-crossover (SCO) materials are sensitive to external stimuli. SCO transition arouses curiosity because the change of the spin state of metal ion involves appearance of serious structural perturbation related to changes of metal-ligand distances. The interest in Fe(II) spin crossover systems is enhanced by the fact that the spin state can be conveniently switched: by changing the temperature, applying pressure, light irradiation or by the action of a chemical agent [1]. Hence, these compounds are considered as materials for potential applications [2] for example in medicinal diagnostic [3], as sensors [4], displays [5] and memory devices. [6]

We have recently investigated pressure induced spin-crossover (SCO) transitions in Fe(II) molecular complexes: **(1)** $[Fe^{II}(H_2B(pz)_2)_2(bipy)]$ and **(2)** $[Fe^{II}(H_2B(pz)_2)_2(phen)]$ pz: pyrazole; bipy: 2,2'-bipyridine; and phen: phenanthroline). At normal conditions **(1)** and **(2)** form monoclinic crystals of space group *C*2/*c*. Both complexes undergo SCO transition when cooled down to 160 K, which is manifested indirectly by abrupt shortening of Fe-N(ligand) distance of about 0.2 Å. While **(1)** remains monoclinic upon further cooling, the low temperature high spin (HS) to low spin (LS) transition in **(2)** is accompanied by the structural transformation from monoclinic *C*2/*c* form to triclinic $P\bar{1}$ phase. Compression of **(2)** decouples SCO and structural transition which allows to detect a monoclinic LS form, which has not been detected at low temperatures. [7],[8]

Acknowledgements: Financial support from regional Nanomat PRRI Project and ERC "E-MOTION" Advanced Grant is gratefully acknowledged.

References

[1] A. B. Gaspar, G. Molnár, A. Rotaru; H. J. Shepherd*, C.R. Chimie*, **21** (2018) 1095.
[2] A. Bousseksou, G. Molnár, L. Salmon, W. Nicolazzi, *Chem. Soc. Rev.*, **40** (2011) 3313.
[3] R. N. Muller, L. V. Elst, S. J. Laurent, *J. Am. Chem. Soc.*, **125** (2003) 8405.
[4] C. Bartual-Murgui, A. Akou, C. Thibault, G. Molnar, C. Vieu, L. Salmon, A. Bousseksou, *J. Mater. Chem. C*, **3,** (2015) 1277.
[5] O. Kahn, C. J. Martinez, *Science*, **279** (1988) 44.
[6] J.-F. Letard, P. Guionneau, L. Goux-Capes, *Top. Curr. Chem.*, **235** (2004) 221.
[7] J.A. Real, C. Muñoz, J. Faus, X. Solans, *Inorg. Chem.*, **36,** (1997) 3008.
[8] A. L. Thompson, A. E. Goeta, J. A. Real, A. Galet, M. Carmen Muñoz, *Chem. Comm.*, **12** (2004) 1390.

P-60

APPLICABILITY OF VEGARD'S LAW FOR NICKEL-MANGANESE OXIDES

Paweł Piszora, Jolanta Darul

Department of Materials Chemistry, Faculty of Chemistry,
Adam Mickiewicz University, Uniwersytetu Poznańskiego 8, 61-614 Poznań, Poland

The shift in lattice parameter is characteristic of substitutional solid-solutions, where the lattice parameter must change in order to accommodate for strain that arises due to the differing atomic sizes of the constituent atoms. However, Vegard's law is rarely followed perfectly and deviations from linear behaviour are much more common.

In practice it is often used to obtain rough estimates when experimental data is not available for the lattice parameter for the system of interest. For systems known to approximately obey Vegard's law, the approximation can also be used to estimate the composition of a solid solution from the knowledge of its lattice parameters, which can be easily obtained from diffraction data.

Ideally, the lattice parameter in a mixed crystal series would obey Vegard's law and vary linearly with the composition. In the case of spinel series the ideal behaviour is approached quite closely in some cases while others show marked deviations. Increasing x in $Ni_xMn_{3-x}O_4$ leads to a reduction in the number of octahedral sites occupied by Mn^{3+} ions, and thus to a reduction in the tetragonal lattice distortion [1]. For x greater than about 0.66 the structure is cubic.

It has been found previously that the inversion degree is dependent on the sintering temperature [2,3]. Both the degree of inversion and the valence of manganese depend on the sample preparation and heat treatment route, and the dimensions of the unit cell vary accordingly [1].

Our research shows a tendency to decrease the volume of $Ni_xMn_{3-x}O_4$ spinels with an increase in x, but with a large dispersion in relation to the dependence determined from the linear interpolation of the volumes of Mn_3O_4 and $NiMn_2O_4$. Establishing a simple relationship between the relative size of ions in the tetrahedral and octahedral sublattices and the size of the unit cell, we observe a similar tendency.

We also analysed the potential influence of cationic vacancies on the deviations from the linear course of the dependence of the mean lattice parameter as a function of x in $Ni_xMn_{3-x}O_4$. A significant influence of the synthesis conditions on the lattice parameter of the obtained oxides can be noticed.

The properties of the nickel-manganese spinel depend on the type and degree of structural defects. The generation of $Ni_xMn_{3-x}O_4$ lattice defects can be controlled by the synthesis conditions, and the lattice parameter can be used as an indicator of the effectiveness of this process.

Literature

[1] A. Díez, R. Schmidt, A. E. Sagua, M. A. Frechero, E. Matesanz, C. Leon, E. Morán, *J. Eur. Ceram. Soc.*, **30(12)** (2010) 2617.
[2] B. Boucher, R. Buhl, M. Perrin, *Acta Crystall. B-Stru.*, **25(11)** (1969) 2326.
[3] F. Guan, Y. Wu, I. Milisavljevic, X. Cheng, S. Huang, *J. Am. Ceram. Soc.*, **104(10)** (2021) 5148.

P-61

PROCEDURE OF INDICATE STABLE CUNI CLUSTERS BASED ON MACHINE LEARNING METHODS

Rafał Stottko, Bartłomiej Szyja

Institute of Advanced Materials, Wroclaw University of Science and Technology, ul. Gdańska 7/9, 50-344 Wrocław

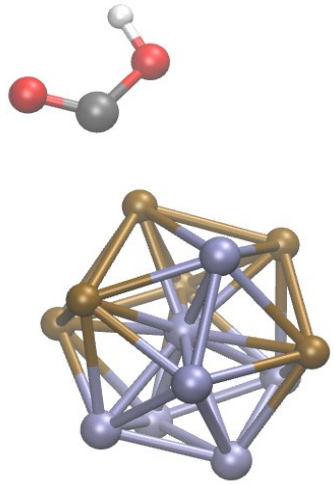

Fig. 1. Example geometry.

The catalytic properties of metallic clusters in the reduction of carbon dioxide have been demonstrated in many studies. One of the interesting subgroups of these compounds are thirteen-atom systems, geometrically similar to the icosahedron with I_h symmetry, containing copper and nickel atoms in their structure.

The problem of identification of the group of catalysts showing the most promising properties still remains unsolved.

This problem, due to a multitude of possible ways of arrangement of metal atoms in the cluster as well as possibilities of attachment of the CO2 molecule resulting from the symmetry operation, becomes too complex a task to justify the investigation of all the systems experimentally or by direct use of the tools of computer chemistry.

Our proposed solution is to study a small fraction of all possible structures on the basis of which an algorithm will be created that generates the remaining clusters in a geometric manner sufficiently close to real, traditionally optimized clusters. The dataset created in this way should then be trained with a machine learning model, so that in effect it is possible to identify those systems that exhibit good stability, saving thousands of computational hours.

The first tested layout generation method of the three considered provides a prediction accuracy higher than 80%.

P-62

ANALIZA RUDY DARNIOWEJ KAWAŁKOWEJ STOSOWANEJ W HISTORYCZNYM BUDOWNICTWIE ŁOWICKIM METODAMI XRD & ICP-OES

Paulina Golis, Andrzej Żarczyński, Waldemar Maniukiewicz, Jakub Kubicki, Wojciech M. Wolf

Politechnika Łódzka, Instytut Chemii Ogólnej i Ekologicznej, ul. Żeromskiego 116, 90-924 Łódź

Rudy darniowe występują w różnych częściach Polski, m.in. w Wielkopolsce, na Mazowszu, Podlasiu, Mazurach, Małopolsce, a także regionalnie na ziemi lubuskiej opolskiej oraz łowickiej. Głównym zastosowaniem rudy darniowej o znaczącej zawartości żelaza było przez wieki hutnictwo, a w przypadku rudy darniowej kawałkowej oprócz hutnictwa - budownictwo. Na terenie Polski znajduje się wiele obiektów sakralnych, obronnych, mieszkalnych, parkowych i gospodarczych wzniesionych z dużym udziałem rudy darniowej [1-5]. W przypadku ziemi łowickiej ruda darniowa kawałkowa była także dość często stosowana jako materiał budowlany. Ślady budownictwa z zastosowaniem tego surowca można znaleźć zarówno w Łowiczu jak i okolicach miasta, zwłaszcza w położonej niedaleko Arkadii [1, 5-7].

Celem pracy było zbadanie składu pierwiastkowego i fazowego pięciu średnich prób luźnej rudy darniowej kawałkowej, pobranej ze środowiska dwóch zabytkowych obiektów w Łowiczu (Baszta gen. Stanisława Klickiego i kapliczka za tzw. Baronią) oraz trzech w Parku Arkadia (Mur z Hermami i Przybytek Arcykapłana, Dom Murgrabiego i Łuk Kamienny, lewy obelisk Ittara). Oznaczono w nich, m.in. zawartość suchej masy i węglanów, pozostałość po prażeniu, udziały wybranych metali oraz niemetali.

Badania obejmowały analizy prób rudy darniowej kawałkowej wykonane, m.in. metodą dyfraktometrii proszkowej (XRD), technikami instrumentalnymi oraz fizykochemicznymi. Do analiz składu fazowego stosowano dyfraktometr polikrystaliczny X`PERT PRO MPD firmy PANanalytical, ze źródłem promieniowania CuKα uzyskiwanego w wyniku monochromatyzacji promieni X na filtrze niklowym. Ocenę składu fazowego badanych prób wykonano przy pomocy programu X`Pert High Score (ver. 4.9) oraz bazy standardów proszkowych ICDD PDF2 (ver. 2020). Analizy zawartości metali w próbach rudy darniowej wykonano metodą atomowej spektrometrii emisyjnej z plazmą sprzężoną indukcyjnie (ICP-OES), po uprzednim roztworzeniu ich w wodzie królewskiej.

Badania prób metodami XRD i ICP-OES wykazały, że chemiczny średni i fazowy skład badanych rud darniowych kawałkowych, zastosowanych w historycznym budownictwie łowickim jest względnie zbliżony. Różnice składu mineralogicznego rud mogą wynikać z różnych warunków środowiska naturalnego w miejscach, gdzie powstała dana ruda. Znanym jest bowiem, iż ruda w centralnej części danego złoża jest zwykle bogatsza w żelazo niż na jego obrzeżach.

Na podstawie badań XRD stwierdzono, że próby rudy zawierały magnetyt (Fe_3O_4), getyt (α-FeO(OH)), krzemionkę i wodę, a część także krzemian wapnia ($CaSiO_3$). Zawartość żelaza w badanych rudach mieściła się w zakresie 21-36%.

Wykazano, że niezwiązana chemicznie woda stanowiła około 10% powietrzno-suchych rud darniowych. Nieznacznie więcej wilgoci zawierały w swojej strukturze próbki pobrane z obiektów w Łowiczu niż w Arkadii. Największą zawartością suchej masy spośród badanych obiektów odznaczał się lewy obelisk Ittara. Ubytek masy podczas prażenia w temperaturze 550^{o}C w stosunku do suszenia w 105^{o}C wahał się w przedziale 6-11% wagowych. Zapewne był on związany z utratą wody krystalizacyjnej ze struktury rudy, jak również z utlenianiem zawartych w niej substancji organicznych.

Literatura

[1] T. Ratajczak, G. Rzepa *Polskie rudy darniowe*, Wydawnictwa AGH, Kraków (2011) 115.
[2] I. Kraczkowska, T. Ratajczak, G. Rzepa, Przegląd Geol., **49(12)** (2001) 1147.
[3] J. Skoczylas, Ochr. Zabytków**, 53(2)** (2000) 206.
[4] D. Kaczorek, M. Sommer, Catena, **54(3)** (2003) 394.
[5] P. Golis, *Analiza rudy darniowej kawałkowej stosowanej w historycznym budownictwie łowickim*, Praca inżynierska, IChOiE, Politechnika Łódzka (2022).
[6] J. Wegner, *Gen. Stanisław Klicki 1775-1847.* Mazowiecki Ośrodek Badań Naukowych MTK w Warszawie im. Stanisława Herbsta, Stacja Naukowa w Łowiczu, 15–18, Łowicz (1990).
[7] W. Warchałowski, Ochr. Zabytków, **51(4)** (1998) 356.

P-63

NEW ALGORITHMS AND INSTRUMENT MODEL REFINEMENT METHODS FOR SIGNAL DETECTION IN TIME-RESOLVED LAUE PHOTOCRYSTALLOGRAPHY DATA ANALYSIS

Piotr Łaski, Dariusz K. Szarejko, Radosław Kamiński, Katarzyna N. Jarzembska

Department of Chemistry, University of Warsaw, Żwirki i Wigury 101, 02-089 Warsaw, Poland

An efficient 1-dimensional seed-skewness (SS) algorithm adapted for X-ray diffraction signal detection along with signal integration procedure is presented. The method performs well for both the standard single-crystal X-ray diffraction data, as well as for time-resolved (TR) Laue photocrystallographic data collected at Advanced Photon Source and European Synchrotron Radiation Facility. It enables for efficient separation of signal from the background in single 1-dimentional data vectors, it is capable of determining small changes of reflection shapes and intensities resulting from exposure of the sample to laser light, and is especially attractive for extracting relatively weak reflections from the background. The last is possible through the adjustment of "trust level" and "signal level" parameters in the algorithm.

Performance of the algorithm is compared with the already reported Kruskal-Wallis test method. Both methods perform competitively in terms of speed and determining the intensity of strong reflections, while the parameterization of the SS method allows for more efficient tuning of the algorithm to improve its sensitivity towards weak reflections.

Furthermore, a novel instrument model refinement approach which allows to obtain precise detection parameters, such as detector distance and X-ray beam centre is presented. It is shown that relatively small adjustments in these parameters can significantly improve orientation-matrix matching procedures necessary during TR Laue data processing.

Finally, a series of TR Laue experiments was carried on a selection of model small molecule complexes, and the resulting data was processed with the use of the novel algorithm. The end results are presented and discussed.

P-64

ESTIMATING COMPLETENESS IN SINGLE-CRYSTAL HIGH-PRESSURE DIFFRACTION EXPERIMENTS

Daniel Tchoń and Anna Makal

Biological and Chemical Research Centre, Faculty of Chemistry, University of Warsaw, Żwirki i Wigury 101, 02-089 Warsaw, Poland

Diamond anvil cells (DAC) can be used to investigate single crystals under pressure by the means of X-ray diffraction (XRD). Structure factors collected in this way provide unique information about the sample, but their quality is never on par with even routine ambient-condition experiments. [1,2] In particular, a 35° opening angle of modern DACs renders up to 97% of reflections inside the limiting sphere inaccessible. Resulting diffraction patterns are thus routinely incomplete, especially so in materials with low internal symmetry. This impedes the crystal structure solution and affects the applicability of some techniques, which require high reciprocal space coverage. [3,4]

The above issue can be circumvented either by merging datasets collected on multiple crystals or by utilising the internal symmetry of one crystal. The first approach requires special infrastructure such as a well-focused incident beam or a gas membrane cells to avoid merging problems. [5] Meanwhile, the other solution calls for very precise control over crystal orientation but can be performed in virtually any laboratory. [6]

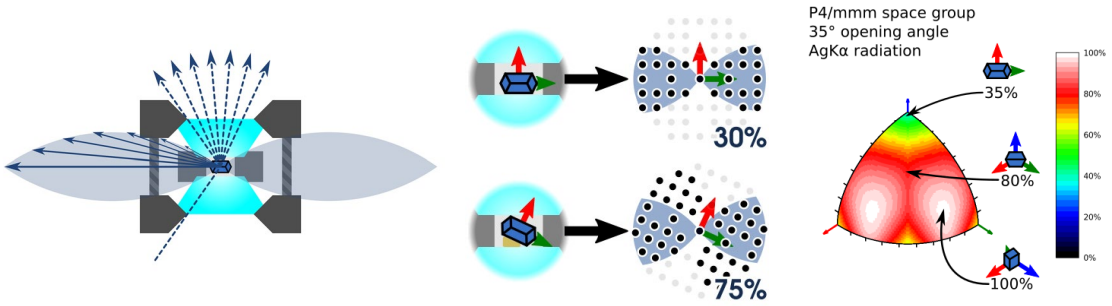

Fig. 1. Orientation of a crystal inside a DAC affects the potency of a HP XRD experiment. Distribution of potency can be estimated and plotted as a function of sample orientation, creating a potency map.

Here, we present potency – maximum attainable completeness – calculated as a function of crystal orientation, opening angle, resolution, and radiation wavelength. Figures and tables describing common experimental set-ups were prepared and general conclusions were drawn. Sample orientation was found to influence the potency more than other factors, to the point where cubic samples were found to offer less data than even orthorhombic ones when placed poorly. To let others test their systems, a dedicated Python library 'hikari-toolkit' was published, while a web server is being prepared.

References

[1] R. J. Angel, *J. Appl. Cryst.*, **37** (2004) 486–492.
[2] A. Katrusiak, *Acta Cryst. A.*, **64** (2008) 135–148.
[3] N. Casati, A. Kleppe, A. P. Jephcoat, P. Macchi, *Nat. Commun.*, **7** (2016) 10901.
[4] D. Jayatilaka, B. Dittrich, *Acta Cryst. A.*, **64** (2008) 383–393.
[5] D. Tchoń, A. Makal, *Acta Cryst. B.*, **75** (2019) 343–353.
[6] D. Tchoń, A. Makal, *IUCrJ*, **8** (2021) 1006–1017.

P-65

LOW-TEMPERATURE PHASE TRANSITION AND HIGH-PRESSURE PHASE STABILITY OF 1H-PYRAZOLE-1-CARBOXAMIDINE NITRATE

Piotr Rejnhardt, Marek Drozd and Marek Daszkiewicz

Institute of Low Temperature and Structure Research, Polish Academy of Sciences, ul. Okólna 2, 50-422 Wrocław, Poland

Chemical compounds with guanidine groups exert plenty of physiological and pharmacological effects and play a key role for muscle activity and in the cardiovascular system, and many guanidines possess antimicrobial activity.[1] Compounds with the guanidinium group have a lot of interesting properties. For example, guanidinium nitrate has a strong crystal strain associated with phase transition resulting in elongation of the samples by over 44 %.[2] Nowadays, one of the most popular substrates for guanylation of amines is 1H-pyrazole-1-carboxamidine, hereafter PyCA, which replaced earlier used *O*-methyl-isourea hydrogensulfate, cyanamide or 3,5-dimethyl-pyrazole-l-carboxamidine nitrate.[3] PyCA has been successfully used in the formation of the guanidinium moiety in alanine and proline amino acids,[4] in the ultrasound-assisted synthesis of substituted guanidines,[5] synthesis of dengue and West Nile virus protease inhibitors[6] and in the synthetic procedure of zanamivir, an anti-influenza A and B drug.[7]

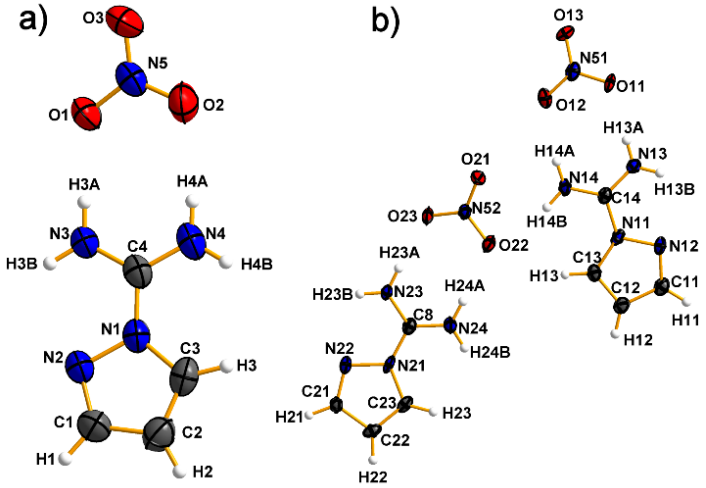

Fig.1. Molecular structures of $(HPyCA)NO_3$ (a) phase (I) at 300 K and (b) phase (II) at 100 K.

Here we present new compound 1H-pyrazole-1-carboxamidine nitrate[8], which was synthesized in the crystalline form. The temperature-dependent X-ray diffraction experiment revealed a reversible continuous phase transition at 174 K from monoclinic space group $P2_1/c$ to triclinic P-1. The mechanism of phase transition mainly refers to the slight movement of nitrate anions leading to disappearance of the 2_1-screw axis and c-glide plane. In contrast to the temperature-dependent experiment, the high-pressure X-ray diffraction detected no phase transition up to 1.27 GPa. This fact is probably associated with the unusual behaviour of unit-cell parameters upon freezing the crystal,

which leads to the increase of unit-cell volume in the narrow temperature range between 174 and 160 K just after the phase transition. Although expansion of the unit cell under pressure has been reported in the literature, but it resulted from the incorporation of guest molecules to the measured crystal.[9] In the case of $(HPyCA)NO_3$, the formula unit is preserved during the temperature-induced phase transition. Therefore, formation of phase II cannot be stimulated by pressure, because this would require a three-dimensional expansion of the unit cell.

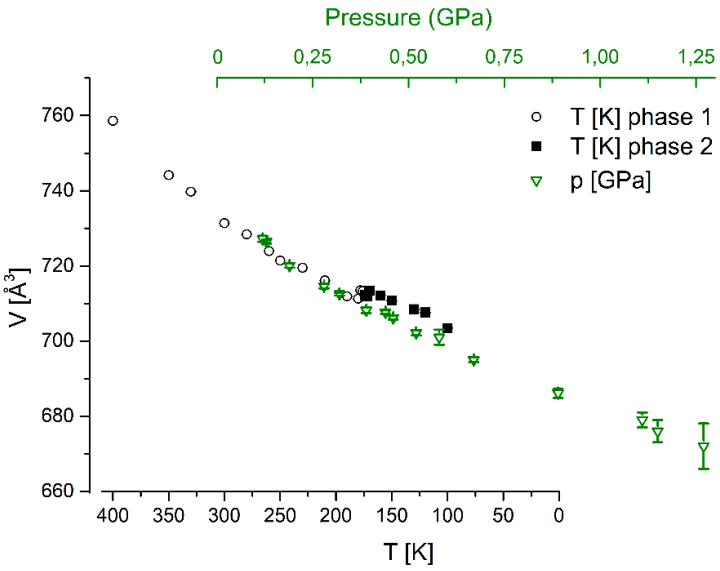

Fig.2. Changes of the unit-cell volume as a function of temperature and pressure. The pressure scale was added to the temperature scale by adjusting the volume change trends for both thermodynamic parameters.

Bibliography

[1] G. J. Durant, Guanidine derivatives acting at histaminergic receptors. *Chemical Society Reviews*, **14** (1985) 375–398.

[2] A. Katrusiak, M. Szafrański, Structural phase transitions in guanidinium nitrate. *Journal of Molecular Structure*, **378** (1996) 205–223.

[3] M. S. Bernatowicz, Y. Wu, G. R. Matsueda, 1H-Pyrazole-1-carboxamidine hydrochloride an attractive reagent for guanylation of amines and its application to peptide synthesis. *Journal of Organic Chemistry*, **57** (2002) 2497–2502.

[4] Z. Zhang *et al.*, Synthesis of alanine and proline amino acids with amino or guanidinium substitution on the side chain. *Tetrahedron*, **56** (2000) 2513–2522.

[5] M. Fujita, Y. Furusho, Ultrasound-assisted synthesis of substituted guanidines using 1H-pyrazole-1-carboxamidine and S-methylisothiouronium sulfate under solvent-free conditions. *Tetrahedron*, **74** (2018) 4339–4342.

[6] N. Kühl *et al.*, A New Class of Dengue and West Nile Virus Protease Inhibitors with Submicromolar Activity in Reporter Gene DENV-2 Protease and Viral Replication Assays. *Journal of Medicinal Chemistry*, **63** (2020) 8179–8197.

[7] J. Magano, Synthetic Approaches to the Neuraminidase Inhibitors Zanamivir (Relenza) and Oseltamivir Phosphate (Tamiflu) for the Treatment of Influenza. *Chemical Reviews*, **109** (2009) 4398–4438.

[8] P. Rejnhardt, M. Drozd, M. Daszkiewicz, Low-temperature phase transition and high-pressure phase stability of 1 H -pyrazole-1-carboxamidine nitrate . *Acta Crystallographica Section B Structural Science, Crystal Engineering and Materials*, **77** (2021) 996–1002.

[9] A. J. Graham, D. R. Allan, A. Muszkiewicz, C. A. Morrison, S. A. Moggach, The Effect of High Pressure on MOF-5: Guest-Induced Modification of Pore Size and Content at High Pressure. *Angewandte Chemie International Edition*, **50** (2011) 11138–11141.

P-66

STRUCTURE MODELLING OF QUASICRYSTALS WITH THE STATISTICAL METHOD

J. Wolny*, R. Strzałka, I. Bugański and J. Śmietańska

Faculty of Physics and Applied Computer Science, AGH University of Science and Technology, Krakow, Poland

**e-mail: wolny@fis.agh.edu.pl*

Since the discovery of quasicrystals, the higher-dimensional method was extensively used to model the atomic structure of quasicrystals and refinement. The basic idea behind this method is a considering of a quasicrystal as a multidimensional object with periodicity. Only by projecting it on the 3D real space, a quasiperiodic arrangement of atoms is obtained. Higher-dimensional method combined with a cluster approach was used to model a vast majority of quasicrystalline systems [1]. An alternative method, named a statistical method, working in real space only and making use of the concept of the average unit cell, was proposed [2]. Results of using both methods are equivalent to some extent, but some differences, e.g., in modeling structural defects, may appear [4].

Over the last years, the statistical method has found its application in the structure refinement of numerous decagonal and icosahedral quasicrystals (e.g., [5,6] or very recently [7]). For the very last result of icosahedral CdYb phase, no assumptions on the cluster type were not made, but only 3D Penrose quasilattice was used to refine the structure. In addition, the influence of phasonic flips on the atomic structure at high temperatures was recently discussed. Finally, the macromolecular system with modulation of the atomic positions was investigated [8].

In this presentation, a short introduction to the statistical method will be followed by some exemplar applications of the approach to real systems, including modeling of phonons and phasons.

Acknowledgements: The authors acknowledge financial support from Polish National Science Center under grant no. 2019/33/B/ST3/02063.

Literature

[1] W. Steurer, *Acta Cryst. A*, **74** (2018) 1.
[2] J. Wolny, B. Kozakowski, P. Kuczera, R. Strzalka, J. Wnek, *Isr. J. Chem.*, **51** (2011) 1275.
[3] R. Strzalka, I. Buganski, J. Wolny, *Crystals*, **6** (2016) 104.
[4] J. Wolny, I. Buganski, P. Kuczera, R. Strzalka, *J. Appl. Cryst.*, **49** (2016) 2106.
[5] P. Kuczera, J. Wolny, W. Steurer, *Acta Cryst. B*, **68** (2012) 578.
[6] I. Buganski, J. Wolny, H. Takakura, *Acta Cryst. A*, **76** (2020) 180.
[7] I. Buganski, R. Strzalka, J. Wolny, *IUCrJ*, *submitted*
[8] J. Smietanska, J. Sliwiak, M. Gilski, Z. Dauter, R. Strzalka, J. Wolny, M. Jaskolski, *Acta Cryst. D*, **76** (2020) 653.

P-67

CRYSTAL STRUCTURE ANALYSIS OF SOME OXYGEN CARRIERS FOR APPLICATION IN CHEMICAL LOOPING COMBUSTION

Rafał Łysowski*, Ewelina Ksepko

Wroclaw University of Science and Technology
Department of Engineering and Technology of Chemical Processes

**e-mail: rafal.lysowski@pwr.edu.pl*

Chemical Looping Combustion (CLC) is a novel, low emissive fuel combustion technology that could be applied to a wide range of fuels to generate energy. It can also be used for syngas production from the gasification of hard coal.

Oxygen carriers for application in CLC are metal oxide-based materials that are capable to accept oxygen in an oxidizing environment and then to release it during direct contact with fuels. Some of those materials are also capable of accepting and releasing oxygen as a result of changes in oxygen partial pressure (pO_2) in their working environment. That effect is often referred as CLOU properties (Chemical Looping with Oxygen Uncoupling). Oxygen carries could be composed of one or several metal oxides with different physicochemical properties. Monophasic oxygen carriers with a spinel or a perovskite structures are particularly interesting because of their high oxygen transport capabilities, often exhibit CLOU properties, and physicochemical stability.

In this work, oxygen carriers of spinel structure, based on iron and copper oxides, were synthesized by mechanical mixing and calcination method. The quality of the obtained oxygen carriers was analysed using X-ray diffractometry (XRD). Structural analysis of synthesized OCs was performed using the Rietveld method and FullProf software.

Acknowledgement: The work was financed from the National Science Centre Poland, Project No. 2020/37/B/ST5/01259.

P-68

STRUCTURAL BEHAVIOR OF $Li_{0.95}Mn_{2.05}O_4$ SPINEL UNDER PRESSURE

J. Darul[1],*, C. Popescu[2], F. Fauth[2] and P. Piszora[1]

[1] Department of Materials Chemistry, Faculty of Chemistry, Adam Mickiewicz University, Uniwersytetu Poznańskiego 8, 61-614 Poznań
[2] CELLS-ALBA Synchrotron Light Facility, 08290 Cerdanyola, Barcelona, Spain

**e-mail: jola@amu.edu.pl*

Tetragonal lithium manganese oxide (LMO) is a key material in the new concept for the design of charge electrode materials. The unique tetragonal spinel phase combines the behavior of a pseudocapacitor and a battery, which results in slowing down the self-discharge process and enhance both the cycle stability and the capacity [1].

In this work, we reported pressure-induced structural changes in $Li_{0.95}Mn_{2.05}O_4$ spinel at two temperatures, 300 K and 380 K, investigated in situ through synchrotron X-ray powder diffraction up to 13 GPa in a diamond anvil cell. Compression-induced strain triggers a cascade of local structure deformations which finally result in the structural phase transition to the high-pressure tetragonal phase [2]. Specifically, we have investigated the dependence of the transformation rate on sample non-hydrostaticity. The non-hydrostatic pressure component induces in the structure a local deformation of coordination polyhedron, enhances the Jahn–Teller deformation and eventually causes a phase transition to the high-pressure tetragonal phase with $c/a > 1$.

Acknowledgements: These experiments were performed at MSPD-BL04 beamline at ALBA Synchrotron with the collaboration of ALBA staff.

Literature

[1] M. Abdollahifa, S. S. Huang, Y. H. Lin, H. S. Sheu, J. F. Lee, M. L. Lu, Y. F. Liao. N. L. Wu,. *J. Power Sources*, **412** (2019) 545–551.
[2] J. Darul, C. Popescu, F. Fauth, P. Piszora, *J. Phys. Chem. C*, **123** (2019) 19288–19297.

P-69

COMPREHENSIVE CHARACTERIZATION OF THE KETOPROFEN-B-CYCLODEXTRIN INCLUSION COMPLEX USING X-RAY TECHNIQUES AND NMR SPECTROSCOPY

Armand Budzianowski[1], Katarzyna Betlejewska-Kielak[2], Elżbieta Bednarek[3], Katarzyna Michalska[2*], and Jan K. Maurin[3]

[1] National Centre for Nuclear Research, A. Sołtana 7, 05-400 Otwock, Poland
Armand.Budzianowski@ncbj.gov.pl
[2] Department of Synthetic Drugs, National Medicines Institute,
Chełmska 30/34, 00-725 Warsaw, Poland
k.kielak@nil.gov.pl
[3] Falsified Medicines and Medical Devices Department, National Medicines Institute,
Chełmska 30/34, 00-725 Warsaw, Poland
(E.B.) e.bednarek@nil.gov.pl; (J.K.M.) j.maurin@nil.gov.pl
(K.M) k.michalska@nil.gov.pl; Tel.: +48-(22)-841-18-88 (ext. 369)

Ketoprofen (**KP**) is an effective NSAID in pain relief and inflammation decrease and is widely used in patients with rheumatoid arthritis and osteoarthritis, gout disorders and other painful conditions. KP is available in both systemic (oral, suppository, or injection) and local topical (patches, compresses, ointments, gels, creams, and lotions) formulations. KP is used in the form of capsules or tablets and has a short elimination half-life (1.5–4 h); therefore, it is administered orally four times daily. As a result, chronic use may cause serious gastric side effects, such as ulcerations and even gastrointestinal bleeding. Therefore, various approaches have been adopted to improving patient compliance by allowing once-daily oral administration of KP. CDs, by forming an inclusion complex, cause beneficial changes in the characteristics of the guest molecule, such as increased solubility, enhanced dissolution properties, improved stability and reduced side effects. The aim of this study [1] was to:

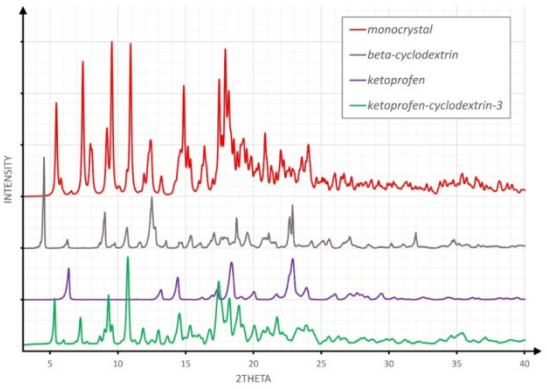

Fig. 1. The comparison of powder diffraction patterns for the product of the heating-under-flux experiment.

- obtain KP/β-CD inclusion complexes by one or more complexing methods,
- grow a single crystal when the XRPD and NMR methods confirmed the formation of the inclusion complexes, and
- comprehensively investigate the inclusion complex of KP/β-CD using XRPD, NMR, and X-ray monocrystalline technique.

Literature

[1] K. Betlejewska-Kielak, E. Bednarek, A. Budzianowski, K. Michalska, J. K. Maurin, *Molecules*, **26(13)** (2021) 4089. DOI: 10.3390/molecules26134089.

LISTA ZAREJESTROWANYCH UCZESTNIKÓW KONWERSATORIUM
LIST OF THE REGISTERED PARTICIPANTS

Elżbieta	**Bartoszak-Adamska**	dr hab.	Department of Crystallography, Faculty of Chemistry, Adam Mickiewicz University, Poznań
Tamara	**Bednarchuk**	dr	Instytut Niskich Temperatur i Badań Strukturalnych im. Włodzimierza Trzebiatowskiego Polskiej Akademii Nauk
Bohdana	**Belan**	PhD	Ivan Franko National University of Lviv
Katarzyna	**Betlejewska-Kielak**	mgr	Narodowy Instytut Leków/National Medicines Institute
Michał	**Białek**	Dr	Uniwersytet Wrocławski
Agata	**Białońska**	dr hab.	Wydział Chemii Uniwersytet Wrocławski
Justyna	**Biesaga**	licencjat	Uniwersytet Wrocławski
Patryk	**Borowski**	BSc	Dept. of Chemistry, University of Warsaw
Iwona	**Bryndal**	Dr	Uniwersytet Medyczny im. Piastów Śląskich we Wrocławiu
Urszula	**Budniak**	mgr	Uniwersytet Warszawski
Armand	**Budzianowski**	dr	Narodowe Centrum Badań Jądrowych
Daria	**Budzikur**	mgr	University of Wrocław
Helena	**Butkiewicz**	mgr inż.	Instytut Chemii Fizycznej Polskiej Akademii Nauk
Jarosław	**Chojnacki**	Profesor	Wydział Chemiczny Politechnika Gdańska
Bartosz	**Cieśla**	Student	Politechnika Gdańska
Anna	**Cociurovscaia**	mgr inż.	Politechnika Łódzka
Jolanta	**Darul**	dr	Department of Materials Chemistry, Faculty of Chemistry, Adam Mickiewicz University, Poznań
Anna Maria	**Dąbrowska**	Mgr	Wydział Chemiczny Politechniki Warszawskiej
Aleksandra	**Deptuch**	dr	IFJ PAN
Krystyna	**Deresz**	Mgr / (Phd Student)	Univeristy of Warsaw, Department of Chemistry
Paulina	**Dominiak**	Profesor	Wydział Chemii Uniwersytetu Warszawskiego
Dawid	**Drozdowski**	Mgr inż.	Instytut Niskich Temperatur i Badań Strukturalnych im. Włodzimierza Trzebiatowskiego Polskiej Akademii Nauk
Michał	**Duda**	dr	Wydział Chemii Uniwersytetu Jagiellońskiego w Krakowie

Konrad	**Dyk**	Mgr	Uniwersytet Marii Curie-Skłodowskiej w Lublinie
Mariya	**Dzevenko**	PhD	Heroes of Kruty Lviv State Lyceum with enhanced military and physical training
Maciej	**Ejnik**	Student	Politechnika Gdańska
Krzysztof	**Ejsmont**	dr hab.	Uniwersytet Opolski
Jarosław	**Fornalski**	mgr	Uniwersytet Wrocławski, Wydział Chemii
Emilia	**Ganczar**	mgr	Uniwersytet Wrocławski, Wydział Chemii
Anna	**Gągor**	dr hab.	Instytut Niskich Temperatur i Badań Strukturalnych PAN
Maria	**Gdaniec**	Prof.	Wydział Chemii, Uniwersytet im. Adama Mickiewicza
Paulina	**Golis**	Inż.	Politechnika Łódzka
Mateusz	**Gołdyn**	Mgr	Faculty of Chemistry, Adam Mickiewicz University
Klaudia	**Górska**	Inż.	Instytut Chemii Ogólnej i Ekologicznej, Wydział Chemiczny, Politechnika Łódzka
Szymon	**Grabowski**	MSc, PhD student	Jagiellonian University, Faculty of Chemistry
Piotr	**Guńka**	dr inż.	Politechnika Warszawska, Wydział Chemiczny
Katarzyna	**Helios**	dr inż.	Politechnika Wrocławska, Wydział Chemiczny / Wrocław University of Science and Technology, Faculty of Chemistry
Felix	**Hennersdorf**	Dr.	Rigaku Oxford Diffraction
Anna	**Hoser**	dr	Uniwersytet Warszawski, Wydział Chemii
Piotr	**Jakieła**	mgr	Malvern Panalytical B.V. Sp. z o.o. Oddział w Polsce
Jan	**Janczak**	profesor	Instytut Niskich Temperatur i Badań Strukturalnych, Polska Akademia Nauk, 50-422 Wrocław
Irena	**Jankowska-Sumara**	dr hab.	Instytut Fizyki, Uniwersytet Pedagogiczny
Mariusz	**Jaskolski**	Prof.	Department of Crystallography, Faculty of Chemistry, A. Mickiewicz University
Róża	**Jastrzębska**		Politechnika Warszawska
Aneta	**Jezierska**	dr hab.	Uniwersytet Wrocławski, Wydział Chemii
Kinga	**Jóźwiak**	mgr	Wydział Chemii, Uniwersytet Wrocławski
Daniel Michał	**Kamiński**	dr hab.	UMCS
Zbigniew	**Karczmarzyk**	Dr hab. inż.	Uniwersytet Przyrodniczo-Humanistyczny w Siedlcach
Hanna	**Kaspiaruk**	licencjat	Uniwersytet Łódzki, Wydział Chemii
Oskar	**Kaszubowski**	Licencjat	Uniwersytet Wrocławski, Wydział Chemii
Marcin	**Kaźmierczak**	Mgr	Uniwersytet Wrocławski
Patrycja	**Kądziałka**	-	Politechnika Wrocławska

Grzegorz	**Kić**	mgr inż.	Labsoft Sp. z o.o.
Vasyl	**Kinzhybalo**	dr	INTiBS PAN
Beata	**Kizior**	drant	Politechnika Wrocławska
Hubert	**Kleinschmidt**	student	Politechnika Gdańska
Agnieszka	**Klonecka**	mgr	Uniwersytet Jagielloński (Narodowe Centrum Promieniowania Synchrotronowego SOLARIS/ Wydział Fizyki, Astronomii i Informatyki Stosowanej)
Andrzej	**Kochel**	dr hab.	Uniwersytet Wrocławski, Wydział Chemii
Dorota	**Kowalska**	dr	Instytut Niskich Temperatur i Badań Strukturalnych PAN
Jacek	**Krawczyk**	dr	Institute of Materials Engineering, Faculty of Science and Technology, University of Silesia in Katowice
Marta	**Krawczyk**	dr	Wydział Farmaceutyczny, Uniwersytet Medyczny im. Piastów Śląskich we Wrocławiu
Monika	**Krawczyk**	dr	Instytut Fizyki Doświadczalnej Uniwersytet Wrocławski
Gratz	**Kristin**	Dr.	Malvern Panalytical GmbH
Katarzyna	**Krupka**	Licencjat	Uniwersytet Wrocławski
Szymon	**Krzywda**	dr hab.	Adam Mickiewicz University
Maria	**Książek**	dr	Instytut Fizyki, Uniwersytet Śląski
Paulina	**Kurowska**	student	Uniwersytet Wrocławski
Joachim	**Kusz**	profesor	Instytut Fizyki, Uniwersytet Śląski
Tadeusz	**Lis**	Prof. dr hab.	Wydział Chemii Uniwersytet Wrocławski
Joanna	**Loch**	dr	Faculty of Chemistry, Jagiellonian University, Krakow
Piotr	**Łaski**	MSc	Dept. of Chemistry, University of Warsaw
Rafał	**Łysowski**	mgr. inż	Politechnika Wrocławska
Izabela	**Madura**	dr hab inż.	Wydział Chemiczny, Politechnika Warszawska
Maura	**Malińska**	dr	Wydział Chemii, Uniwersytet Warszawski
Paulina	**Marek-Urban**	mgr inż.	Politechnika Warszawska, Wydział Chemiczny
Liliana	**Mazur**	dr hab.	Instytut Nauk Chemicznych, Wydział Chemii Uniwersytet Marii Curie-Skłodowskiej w Lublinie
Adrian	**Mermer**	MSc	Uniwersytet Wrocławski
Maja	**Morawiak**	dr inż.	Instytut Chemii Organicznej PAN
Marzena	**Nowacka**	Mgr inż.	Międzynarodowy Instytut Biologii Molekularnej i Komórkowej
Przemysław	**Nowak**	Inż.	Politechnika Łódzka, Wydział Chemiczny, Instytut Chemii Ogólnej i Ekologicznej
Weronika	**Nowak**	mgr	Uniwersytet im. Adama Mickiewicza w Poznaniu

Klaudia	**Nowakowska**	mgr	Uniwersytet Jagielloński w Krakowie
Waldemar	**Nowicki**	Prof. UAM dr. hab.	Uniwersytet im. Adama Mickiewicza w Poznaniu
Andrzej	**Okuniewski**	dr inż.	Politechnika Gdańska
Andrzej	**Olczak**	dr hab.	Politechnika Łódzka
Damian	**Paliwoda**	Dr	CNRS Laboratoire de Chimie de Coordination
Jesica	**Pantaz**	Master's degree in science	Antofagasta University
Anna	**Pietrzak**	dr inż.	Politechnika Łódzka
Agnieszka	**Pietrzyk-Brzezińska**	Dr inż.	Instytut Biotechnologii Molekularnej i Przemysłowej, Politechnika Łódzka
Paweł	**Piszora**	dr hab.	Department of Materials Chemistry, Faculty of Chemistry, Adam Mickiewicz University, Uniwersytetu Poznańskiego
Kinga	**Pokrywka**	Mgr	Instytut Chemii Bioorganicznej Polskiej Akademii Nauk
Kamila	**Pruszkowska**	mgr	Uniwersytet Warszawski
Anna	**Pyra**	Dr	Uniwersytet Wrocławski
Piotr	**Rejnhardt**	Mgr Inż.	Instytut Niskich Temperatur i Badań Strukturalnych PAN we Wrocławiu
Piotr	**Salwa**	Mgr inż.	Instytut Inżynierii Materiałowej, Uniwersytet Śląski w Katowicach
Jarosław	**Serafińczuk**	dr hab. inż.	Politechnika Wrocławska
Miłosz	**Siczek**	Dr	Wydział Chemii, Uniwersytet Wrocławski
Magdalena	**Siedzielnik**	mgr inż.	Politechnika Gdańska
Yurii	**Slyvka**	Dr.	Ivan Franko National University of Lviv
Joanna	**Sławek**	dr inż.	NCPS Solaris, Uniwersytet Jagielloński
Vernon	**Smith**	Dr.	Bruker AXS GmbH
Paulina	**Sobczak**	mgr inż.	Politechnika Łódzka
Aleksandra	**Sokołowska**	Licencjat	Wydział Chemii Uniwersytet Wrocławski
Magdalena	**Stępień**	mgr	Wydział Chemii Uniwersytetu Wrocławskiego
Rafał	**Stottko**	-	Politechnika Wrocławska
Radosław	**Strzałka**	dr inż.	AGH Akademia Górniczo-Hutnicza im. Stanisława Staszica w Krakowie
Jarosław	**Sukiennik**	mgr	Instytut Chemii Ogólnej i Ekologicznej Politechniki Łódzkiej
Kinga	**Suwińska**	Prof. dr. hab.	Uniwersytet Kardynała Stefana Wyszyńskiego w Warszawie

Małgorzata	**Szczesio**	dr hab. inż.	Instytut Chemii Ogólnej i Ekologicznej, Wydział Chemiczny, Politechnika Łódzka
Małgorzata	**Szklorz**	mgr inż.	udział prywatny
Anna	**Ściuk**	mgr	Uniwersytet Jagielloński
Katarzyna	**Ślepokura**	dr hab.	Uniwersytet Wrocławski, Wydział Chemii
Daniel	**Tchoń**	mgr	Wydział Chemii Uniwersytetu Warszawskiego
Waldemar	**Tejchman**	dr hab.	Uniwersytet Pedagogiczny im. Komisji Edukacji Narodowej w Krakowie
Aleksandra	**Tołoczko**	Mgr	Uniwersytet Wrocławski, Wydział Chemii
Paweł	**Tomaszewski**	dr	INTiBS PAN
Kamil	**Twarów**	Mgr	Uniwersytet Wrocławski, Wydział Chemii
Karolina	**Urbanowicz**	Inż.	Politechnika Warszawska
Marek	**Wołcyrz**	Prof.	Instytut Niskich Temperatur i Badań Strukturalnych PAN, Wrocław
Krzysztof	**Woźniak**	Profesor	Wydział Chemii, Uniwersytet Warszawski
Karolina	**Wrochna**	Student	Politechnika Warszawska Wydział Chemiczny
Karol	**Wydra**	mgr	Wydział Chemii Uniwersytetu Wrocławskiego
Waldemar	**Wysocki**	Dr	Instytut Nauk Chemicznych Wydział Nauk Ścisłych i Przyrodniczych Uniwersytet Przyrodniczo-Humanistyczny w Siedlcach
Patrycja	**Wytrych**	mgr	Wydział Chemii Uniwersytetu Wrocławskiego
Anna	**Zep**	Dr	Anton Paar Polska / Uniwersytet Warszawski
Maciej	**Zieliński**	dr inż.	Narodowe Centrum Badań Jądrowych (National Centre for Nuclear Research)
Dagmara	**Ziembicka**	Master of Engineering	Department of Organic Chemistry, Medical University of Gdańsk
Aleksandra	**Zwolenik**	lic.	Wydział Chemii, Uniwersytet Warszawski
Andrzej	**Żarczyński**	dr inż.	Politechnika Łódzka, Instytut Chemii Ogólnej i Ekologicznej
Ewa	**Żesławska**	dr hab.	Uniwersytet Pedagogiczny

INDEKS AUTORÓW PRAC / INDEX OF AUTHORS

Normalną czcionką zaznaczono autorów prezentujących, *czcionką pochyłą współautorów.*
Presenting authors are shown in normal font, *co-authors in italics*.

Zbigniew	***Czapla***	*P-51*
Grzegorz	***Czernel***	*O-13*
Oksana	***Danylyuk***	*O-07*
Jolanta	**Darul**	*P-60*, P-68
Marek	***Daszkiewicz***	*P-12*, *P-56*, *P-65*
Anna Maria	**Dąbrowska**	P-10
Zofia	***Dega-Szafran***	*P-15*
Aleksandra	**Deptuch**	P-48
Krystyna	**Deresz**	P-49
Anna	***Dołęga***	*P-13*, *P-26*
Paulina	**Dominiak**	O-17
Maciej	***Dranka***	*P-19*
Marek	***Drozd***	*O-13*, *P-65*
Dawid	**Drozdowski**	O-20
Marta K.	***Dudek***	*P-31*
Krzysztof	***Durka***	*P-30*, *P-40*, *P-41*
Konrad	**Dyk**	O-13
Mariya	**Dzevenko**	*P-11*, P-12
Jolanta	***Ejfler***	*P-36*
Maciej	**Ejnik**	P-13
Francois	***Fauth***	*P-68*
Katarzyna	***Fedoruk***	*O-20*
Aleksander	***Filarowski***	*O-02*
Jarosław	**Fornalski**	P-14
Andrzej	***Fruziński***	*P-37*
Roman	***Gajda***	*O-01*
Emilia	**Ganczar**	O-03, P-06
Małgorzata	***Gazińska***	*P-36*
Anna	***Gągor***	*O-20*
Miroslaw	***Gilski***	*P-03*, *P-04*
Roman	***Gladyshevskii***	*P-11*, *P-12*
Katarzyna	***Gobis***	*P-16*, *P-37*, *P-44*
Paulina	***Golis***	*P-62*
Mateusz	**Gołdyn**	P-15, *P-32*
Evgeny	***Goreshnik***	*P-33*

Tomasz	***Goryczka***	*O-21*
Tomasz	***Góral***	*O-17*
Klaudia	**Górska**	P-16
Szymon	**Grabowski**	P-55
Kristin	**Gratz**	O-16
Wojciech	***Grudziński***	*O-13*
Barbara	***Gruza***	*O-17*
Marlena	***Gryl***	*P-55*
Marta	***Grzechowiak***	*P-04*
Nurbey	***Gulia***	*P-14*
Piotr	**Guńka**	P-17
Marek	***Gusowski***	*P-50*
Jadwiga	***Handzlik***	*P-46*
Katarzyna	**Helios**	O-04
Felix	**Hennersdorf**	O-14
Yuriy	***Horak***	*O-13*
Paweł	***Horeglad***	*P-10*
Anna	**Hoser**	O-09
Andreas	***Hoser***	*P-48*
Barbara	***Imiolczyk***	*P-03*, *P-04*
Dagmara	***Jacewicz***	*P-49*
Ewelina	***Jach***	*P-50*
Piotr	**Jakieła**	O-16
Jan	**Janczak**	P-18
Tomasz	***Janecki***	*P-31*
Irena	**Jankowska-Sumara**	O-18
Katarzyna N.	***Jarzembska***	*P-47*, *P-49*, *P-63*
Mariusz	***Jaskolski***	*P-03*, *P-05*, *P-04*
Róża	**Jastrzębska**	P-19
Aneta	***Jezierska***	*O-02*, *P-25*
Kunal Kumar	***Jha***	*O-17*
Łukasz	***John***	*P-43*
Kinga	**Jóźwiak**	O-02
Anna	***Kamecka***	*P-42*
Radosław	***Kaminski***	*P-47*, *P-49*, *P-63*

Daniel M.	***Kamiński***	*O-13*
Agnieszka	***Kania***	*P-38*
Zbigniew	**Karczmarzyk**	P-20, *P-42*
Hanna	**Kaspiaruk**	P-21
Oskar	**Kaszubowski**	P-22
Marcin	**Kaźmierczak**	P-23
Patrycja	**Kądziałka**	*P-03*, P-56
Mateusz	***Kciuk***	*P-20*
Anna	***Kędziora***	*O-04*
Grzegorz	**Kić**	O-15
Edyta	***Kierasińska***	*P-36*
Vasyl	**Kinzhybalo**	*O-12*, *O-13*, P-24, *P-29*, *P-51*
Beata	**Kizior**	P-25
Hubert	**Kleinschmidt**	P-26
Agnieszka	**Klonecka**	P-02, *P-03*
Jae-Hyeon	***Ko***	*O-18*
Andrzej	**Kochel**	*O-02*, P-28
Anna	***Komasa***	*P-15*
Izabela	***Korona-Głowniak***	*P-16*, *P-38*
Sandra	***Kosiorek***	*O-07*
Jacek	***Koszuk***	*P-31*
Daria	***Kowalkowska-Zedler***	*P-09*
Dorota A.	**Kowalska**	*P-11*, P-50
Maciej	***Kozak***	*P-02*
Marta S.	**Krawczyk**	P-27
Monika K.	**Krawczyk**	P-51
Jacek	**Krawczyk**	P-57
Ewelina	***Ksepko***	*O-22*, *P-67*
Maria	**Książek**	P-52, *P-53*
Jakub	***Kubicki***	*P-62*
Paulina	**Kurowska**	P-29
Joachim	**Kusz**	*P-52*, P-53
Aneta	***Lewandowska***	*P-15*
Krzysztof	***Lewiński***	*P-05*
Rafał	***Lipiński***	*P-24*

Marek	*Paściak*	*O-18*
Bogusław	*Penc*	*P-48*
Anna	*Pietrzak*	*P-31*
Agnieszka	*Pietrzyk-Brzezińska*	*P-01*
Paweł	Piszora	P-60, *P-68*
Agnieszka	*Pladzyk*	*P-09*
Nazariy	*Pokhodylo*	*P-33*
Kinga	Pokrywka	P-04
Catalin	*Popescu*	*P-68*
Carla	*Pretorius*	*P-47*
Anna	Pyra	P-07
Piotr	Rejnhardt	O-06, *P-56*, P-65
Toms	*Rekis*	*O-09*
Andreas	*Roodt*	*P-47*
Miłosz	*Ruszkowski*	*P-05*
Piotr	Salwa	O-21
Volodymyr	*Sashuk*	*O-07*
Dominik	*Schaniel*	*P-49*
Svitlana V.	*Shishkina*	*P-56*
Miłosz	*Siczek*	*P-23*, *P-39*
Magdalena	*Siedzielnik*	*P-26*
Adam	*Sieradzki*	*O-20*
Julia	*Skowronek*	*P-15*
Agnieszka	*Skórska-Stania*	*P-38*
Yurii	Slyvka	P-33
Joanna	*Sławek*	*P-02*
Vernon	Smith	O-15
Paulina	Sobczak	P-34
Aleksandra M.	*Sokołowska*	*P-24*
Aleksandra R	Sokołowska	P-35
Dagmara	*Stefańska*	*O-20*
Magdalena	Stępień	P-36
Marcin	*Stolarczyk*	*P-07*
Rafał	Stottko	P-61
Radosław	Strzałka	O-19, P-66

Jarosław	**Sukiennik**	P-37
Dariusz K.	***Szarejko***	*P-63*
Małgorzata	***Szczesio***	*P-16*, *P-37*, *P-44*
Bartłomiej M.	***Szyja***	*P-25*, *P-61*
Andrzej	***Szytuła***	*P-48*
Anna	**Ściuk**	P-05
Katarzyna	***Ślepokura***	*P-08*, *P-22*, *P-24*, *P-29*
Joanna	***Śmietańska***	*P-66*
Daniel	**Tchoń**	P-64
Waldemar	**Tejchman**	P-38
Aleksandra	**Tołoczko**	P-39
Paweł E.	**Tomaszewski**	P-54
Monika	***Trzebiatowska***	*P-50*
Agata	***Trzęsowska-Kruszyńska***	*P-34*
Kamil	**Twaróg**	P-28
Yuriy	***Tyvanchuk***	*P-48*
Karolina	**Urbanowicz**	P-40, *P-41*
Józef	***Utko***	*P-43*
Laure	***Vendier***	*P-59*
Marek	***Weselski***	*P-52*, *P-53*
Agnieszka	***Wojciechowska***	*O-04*
Wojciech M.	***Wolf***	*P-31*, *P-62*
Janusz	***Wolny***	*O-19*, *P-66*
Krzysztof	**Woźniak**	O-01, *O-17*, *P-30*, *P-40*, *P-41*
Karolina	**Wrochna**	P-41
Karol	**Wydra**	O-12
Waldemar	**Wysocki**	P-42
Rafał	***Wysokiński***	*O-04*
Patrycja	**Wytrych**	P-43
Jan K.	***Zaręba***	*O-20*
Dagmara	**Ziembicka**	P-44
Maciej	***Zubko***	*O-21*
Aleksandra	**Zwolenik**	P-45
Andrzej	**Żarczyński**	P-62
Ewa	**Żesławska**	*P-38*, P-46

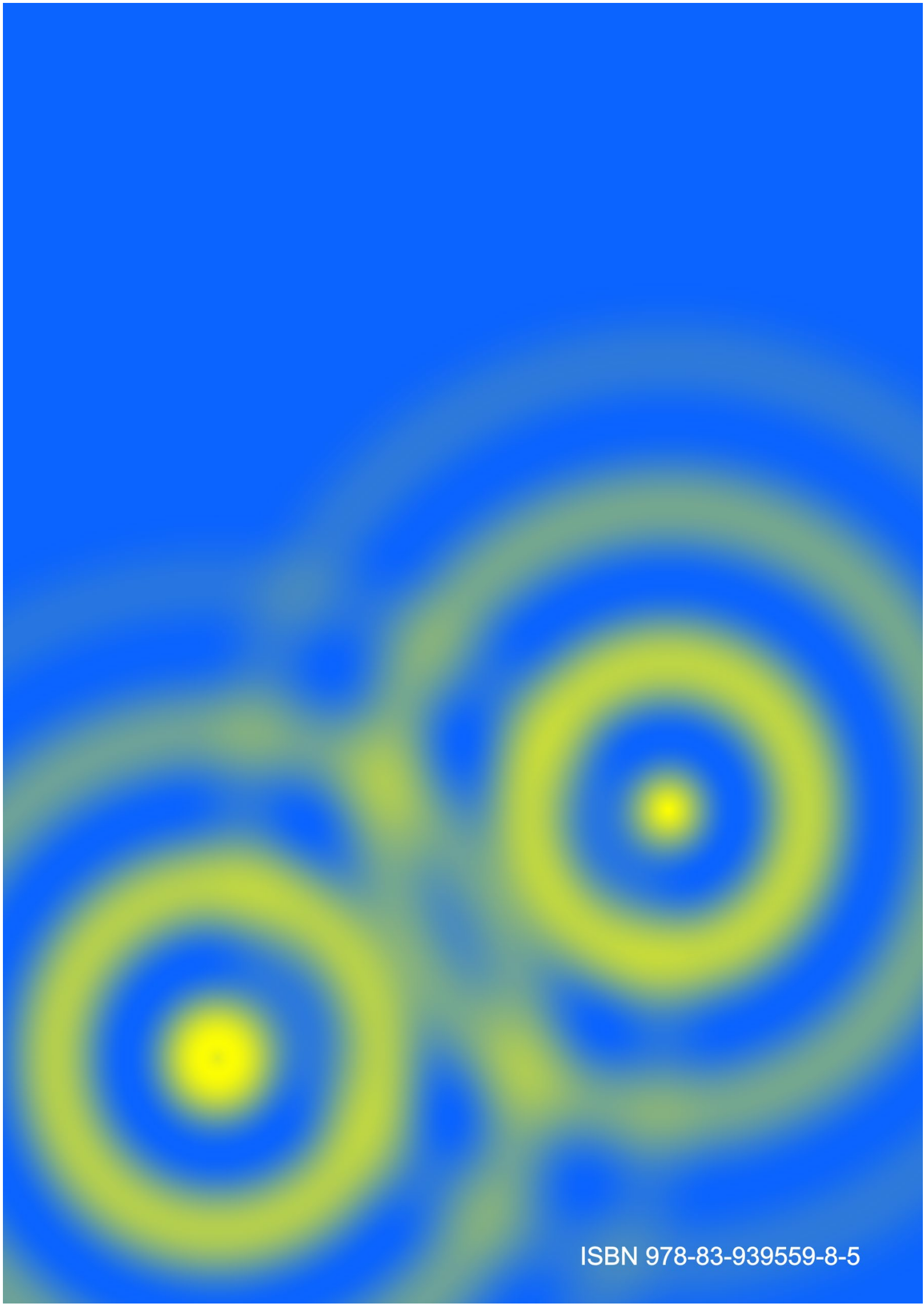

ISBN 978-83-939559-8-5